Bicuspid aortic valve and associated aortopathy: a combined biomechanics, histological and genetic analysis

A thesis submitted to Imperial College London

for the degree of Doctor of Philosophy

by

Stamatia Prapa

June 2013

Department of Adult Congenital Heart Disease

National Heart and Lung Institute

Imperial College London

Declaration

I hereby certify that all material in this dissertation is the product of original research. Any presented work which is not my own has been appropriately acknowledged.

Abstract

Bicuspid aortic valve (BAV) is the most common inborn heart defect and a continuum of a disease process affecting the aortic valve and the thoracic aorta with an increased risk of thoracic aortic aneurysm (TAA) formation and dissection. Aortic dilatation may be related to haemodynamic perturbations or intrinsic wall abnormalities. The aim of this thesis was to investigate the relative contribution of these parameters to BAV aortopathy via integrated analyses.

Distribution of circumferential stress in the aorta of BAV patients planned to undergo surgery was analysed using computed tomography imaging and computational modelling. During surgery, aortic biopsies were taken from discrete areas and examined for histological abnormalities. Maximal mechanical stress occurred in the medial ascending aorta in the majority of cases with integrated analyses exhibiting a positive correlation between aortic fibrosis and mechanical stress, both in the root and the ascending aorta. The degree of histological abnormalities and transforming growth factor beta (TGFβ) activation was also assessed in collected tissue biopsies. Patients with either root dilatation and/or predominant regurgitant valve disease had greater levels of medial wall degeneration in their ascending aorta whereas enhanced TGFβ signalling was present in aneurysmal but also, non-dilated BAV aortic segments, pointing to a genetic trigger. Copy number variation (CNV) analyses in a larger BAV cohort revealed a large heterozygous deletion in the angiotensin converting enzyme (*ACE*) gene and targeted next-generation sequencing revealed previously reported variants in *NOTCH1*, *COL3A1*,

and *APOE* genes with additional discovery of a large number of likely pathogenic variants in genes related to BAV formation and aortopathy.

In conclusion, different BAV aortic phenotypes were recognised and further analysed. The presence of multiple likely pathogenic variants in sequenced patients suggests a polygenic nature of BAV disease which, in conjuction with local haemodynamic perturbations, supports a mutlifactorial origin of BAV aortopathy.

List of contents

List of Figures

List of Tables

Abbreviations

3D Three-dimensional
4D Four-dimensional
AAA Abdominal aortic aneurysm
ACE Angiotensin converting enzyme
ACTA A-smooth actin
ALP Alkaline phosphatase
Ao Aortic
APC Adenomatosis polyposis coli
AR Aortic regurgitation
ARB Angiotensin receptor blocker
AS Aortic stenosis
ASD Atrial septal defect
ASI Aortic size index
ASO arterial switch operation
ATI Angiotensin II type I receptor
AVR Aortic valve replacement
BAC Bacterial artificial chromosome
BAV Bicuspid aortic valve
BMP Bone morphogenic protein
BRU Biomedical research unit
BSA Body surface area
cDNA Complementary DNA
CGH Comparative genomic hybridization
CHD Congenital heart disease
CMR Cardiac magnetic resonance
CNC Cardiac neural crest
CNS Central nervous system
CNV Copy number variation
CNVE Copy number variation event
CMR Cardiac magnetic resonance
CoA Coarctation of the aorta
COL3A1 Type III procollagen
COL3A1 Type III procollagen

CT Computed tomography
DAB chromogen 3,3’-diaminobenzidine
DDR Deletion-to-duplication ratio
ECM Extracellular matrix
EMT Endothelial mesenchymal transformation
ENG Endoglin
eNOs Endothelial nitric oxide synthase
ES Eisenmenger syndrome
EVG Elastic Van Gieson
FBN1 Fibrillin-1
FEA Finite element analysis
FN1 Fibronectin-1
Fz Frizzled
GABA gamma-aminobutyric acid
GPCR G-protein coupled receptor
GSK3 glycogen synthase kinase-3
HGS Histology grading score
HLHS Hypoplastic left heart syndrome
IMS Industrial Methylated Spirits
KPa Kilopascals
LDS Loeys Dietz syndrome
LLC Large latent complex
LPA Left pulmonary artery
LOD score Logarithm (base 10) of odds
LRP Lipoprotein receptor-related
LV Left ventricular
LVOTO Left ventricular outflow tract obstruction
MAD Median absolute deviation
MAF Minor allele frequency
MAPK Mitogen activated protein kinase
MFS Marfan syndrome
MMP Matrix metalloproteinase
MRI Magnetic resonance imaging
NFATc1 Activated T-cell protein 1
NGS Next generation sequencing

PAH Pulmonary arterial hypertension
PBS Phosphate buffered saline
PCR polymerase chain reaction
PDA Patent arterial duct
pSmad2 Phosphorylated Smad2
PT Pulmonary trunk
PT/Ao MT Pulmonary trunk-to-aortic media thickness
PWS Peak wall stress
QC Quality control
RAS Renin angiotensin system
RhoA Ras homolog gene family
R-L Fusion of right- and left-coronary leaflets
R-N Fusion of right- and non-coronary leaflets
ROCK Rho kinase
RPA Right pulmonary artery
SAC Sum of auto-correlation
SNP Single nucleotide polymorphism
SOX9 Sex determining region Y box-9
STJ Sinutubular junction
TAA Thoracic aortic aneurysm
TAV Trileaflet aortic valve
TGA Transposition of the great arteries
TGFβ Transforming growth factor beta
TGFBR Transforming growth factor-beta receptor
TIMP Tissue inhibitor of matrix metalloproteinase
TOF Tetralogy of Fallot
UTR Prime untranslated region
VEGF Vascular endothelial growth factor
VSD Ventricular septal defect
VSMC Vascular smooth muscle cell
WSS Wall shear stress

Acknowledgements

First and foremost, I would like to thank my primary supervisor, Prof. Gatzoulis, for his endless support, motivational advice, warmth, and kindness. He has acted as an excellent supervisor but also, as a fatherly figure throughout these challenging years, seeing me through my first academic steps and transition to clinical training. I am indebted to him for giving me the opportunity to become part of his team and investing me with his knowledge.

Likewise, I would like to thank Prof. Ho, my secondary supervisor, who has also graciously supported me all the way through and continues to provide me with exciting new academic challenges. Prof. Ho also introduced me to the wonderful team of the Cardiac Morphology Unit, Royal Brompton Hospital, and in particular to Karen McCarthy, whom I thank for her teaching and for making this work seem effortless. My special thanks go to the rest of my supervisors, Prof. Johnson and Dr. Babu-Narayan for giving me instrumental advice in the beginning of this project and supporting me all the way through to key edits of this dissertation. I am lucky to consider Sonya a personal friend and could not have made it without her warm smile during challenging moments of this research. I am also grateful to Prof. Collins, my mentor, who guided me from the very beginning of this project and made sure that I was well supported.

During these years, I was also lucky to have a number of informal supervisors. Just to name a few, I would like to thank Dr. Dimopoulos who introduced me to key research methodology but also, acted as a mentor and generously gave me numerous opportunities to complete exciting work with him. I am also thankful to Mr. Shore for making this

project possible and introducing me to a number of key ICL faculty members. Mr. Shore, along with Mr. Sethia and Mr. Uemura, have also provided key surgical support to this study and facilitated the collection of targeted tissue biopsies. Finally, I am thankful to Dr. Kilner and Dr. Rubens for their generous help with pre-operative imaging, without which the computational modelling aspects of this study would not have been possible.

A number of key collaborators were necessary to complete this multidisciplinary research. Prof. Pepper has acted as an informal supervisor of this thesis, providing me with essential academic support, and led the way to exciting collaborations. Prof. Xu kindly welcomed me to the Chemical Engineering department, ICL, and with the support of Dr. Torii, taught me the fundamentals of computational modelling. I am especially thankful to Prof. Cook, who not only introduced me to the field of clinical genetics but also, gave me tremendous opportunities to extend this work, via collaborations with the Wellcome Trust Sanger Institute and the Cardiovascular Biomedical Research Unit of the Royal Brompton Hospital.

Finally, I am thankful to a number of old and new friends, including fellows of the Adult Congenital Heart Disease Unit, Royal Brompton Hospital, who were there when most needed. This research is dedicated to my family; my parents, Sotiris and Evangelia, for their immense support and for teaching me that “the sky is the limit” and my sisters, Vicky and Iliana, for standing by me throughout the joyful and stressful moments of this journey.

Chapter 1. Introduction

Abbreviations

4D Four-dimensional
ACE Angiotensin converting enzyme
ACTA A-smooth actin
ALP Alkaline phosphatase
APC Adenomatosis polyposis coli
ASD Atrial septal defect
ATI Angiotensin II type I receptor
BAV Bicuspid aortic valve
BMP Bone morphogenic protein
CGH Comparative genomic hybridization
CHD Congenital heart disease
COL3A1 Type III procollagen
ECM Extracellular matrix
EMT Endothelial mesenchymal transformation
ENG Endoglin
eNOs Endothelial nitric oxide synthase
FBN1 Fibrillin-1
FN1 Fibronectin-1
Fz Frizzled
GABA gamma-aminobutyric acid
GPCR G-protein coupled receptor
GSK3 glycogen synthase kinase-3
LDS Loeys Dietz syndrome
LLC Large latent complex
LRP Lipoprotein receptor-related

MAPK Mitogen activated protein kinase

MFS Marfan syndrome

MMP Matrix metalloproteinase

MRI Magnetic resonance imaging

NFATc1 Activated T-cell protein 1

PAH Pulmonary arterial hypertension

PDA Patent arterial duct

PWS Peak wall stress

RAS Renin angiotensin system

RhoA Ras homolog gene family

R-L Fusion of right- and left-coronary leaflets

R-N Fusion of right- and non-coronary leaflets

ROCK Rho kinase

SOX9 Sex determining region Y box-9

TAA Thoracic aortic aneurysm

TAV Trileaflet aortic valve

TGFβ Transforming growth factor beta

TGFBR Transforming growth factor-beta receptor

TIMP Tissue inhibitor of matrix metalloproteinase

VEGF Vascular endothelial growth factor

VSD Ventricular septal defect

VSMC Vascular smooth muscle cell

WSS Wall shear stress

1.1 Valve anatomy and disease

The human heart is a key component of the cardiovascular system acting as a beating pump that circulates blood around the body. Its anatomy can be considered in three segments: the collecting chambers, known as atria, the pumping chambers, known as ventricles, and the great arteries, namely the aorta and pulmonary artery. A muscular layer called septum separates the heart into right and left, with each side facilitating the pulmonary and systemic circuits, respectively. Unidirectional blood flow through these chambers is ensured by the presence of four heart valves; two atrioventricular valves separate the atria from the ventricles, with the tricuspid valve on the right and the mitral valve on the left, and two semilunar valves, including the pulmonary and aortic valves, separate the ventricles from the respective great arteries.

Despite their similar function, valve anatomies differ with the atrioventricular valves made up of two (mitral) or three (tricuspid) valve leaflets resembling circular curtains with the external support of chordae tendineae attaching the leaflets to the ventricular papillary muscles (Anderson et al., 2000). In contrast, the term “cusps” is used to describe the three leaflets of the semilunar valves (aortic and pulmonary) situated in the great arteries leaving the heart. The latter lack external support with the exception of the aortic annulus, a fibrous structure attaching the root of the aorta to the left ventricle.

With an average adult heart rate of 70 beats per minute, heart valves open and close more than 100,000 times per day determining the pathway of blood flow through the heart. In order to withstand this continuous cyclic shear stress, valve leaflets develop an intricate connective tissue architecture comprised of interstitial cells, stratified extracellular matrix

(ECM), and a peripheral layer of endothelial cells responsive to biomechanical stimuli (Armstrong and Bischoff, 2004). Disruption of this architecture at birth or later in life results in development of valve disease, either in the form of regurgitation, with incomplete coaptation of the leaflets leading to backward flow, or stenosis, with narrowing of the valve opening leading to outflow obstruction.

Congenital valve defects are inborn abnormalities occurring during fetal life disrupting valve formation. Bicuspid aortic valve (BAV) (OMIM # 109730, Figure 1.1) is the most common congenital cardiac malformation with a prevalence of 0.5% - 2% in the general population (Basso et al., 2004, Braverman et al., 2005). BAV is characterised by the presence of two instead of three valve leaflets with an increased predisposition to a number of complications including infective endocarditis and valvular dysfunction (Ward, 2000). The majority of BAV patients will require valve surgery during their lifetime, predominantly due to significant aortic stenosis in early childhood, aortic regurgitation into adolescence and calcific valve disease later in adulthood (Lewin and Otto, 2005).

The incidence of aortic stenosis in BAV varies from 5 to 50% based on surgical series and is affected by the age of studied populations, with increased prevalence in older subjects (Braverman et al., 2005). Despite the same underlying mechanisms of senile valve degeneration, involving lipid deposition, inflammation, and ultimate calcification, BAV leaflets are more susceptible to the above process with higher rates of progressive aortic stenosis compared to trileaflet aortic valves (Braverman et al., 2005, Robicsek et al., 2004). In contrast, aortic regurgitation in BAV is less common with an incidence of

1.5 to 10% (Roberts et al., 1981) and can be the inherent result of redundant leaflet architecture or the secondary outcome of endocarditis, aortic dilatation, and dissection, as described later (Ward, 2000). Overall, up to 33% of BAV patients will require valve surgery during their lifetime, for either aortic stenosis or regurgitation (Fernandes et al., 2007, Keane et al., 1993).

1.2 Aortic anatomy and disease

Over the past decades, perception of BAV has shifted from an isolated valve defect to a continuum disease process affecting the entire aortic root and ascending aorta (Tadros et al., 2009). These two segments are the proximal parts of the thoracic aorta, the main artery arising from the left ventricle supplying the human body with oxygenated blood to the level of the diaphragm. The aortic root forms a bridge between the left ventricle and the ascending aorta guarded by the aortic valve leaflets with three small dilatations immediately above it called sinuses. Out of the anterior and left posterior sinuses rise the mouths of the right and left coronary arteries, respectively, supplying the heart, with the third bulge called the non-coronary sinus (Anderson, 2007). The anatomical border between the aortic root and the ascending aorta is defined as the sinutubular junction. At this point the ascending aorta becomes a tubular structure with an approximate length of 5cm followed by the aortic arch, supplying the chest, upper limbs, head, and neck with numerous branching vessels.

All arterial walls have the same triple layer composition of an innermost layer constituted by endothelial cells on a basic membrane (intima), a middle layer containing muscle tissue and elastic fibres (media), and an outer layer comprising connective tissue

(adventitia). BAV patients are at an increased risk of developing thoracic aortic aneurysm (TAA), which is a localized balloon-like bulge in the vessel wall. TAA is a silent disease that can progress over the years with no symptoms. As aneurysm size increases, so does the risk of developing a tear in the intima (called aortic dissection) allowing blood flow into the media with complete separation of the two layers. These tears can propagate antero- or retro- gradely leading to reduced organ perfusion, haemodynamic compromise and ultimately, complete rupture of the aortic wall with subsequent death in the absence of timely intervention. Severe aortic regurgitation can also occur due to incomplete coaptation of the valve leaflets when the tear extends to the aortic root.

Aortic dilatation in BAV disease is present in early stages of life with TAA formation in approximately 40% of adult patients (El-Hamamsy and Yacoub, 2009b, Beroukhim et al., 2006). The estimated risk of aortic dissection in BAV patients is 5-10 times higher compared to the general population, based on necropsy series (Larson and Edwards, 1984, Ward, 2000). Review of the Yale clinical series revealed higher aneurysm annual growth rate in BAV compared to tricuspid aortic valve (TAV) patients but similar rates of aortic dissection and rupture (Davies et al., 2007). As discussed later, identification of risk factors for aneurysm formation in BAV patients is fundamental to avoid the catastrophic complications of aortic wall dissection.

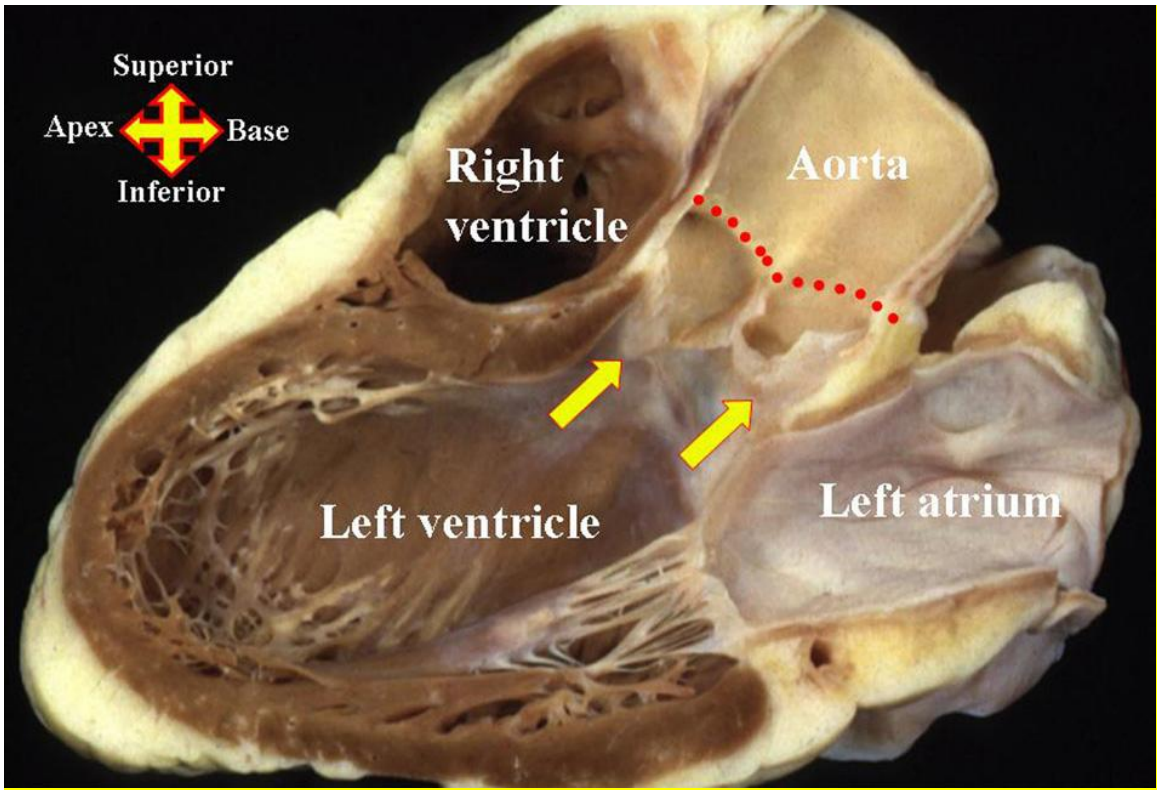

Figure 1.1 Human heart morphology. In this section, all three segments of the left heart can be seen including the smooth walled collecting chamber (left atrium), the muscular walled pumping chamber (left ventricle), and the aortic valve leaflets (yellow arrows) within the aortic root. The root extends from the ventriculo-aortic to the sinutubular junction (marked with red dotted line), after which the aorta becomes a tubular structure (Anderson, 2007).

1.3 Structure and ontology of the bi-leaflet aortic valve

The term BAV has been used to describe a broad spectrum of aortic valve malformations with the diagnostic criteria of a BAV first classified by Osler in 1886 (Braverman et al., 2005). According to general consensus, there are two morphological types of BAV, determined by the number of commissures. In the case of complete absence of one commissure, the result is a 'true' BAV with either anterior-posterior or lateral-lateral orientation of the free edges of the leaflets. In a 'functional' BAV, there are three commissures, one of which is often hypoplastic. In these cases, the malformed

commissure, also known as a raphe, represents the fused area between the two adjacent leaflets. The orientation of the raphe in relation to the sinuses, defines the further subtype of a functional BAV, with the commonest type being right-left (R-L) followed by right-non coronary (R-N) functional BAV (Figure 1.2) (Russo et al., 2008). Less frequent types of BAV with two raphes have also been described (Sievers and Schmidtke, 2007).

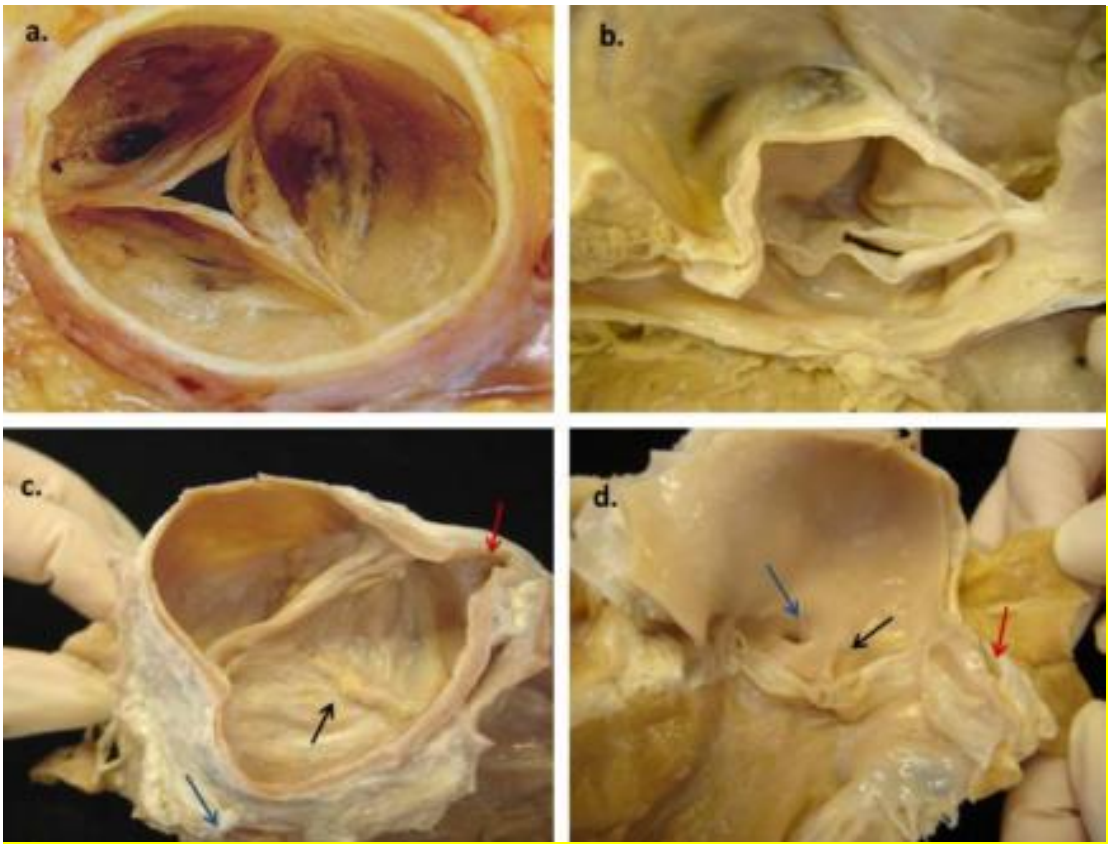

Figure 1.2 BAV morphological subtypes. The commonest subtypes of BAV are exhibited, as seen in human specimens (Cardiac Morphology Unit, Royal Brompton Hospital). A normal tri-leaflet aortic valve is comprised of three leaflets and three commissures (a). In the case of complete absence of one commissure, the result is a 'true' BAV consisting of only two sinuses, two leaflets and two fully developed commissures (b). In a functional BAV (c and d), there are three sinuses and three leaflets, but two of the leaflets and sinuses are underdeveloped leaving a raphe in between as a putative commissure. The commonest morphologic types of BAVs are the right-left (c) and right-non coronary (d) functional BAVs. The black arrow marks the raphe, the red arrow the left coronary artery, and the blue arrow the right coronary artery.

The process of valvulogenesis initiates when the heart is a tube consisting of an inner layer of endothelial cells, an outer layer of myocardial cells, and the in-between ECM (cardiac jelly) (Armstrong and Bischoff, 2004). Following right-ward looping of the heart, endothelial-mesenchymal transformation (EMT) takes place, with proliferation and differentiation of a special subset of endothelial cells into mesenchymal cells. The EMT results in thickening of the cardiac jelly in the regions of the atrioventricular and outflow tract and subsequent formation of the endocardial cushions.

A large number of signalling pathways have been involved in EMT and endocardial cushion formation, including family members of transforming growth factor beta (TGFβ) and vascular endothelial growth factor (VEGF), *NOTCH1*, Wnt/β-catenin, and nuclear factor of activated T-cell protein 1 (*NFATc1*) (Armstrong and Bischoff, 2004, Chakraborty et al., 2010). Complex signalling interactions between the above pathways give rise to the mitral and tricuspid valves in the atrioventricular canal. In the outflow tract, neural crest cells migrate from the branchial arches to the endocardial cushions and contribute to the formation of the aortic and pulmonary valves and the aorticopulmonary septation of the outflow tract (Kirby et al., 1983). In a healthy fetus, the EMT process and subsequent endocardial cushion remodelling lead to the formation of a trileaflet aortic valve. As described in the following sections, disruptions in key embryological pathways can lead to congenital valve defects and in particular, development of BAV.

TGFβ family members, including bone morphogenetic proteins (BMPs) and TGFβs, act as signaling partners in endocardial cushion formation. They interact with transmembrane

TGFβ receptors via phosphorylation, which in turn, phosphorylate and activate Smad proteins in the cytoplasm (Shi and Massague, 2003). The downstream transcription factors of TGFβ and BNP signalling activated by Smads are currently not well defined (Armstrong and Bischoff, 2004). However, there is evidence of hypoplastic cardiac cushion formation in mice genetically disrupted for BMP, including double mutants for BMP-6 and BMP-7 (bmp6_/_; bmp7_/_) and mutants for *ALK3* gene (ALK3_/_) encoding a BMP receptor with additional decrease of TGFβ expression (Gaussin et al., 2002, Kim et al., 2001).

VEGF, a key regulator of physiological angiogenesis during embryologic development, is also thought to be a specific mediator of cardiac valve development via signaling on the endothelial cell surface in the cushion forming regions (Miquerol et al., 1999). Lack of VEGF during valve development leads to insufficient endothelial cell proliferation and thus, inadequate number of endothelial cells for EMT with hypoplastic/absent cardiac cushion formation. Environmental conditions, such as hyperglycaemia, can reduce VEGF expression with subsequent inhibition of EMT of the atrioventricular cushions (Enciso et al., 2003).

Transcription factor *NFATc1* is part of the nuclear factor of activated T-cell (NFAT) protein family involved in the regulation of cell differentiation and endocardial cushion development (Armstrong and Bischoff, 2004). Expression of *NFATc1* in the developing heart overlaps spatiotemporally with that of VEGF with evidence of interaction between the two factors in cultures of human pulmonary valve endothelial cells (Johnson et al., 2003). *NFATc1* signalling is also part of the calcineurin/NFAT pathway (Figure 1.4),

with knockout of calcineurin gene in mice resulting in complete absence of the aortic and pulmonary valves (Lin et al., 2012).

A number of transcription factors have been associated specifically with BAV formation. A characteristic example is that of a transcription factor central to the EMT process, *NOTCH1*, associated with development of BAV and calcific aortic valve disease in humans (Garg et al., 2005). *NOTCH1* gene encodes a transmembrane protein regulating cell fate decisions involved in the development of the atrioventricular canal, ventricular myocardium and cardiac outflow tract (Niessen and Karsan, 2008). Downregulation of *NOTCH1* and its receptor ligand, *JAG1* (Figure 1.4), has been exhibited in GATA5 null mice with BAV (Laforest et al., 2011). *NOTCH1* regulation of aortic valve calcification, a pathology commonly seen in BAV patients, appears to take place via a sex determining region Y (SRY)-box 9 (*SOX9*)-dependent pathway (Acharya et al., 2011). Of note, *NOTCH1* signalling also participates in the differentiation of cardiac neural crest cells into smooth muscle cells contributing to the development of the great vessels, thus providing a genetic linkage to the BAV-TAA phenotype, as discussed later (Laforest and Nemer, 2012).

Lack of another transcription factor expressed in the atrioventricular and outflow tract endocardial cushions*, GATA5,* results in partial penetrance of BAV with a prevalence of 26% in null mice (Laforest et al., 2011). Heterozygous mice for *NKX2.5*, a cardiac homeobox gene associated with a number of congenital heart disease (CHD) lesions in humans, have an 8-fold increased prevalence of stenotic BAVs compared to wild-type mice (Biben et al., 2000).

Sans-Coma et al. were the first to exhibit that fusion of the right and left valve cushions plays a crucial role in BAV morphogenesis, using inbred Syrian hamsters with high prevalence of BAV (Sans-Coma et al., 1996). Interestingly, a recent study in endothelial nitric oxide synthase (eNOS) knock-out mice provided evidence on distinct aetiologies of functional BAVs, showing that R-N BAVs result from abnormal cardiac cushion formation occuring prior to the septation of the cardiac outflow tract, whereas R-L BAVs develop due to abnormal outflow tract septation (Figure 1.3) (Fernandez et al., 2009). The authors argue that eNOS may have a role in cardiac cushion formation and the EMT process in R-N BAVs whereas neural crest cell defects may underlie the abnormal outflow tract septation in R-L BAVs.

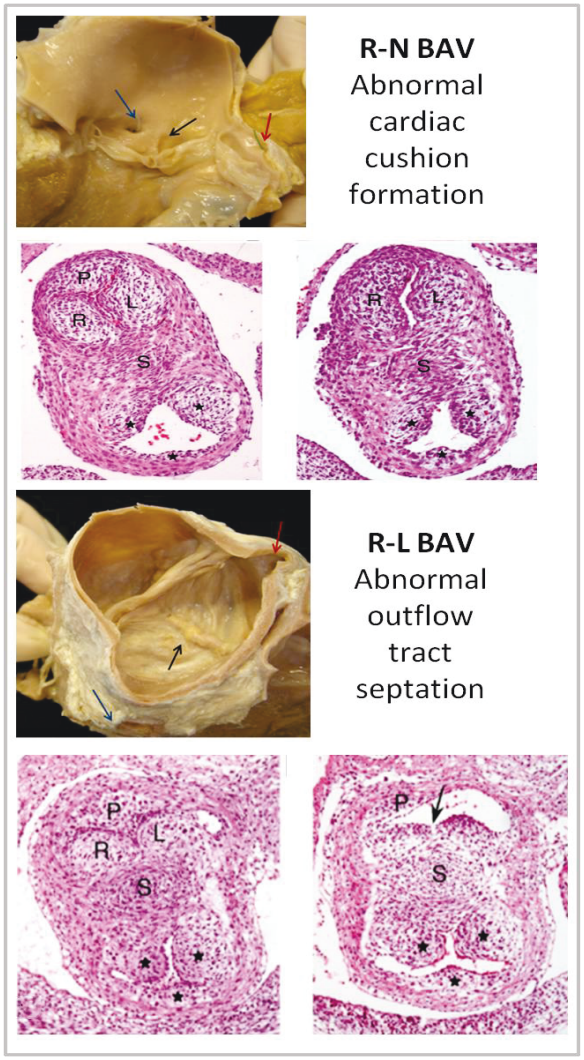

Figure 1.3 Distinct aetiology of functional BAVs. Right-non coronary (R-N) BAVs result from abnormal cardiac cushion formation whereas right-left (R-L) coronary BAVs result from abnormal outflow tract septation. Histology images by Fernandez et al.(Fernandez et al., 2009): Transverse sections of the developing outflow tract in mouse (upper panel) and hamster (bottom panel) BAV animal models (Haematoxylin-eosin stain, x100 magnification). *Pulmonary valve cushions, L; left aortic valve cushion; P posterior (noncoronary) aortic valve cushion; R right aortic valve cushion; S, outflow tract septum. Human aortic valve specimens from Cardiac Morphology Unit, Royal Brompton Hospital.

Nitric oxide synthase enzymes convert L-arginine to L-citrulline leading to production of nitric oxide (Figure 1.4), a signalling molecule involved in multiple processes including cell proliferation, differentiation and apoptosis. Release of eNOs is primarily regulated by Ca+2/CaM (calcium/calmodulin) in an autoinhibitory manner (Salerno et al., 1997). Endothelial nitric oxide is involved in both cardiac embryogenesis and post-developmental vascular remodelling (Liu et al., 2013). A strong association has been exhibited between eNOs deficiency and development of BAV in mice (Lee et al., 2000). Expression of eNOs is shear-dependent (by the protein kinase B/Akt (Akt)-dependent mechanism), which is similar to the EMT process, and thus, deficiency of its activation might affect cardiac cushion formation (Groenendijk et al., 2004).

The Wnt/β-catenin signal transduction pathway, initially linked to carcinogenesis, has many additional disease connections as well as an established role in embryologic development (Clevers and Nusse, 2012). Wnt signalling initiates when Wnt proteins bind to a heterodimeric receptor complex, consisted of a Frizzled (Fz) protein, part of the G-protein coupled receptors (GPCRs) family, and a lipoprotein receptor-related protein (LRP)-5/6 (Figure 1.4). Activation of the receptor leads to cytoplasmic accumulation of β-catenin which would otherwise not be possible due to its degradation by a destruction complex, including Axin-1, adenomatosis polyposis coli (APC), and glycogen synthase kinase 3 (GSK3) proteins. The role of Wnt/β-catenin signalling in valve formation has been shown in various animal models (Gitler et al., 2003, Hurlstone et al., 2003). More recently, mutations in the gene encoding for Axin-1 have been linked to BAV disease in humans, with no clear mechanistic hypothesis (Wooten et al., 2010).

Selected aforementioned pathways contributing to aortic valve/BAV formation are illustrated in Figure 1.4, including the Ca+2/CaM (calcium/calmodulin) regulated expression of eNOs and *NFATc1*, the association of key transcription factors *NOTCH1* and *GATA5*, and the Wnt/β-catenin pathway. Genes highlighted in purple in this image were selected for targeted next-generation sequencing and are discussed in more detail in **Chapter 7**).

Figure 1.4 Molecular pathways involved in BAV formation.

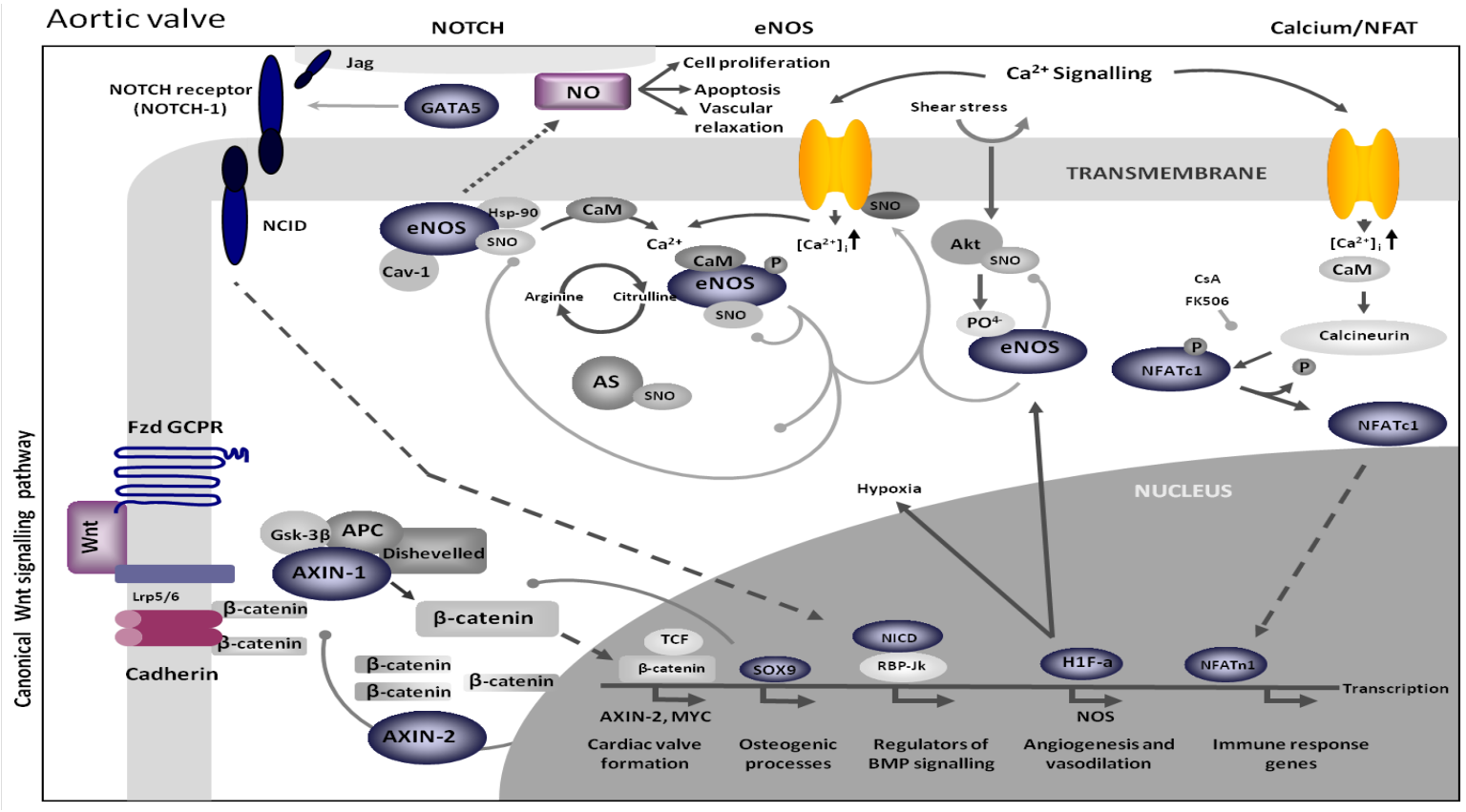

Key: AKT, aka Protein Kinase B; APC, adenomatous polyposis coli; AS, argininosuccinate synthetase; AXIN, AXis Inhibitor; Ca, calcium; [Ca2+]I, intracellular calcium concentration; CaM, calmodulin; Cav-1, caveolin-1; CsA, cyclosporine A; eNOS, endothelial nitric oxide synthase; FK, tacrolimus; Fzd, frizzled; GPCR, G protein coupled receptors; GSK-3, Glyogen synthase kinase-3; HIF-1^{α}, Hypoxia inducible factor 1^{α} ; Hsp-90, Heat shock protein 90; LRP, low density lipoprotein receptor related protein; NCID, NOTCH Intracellular Domain; NFATn/c, Nuclear Factor nucleus (n) or cytocol (c) located; NOS, nitric oxide synthase; RBP-Jk, Recombination Signal-Binding Protein 1 for J-Kappa; SNO, S-nitrosylation; SRY, sex determining region Y; TCF, T cell factor.

1.4 Mechanisms underlying BAV aortopathy

Aortic dilatation in BAV patients is progressive and may be related to haemodynamic abnormalities, secondary to stress exerted on the aortic wall by eccentric turbulent flow through the abnormal BAV leaflets, or to genetic abnormalities of the aorta, secondary to a common developmental defect affecting the aortic valve and aortic wall (Fedak et al., 2002). The latter is supported by evidence of histological abnormalities in the BAV aorta, commonly known as Erdheim's cystic medial necrosis, characterised by elastic fibre fragmentation, non-inflammatory loss of vascular smooth muscle cells (VSMCs) and accumulation of basophilic ground substance within cell-depleted areas of the media (Niwa et al., 2001, McKusick, 1972, Parai et al., 1999).

The proposed culprit lesion in BAV aortopathy is deficiency of a large protein forming extracellular microfibril suprastructures, fibrillin-1, leading to detachment of VSMCs from elastin and collagen and release of matrix-metalloproteinases (MMPs) (Fedak et al., 2003). MMPs belong to a family of proteases that possess proteolytic properties and are synthetized by a number of cells, including VSMCs, in response to local haemodynamic environment and various disease states. MMP-2 (gelatinase A) and MMP-9 (gelatinase B) are the most commonly encountered metalloproteinases in the ascending aorta and their activity, involving degradation of type IV, elastin, and fibrillar collagens, has been shown to be increased in BAV aneurysms compared to aneurysmal tissue from TAV patients (LeMaire et al., 2005, Ikonomidis et al., 2007). Expression of MMPs is normally kept under tight control predominantly by tissue inhibitors of metalloproteinases (TIMPs), with TIMP-1 being the most common in the aorta produced by VSMCs and

fibroblasts. The balance of expression of MMPs and TIMPs also appears to be associated with aneurysm formation, although several studies have shown conflicting patterns of MMP/TIMP expression, possibly due to differences in sites of aortic tissue sampling (El-Hamamsy and Yacoub, 2009a).

Medial degeneration of the BAV aortic wall resembles histopathologic changes seen in other connective tissue disorders, such as Marfan syndrome, in favour of an inherent structural defect of the aortic wall (Niwa et al., 2001). Additional arguments supporting the genetic aortopathy theory include the presence of greater degrees of dilatation in BAV, both in the absence of valvular disease, compared to age-matched healthy individuals, and in the presence of valvular stenosis/regurgitation, compared to TAV patients matched for haemodynamic severity of valvular lesions (Girdauskas et al., 2011a). Moreover, progressive aortic dilation in BAV patients following aortic valve replacement and thus, removal of any additive haemodynamic influence, further points to a genetic origin of BAV-TAA (Andrus et al., 2003).

However, recently arising evidence contradicts the single-sided genetic theory of aortopathy and highlights the presence of jet eccentricity in stenotic but also, 'normally' functioning BAVs, causing altered blood flow patterns from a very young age (Girdauskas et al., 2011a). As discussed later, this altered haemodynamic environment can lead to locally exerted stress with asymmetrical patterns of dilation and corresponding histopathologic lesions (i.e., flow-induced vascular remodeling) (Lehoux et al., 2002). Moreover, despite the evidence of ongoing aortic dilatation following aortic

valve replacement in BAV, there are no comparative reports in the literature showing that the TAV aorta behaves differently postoperatively (Andrus et al., 2003).

1.4.1 Haemodynamic theory

Intrinsic structural abnormalities of the BAV aortic wall may be augmented by altered blood flow patterns secondary to the malformed aortic valve. In vitro cultures of human endothelial cells have exhibited the capacity of the latter to respond to different levels of wall shear stress (WSS) with downstream alteration of the underlying VSMCs' proliferative, contractile, or synthetic properties (El-Hamamsy and Yacoub, 2009a, Topper et al., 1996). Morphological subtypes of BAV have a different natural history which may relate to their corresponding haemodynamic effects; anterior-posteriorly oriented BAVs are more likely to develop regurgitation, whereas right-left oriented BAVs are more prone to stenosis, resulting in different flow patterns in the aorta (Hope et al., 2010, Sonoda et al., 2008). Consequently, regurgitant BAVs are thought to increase wall tension, due to higher stroke volumes, and correlate with aortic root dilatation (Tadros et al., 2009). In contrast, stenotic BAVs generate a high-velocity jet with increased longitudinal, rather than radial, stress on the right anterolateral wall of the ascending aorta, creating an asymmetric "bulge" in the same region (Tadros et al., 2009).

The contributory role of haemodynamics has been investigated in aortic tissue specimens from patients with stenotic BAVs, exhibiting increased VSMC apoptosis and differences in ECM content in the convexity (versus the concavity) of the ascending aorta, where wall stress is expected to be higher (Della Corte et al., 2008). The so-called "post-stenotic dilatation" theory has also been assessed by four-dimensional (4D) flow magnetic

resonance imaging (MRI) exhibiting eccentric systolic flow contributing to focal elevations in WSS, even in the absence of stenotic BAV disease (Figure 1.5) (Hope et al., 2010). Interestingly, the patterns of eccentric flow in the latter study differed between subtypes of functional BAVs and may account for differences in their natural history; R-L BAV has been associated with dilatation of the aortic root at a younger age and more severe medial wall degeneration of the ascending aorta whereas R-N BAV has been linked to increased dimensions of the aortic arch (Schaefer et al., 2008, Fazel et al., 2008).

Figure 1.5 Evidence of haemodynamic influence on BAV aortopathy. A. Coronal cardiac magnetic resonance image (MRI) of a BAV patient with stenotic valve disease. A jet lesion directed to the anterior-lateral portion of the ascending aorta can be viewed, with asymmetrical dilatation of the vessel wall at the same level. Four-dimensional MRI flow studies in patients with right-left (R-L) (**B**) and right-non coronary (R-N) (**C**) functional BAVs exhibited differential eccentric systolic flow patterns, even in the absence of stenotic disease. Image A, courtesy of S. Babu-Narayan, Royal Brompton Hospital. Images B and C from Hope et al.(Hope et al., 2010)

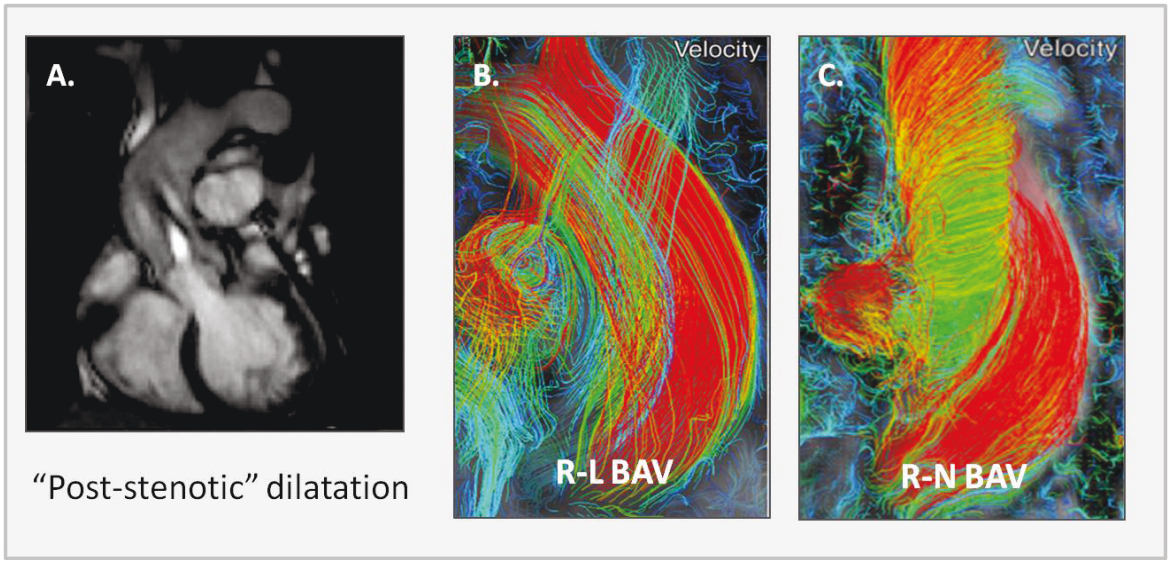

1.4.1.1 Pulmonary arterial hypertension as an aortopathy model

Pulmonary arterial hypertension (PAH) is defined as a sustained increase of blood pressure in the pulmonary circulation to more than 25mmHg at rest or 30mmHg with physical exertion (Farber and Loscalzo, 2004). PAH can be idiopathic or secondary to a number of pathologies including left-sided heart disease, lung disease and/or hypoxemia, chronic thromboembolic disease, and congenital left-to-right intracardiac shunts. Regardless of the primary underlying cause, vascular changes in the pulmonary circulation are common and include vasoconstriction, proliferation of smooth muscle and endothelial cells, and thrombosis.

In the setting of congenital heart disease (CHD), PAH develops when incomplete separation of the pulmonary and systemic circulations forces blood to flow from the high-pressure systemic circulation to the low-pressure pulmonary circulation, described as left-to-right shunting. Eisenmenger syndrome is the extreme manifestation of PAH associated with congenital heart defects and consists of pulmonary hypertension in the presence of reversed or bidirectional shunting and cyanosis. Shunting may occur at different levels and associated defects can be divided into pre-tricuspid, i.e. atrial septal defects (ASDs), or post-tricuspid, i.e. non-restrictive ventricular septal defects (VSDs), patent ductus arteriosus (PDA) and aortopulmonary windows.

PAH is primarily considered a disease of the small muscular distal pulmonary arteries. However, the large elastic pulmonary arteries are also affected in the setting of PAH and CHD, with previous reports of aneurysmal dilatation, atherosclerosis and thrombosis (Heath et al., 1960, Broberg et al., 2007, Daliento et al., 2002). As discussed later in

Chapter 5, arterial wall remodeling in the setting of PAH can serve as an aortopathy model to study medial wall changes in relation to elevated haemodynamic stress. Moreover, as inherent abnormalities of the great arteries have been previously reported in a variety of CHD lesions (Niwa et al., 2001), similar to those seen in BAV, the PAH/CHD model can provide information on the additive contribution of haemodynamic stress to intrinsic structural wall defects (Prapa et al., 2013).

1.4.2 Genetic theory

The origin of BAV is speculated to be hereditary with familial studies demonstrating the occurrence of a BAV in approximately 9% of first-degree relatives of affected individuals with an autosomal dominant pattern of inheritance with reduced penetrance (Huntington et al., 1997, Fedak et al., 2002). Development of TAA as an isolated feature can also run in families following the same pattern of inheritance (Milewicz et al., 1998). Interestingly, affected BAV family members may have isolated thoracic aortic dilatation or increased aortic stiffness in the absence of BAV, suggesting a common genetic background of BAV and TAA as variable manifestations of the same disease (Hiratzka et al., 2010, Loscalzo et al., 2007).

Interestingly, BAV patients exhibit similar degenerative changes in the media of their aortic root and pulmonary trunk, with the two segments sharing the same embryologic origin of the conotruncus (de Sa et al., 1999). This finding points further to a genetic origin of aortopathy in BAV disease but also has clinical implications in surgical replacement of the BAV. Ross procedure is a type of aortic valve replacement involving excision of the pulmonary valve and a segment of the pulmonary artery with their

placement in the aortic position. This procedure is particularly advantageous in young patients with BAV requiring valve replacement, as the pulmonary autograft lasts longer compared to bioprostheses and does not require anticoagulation, as with mechanical valves. However, Ross procedure remains a source of controversy in BAV with evidence of poor durability of the pulmonary autograft, due to the above described histopathological abnormalities (Takkenberg et al., 2009).

The specific gene product responsible for development of TAA in BAV disease remains elusive and is speculated to be a structural protein or one with a vital role in cardiac development. Candidate genes central to the contractile apparatus of the aortic media include *MYH11* and *ACTA2* (Figure 1.6). Mutations in the *MYH11* gene, encoding the major contractile protein βMHC in VSMCs, have been linked to familial TAA associated with PDA and less frequently, BAV (Zhu et al., 2006, Pannu et al., 2007). Similarly, mutations in the *ACTA2* gene, which encodes α-smooth muscle actin, cause non-syndromic TAA associated with PDA, BAV and other features of unknown frequency, such as livedo reticularis and iris flocculi (Guo et al., 2007, Fatigati and Murphy, 1984). Another candidate gene is *FN1,* encoding for fibronectin-1, a collagen-binding glycoprotein interacting with ECM elements leading to microfilament bundle formation via a downstream cascade of Ras homolog gene family member (RhoA) and rho kinases (ROCKs) (Figure 1.6) (Yoneda et al., 2007). Stress-dependent upregulation of *FN1* has been previously shown in the BAV ascending aorta (Della Corte et al., 2008) although mutations in this gene have not been identified in BAV patients.

Additional target genes for BAV aortopathy relate to the synthetic properties of VSMCs and have been linked to connective tissue disorders, such as Marfan (MFS) and Loeys-Dietz (LDS) syndromes. Surprisingly, despite the common finding of fibrillin-1 deficiency seen in the MFS and BAV aneurysmal aorta, mutations in *FBN1* gene encoding for this protein are present in MFS but not in BAV patients (Dietz et al., 1991, Robinson and Godfrey, 2000). Recent insights into inherited forms of aortopathy have also highlighted the central role of TGFβ signalling in TAA formation with the general mechanistic hypothesis of *FBN1* deficiency making sequestered TGFβ more accessible to activation leading to matrix proteolysis (Carta et al., 2009).

TGFβ is a multifunctional cytokine, with synthetic and apoptotic properties, that not only participates in cardiac valve formation as mentioned above, but also in post-developmental ECM homeostasis (Goumans et al., 2009, Owens and Wise, 1997, Cordenonsi et al., 2003). Its bioavailability is regulated by the large latent complex (LLC) which interacts with fibrillin-1 and contains TGFβ in an inactive state (Figure 1.6) (El-Hamamsy and Yacoub, 2009a, Carta et al., 2009). Once active TGFβ is released in the ECM, it binds to its ligand-activated receptors and stimulates signalling via "canonical" and "non-canonical" pathways, with shared key terminal evens including MMP-mediated proteolysis (Figure 1.6) (Derynck and Zhang, 2003). Canonical signalling relies on a Smad-dependent signalling cascade involving nuclear translocation and phosphorylation of a family of transcriptional factors (Smads) with subsequent expression of targets, such as MMPs. Ligand-activated TGFβ receptors can also stimulate signalling via non-canonical pathways, including the mitogen-activated protein kinase (MAPK) cascade

which cross-talks with the angiotensin converting enzyme (ACE) cascade, as seen in Figure 1.6 (Lindsay and Dietz, 2011).

Increased TGFβ signalling is seen in the dilated aorta of BAV, MFS, and LDS patients with the latter testing positive for mutations in the TGFβ receptor type I (*TGFBR1*) and type II (*TGFBR2*) genes (Gomez et al., 2009, Loeys et al., 2006). However, similar with *FBN1*, despite the common histopathological lesions seen in the BAV and LDS aorta, patients with BAV do not carry mutations in *TGFBR1* or *TGFBR2* gene (Arrington et al., 2008).

Other potential genes include type III procollagen (*COL3A1*) and *PLOD1/3* involved in collagen metabolism and associated with aneurysm formation in Ehlers-Danlos syndrome (Beridze and Frishman, 2012, Takaluoma et al., 2007, Salo et al., 2008) as well as the *SLC2A10* gene associated with aortic tortuosity syndrome (Figure 1.6) (Coucke et al., 2006). *PLOD1/3* genes encode for lysyl hydroxylase 1 and 3, respectively, which are oxygenase enzymes involved in the post-translational modification of pro-collagen in the endoplasmic reticulum necessary to the formation and stabilisation of collagen (Figure 1.6). *SLC2A10* gene (also known as *GLUT10*) encodes the integral membrane protein glucose transporter type 10 and is highly expressed in the mitochondria of VSMCs protecting cells from oxidative injury (Lee et al., 2010). The genetic cause of syndromic and non-syndromic forms of TAA is summarized in Table 1.1 and further discussed in **Chapter 7** as genetic insights from inherited forms of aortopathy guided our gene selection process for next-generation sequencing in BAV.

TAA formation in BAV may also be owing to aberrations in genes involved in the development of the great vessels and the aortic valve during embryogenesis, such as *NOTCH1* and endoglin (*ENG*) (Niessen and Karsan, 2008, Qu et al., 1998). In fact, *NOTCH1* mutations have been linked to the sporadic BAV-TAA phenotype (McKellar et al., 2007), and *ENG*, a type I membrane glycoprotein interacting with TGFβ receptor and BMP singalling cascade (Figure 6.1), may also contribute to TAA formation (Li et al., 1999, Wooten et al., 2010).

However, familial studies have exhibited that *NOTCH1* mutations are exceedingly rare and, although they may represent susceptibility alleles for the BAV-TAA phenotype, additional genetic aberrations most likely contribute to its phenotypic expression (Kent et al., 2013, McBride et al., 2005). Human tissue studies have also reported reduced eNOs expression in the ascending aorta of BAV patients compared to patients with a tri-leaflet aortic valve (Aicher et al., 2007). Despite the strong association between eNOs deficiency and BAV formation in mice (Lee et al., 2000), BAV patients have not been tested for mutations in this gene.

Figure 1.6 provides an overview of selected molecular pathways involved in TAA formation, including canonical and non-canonical TGFβ signalling and its crosstalk with the ACE pathway, *FN1* gene signalling cascade determining the VSMC synthetic phenotype with downstream transcription of contractile protein genes (*MYH11* and *ACTA2*), as well as *PLOD1/3* and *SLC2A10* genes. Genes highlighted in blue underwent targeted next-generation sequencing and are further discussed in **Chapter 7**. Involvement

of angiotensin converting enzyme (*ACE*) gene in TAA formation is discussed under "future directions" section of this chapter.

Table 1.1 Summary of inherited forms of thoracic aortic aneurysm (TAA), modified from Canadas et al.(Canadas et al., 2010).

Disease	Phenotype	Known mutated genes	Inheritance	Pathophysiology
Syndromic				
Marfan syndrome(Canadas et al., 2010)	Aortic root aneurysm , ectopia lentis, skeletal abnormalities, dural ectasia, lung disease	*FBN1*	AD	Fibrillin-1 deficiency and increased TGFβ signalling
Marfan-like syndrome(Loeys et al., 2006)	Overlap with Loeys-Dietz syndrome	*TGFBR2*	AD	Increased TGFβ signalling
Loeys-Dietz syndrome(Loeys et al., 2006)	Aneurysm of aortic root and other vessels, aortic tortuosity, hypertelorism, cleft palate or abnormal uvula, craniofacial, skeletal and cutaneous abnormalities, PDA, ASD	*TGFBR1, TGFBR2*	AD	Increased TGFβ signalling
Ehlers-Danlos syndrome(Beridze and Frishman, 2012)	Spontaneous arterial, intestinal or uterine rupture, characteristic facial appearance, translucent skin with easy bruising, hypermobile joints	*COL3A1*	AD	Abnormal type III collagen production
Arterial tortuosity syndrome(Coucke et al., 2006)	Tortuosity, stenosis, and dilatation of major arteries, joint hypermobility, elongated face, hernias	*SLC2A10*	AD	Deficiency of glucose transporter (GLUT10) and increased TGFβ signalling
Turner syndrome(Lin et al., 1998)	TAA, short stature, webbed neck, widely spaced nipples, gonadal dysfunction, BAV, aortic coarctation	45, X0	-	Cystic medial necrosis
Non-syndromic				
TAAD-PDA(Zhu et al., 2006, Pannu et al., 2007) **TAAD2**(Pannu et al., 2005) **TAAD4**(Guo et al., 2007)	Familial TAA* & PDA, BAV Cerebral, carotid and popliteal aneurysms Levido reticularis, iris floculi, PDA, BAV	*MYH11* *TGFBR2* *ACTA2*	AD	Abnormal smooth muscle βMHC production with upregulated IGF-1 and Ang II signalling Increased TGFβ signalling Abnormal α-smooth muscle actin production
Bicuspid aortic valve(Tadros et al., 2009, Garg et al., 2005)	TAA, valvular dysfunction	*NOTCH1*	AD	Fibrillin-1 deficiency, increased TGFβ signalling, haemodynamic perturbations secondary to the malformed valve

*Selected familial TAA syndromes with known mutated genes. Abbreviations: AD, autosomal dominant; Ang, angiotensin; ASD, atrial septal defect; BAV, bicuspid aortic valve; IGF, insulin growth factor; PDA, patent ductus arteriosus; TAAD, thoracic aortic aneurysm and dissection; TGF, transforming growth factor.

Figure 1.6 Molecular pathways involved in inherited forms of aortopathy.

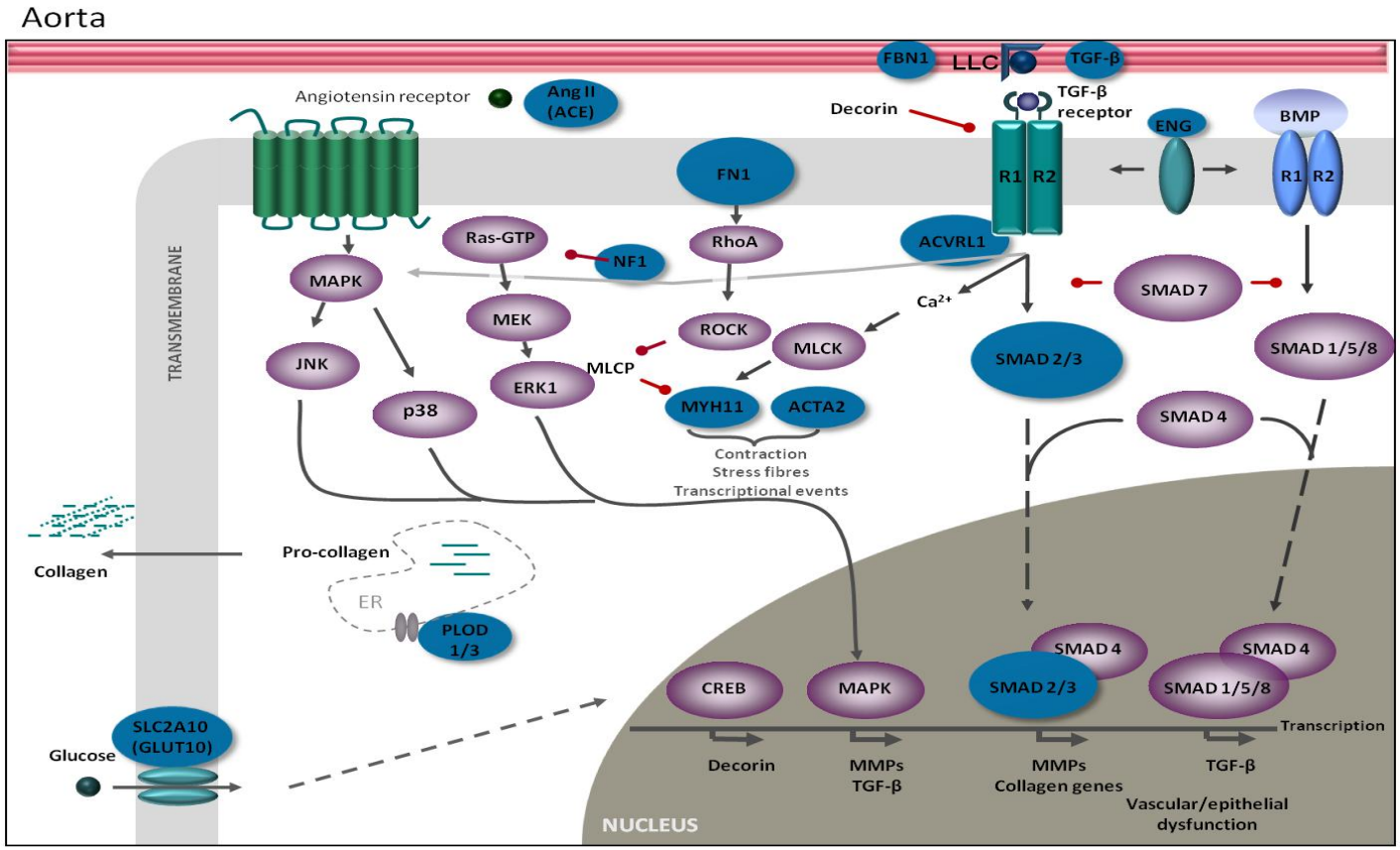

Key: ACTA2, smooth muscle alpha actin 2; ACVRL1, activin receptor-like kinase-1; AngII, angiotensin II; BMP, bone morphogenic protein; CREB, cAMP response element-binding protein; ENG, endoglin; ER, endoplasmic reticulum ; FBN1, fibrillin-1; FN1, fibronectin-1; JNK, c-Jun N-terminal kinase; LLC, large latent complex; MAPK, mitogen-activated protein kinase (aka ERK); MLCK, myosin light chain kinase; MLCP, myosin light chain phosphatase; MMPs, matrix metalloproteinases; NF1, neurofibromin-1; PLOD, 2-oxoglutarate 5-dioxygenase; RhoA, Ras homolog gene family member A; ROCK, Rho-associated protein kinase; SLC2A10/GLUT10, solute carrier family 2 member 10; TGF-B, transforming growth factor beta.

1.5 Future directions in management of BAV aortopathy

The therapeutic mainstay of TAA continues to be early diagnosis via imaging of the thoracic aorta with timely surgical intervention (Hiratzka et al., 2010). Although radiographic screening is valuable, many patients who have an increased risk of developing aneurysms in later life may not have recognisable enlargement of the aorta at the time of screening even with state-of-the-art imaging technologies (Prapa and Ho, 2012). Timely correction of TAA in BAV is fundamental and should rely on in depth understanding of the pathogenetic mechanisms implicated in the degradation of the aortic wall.

Appreciation of the genetic component of BAV aortopathy has been recently reflected by the American College of Cardiology guidelines on thoracic aortic disease management, with lowering of the traditional threshold of 50mm for elective replacement of the aorta to 40mm, similar to the cut-off suggested for other connective tissue disorders (Hiratzka et al., 2010). However, as our understanding of BAV- TAA pathophysiology increases, novel promising therapeutic strategies and risk stratification tools should be gradually translated into clinical practice.

1.5.1 Pharmacological treatment

Insights into MFS pathophysiology, which has served as the typical aortopathy model in inherited TAA disease, have led to emergence of novel pharmacological treatments. Beta blockers (b-blockers), a class of drugs interfering with the action of endogenous catecholamines epinephrine (adrenaline) and norepinephrine (noradrenaline) on the sympathetic nervous system via blockage of b-adrenergic receptors, are used extensively in daily clinical practice for treatment of hypertension, arrhythmias, coronary artery disease and heart failure. Prophylactic b-blockade has been shown to be beneficial in a subset of MFS patients with reduction in rates of

aortic root dilatation and improved survival (Shores et al., 1994, Rossi-Foulkes et al., 1999). Its therapeutic benefit may be secondary to negative chronotropy and inotropy (reduction of force and rate of contraction in the heart) resulting in decreased arterial stress (Milewicz et al., 2005). Prophylactic administration of b-blockers in BAV disease is currently based on consensus opinion and recommended in patients with aortic dilatation (>40mm) without significant aortic regurgitation (Bonow et al., 2006).

Another antihypertensive drug, the angiotensin II type 1 receptor (AT1) blocker, losartan has been shown to improve the aortic phenotype in fibrillin-1 deficient mice (Habashi et al., 2006). Angiotensin I-converting enzyme (ACE) is a key component of the renin-angiotensin system (RAS) hydrolysing angiotensin I into angiotensin II, a potent vasopressor that stimulates aldosterone with salt and water reabsorption (Heeneman et al., 2007). Administration of AT1 blocker, losartan, has been shown to attenuate the aortic phenotype in both animal models and children with MFS (Habashi et al., 2006, Brooke et al., 2008). Following establishment of aortic root aneurysm at 7 weeks of age, 6-month treatment with losartan prevented elastic fragmentation and reduced TGFβ signalling in the aortic media, compared to a b-blocker (propranol) whose beneficial effect was restricted to reduction of aortic root growth rate (Habashi et al., 2006).

The cross-talk between TGFβ and angiotensin II pathways remains poorly understood although it has been reported that angiotensin II has the capacity to induce TGFβ1 activity via the AT1 receptor and can also activate the SMAD signalling cascade in a TGFβ-independent manner via the MAPK cascade (Figure 1.6) (Cohn et al., 2007, Zhou et al., 2006, Rodriguez-Vita et al., 2005). The beneficial effect of angiotensin II blockade has been recently exhibited in a pilot study in children with MFS (Brooke et al., 2008) and is further validated by ongoing clinical

trials (Lacro et al., 2007). Findings from these studies may also be applicable to BAV patients in the future and would necessitate similar clinical trials in BAV patient cohorts.

Doxycycline, a derivative of tetracycline, acts as a non-specific MMP inhibitor, independent of its antimicrobial properties inhibiting bacterial protein synthesis, and has been shown to attenuate elastic fragmentation in MFS mouse models (Chung et al., 2008) which may be applicable in the treatment of BAV patients with TAA.

1.5.2 Emerging risk stratification tools in BAV-TAA

1.5.2.1 Novel imaging

According to La Place's law, wall tension increases with aortic radius (Humphrey, 2008). However, variables other than aortic diameter, such as aortic elasticity, may allow earlier evaluation of abnormal loads in the aortic wall (Baumgartner et al., 2005, Nistri et al., 2008). Nistri et al have exhibited abnormal aortic stiffness in BAV patients with absent or mild valvular disease and non-aneurysmal aortic dilatation (Nistri et al., 2008). Direct indicators of elevated mechanical stress include peak wall stress (PWS) and WSS which can now be measured with use of computational modelling methods (Giannakoulas et al., 2009, El-Hamamsy and Yacoub, 2009a). Both PWS and WSS are known to be reliable markers of the risk of abdominal aortic rupture (Venkatasubramaniam et al., 2004, Fillinger et al., 2003) and may also affect TAA formation by complex mechanotransduction pathways (Humphrey, 2008, El-Hamamsy and Yacoub, 2009a). Moreover, local haemodynamic perturbations secondary to different morphological BAV subtypes can now be visualised *in vivo* by advanced MRI techniques (Hope et al., 2010). As quantification of this imaging data becomes increasingly available (Gatehouse et al., 2005, Hope et al., 2011), WSS measurements via phase contrast MRI may serve as an additional risk stratification tool in BAV disease (Barker et al., 2010).

Apart from advanced MRI and computational imaging, molecular imaging of aortic aneurysms may also hold a promising future (Buxton, 2012). *In vivo* molecular imaging has been shown to be feasible in examination of aortic valve pathophysiology in hypercholesterolaemic apolipoprotein-E deficient mice (Aikawa et al., 2007). Via usage of a panel of near-infrared fluorescence imaging agents, key cellular events in early aortic valve disease were captured, including endothelial cell and macrophage activation, proteolytic activity, and osteogenesis. Similar techniques may be applicable in the future in human aortas, allowing the detection of spatiotemporal patters of MMP activity and thus, earlier identification of BAV patients predisposed to TAA formation.

1.5.2.2 Genetic screening

Targeted sequencing for a panel of inherited aortopathy genes is now suggested for patients with TAA with a positive family history and/or associated syndromic clinical features (Hiratzka et al., 2010). Moreover, screening of first-degree relatives of BAV patients is recommended for the presence of BAV and asymptomatic TAA (Hiratzka et al., 2010). However, genetic screening tools specific to BAV disease are currently lacking. This may be owing to the wide phenotypic diversity of BAV, which may not only present in association with TAA but can also be part of a broader spectrum of abnormalities such as hypolastic left heart syndrome (Laforest and Nemer, 2012, Hinton, 2012). Recent advances in genetics, such as next-generation sequencing, are vastly changing the landscape of clinical genomics and may serve as novel research tools for identification of specific susceptibility genes for BAV aortopathy (Ware et al., 2012).

Over the past decades, Sanger sequencing has served as the gold standard technology for DNA sequencing using fluorescently labelled terminating nucleotides and electrophoresis. Despite its advantages, sequencing of the whole human genome as part of the human genome project with

Sanger sequencing took over 10 years to complete with a cost of US$2.7 billion (Berglund et al., 2011). Next-generation sequencing technologies developed in the past decade allow massively parallel DNA sequencing with a considerably lower cost per sequenced base (Ware et al., 2012). These technologies serve not only as research tools but also as diagnostic screening tools for cardiovascular conditions, such as inherited cardiomyopathies and arrhythmia syndromes (Meder et al., 2011, Herman et al., 2012, Ware et al., 2013). Application of next-generation sequencing in BAV could allow low-cost genetic screening of these patients, provided that suitable genes predisposing to disease traits are identified.

1.4 Study aims

In summary, despite the exponential research in the field of BAV aortopathy, novel risk stratification tools for predicting natural history of TAA and guiding the timing of prophylactic surgical intervention on the BAV aorta are lacking. The proposed study will use established computational, histopathological and genetic methods to explore the following hypotheses:

1. Asymmetric formation of TAA in BAV disease is related to heterogeneous wall stress distribution and varying degrees of histopathological abnormalities at different levels of the aorta.

2. Genetic aberrations underlie the formation of BAV and associated aortopathy.

The aims of the present study are:

1. To investigate the role of structural finite-element analysis in BAV aortopathy and assess the distribution of mechanical stress and severity of corresponding structural abnormalities in the BAV aorta.

2. To assess the degree of histological abnormalities and TGFβ signalling in distinct clinical phenotypes of BAV-TAA.

3. To assess the presence of copy-number variation in BAV disease.

4. To develop a panel of genes for targeted next-generation sequencing in BAV disease.

Chapter 2. General methods

Abbreviations

3D Three-dimensional
BAV Bicuspid aortic valve
BAC Bacterial artificial chromosome
BSA Body surface area
BRU Biomedical research unit
CHD Congenital heart disease
cDNA Complementary DNA
CGH Comparative genomic hybridization
CNV Copy number variation
CMR Cardiac magnetic resonance
CT Computed tomography
EVG Elastic Van Gieson
FEA Finite element analysis
DAB chromogen 3,3'-diaminobenzidine
IMS Industrial Methylated Spirits
KPa Kilopascals
MRI Magnetic resonance imaging
NGS Next generation sequencing
PBS Phosphate buffered saline
PCR polymerase chain reaction
PDA Patent arterial duct
VSMC Vascular smooth muscle cell

2.1 Patient Population

Ethical approval was granted by the Royal Brompton Hospital Research Ethics Committee (09/H0708/36) for the whole of this study. All participants were provided with information sheets and appropriate written informed consent was obtained.

2.1.1 Inclusion criteria

Patients with BAV scheduled to undergo aortic valve replacement and/or ascending aortic surgery were included in the study (**Chapters 3 and 4**). Both adult and paediatric BAV cases were included, with appropriate age matching of control samples (**Chapter 4**). Patients with previous known BAV requiring a second operation due to postoperative complications were also recruited. For the control group (**Chapter 4**), age-matched structurally normal hearts were retrieved from patients who had not died from cardiovascular disease, held at the Cardiac Morphology Unit and the Department of Histopathology, Royal Brompton Hospital. The latter heart biobank was also used in **Chapter 5** to study cases with congenital heart disease and pulmonary arterial hypertension (detailed methods provided in respective chapter due to distinct study population). In **Chapter 6**, copy number variation data from the Wellcome Trust Control Consortium 2 were used as a control group (Bochukova et al., 2010).

For the genetic studies (**Chapters 6 and 7**), BAV patients undergoing surgery (previous group) were recruited in addition to BAV patients attending the Adult Congenital Heart Disease Unit outpatients' clinic, Royal Brompton Hospital.

2.1.2 Exclusion Criteria

The following patients were excluded from this study:

1. Patients with clinical features of developmental syndromes, multiple major developmental abnormalities or major cytogenetic abnormalities.
2. Patients fulfilling standard diagnostic criteria for Turner syndrome or connective tissue disorders, such as Marfan and Ehlers-Danlos syndromes (Hiratzka et al., 2010).
3. Patients with inflammatory aortic disease.
4. Patients with BAV and associated congenital cardiac defects, other than ventricular septal defect, coarctation of the aorta and PDA.
5. Patients unwilling or unable to provide written informed consent.

2.1.3 Phenotyping

For patients undergoing surgery, the morphology of the BAV valve (true or functional and further sub-types) was assessed at the time of the operation. In the instance of previous aortic valve replacement, medical notes and pre-operative imaging (echocardiography or MRI) was assessed to delineate the valve morphology.

Cardiac magnetic resonance (CMR) imaging (Siemens 1.5T) was used for examination of BAV morphological subtypes, presence of valvular disease, and aortic diameter measurements in the overall study population. An electronic calculator using aortic diameter and body surface area (BSA) was employed for calculation of z-scores (z-value = (measured diameter – predicted diameter)/standard deviation of residuals) at selected CMR-standardized aortic sites (aortic sinus, sinutubular junction, ascending aorta at level of right pulmonary artery, and ascending aorta proximal to the innominate artery) (Kaiser et al., 2008). A clinical cut-off of z-score > 2 standard deviations was used to define the presence of dilatation at specified aortic segments (Kim et al., 2011).

For patients participating in the computational modelling study (**Chapter 3**), computed tomography (CT) angiograms were used for aortic diameter measurements and three-dimensional (3D) reconstruction of their aortas (methods described below).

Additional individual review of patient echocardiograms (Hewlett Packard Sonos 5500) was performed in cases where assessment of BAV morphology from CMR images was indeterminate.

All scans (MRI, CT and echocardiograms) used for assessment of valvular disease and aortic diameter measurements were clinically indicated and obtained up to 6 months prior to surgical procedure, as part of the diagnostic work-up of BAV patients undergoing surgery.

2.1.4 BAV patient cohort characteristics

Overall, a total number of 110 BAV patients were recruited for various aspects of this study with an overall mean age of 24,47 years (standard deviation 14,56 years). A selection bias may have been inevitably introduced in the study as a significant proportion of patients (37%, table 2.1) attended for cardiovascular surgery at the time of recruitment and therefore, may represent the more severe spectrum of BAV disease. Equally, 32% of the BAV patient population had initially presented at a younger age (<16 years of age, table 2.1) and may potentially harbour a greater number of genetic risk factors predisposing to BAV-associated complications compared to the remaining study population. However, it was important to include the above sub-cohorts in our study, both for collection of surgical tissue samples (**Chapters 3 and 4**) as well as investigation of genetic aberrations in BAV disease (**Chapters 6 and 7**).

The majority of recruited patients were morphologically phenotyped via MRI for both aortic valve morphology and aortopathy (Table 2.1). The remaining patients were assessed with echocardiography, a method also considered to be reliable in the assessment of aortic valve

morphology, except in the presence of heavy valve calcification where operative notes were used (Chan et al., 1999). In 19% of cases, BAV morphology was not available due to valve replacement or valvotomy taking place in early childhood with unavailable imaging and/or operative notes. Despite the above limitations, uniform methods of aortopathy assessment were used in chapters were correlations between diameter measurements and other features were attempted, applying CT in **Chapter 3**, and MRI in **Chapter 4**.

Details of previous operations, cardiovascular risk factors, and BAV-associated CHD lesions in recruited patients are given in the respective chapters.

Table 2.1 Bicuspid aortic valve (BAV) patient cohort characteristics

BAV patient cohort characteristics (n, %)	**Number of recruited patients (total n= 110)**
Presentation at early age (<16y)	36 (32)
At time of recruitment, attending for:	
Surgery	41 (37)
Regular follow-up	69 (63)
BAV morphology phenotyping:	
Magnetic resonance imaging	79 (72)
Echocardiography	2 (2)
Operative notes (heavily calcified valve)	8 (7)
Unavailable	21 (19)
Aortic measurements:	
Magnetic resonance imaging	92 (83)
Computed tomography	14 (13)
Echocardiography	4 (4)
Previous surgery	93 (84)
Multiple reoperations	36 (32)

2.2 Computational modelling

Methods described below have been previously validated by our group (Prof. XY Xu, Department of Chemical Engineering) for three-dimensional reconstructions of thoracic aortic aneursyms (Borghi et al., 2006) and subsequent simulation analyses (Cheng et al., 2010) as well as by other researchers applying similar computational software to study distribution of mechanical stress in thoracic and abdominal aneurysms (Nathan et al., 2011b, Giannoglou et al., 2006).

2.2.1 Data acquisition

All patients underwent CT (Siemens 64) imaging pre-operatively, as part of their routine care. Contrast enhanced aortic angiograms obtained from these studies were processed via a MATLAB software (Materialise® Mimics® version 14) to build patient-specific 3D models of the aortic root and ascending aorta (Cheng et al., 2010).

2.2.2 Segmentation

A segmentation technique, based on thresholding and region-growing methods, was employed to extract, slice by slice, the contour of the aortic wall. First, a threshold was set for the image intensity that represents the entire thoracic aorta. The software created a mask consisting of all pixels that fall within the defined range and this was in turn used to build a 3D image. The derived images were then cropped to decrease the number of pixels picked up from the surrounding chest cavity (Figure 2.1).

Figure 2.1 Representation of thresholding, viewed as an CT slice (a) and as a 3D image, before (b) and after (c) appropriate cropping.

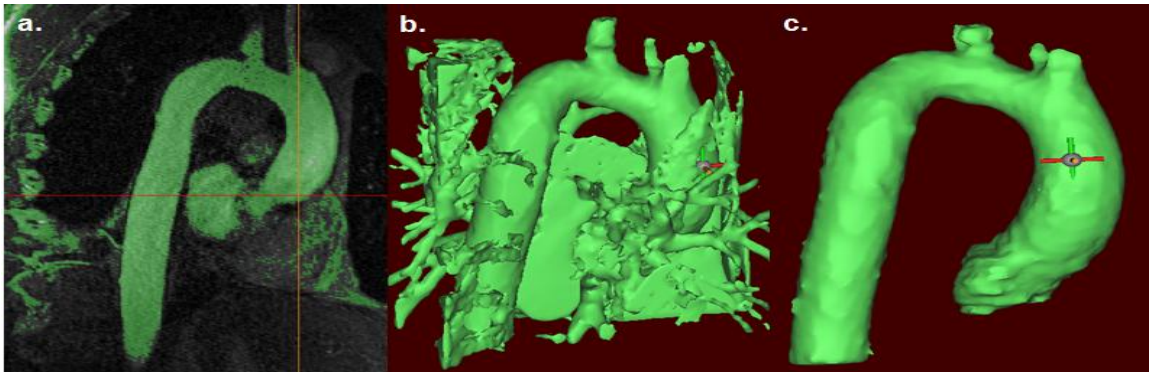

Following creation of a mask representing the thoracic aorta, the geometry was cut down in order to isolate the aortic root and ascending aorta (Figure 2.2a-b). Following this, the vessel was smoothed to avoid any unexpected high circumferential stress regions during haemodynamic simulations from rough surfaces or harsh corners induced by image noise or cardiac motion (Redaelli A, 2002). At this point, it was important to smooth the geometry adequately to remove any misrepresentations of the vessel but at the same time, not so much so that important geometrical features, such as convexity angle or vessel diameter, were altered which would lead to errors in simulation results (Figure 2.2c).

Lastly, as the mask was created based on contrast data outlining the inner lumen of the aorta, the outer wall of the vessel had to be created. To that end, the finalized 3D mask was dilated (Figure 2.2d) applying a uniform wall thickness of 1.5mm. In a similar study, Nathan and colleagues applied a uniform thickness of 2mm based on echocardiographic data (Nathan et al., 2011b). However, *in vivo* testing of dilated BAV aortic tissue rings reveal a thinner aortic wall compared to normal and TAV subjects, with wall thickness varying between 1.3 to 2.1 mm (Choudhury et al., 2009).

Figure 2.2 Three-dimensional (3D) aortic models. The complete aortic root and ascending aorta, viewed as a CT slice (a) and a 3D image, pre (b) and post (c) smoothing. The created outer wall of the aorta is also viewed (d) as a 3D image.

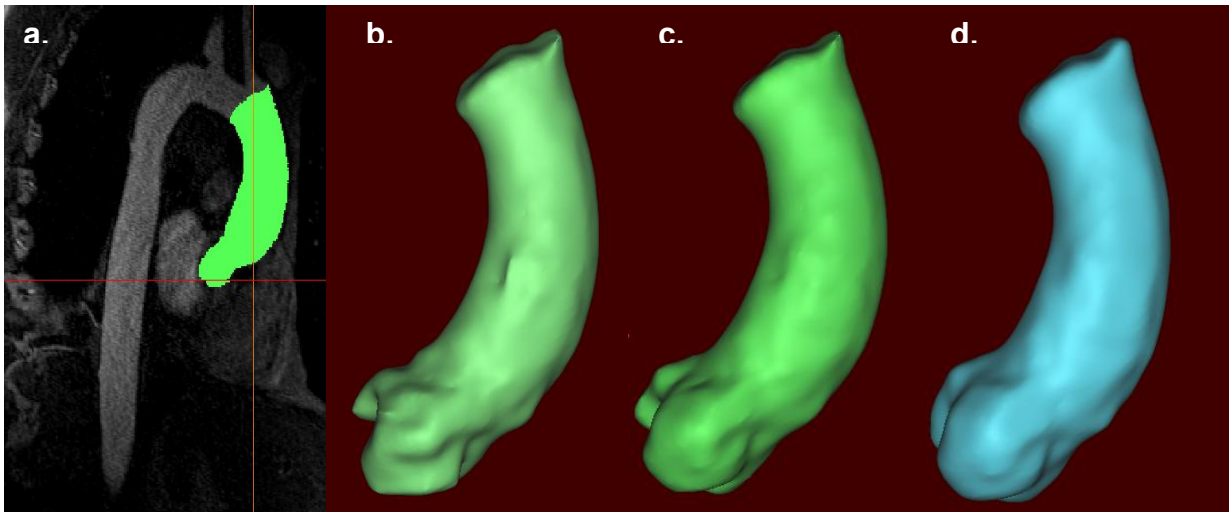

2.2.3 Discretisation

The 3D aortic model was imported into a mesh generator (ANSYS ICEM CFD© version 12) and broken down into smaller regular elements (termed meshing) in order to obtain a solution from haemodynamic simulation (Figure 2.3).

Figure 2.3 Meshing. The geometry of the aortic root and ascending aorta is viewed, before (a) and after meshing (b). The meshed geometry is chopped at the mid level of the sinuses and before the origin of the brachiocephalic artery, to create the aortic inlet (c) and outlet (d) respectively.

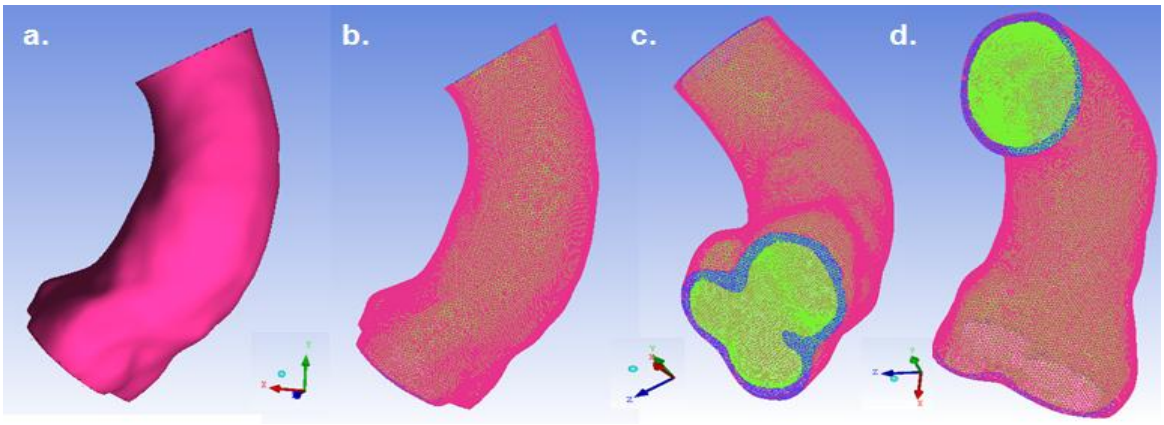

In patients with aneurysms of the distal ascending aorta, the aortic arch was incorporated into the model.

2.2.4 Structural analysis

Structural finite element analysis (FEA) was then performed; pre-defined loads were applied to the 3D aortic model and the distribution of mechanical stress, exerted perpendicularly to the aortic wall, was calculated in response to the applied pressure (Figure 2.4). The arterial wall was assumed to be a linearly-elastic material with its density, elastic modulus and Poisson's ratio at 1000kg/m³, 3MPa and 0.45, respectively. Both proximal and distal ends of the aortic model were fixed to mimic the anatomical tethering between the aortic root and arch arteries. Subsequently, a uniform loading pressure of 40mmHg (pulse pressure resulting from a 120/80mmHg blood pressure) was applied to the model. The distribution of mechanical stress was measured in kilopascals (KPa), using Von Mises stress which represents the total compression/tension field created by elastic deformation of the studied material.

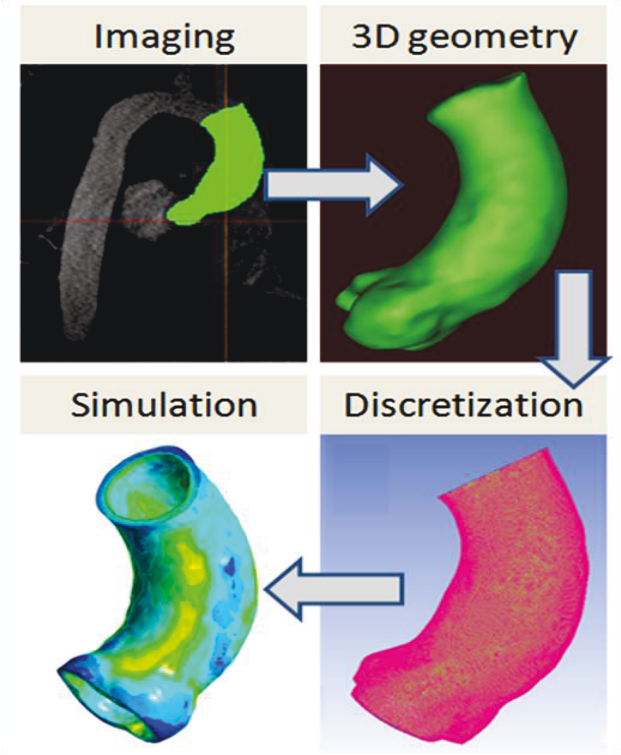

Figure 2.4 Summary of structural finite element analysis. Patient-specific three-dimensional (3D) models of the aortic root and ascending aorta were built using computed tomography (CT) contrast-enhanced angiograms. The lumen borders were smoothed, a uniform wall thickness of 1.5mm was applied, and the model was segmented into smaller elements (nodes). A uniform loading pressure of 40mmHg was applied to the created "mesh" of the aorta and a colour-coded map of the distribution of circumferential stress, exerted perpendicularly to the aortic wall, was calculated in response to the applied pressure.

2.3 Aortic tissue sampling

Intra-operatively, tissue samples were collected from distinct regions of the aortic wall and labelled according to their area of origin. Efforts were made to consistently collect tissue from the aortic root (level of sinuses of Valsalva) and the ascending aorta (1cm distal to the level of sinutubular junction), depending on the type of surgical procedure. In patients undergoing aortic valve replacement, the explanted aortic valve leaflets were also harvested. Figure 2.5 provides vivid examples of how the collected samples were marked before being further processed. Collected specimens were fixed in 10% buffered formalin saline and stored at room temperature for subsequent histological and immunohistochemical analyses.

Figure 2.5 Examples of aortic tissue labelling.

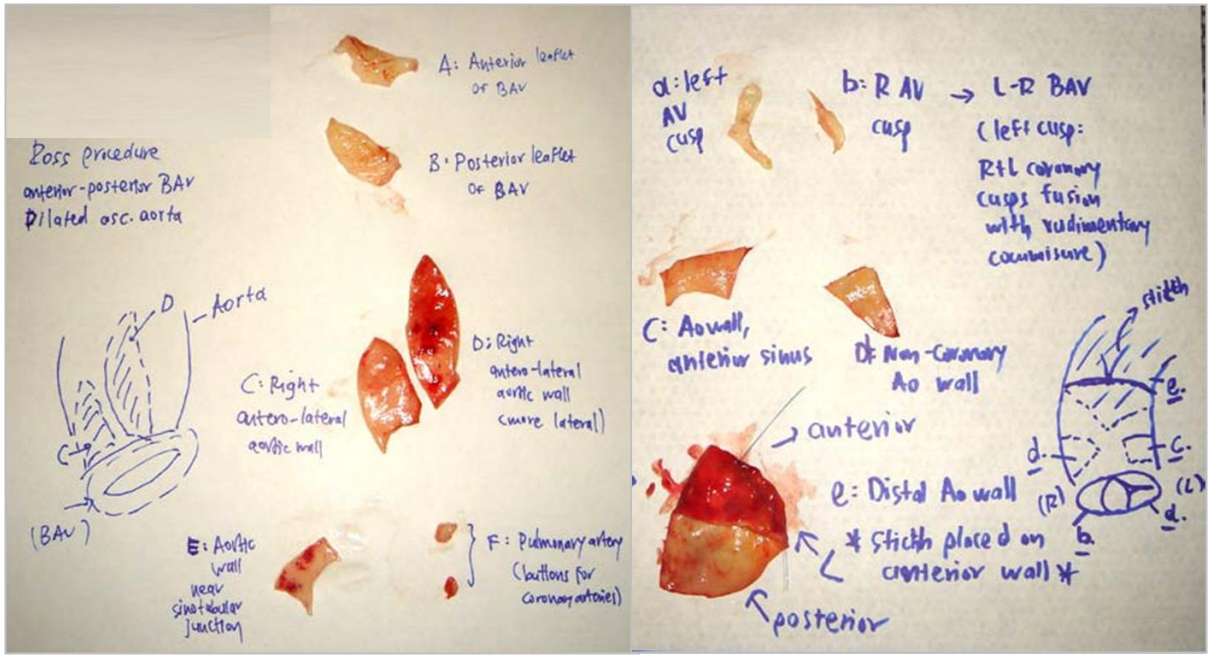

2.4 Histology and immunohistochemistry

2.4.1 Processing of aortic sections

From fixation in 10% formalin, tissue sections were routinely processed through increasing grades of alcohol (70%-100% Industrial Methylated Spirits, IMS) before xylene clearing, immersion in paraffin wax for a minimum of 2 hours, and embedment in fresh paraffin wax. Serial sections were cut at 6μm using a rotary microtome (RMC Rotary Microtome MT 960) and Accu-Edge® low profile disposable blades for histological and immunohistochemical examination. For histological assessment, the sections were floated out onto a waterbath at 55°C and mounted onto glycerin albumin coated twin frost glass slides. These were then placed for 3 hours in a section drier before use. Sections at 6μm for immunohistochemical staining were also floated out into a 55°C waterbath but mounted onto silane coated twin frost glass slides.

2.4.2 Histological examination

Sister sections of the aorta from each paraffin block were stained with elastic van Gieson (EVG), alcian blue, and haematoxylin/eosin stains and examined under light microscopy for medial wall abnormalities. EVG was used for examining elastic fibers (fibrosis and elastic fragmentation), alcian blue for basophilic ground substance (cyst-like formations), and haematoxylin/eosin for cell nuclei (medionecrosis). Structural defects of the media were categorized in 4 distinct grades (0-3) according to the criteria proposed by Schlatmann and Becker (Schlatmann and Becker, 1977) adapted from our group (Tan et al., 2005): grade 0 denoted absence of lesions and grades 1-3 were used according to severity of processes (Figure 2.6). All sections were examined separately by two observers, with repeat evaluation by a blinded third observer in cases of discrepancy. A cumulative histology grading score was calculated to assess the severity of medial wall degeneration; points were assigned for each

histological feature based on the grade of severity (grade 0 = 0 points, grade 1 = 1 point, grade 2 = 2 points, grade 3 = 3 points).

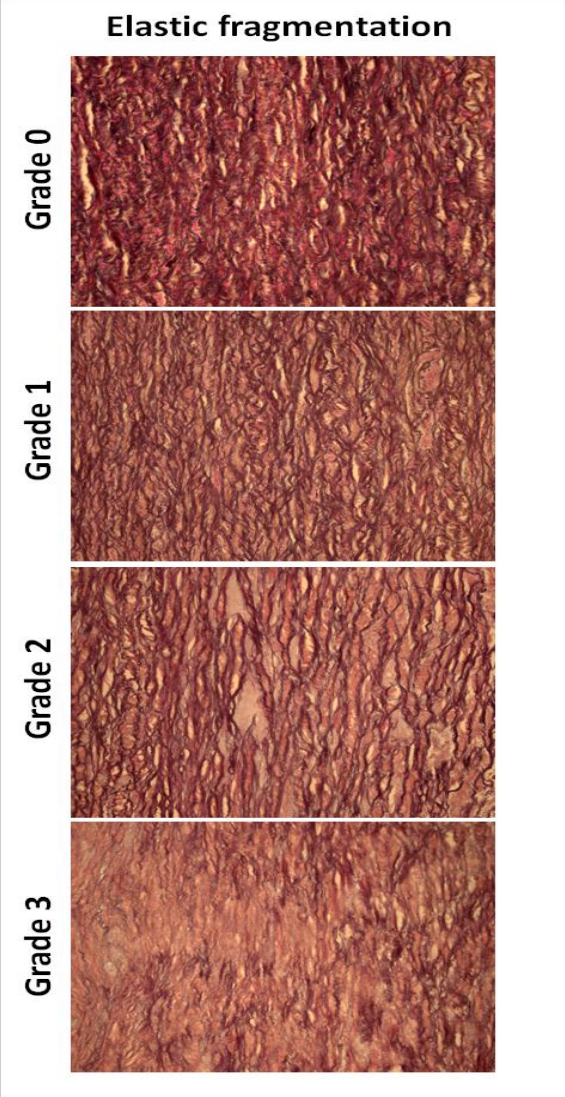

Figure 2.6 Histological grades of medial elastic fragmentation. The range of elastic fragmentation can be visualized in a series of ascending aortic tissue biopsies (elastic van Gieson stain, magnification x200). Grade 0 is seen in a healthy control with parallel distribution of intact elastic lamellae (*purple*); grades 1 and 2 denote mild and moderate elastic fragmentation with accumulation of ground substance (*pink*); grade 3 shows severe elastic fragmentation with complete loss of elastic lamellae involving large areas of the media.

2.4.3 Immunohistochemical protocol

Sections adjacent to the histology stained slides were deparaffinized and then rehydrated in descending grades of alcohol.

1. The endogenous peroxide enzyme activity in the tissue was blocked with a 30% hydrogen peroxide solution in methanol (1:10) for 10 minutes at room temperature. This was washed off

the sections with phosphate buffered saline (PBS) solution at pH 7.2. The tissues were incubated with normal goat serum (*Vector, Peterborough*) for 10 minutes at room temperature to block non-specific binding of the negatively charged primary antibody to non-antigenic positive sites in the tissue.

2. The sections were washed with PBS buffer and specific antigen retrieval methods were optimised for anti-pSmad2 (*Merck Biosciences*) with application of 0.4% pepsin for 20 minutes to induce unmasking of the antigenic sites.

3. Immunohistochemical staining was performed using commercially available pSmad2 (*Merck Biosciences*) diluted with PBS (pH 7.2) at the determined optimal working dilution of 1:15 with subsequent incubation (37˚C) of tissues for 2 hours.

4. Following washing steps using PBS (pH7.2) between each stage, the biotinylated secondary antibody (rabbit IgG; *Vector*) was applied at 37˚C for 15 minutes. An avidin-biotin peroxidase complex was then added for 15 minutes at 37˚C using VectorStain *Elite*® ABC (*Vector*).

5. The reaction was visualised by the addition of a chromogen 3,3'-diaminobenzidine (DAB) with 30% H_2O_2 for 1-5 minutes and the remaining tissues lightly counterstained with Harris Haematoxylin solution for 1.5 minutes before the slides were placed in xylene solution for 15 minutes. The tissue sections were then cover-slipped using DPX histology mountant.

Of note, the primary antibody was replaced with rabbit non-immune IgG solution at same concentration of the pSmad2 antibody to ensure the specificity of its interaction in tissues.

2.4.4 Immunohistochemical grading

All pSmad2 immunolabelled sections were examined by light microscopy and compared with EVG stained sections to determine the discrete zones of the aortic wall. Comparable views were observed in antibody labelled slides of the controls.

A section through the aortic wall from adventitia to intima was viewed at 20x magnification. Using an image analysis system (Quantimet 500C QWIN V02.00B; *Leica, Cambridge*), the extent of immunoreaction for the intima, media and adventitia was determined by viewing the tissue section and all calls were counted in a measured frame area. Sections were assessed for specifically localized staining in the nucleus of VSMCs: positive cells had brown DAB nuclei and negative cells had blue Harris Haematoxylin stained nuclei. Data are expressed as the percentage of positive pSmad2 nuclei in each aortic wall layer. All slides were reviewed jointly by two observers.

A detailed list of used chemicals and materials (source in brackets) is included below:

- 3-aminopropyltriethoxy-silane (Sigma-Aldrich)
- 3,3'-diaminobenzidine chromogen (Sigma-Aldrich)
- Accu-Edge® low profile disposable blades (RA Lamb)
- Elite Immunohistochemistry Kit (Vector laboratories)
- Eppendorf Pipette tips. Volumes 0.1 – 5000µl (VWR)
- Ethanol (VWR)
- Glycerin albumin (RA Lamb, East Sussex)
- Harris Haematoxylin solution (VWR)
- Hydrogen peroxide [H2O2] (VWR)

- Industrial methylated spirits (VWR)

- Mouse and goat serum (Vector laboratories)

- Paraffin section waterbath (RA Lamb)

- Paraffin wax (VWR)

- Pepsin (Sigma-Aldrich, Dorset)

- Pipettes – Eppendorf Research. Volume 0.1 – 5000µl (VWR)

- Phosphate buffered saline tablets (Sigma-Aldrich)

- pSmad2 Rabbit IgG antibody (Merck)

- Section Drier (RA Lamb)

- Super Premium twin frost microscope slides 75 x 25 x 1.0mm (VWR)

- Tris (hydroxyl) methylamine (Sigma-Aldrich)

- Winsor Incubator (RA Lamb)

- Xylene (mixed isomers) (Genta Medical, York)

- All histological stains sourced from RA Lamb, East Sussex UK and VWR, Leicester, UK

Haematoxylin & Eosin: containing Harris haematoxylin.

PAS -alcian blue: containing Periodic Acid, Schiff Reagent and Alcian blue.

Elastic Van Geison: containing Millers Elastic Haematoxylin and Van Geison.

2.5 Purification and quantification of DNA

From each patient, 20 ml of venous blood were collected in EDTA tubes and stored at -80˚ C for future DNA extraction. In patients refusing blood sampling, Oragene DNA Self-Collection kits were used for storage of 2 ml of saliva in room temperature.

An automated DNA purification system (BioRobot EZ1) available at the Cardiovascular Biomedical Research Unit (BRU), Royal Brompton Hospital, was used for DNA extraction. The EZ1 utilizes silica-magnetic-particle technology for high-throughput DNA extraction. The EZ1 DNA Blood kit (Qiagen) was used for DNA purification (elution volume of 200 µL) from 350 µL of whole blood, as per the manufacturer's standardized protocol. A spectrophotometer (NanoDrop™) was used for calculation of concentration (µg/ml) of the extracted DNA by measuring the absorbance at 260 nm (A260). Tubes containing DNA were applied to a magnetic separator (Qiagen 12-Tube Magnet) for 1 minute and 10 µl of isolated DNA were used for quantification, following calibration of the spectrophotometer with distilled water. The purity of extracted DNA was determined by calculating the ratio of corrected absorbance at 260 nm to corrected absorbance at 280 nm, i.e., (A260 – A320)/(A280 – A320) with an acceptable A260/A280 ratio of 1.7–1.9 (Wilfinger et al., 1997).

The EZ1 DNA Tissue kit (Qiagen) was used for DNA purification from the collected saliva samples. Due to lack of a standardized protocol for EZ1 DNA extraction from Oragene saliva kits, the following trials were undertaken (data reported for the same sample):

- 200µL neat sample with no pre-treatment with selected elution volume of 200µL: DNA concentration 24µg/ml, A260/A280 2.6.
- 50µL sample with pre-treatment (140ul buffer G2 and 10ul proteinase K) and selected elution volume of 100µL: DNA concentration 16.5µg/ml, A260/A280 2.6.
- 200µL neat sample with incubation at 50˚C for 2 hours and selected elution volume of 50µL: DNA concentration 68µg/ml, A260/A280 1.9.

In view of the maximal DNA yield obtained with saliva incubation at 50˚C, the last out of the three protocols was applied for DNA extraction from collected saliva samples.

2.6 Statistical analyses

Data analysis was performed using IBM SPSS Statistics 19.0 (**Chapters 3, 4, and 5**). Continuous variables are expressed as median with range and categorical data as number with percentages. Comparisons between groups were performed using the Wilcoxon rank sum test or the Fisher exact test accordingly. A two-tailed p value < 0.05 was considered indicative of statistical significance. Spearman's rank correlation coefficients were used to assess the relationship between circumferential stress and examined parameters (**Chapter 3**), between pSmad2 signalling and histological features (**Chapter 4**), and between medial hypertrophy and histology grading score (**Chapter 5**).

Separate bioinformatic analyses were performed for genetic sequencing results, which are detailed in **Chapters 6 and 7**.

2.7 Genetic analyses

Sequencing of DNA samples for copy number variation analyses was performed by collaborators at the Wellcome Trust Sanger Institute, Cambridge, and for targeted next-generation sequencing, by collaborating team-members of the cardiovascular BRU, Royal Brompton Hospital. The following sections summarize the basic principles of the above techniques with a detailed description of post-calling data processing and interpretation included in the relevant chapters (**Chapter 6 and 7**).

2.7.1 Array comparative genomic hybridization

Until recently, sequencing of the human genome focused on variation at either the chromosomal or nucleotide level with reduced knowledge on structural variants of an intermediate size. Array comparative genomic hybridization (CGH) is a technique which allows the identification of submicroscopic chromosomal copy number variants (CNVs), ranging from ~1 kb to 3 Mb in

size, at the genome wide level (Feuk et al., 2006). The principle of this method relies on comparison of copy number variation between a genome of interest and a reference sample.

DNA fragments of test and reference samples are differentially labelled and competitively hybridized to target arrays (eg, BAC clones, cDNAs, oligonucleotides) with extensive coverage of the human genome. Following hybridization of DNA fragments with their respective probes, a fluorescence ratio from each probe (test:reference) is used to detect copy number differences between the two samples, with a duplication or deletion in a genomic region expressed by a relevant increase or decrease of the relative ratio (Figure 2.7) (Wain et al., 2009). Derived intensities are transformed to log2 ratios for further data processing.

In this study, a variation of the array-CGH approach was applied with usage of hybridization intensities derived from spotted oligonucleotides on Affymetrix Genome-Wide Human SNP Array 6.0 (Aros, Inc.) (Feuk et al., 2006). DNA samples from BAV patients were run on the Affymetrix array and the derived hybridization intensities were compared to genotyping data from Wellcome Trust Control Consortium 2 donors assayed on the same platform (Bochukova et al., 2010).

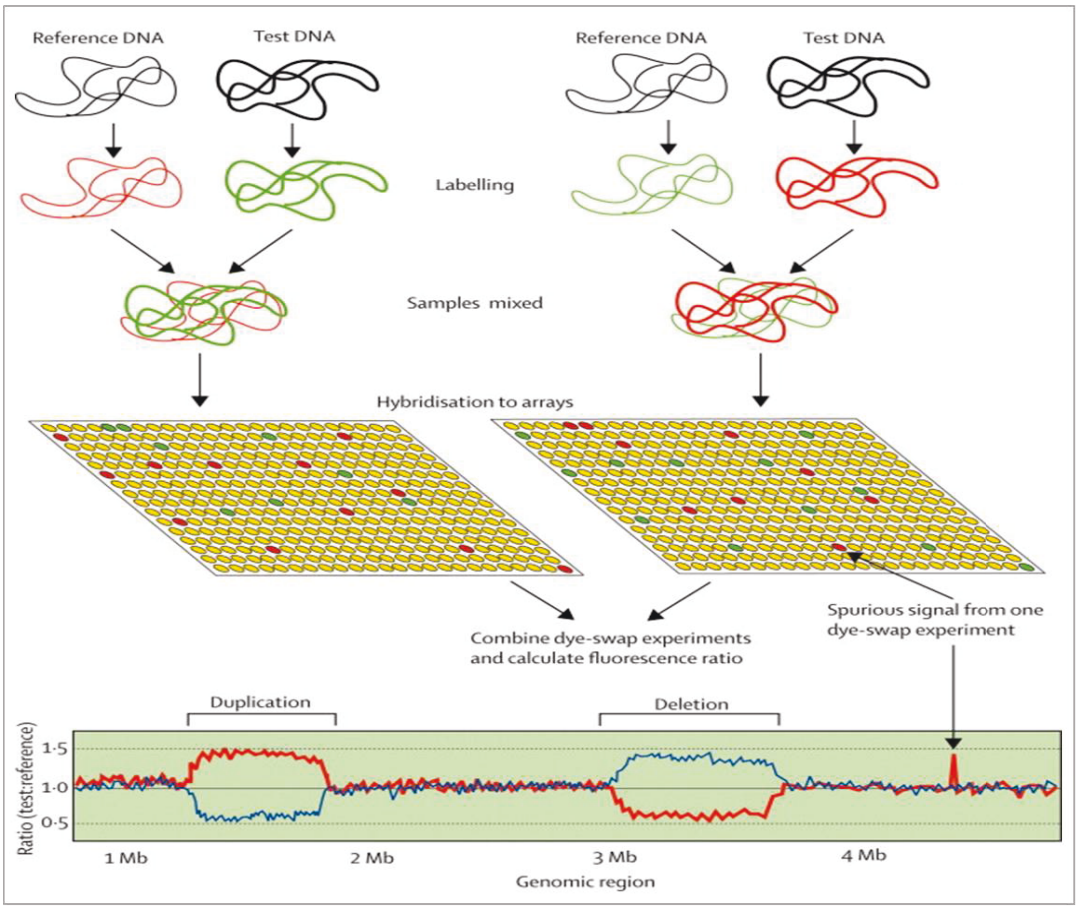

Figure 2.7 Array comparative genomic hybridization. Differentially labelled fragments from test and reference DNA are mixed and hybridized to a target array spoted with cloned DNA fragments from across the whole human genome. Following hybridization of DNA samples with their corresponding probes, the ratio of fluorescence in each probe (test: reference) is used to reveal genomic regions of copy number variations (red line: original hybridization; blue line: dye-swapped hybridization). Equal copy number for test and reference DNA result in a ratio of 1, with duplications identified by a ratio >1 and deletions by a ratio < 1. Derived fluorescence intensities are then transformed to log2 ratios for further data processing. Image from Wain and colleagues (Wain et al., 2009).

2.7.2 Targeted next-generation sequencing

Changes in the field of clinical medicine are imminent as next-generation sequencing (NGS) techniques offer the potential of high-throughput sequencing at continuously lowering costs (Ware et al., 2012, Metzker, 2010). NGS approaches parallelize the sequencing process, producing sequences of up to 50 billion bases per day compared to the 2 million bases via high-throughput Sanger sequencing (Ware et al., 2012). The technology used in this study (SOLiD

platform, Life Technologies) amplifies sequencing via fragmentation of genomic DNA followed by magnetic bead tagging of each fragment (http://www.chem.agilent.com/Library /usermanuals/Public/G753090004_SureSelect_SOLiD5500Multiplexed.pdf). Following bar-coding, samples are pooled for emulsion polymerase chain reaction (PCR) and the resulting clonally amplified DNA is bound to a glass slide. Then, massively parallel sequencing takes place via multiple rounds of hybridization, ligation, and cleavage of dye-labeled oligonucleotide probes followed by alignment of DNA sequence to a reference genome for decoding (Metzker, 2010). Generated reads are de-multiplexed and bioinformatically processed (details in **Chapter 7**).

An additional advantage of NGS techniques is that of whole-exome sequencing, allowing for selective sequencing of the coding regions of the human genome. Enrichment of targeted genomic regions can be achieved via PCR or hybridization methods (Ware et al., 2012). In this study, DNA libraries were constructed using the SureSelectXT Target Enrichment System (Figure 2.8) with "custom-made" RNA baits for all exons of 63 genes of interest (design details in **Chapter 7**). Targeted genomic areas were then enriched and barcoded, as described above, followed by NGS to screen for sequence variants.

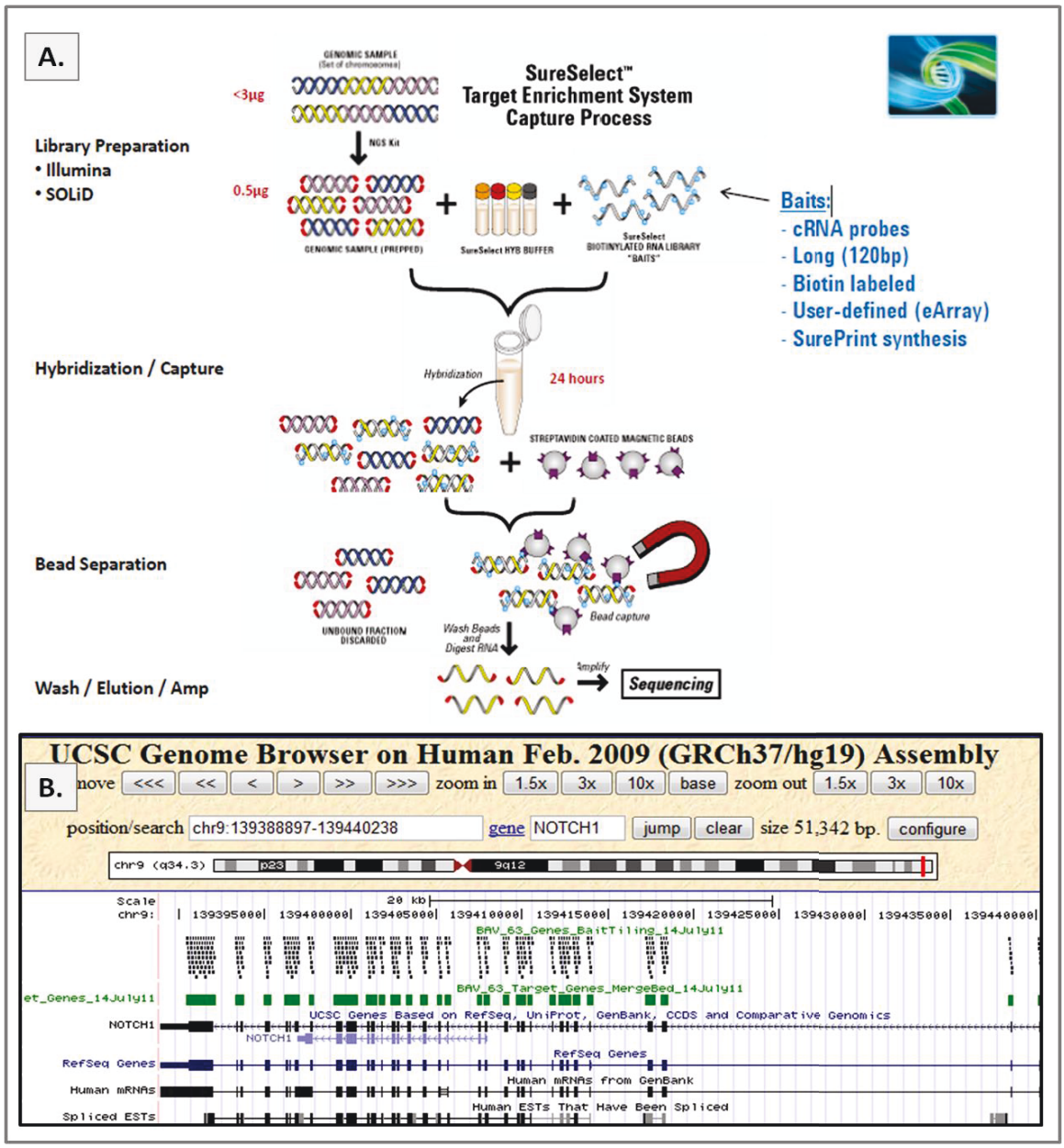

Figure 2.8 Sureselect target enrichment system for next-generation sequencing. A. The process of hybridization and capture of selected genomic regions via complementary RNA (cRNA) baits can be viewed. Genomic DNA is initially sheared and prepped with repair of blunt-ended DNA fragments and ligation of adapter modified-ends (*library preparation*). The prepped DNA is incubated in solution with the biotinylated RNA library ('baits') for 24h. Targeted genomic regions are captured by hybridization to the custom-designed cRNA oligonucleotide baits (*hybridization/capture*), isolated (via *magnetic bead separation*) and further amplified via polymerase chain reaction (PCR) for sequencing. B. Coverage of NOTCH1 gene exons (green) by "custom-made" complementary RNA baits (black dots in upper section of image). Figure A from http://www.chem.agilent.com/ Library/brochures/5990-3532en_lo%20CMS.pdf

Chapter 3. Finite-element analysis

Abbreviations

3D Three-dimensional
4D Four-dimensional
AAA Abdominal aortic aneurysm
AR Aortic regurgitation
AS Aortic stenosis
ASI Aortic size index
BAV Bicuspid aortic valve
CT Computed tomography
FEA Finite element analysis
HGS Histology grading score
MFS Marfan syndrome
MRI Magnetic resonance imaging
KPa Kilopascal
TAA Thoracic aortic aneurysm

3.1Abstract

Background: BAV is the commonest inborn heart defect predisposing affected individuals to a higher risk of TAA formation and dissection. Although there is a genetic component underlying TAA susceptibility, the local haemodynamic environment also plays an important role and is currently a critical gap in our understanding of the evolution of BAV-associated disease. We have generated the hypothesis that circumferential stress is different between the various aortic phenotypes in BAV and that it corresponds to the severity of the structural abnormalities in the aortic wall.

Methods: The 3D geometry of the thoracic aorta was constructed using CT angiography for BAV patients about to undergo surgery. The 3D models were broken down into smaller elements and circumferential stress, exerted perpendicularly to the aortic wall, was calculated in response to applied predefined loads via structural FEA. During surgery, aortic tissue biopsies were collected from discrete areas and the degree of medial wall degeneration was correlated to the calculated circumferential stress.

Results: Ten BAV patients (90% male) with a median age of 27 years [2-68] were studied. Maximal circumferential stress (KPa) normalised by aortic size index (ASI, cm/m²) was higher in the ascending aorta of patients with aortic regurgitation compared to those with aortic stenosis (42.6 [32.2-155.3] vs 14.5 [3.7-19.2] KPa; p= 0.025). Maximal stress in the ascending aorta occurred above the left coronary sinus in 80% of patients. A shift in stress location from the convex to the concave ascending aorta was observed as the asymmetry of the antero-lateral "bulge" increased. A positive correlation between the severity of fibrosis and corresponding stress was noticed both in the aortic root (ρ=0.79, p=0.033) and ascending aorta (ρ=0.76, p=0.044), with additional associations between stress, cyst-like formations (ρ=0.86, p=0.012)

and overall histology grading score (ρ=0.80, p=0.031) at the aortic root level when stress was normalised by ASI.

Conclusion: Our integrated analyses propose a link between radial stress and altered elastic component of the aortic media, with varied maximal stress location in distinct BAV aortic phenotypes. Aortic geometry should be taken into consideration in future studies examining the haemodynamic theory of BAV aortopathy.

3.2 Introduction

BAV is considered as a continuum of an inherent disease process affecting not only the aortic valve, causing it to have two instead of three leaflets, but also the aortic root and ascending aorta (Tadros et al., 2009). Despite the well recognized aortic dilatation associated with BAV disease, the natural history of the affected aortic segments remains largely unknown (Fedak et al., 2002). The lifetime likelihood of aortic dissection in BAV may be lower compared to other inborn abnormalities (5% versus 40% in MFS), but accounts for a larger number of incidents due to its higher prevalence in the general population (0.5 - 2%), comprising the commonest inborn heart defect (Tadros et al., 2009, Huntington et al., 1997, Braverman et al., 2005). Maximal aortic diameter is an established predictor of aortic dissection and rupture and to date, has been used as the single criterion for monitoring TAA formation in BAV disease (Prapa and Ho, 2012). While radiographic screening in BAV disease is valuable, many patients at a higher risk of TAA formation in later life may not have recognisable aortic enlargement at the time of testing, highlighting the need for further risk stratification tools (**Chapter 1**).

Considerable research in BAV patients over the past decade has sought to resolve the debate of haemodynamic versus genetic abnormalities causing the aorta to dilate. The resulting data have not only enhanced our understanding of the disease but also given rise to potential novel tools to

assess risk of TAA formation (Girdauskas et al., 2011a). Although genetic screening of BAV patients is not routinely available, our appreciation of the genetic aspects of TAA pathogenesis has led to the proposal of a lower threshold for elective surgery in BAV disease by the most recent American College of Cardiology/American Heart Association guidelines, similar to other connective tissue disorders (Girdauskas et al., 2011a, Hiratzka et al., 2010). On the other hand, the so-called "post-stenotic dilatation" theory, advocating elevated stress on the convexity of the ascending aorta due to disturbed blood flow downstream of a BAV stenotic lesion, has been further investigated by 4D magnetic resonance (MR) imaging suggesting disturbed flow patterns even in the absence of aortic stenosis (AS) and/or regurgitation (AR) (Girdauskas et al., 2011a, Hope et al., 2010).

The prognostic value of the wealth of structural and functional information currently obtained by advanced cardiovascular imaging in BAV disease remains to be seen. Computational modelling offers the advantage of rigorous utilization of the above data in the field of arterial biomechanics, allowing for validation of clinically relevant hypotheses (Giannakoulas et al., 2009). In fact, peak mechanical stress calculated by FEA has been shown to be superior to maximal aortic diameter for prediction of aortic dissection in patients with abdominal aortic aneurysms (Fillinger et al., 2003). The application of a similar model to study the effect of mechanical stress on TAA formation on the basis of geometrical features of the vessel wall would be particularly advantageous in the setting of BAV disease. The aim of this study was to address this critical gap in our understanding of BAV aortic "mechanical homeostasis", by utilization of pre-operative imaging combined with computational modelling to assess the distribution of mechanical stress and severity of corresponding structural abnormalities in the BAV aorta.

3.3 Methods

3.3.1 Summary

Informed consent was obtained from patients with BAV planning to undergo surgery at the Royal Brompton Hospital. Patients with developmental syndromes, major cytogenetic abnormalities and connective tissue disorders, such as MFS, were excluded from the study. Imaging data obtained preoperatively via CT angiography were used to study the distribution of mechanical stress in the proximal aorta, applying computational modelling methods. During the operation, aortic tissue samples were collected from discrete areas of the aortic root and ascending aorta and histological analyses were performed. A detailed description of methods is included in **Chapter 2**.

For each patient, maximal circumferential stress was reported at the level of the aortic root and ascending aorta. In addition, mean circumferential stress was calculated in areas of the aortic wall corresponding to the sites of tissue sampling during surgery (Figure 3.1).

Figure 3.1 Circumferential stress measurements. The result of finite element analysis as derived by ANSYS ICEM CFD© version 12 software can be viewed. The colour-coded three-dimensional map depicting the distribution of circumferential (Von Mises) stress (Pa) was reviewed and for each patient, maximal stress (red arrow) was reported at the level of the aortic root and ascending aorta. In addition, mean stress (green arrow) was calculated in areas of the aortic wall corresponding to the sites of tissue sampling during surgery. In this particular case, as the patient underwent aortic valve replacement, a single biopsy was collected from the anterior proximal aorta.

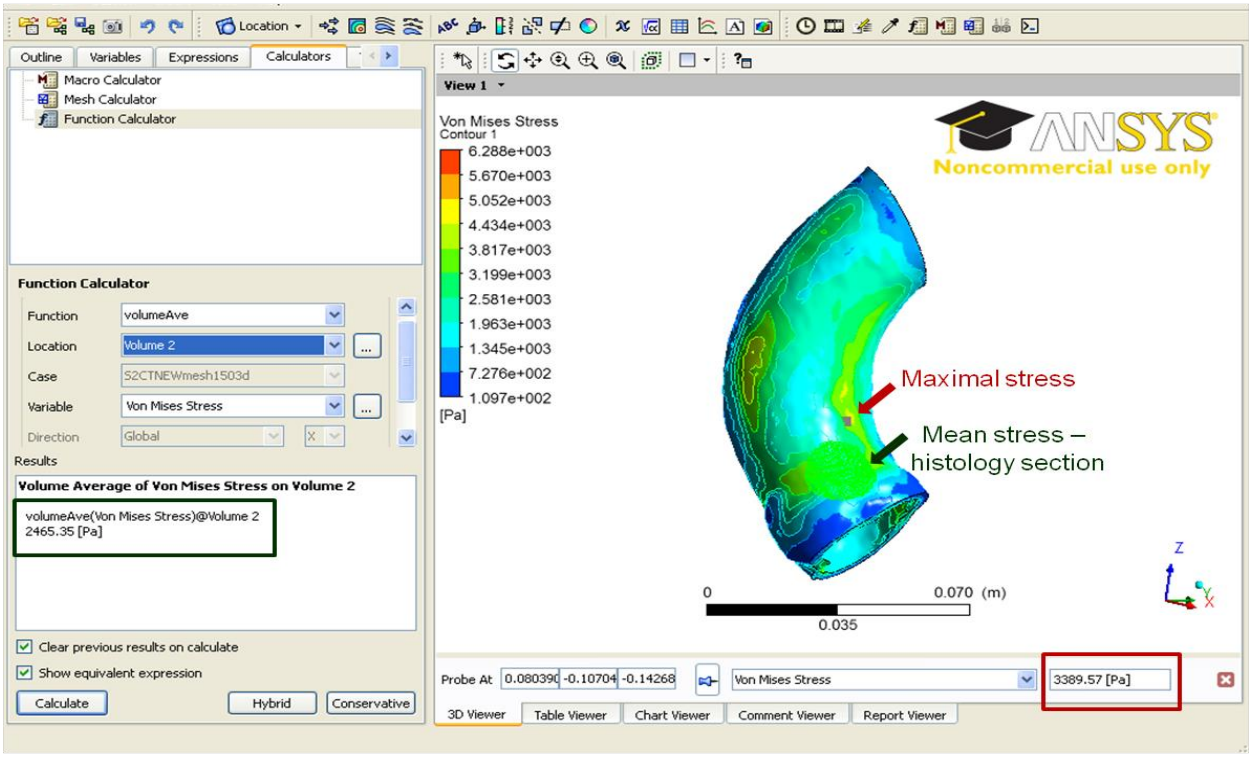

3.3.2 Technical difficulties over course of the study

When this study was initially designed, as it was the first of its kind involving integrated histological and computational modelling analyses, we used differential degrees of medial wall degeneration between the convexity and concavity of the ascending aorta in BAV patients with aortic regurgitation (2.5 versus 1.7 grades with a population standard deviation of 0.6) for our power calculations (Cotrufo et al., 2005). In order to detect a difference of 0.8 grades between areas of high and low mechanical stress (paired analyses) at a significance level of 0.01 and a power of 90%, we would need to recruit 12 patients. A total of at 15 patients was set as a target to adjust for technical difficulties in the harvesting, processing and analysis of tissue samples.

As mentioned in **Chapter 2**, all preoperative imaging scans were clinically indicated and obtained up to 6 months prior to surgical procedure, comprising a part of the diagnostic work-up of BAV patients undergoing surgery. Preoperative magnetic resonance imaging (MRI) is increasingly employed in BAV patients as it provides accurate aortic diameter measurements as well as functional data related to valvular disease and left ventricular function. In contrast, computed tomography (CT) angiograms are considered to be the gold standard for three-dimensional (3D) reconstructions of the aorta but subject patients to significant radiation exposure and are usually performed preoperatively when more detailed aortic anatomy is required for surgical planning or CT coronary angiography is performed simultaneously to assess for presence of coronary artery disease (Rengier et al., 2013).

In order to increase the number of recruited patients for this study, it was initially decided to use preoperatively obtained MRI angiograms for 3D reconstructions. However, their use would mandate an MRI slice thickness of <2mm (Rengier et al., 2013) with greater slice thicknesses leading to potential loss of important geometrical features and subsequent errors in computational modelling simulations. The above limitation was confirmed in a pilot study employing a "standard" 5mm slice thickness MRI angiogram for 3D reconstruction of the aorta, which was felt to be suboptimal (Figure 3.2). Unfortunately, the lower slice thickness parameter is rarely set outside research context limiting the use of clinically indicated preoperatively obtained MRI scans of BAV patients. As a result, it was decided to restrict our applied methodology to use of preoperative CT angiograms for all of our 3D reconstructions.

Figure 3.2 Pilot three-dimentional (3D) reconstruction employing magnetic resonance imaging (MRI). The complete structural analysis of a patient undergoing the Ross procedure for severe aortic stenosis can be seen with colour coded mechanical stress distribution in the anterolateral (a), posterior (b) and medial (c) wall of the aortic root and ascending aorta. As visualised in the images, 3-D reconstruction with use of 5mm slice thickness MRI, leads to poor depiction of geometrical features of the vessel wall and may result in significant simulation errors.

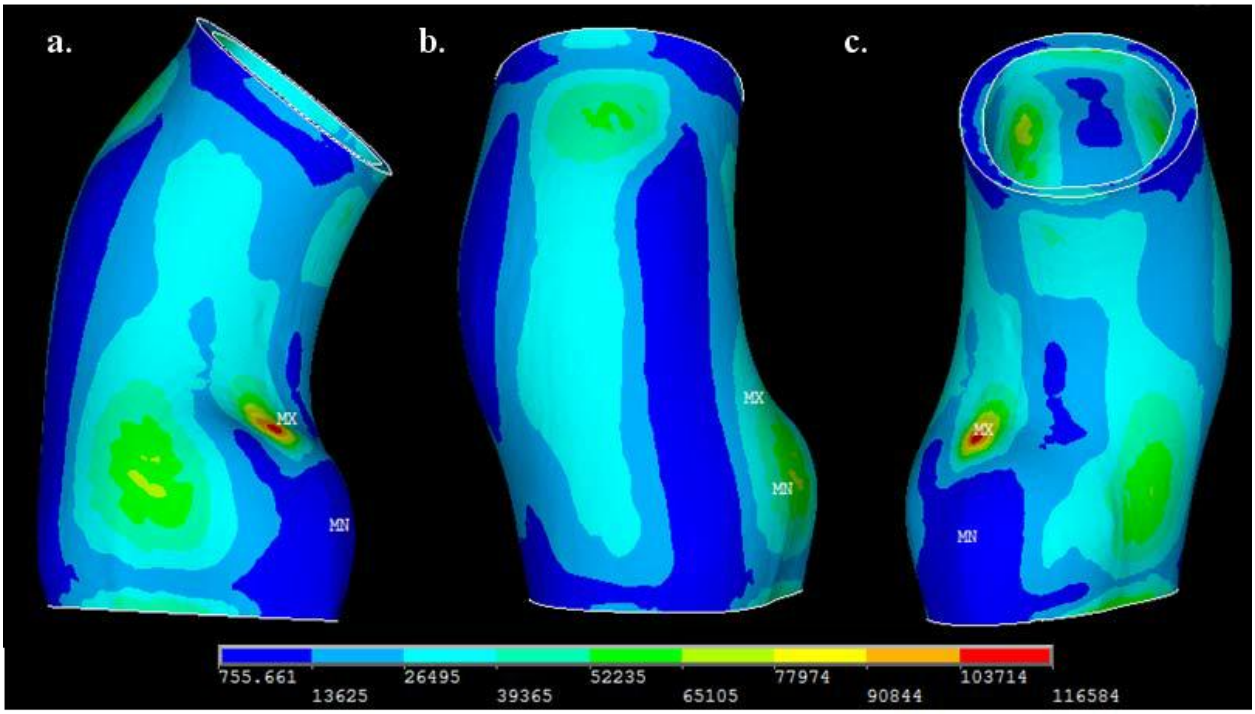

3.4 Results

3.4.1 Patient characteristics

Patient characteristics are summarized in Table 3.1. A total of 10 BAV patients planning to undergo surgery were recruited. Median age was 27 years [2-68], 90% of participants were male. The majority of patients had aortic valve disease (90%); three had AS and six had AR. A single 68y old patient had systemic hypertension (patient #10) treated with a calcium-channel blocker with none of the remaining patients having any cardiovascular disease risk factors (diabetes, hypertension, smoking) or being on any cardiovascular medication. Two patients (#4 and #9 had repaired coarctation of the aorta) and a single patient (patient #6) had a spontaneously closed ventricular septal defect. None of the remaining patients had any BAV-associated congenital heart defects, as outlined in the inclusion criteria in **Chapter 2**.

Biopsies were collected from multiple areas of the aortic wall, depending on the type of surgical procedure, with recording of the exact site of tissue collection.

Table 3.1 Patient characteristics

Pt	Sex	Age (y)	BAV type	BAV Disease	BAV Degree	Ao Root (cm)	Asc Ao (cm)	BSA	Surgical procedure	Aortic samples Root	Aortic samples Asc Ao
1.	M	2	True	AS	Severe	1.4	2.3	0.59	Ross	+	+
2.	M	14	R-N	AR	Moderate	2.8	5.6	1.66	Ao root & arch replacement	+	+
3.	M	22	True	AS	Severe	3.1	2.9	1.78	Ross	+	+
4.	M	24	True	-	-	6.4	1.7	2.07	VSARR	+	-
5.	M	26	NA	AR	Moderate	6.6	3.9	1.91	ARR	+	-
6.	F	28	R-N	AR	Severe	4.0	5.4	1.74	Bentall	+	+
7.	M	29	R-L	AR	Severe	3.4	2.6	2.08	AVR	-	+
8.	M	34	R-N	AR	Severe	3.8	5.2	1.84	AVR & Asc Ao replacement	-	+
9.	M	37	True	AR	Mild	6.3	3.0	2.09	VSARR	+	-
10.	M	68	R-L	AS	Severe	3.2	3.2	2.05	AVR	-	+

Abbreviations: Ao, aortic; ARR, aortic root replacement; Asc, ascending; AVR, aortic valve replacement; BAV, bicuspid aortic valve; BSA, body surface area; Pt, patient; R-L, fusion of right and left coronary leaflets; R-N, fusion of right and non-coronary leaflets; VSARR, valve sparing aortic root replacement.

3.4.2 Maximal Mechanical Stress

Overall, three aortic phenotypes, related to BAV disease, were analysed (Figure 3.3). Within the 3 aortopathy groups, there were no significant differences in absolute or normalised maximal stress in the ascending aorta compared to the aortic root (Figure 3.3).

Figure 3.3 Analyzed BAV aortic phenotypes and corresponding maximal stress values. Ao root, aortic root; asc ao, ascending aorta; ASI, aortic size index; max, maximal. Aortic images created by artist for purpose of thesis chapter.

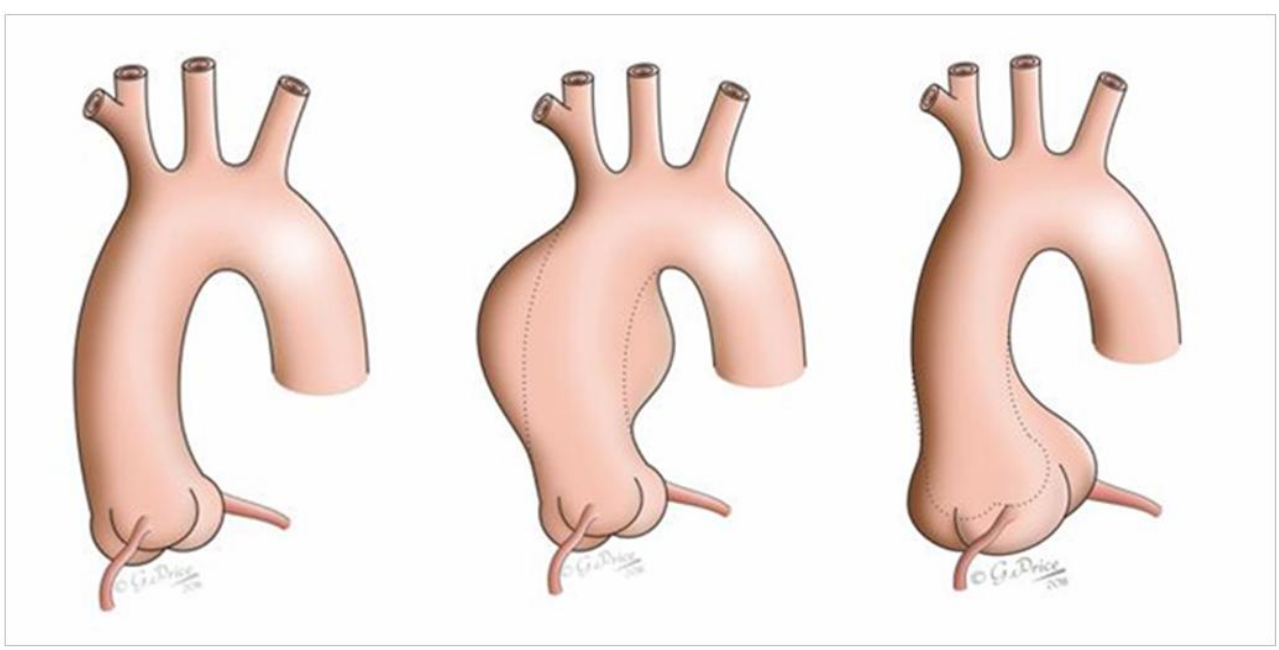

Aortic phenotype	Mild dilatation (n=3)	Asc Ao aneurysm (n=4)	Ao Root aneurysm (n=3)	p value*
Ao Root Max Stress (kPa)	24.8 (4.4-75.5)	66.1 (12.2-154.3)	77.9 (67.3-120.4)	0.445
Asc Ao Max Stress (kPa)	31.3 (5.8-47.6)	130.7(56.6-523.6)	46.4 (41.5-46.4)	
Ao Root Max Stress/ASI	14.2 (2.8-46.3)	28.7 (5.9-91.3)	25.2 (19.4-40.0)	0.114
Asc Ao Max Stress/ASI	19.2 (3.7-38.1)	47.1 (14.5-155.3)	32.2 (20.3-56.6)	

* Paired analysis in overall population. Separate paired analysis within the 3 aortopathy groups did not reveal any significant differences in neither absolute nor normalized maximal stress in ao root versus asc ao.

Table 3.2 Maximal circumferential stress (in all subjects sub-divided by BAV morphology and disease). A single subject was not included in the first part of the table as BAV morphology was not available in this case (patient #5, table 3.1).

Stress	**BAV Groups**			
Maximal Stress (KPa) location		**BAV Subtypes**		
	True (n=4)	**R-L (n=2)**	**R-N (n=3)**	**p value*¹**
Aortic root normalised for root ASI	19.4 (6.3-40.0)	24.6 (2.8-46.3)	51.0 (5.9-91.3)	0.580
Ascending aorta normalised for asc ao ASI	20.3 (14.5-56.6)	20.9 (3.7-38.1)	51.6 (42.5-155.3)	0.139
Maximal Stress (KPa) location		**BAV Disease**		
	AR (n=6)	**AS (n=3)**	**None (n=1)**	**p value*²**
Aortic root normalised for root ASI	46.3 (5.9-91.3)	6.3 (2.8-14.2)	25.2	0.101
Ascending aorta normalised for asc ao ASI	42.6 (32.2-155.3)	14.5 (3.7-19.2)	95.0	**0.025**

*¹ Kruskall-Wallis test for comparisons between 3 groups

*² Mann-Whitney test for comparisons between 2 groups (AR versus AS)

Abbreviations: Ao, aortic; AR, aortic regurgitation; AS, aortic stenosis; Asc, ascending; ASI, aortic size index; BAV, bicuspid aortic valve; R-L, fusion of right and left coronary leaflets; R-N, fusion of right and non-coronary leaflets.

Similarly, no differences in stress values were noticed between different morphological subtypes of BAV (Table 3.2). The normalised maximal stress in the ascending aorta was higher in patients with AR compared to those with AS (42.6 [32.2-155.3] vs. 14.5 [3.7-19.2] KPa; p= 0.025, Table 3.2). Absolute values of maximal stress did not correlate with maximum diameters, both at the level of the root (ρ= 0.23, p=0.511) and the ascending aorta (ρ= 0.44, p=0.199). Similarly, no correlation was found between maximal stress and

maximum ASI in the aortic root (ρ= 0.24, p=0.489) and the ascending aorta (ρ= 0.57, p=0.08).

The regional distribution of maximal stress was investigated. Patient-specific 3D wall stress distributions with absolute values of maximal stress are depicted in Figure 3.4 and Table 3.3, respectively. In the majority of patients (8/10, 80%), maximal stress was located on the concave aspect of the ascending aorta above the left coronary sinus. In a single patient (1/10, 10%), maximal stress occurred on the convex aspect of the ascending aorta above the right coronary sinus and in another patient (1/10, 10%), it was located on the anterior aspect of the ascending aorta.

Table 3.3 Absolute values of maximal stress and aortic radius measurements. Patient numbers correspond to table 3.1 and figure 3.4.

Pt		Diameter (cm)	Z score	ASI (cm/m²)	Max Stress (KPa)
1.	Root	1.4	-.66	2.37	14.94
	Asc Ao	2.3	4.99	3.90	56.59
2.	Root	2.8	1.02	1.69	154.35
	Asc Ao	5.6	16.72	3.37	523.57
3.	Root	3.1	1.93	1.74	24.80
	Asc Ao	2.9	2.78	1.63	31.35
4.	Root	6.4	14.94	3.09	77.91
	Asc Ao	1.7	-4.21	.82	46.41
5.	Root	6.6	16.23	3.46	67.30
	Asc Ao	3.9	7.35	2.04	41.53
6.	Root	4.0	5.81	2.30	117.36
	Asc Ao	5.4	15.43	3.10	160.15
7.	Root	3.4	2.30	1.63	75.55
	Asc Ao	2.6	0.25	1.25	47.66
8.	Root	3.8	4.69	2.07	12.26
	Asc Ao	5.2	14.11	2.38	101.30
9.	Root	6.3	14.46	3.01	120.41
	Asc Ao	3.0	2.24	1.44	46.41
10.	Root	3.2	1.54	1.56	4.44
	Asc Ao	3.2	3.35	1.56	5.78

Abbreviations: Ao, aortic; Asc, ascending; ASI, aortic size index; Max, maximal; Pt, patient.

Figure 3.4 Overview of range (KPa) and location of circumferential stress in studied BAV subjects. The convexity and concavity of the ascending aorta can be viewed in all cases. Patient numbers correspond to tables 3.1 and 3.3.

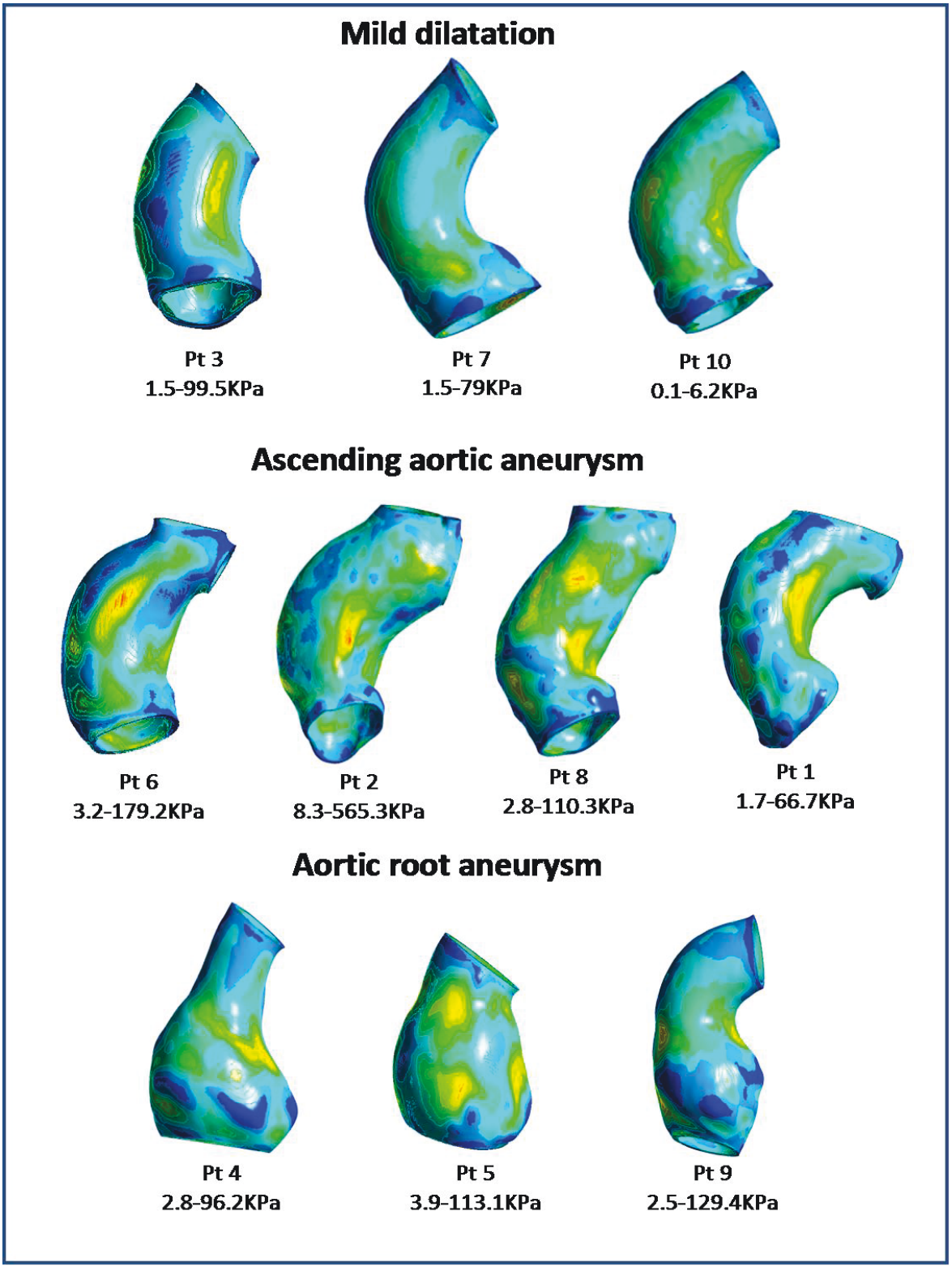

3.4.3 Histological abnormalities

The vast majority of BAV patients had severe medial wall abnormalities (≥ grade 2) involving their ascending aorta, including elastic fragmentation (85%), fibrosis (28%) and cyst-like formations (42%). Medionecrosis was rarely seen and was found to be mild (grade 1) in 14% of samples. In the aortic root, severe elastic fragmentation was present in 28% of samples, fibrosis in 42%, cyst-like formations in 42% and medionecrosis in none (Figure 3.5). The median histology grading score (HGS) was 4.5 [3-7] in the ascending aorta and 3.5 [2-5] in the aortic root. No significant differences in HGS were noticed between aortic phenotypes or BAV morphological subtypes. When subdivided by aortic valve disease, patients with AR had a significantly higher HGS compared to those with AS (6 [5-7] vs. 3.5 [3-4]; p=0.029) in their ascending aorta.

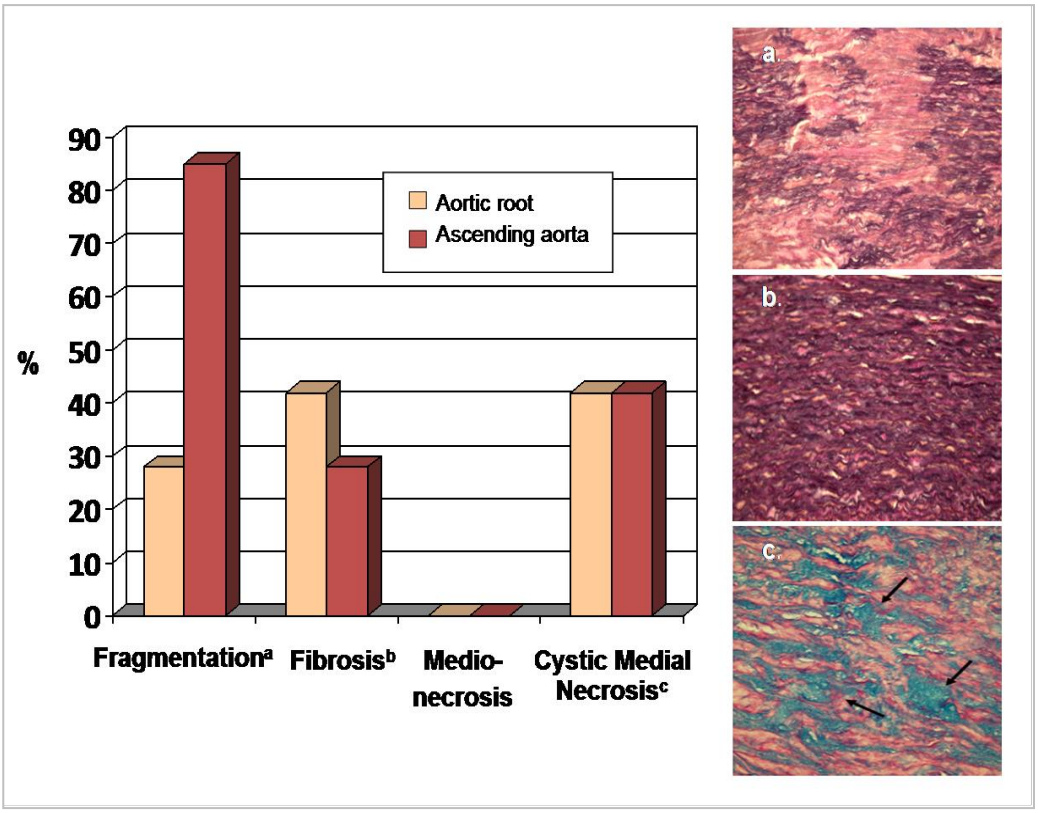

Figure 3.5 Percentage of severe medial wall abnormalities (≥ grade 2) in collected tissue biopsies. The right-sided panel illustrates the presence of elastic fragmentation (a), fibrosis (b), and cyst-like formations (c, black arrows) on microscopy (x200 magnification, a and b, elastic van Gieson; c, alcian blue stain).

3.4.4 Integrated analyses

The degree of medial wall abnormalities was correlated to the mean mechanical stress in the corresponding areas of the aortic wall (Figure 3.6). In the aortic root samples, the normalised mechanical stress correlated with the severity of fibrosis (ρ= 0.85, p=0.015), cyst-like formations (ρ= 0.86, p=0.012), and overall HGS (ρ= 0.80, p=0.031). In the ascending aorta, a positive correlation was noticed between normalised mechanical stress and fibrosis (ρ= 0.76, p=0.044). When absolute values of mechanical stress were used, a positive correlation was noticed between stress and fibrosis, both in the aortic root (ρ= 0.79, p=0.033) and the ascending aorta (ρ= 0.76, p=0.044).

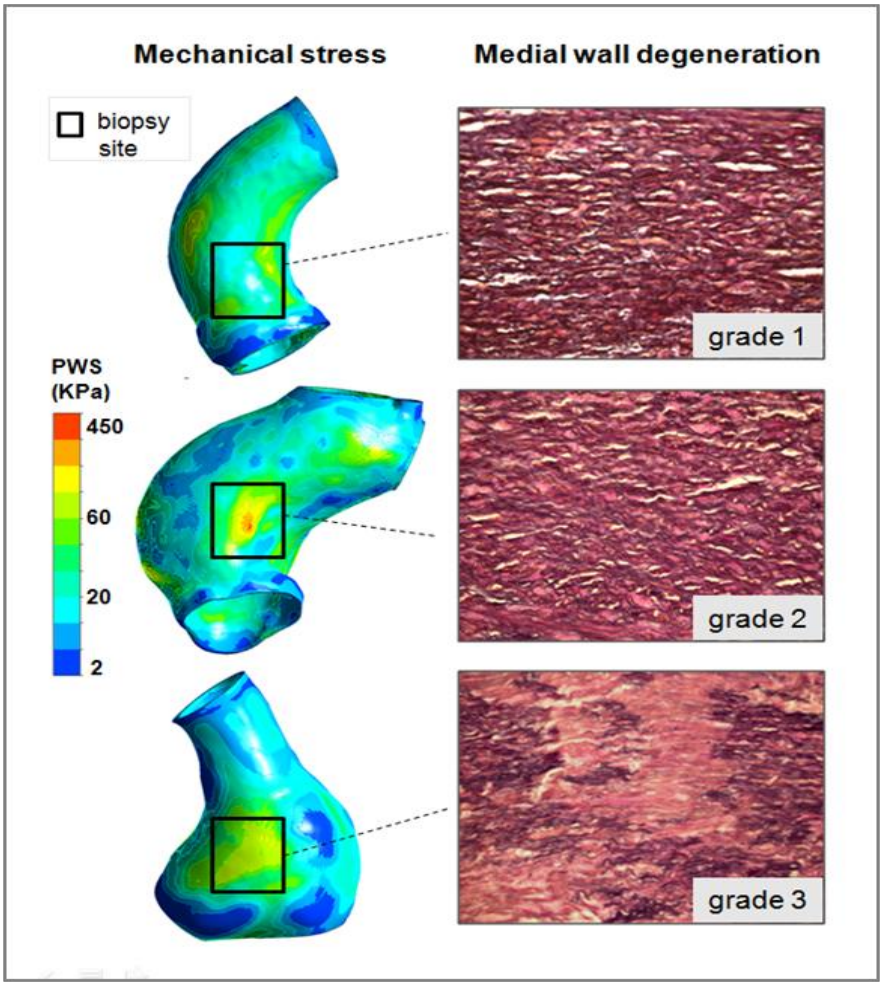

Figure 3.6 Representative overview of correlations between the degrees of medial wall abnormalities and mean circumferential stress in the corresponding areas of aortic wall tissue biopsies. Three aortic phenotypes can be seen in descending order (mild dilatation, ascending aortic aneurysm, aortic root aneurysm) with examples of corresponding degrees of elastic fragmentation (x200, elastic van Gieson stain).

3.5 Discussion

This study demonstrates that mechanical stress distribution differs between BAV aortic phenotypes, with maximal stress located in the concave aspect of the ascending aorta in the majority of cases. Combined biomechanical and histological analyses exhibited a strong positive correlation between the degree of fibrosis and mechanical stress, both in the aortic root and the ascending aorta. When mechanical stress was normalised to ASI, additional positive correlations were noticed between stress, cyst-like formations, and overall histology grading score at the level of the aortic root.

3.5.1 Maximal mechanical stress

To date, the distribution of mechanical stress in the BAV aorta has been investigated by a single group; Nathan and colleagues compared equal numbers of BAV and TAV adult patients (n=20) and reported increased 99^{th} percentile wall stress in the ascending aorta of BAV patients, regardless of aortic diameter (Nathan et al., 2011b). Similarly to our findings, the authors reported no differences in 99^{th} percentile wall stress between different BAV morphological subtypes (Nathan et al., 2011b) albeit higher normalised maximal stress was noticed in our BAV subjects with AR compared to those with AS, which reached statistical significance at the level of the ascending aorta (Table 3.2). Direct comparisons of reported stress values with our findings in BAV subjects are not possible due to the different intraluminal applied pressure, despite similar material properties of the vessel wall (Giannakoulas et al., 2005). However, differences in location of stress may be more important than actual values, especially in the instance of higher stress in the convexity of the ascending aorta where type A dissections typically occur (Nathan et al., 2011b). Nathan et al. reported maximal stress above the left coronary sinus in 50%, above the right coronary sinus in 45%, and in the distal ascending aorta in 5% of BAV cases whereas in the majority of TAV aortas (65%), maximal stress was located above the left coronary sinus (Nathan et al.,

2011b). In our study, maximal stress occurred in the concavity of the ascending aorta (above the left coronary sinus) in the vast majority (90%) of BAV patients. This suggests that stress patterns in our subjects are geometry-driven as most of them had similar geometrical features with a "bulge" in the anterolateral portion of the ascending aorta characteristic of BAV disease (Figure 3.4).

Despite differences in pathophysiology and location, virtual models of abdominal aortic aneurysms (AAA) can be used to partly explain the location of mechanical stresses in the ascending aorta. Previous studies have investigated the effect of bulge shape asymmetry in AAA biomechanics and reported changes in the location of maximal stress in relation to the altered shape of the aneurysm sac. Both static (Vorp et al., 1998) and fluid-structure interaction analyses (Scotti et al., 2005), have reported a shift in location of circumferential stress in AAA sac from the distal ends of the anterior wall to the midsection of the posterior wall as asymmetry increases, which may be explained by the increasing curvature of the sac allowing accelerated flow in the opposite (posterior) area (Figure 3.7) (Scotti et al., 2005). Similarly, it may be that mechanical stress distribution in the ascending aorta shifts from the distal ends of the bulge in the anterolateral wall (including the area above the right coronary sinus) to the posterior-medial wall as asymmetry of the bulge increases. Although theoretical aneurysm models are outside the scope of this study, the stress patterns of the aneurysms in our BAV subjects would support this theory (Figure 3.4). As the bulge asymmetry increases from patient 6 (with dilatation extending to the sinutubular junction) to patient 2 and patient 8 (with a prominent anterolateral bulge proximally), the location of maximal circumferential stress shifts from the anterior aorta (patient 6) to the medial wall (patient 2) and finally, the area above the left coronary sinus (patient 8). Due to the more uniform dilatation noted in BAV cases with aortic root dilatation, interpretation of stress distribution in this area would need to follow different theoretical models of spherical aneurysms exhibiting maximum

circumferential stress near the junction of the aneurysm, as seen in patients 4 and 9 in our study (Stringfellow et al., 1987).

Figure 3.7 Computational modelling in abdominal aortic aneurysm (AAA). Both static (A) and fluid-structure interaction analyses (B) have reported a shift in location of circumferential stress (N/cm^2) in the AAA sac from the distal ends of the anterior wall to the midsection of the posterior wall as asymmetry (expressed by the β parameter) increases. Both images depict AAA virtual models of increasing sac asymmetry and uniform wall thickness; A. is adjusted by Vorp et al. and shows anterior (left column) and posterior views (right column) of Von Mises stress (Vorp et al., 1998) and B. is adjusted by Scotti et al. and shows anterior/left lateral views of displacement (left column) and Von Mises stress (right column) (Scotti et al., 2005).

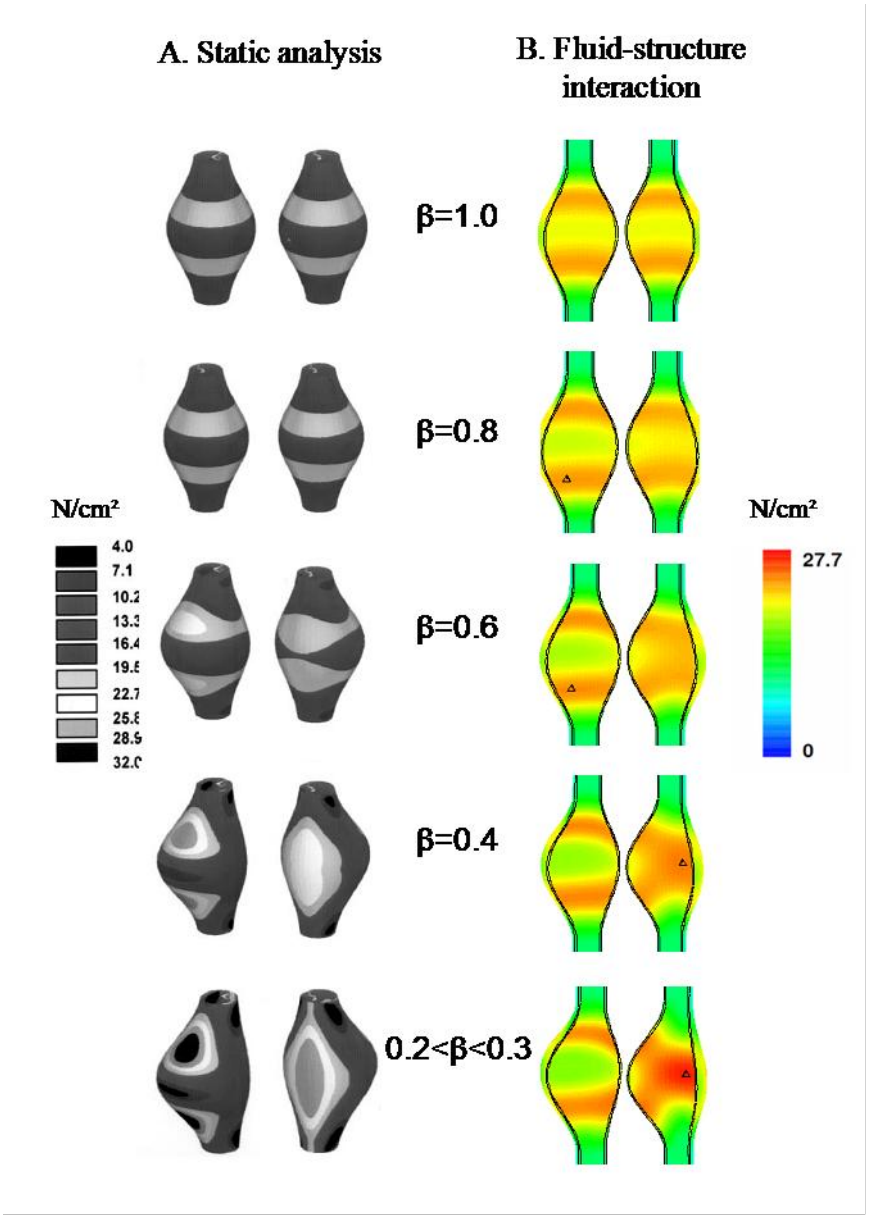

3.5.2 Integrated analyses

This study also investigated associations between histological abnormalities and corresponding stress in the BAV aorta, although the prognostic value of the former remains elusive (Prapa and Ho, 2012). In fact, the presence of structural wall abnormalities in BAV disease may not precipitate aortic dissection in isolation but make the aorta susceptible to such an event. External factors, such as acute exertion and emotion, can trigger the onset of aortic dissection in a genetically "weakened" aorta with aneurysm rupture occurring when the developing mechanical stress exceeds the tensile strength of the aortic wall (Elefteriades and Farkas, 2010, Vorp et al., 1998). However, it remains unclear whether structural changes in the BAV aorta are purely inherent or the result of external haemodynamic factors, including increased mechanical stresses as the diameter enlarges (Schlatmann and Becker, 1977).

Okamoto et al. studied the influence of histological structural changes in the ascending aorta of BAV and MFS patients on wall stress and distensibility by fitting *in vivo* elastic tissue properties into a cylindrical mathematical model of the aorta (Okamoto et al., 2003). The authors reported reduced distensibility of the ascending aorta in BAV patients with greater degrees of elastic fragmentation. However, no differences in mean circumferential stress were noticed in their studied groups, although the frequency of severe fibrosis and medionecrosis was lower in their tissue samples compared to other studies (Schlatmann and Becker, 1977). By examining the effect of patient-specific aortic geometry (rather than elastic properties) on circumferential stress, we report a positive correlation between increased stress and severity of fibrosis, both in the aortic root and the ascending aorta. Arterial remodelling in response to increased radial stress has been studied extensively in patients with systemic hypertension, exhibiting altered contribution of elastic components of the media (fracture of elastic lamellae and increased collagen turnover) leading to dilatation, increased wall thickness and stiffness of the vessels (Humphrey, 2008). Similarly, in congenital heart

disease, whereby the great arteries are “inherently” abnormal, severe fibrosis with increased elastin/collagen ratio has been described by our group in the pulmonary artery of patients exposed to long-standing elevated pulmonary arterial pressures (**Chapter 5**) (Prapa et al., 2013).

When stress was normalised for ASI, a stronger correlation with fibrosis was noticed in the aortic root with additional associations between stress, cyst-like formations and overall HGS at the same level. Cyst-like formations in the media have been described as the only potential histological abnormality distinguishing the dissecting aorta from normotensive and hypertensive controls (Manley, 1964). It has been previously proposed that the root dilatation phenotype accompanied by varying degrees of aortic insufficiency may represent the predominantly genetic form of BAV disease (Girdauskas et al., 2011a), as it would be less influenced by altered haemodynamic factors compared to the ascending aorta which is subjected to eccentric blood-flow patterns and focally elevated WSS, even in the absence of AS (Hope et al., 2010). However, in our study, the degree of histological abnormalities in the root was not greater compared to that of the ascending aorta, although when subdivided by aortic valve disease, patients with pure AR had a significantly higher HGS in their ascending aorta, in agreement with previous findings (Roberts et al., 2011). It is, therefore, possible that mechanical (rather than shear) stress has a greater pathophysiologic effect on aortic root dilatation, especially in view of the fact that the majority of our BAV subjects had regurgitant valves subjecting the aorta to higher stroke volumes rather than stenotic valves causing eccentric jet lesions in the distal ascending aorta with potentially corresponding asymmetric structural abnormalities (Tadros et al., 2009, Della Corte et al., 2008).

3.5.3 Limitations

This study has several limitations in relation to vessel wall properties incorporated into the finite-element analyses. Firstly, the arterial wall was assumed to have uniform elastic

properties in all subjects with properties of an isotropic linearly-elastic material. Although similar wall characteristics have been applied in equivalent studies in BAV disease (Nathan et al., 2011b), a more accurate method would be that of mechanical testing of our collected tissue biopsies and incorporation of *in vivo* elastic properties into our model. Another assumption is that of uniform wall thickness in all of our subjects; Scotti and colleagues studied the effect of differential wall thickness in AAA models and showed that uniform thickness may underestimate peak stress by an average of 9.4% when applying quasi-static computational conditions (Scotti et al., 2005). However, *in vivo* examination of BAV aneurysmal aortic tissue rings failed to exhibit significant variations in regional wall thickness (Choudhury et al., 2009). Finally, an important limitation is that of the applied computational method *per se*, as our model did not take into consideration the effect of 3D time-varying blood flow, allowing calculation of WSS, which may have an important haemodynamic effect especially in stenotic BAV disease (Girdauskas et al., 2011a). Although fluid-structure interaction analysis would reflect more accurately the *in vivo* haemodynamic conditions, it would also require a significantly greater amount of workload with an estimated 23-fold increase in computational costs, restricting its current role as a readily accessible risk stratification tool for clinicians (Scotti et al., 2005). Analyses are also limited by the lack of controls, restricted numbers, and varying age of our subjects which may impose additional effects on the elastic properties of their aortic walls. Aortic geometry has been previously reported to be an established contributing factor to aneurysm expansion and rupture potential, regardless of the heterogeneity of the wall (Scotti et al., 2005). Despite its limitations, this study is the first of its kind to assess the effect of patient-specific aortic geometry on circumferential stress and corresponding histological abnormalities in a typical group of BAV patients who would be expected to present to a Congenital Heart Disease Unit.

3.6 Conclusions

This study employs patient-specific 3D aortic models combined with structural finite-element analysis to study the effect of geometrical features of BAV aortic phenotypes on circumferential stress and corresponding histological abnormalities. Overall, maximal stress occurred above the left coronary sinus in the majority of patients with maximal stress location shifting from the convex to the concave aspect of the vessel wall as asymmetry of the anterolateral bulge increased. Future sequential static computational analyses in enlarging or dissected BAV aortas will be able to validate the prognostic value of maximal mechanical stress, as has been carried out in AAA disease (Fillinger et al., 2003). Our integrated analyses propose a link between radial stress and altered elastic component of the BAV aortic media, which may be competitive or synergistic to that of shear stress assessed by fluid-structure interaction analyses or 4D MR imaging (Cheng et al., 2010, Hope et al., 2010). As more advanced tools are becoming available to clinicians, it would be safe to assume that we are moving away from the "aortic diameter criterion" and closer to individualized risk stratification and management of BAV disease.

Chapter 4. BAV aortic phenotypes

Abbreviations

ACE Angiotensin converting enzyme
AR Aortic regurgitation
ARB Angiotensin receptor blocker
AS Aortic stenosis
AVR Aortic valve replacement
BAV Bicuspid aortic valve
CMR Cardiac magnetic resonance
CNC Cardiac neural crest
ECM Extracellular matrix
FBN1 Fibrillin-1
LDS Loeys Dietz syndrome
MMP Matrix metalloproteinase
pSmad2 Phosphorylated Smad2
TGFβ Transforming growth factor-beta
TGFBR Transforming growth factor-beta receptor
VSMC Vascular smooth muscle cell

4.1 Abstract

Background: TGFβ signalling plays a central role in vascular remodelling and aneurysm formation. A hypothesis of lineage-specific capacity in TGFβ responsiveness has recently emerged which may explain the different patterns of aortopathy in BAV disease. To that end, we aimed to assess the degree of histological abnormalities and TGFβ activation in the mesoderm-derived aortic root and ectoderm-derived ascending aorta of BAV patients.

Methods: Aortic tissues from BAV patients and controls sampled at the level of sinuses of Valsalva and distal ascending aorta were examined via light microscopy for histological abnormalities and nuclear phosphorylated Smad2 (pSmad2) signalling, a marker of TGFβ activation. A detailed histology grading score was used to assess the severity of medial wall abnormalities. Immunohistochemical data was expressed as the percentage of positive pSmad2 nuclei in each aortic wall layer.

Results: Aortic specimens collected during surgery from 18 BAV patients (median age 22.5 [2–39]) were compared to 12 age-matched controls. Paired analysis in BAV patients reported a higher cumulative histology grading score in the ascending aorta compared to the root (5.5, [2-9] versus 4, [2-7]; p=0.004), which was persistently greater in patients with regurgitant valve disease (6, [2-9] versus 4, [2-6]; p=0.026), and in patients with aortic root dilatation (6, [3-9] versus 4, [2-6]; p=0.029). At immunohistochemistry, pSmad2 signalling was significantly higher in the BAV media compared to controls, both in the aortic root (38.7 [14-61] versus 10.7 (2-36), p<0.001) and in the ascending aorta (40.3 [4-54] versus 7.9 [3-46], p=0.001). Medial pSmad2 activation did not differ significantly between the ascending aorta and root of BAV patients, with or without respective aortic dilatation. In the overall population, a positive correlation was noticed between the degree of pSmad2 signalling in the media and the severity of medial wall abnormalities, both in the aortic root (ρ=0.57; p=0.001) and the ascending aorta (ρ=0.6; p<0.001).

Conclusion: The dilated aortic root phenotype may represent the primarily genetic form of BAV disease as patients with either root dilatation and/or predominant regurgitant valve disease had greater levels of medial wall degeneration in their ascending aorta. Enhanced TGFβ signalling appears to play a key role in BAV aortopathy. The presence of increased pSmad2 activation in non-dilated BAV aortic segments points to a genetic trigger, with no differences in signalling between the mesoderm-derived root and the ectoderm-derived ascending aorta.

4.2 Introduction

The heterogeneous nature of BAV disease has been increasingly recognized over the past decades, with extensive research focusing on discrete clinical phenotypes and their respective pathophysiology (Tadros et al., 2009, Girdauskas et al., 2011a). As seen in **Chapter 3**, different patterns of BAV aortopathy include typical asymmetric enlargement at the convexity of the ascending aorta, and isolated aortic root dilatation (Della Corte et al., 2007, Bauer et al., 2006, Cotrufo and Della Corte, 2009, Nistri et al., 1999). These phenotypes may be secondary to haemodynamic stress-induced vascular remodelling although our integrated analyses in **Chapter 3** suggested that genetic factors may be equally operative (Robicsek et al., 2004, Hope et al., 2010, Hinton, 2012). Irrespective of potential underlying mechanisms, the end-result of medial wall degeneration in the BAV ascending aorta has been established whereas, to date, no surgical reports have focused on the histopathology of the aortic root in the same setting (Girdauskas et al., 2011a, Fedak et al., 2003).

The central role of increased TGFβ signalling in inherited aortopathy has recently emerged (Lindsay and Dietz, 2011, El-Hamamsy and Yacoub, 2009a). TGFβ is a multifunctional cytokine, with synthetic and apoptotic properties, that participates in extracellular matrix (ECM) homeostasis (Goumans et al., 2009, Owens and Wise, 1997, Cordenonsi et al., 2003). Its bioavailability is partially regulated by fibrillin-1 which interacts with the large latent

complex containing TGFβ in an inactive state (Figure 4.1) (El-Hamamsy and Yacoub, 2009a, Carta et al., 2009). Once released in the ECM, TGFβ and its ligand-activated receptors can stimulate signalling via "canonical" and "non-canonical" pathways (Derynck and Zhang, 2003). The former involves nuclear translocation and phosphorylation of a family of transcriptional factors (Smads) with subsequent expression of targets, such as MMPs, leading to ECM proteolysis (Ma et al., 1999, El-Hamamsy and Yacoub, 2009a).

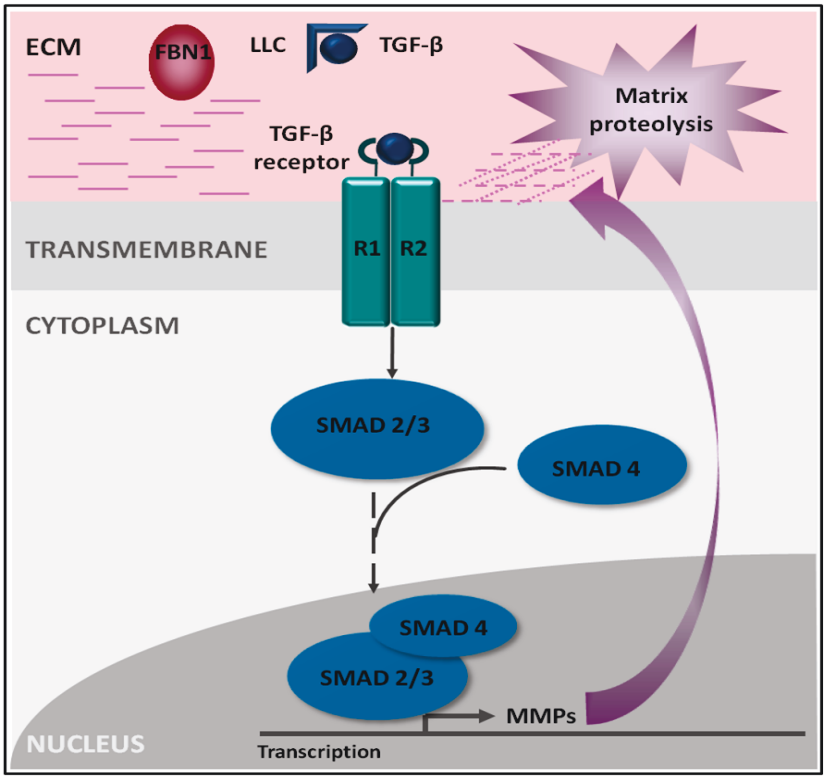

Figure 4.1 Canonical (Smad-dependent) transforming growth factor-β (TGFβ) signalling pathway. Normally, TGFβ remains in an inactive state by binding to the large latent complex (LLC) which interacts with fibrillin-1 (FBN1) in the extracellular matrix (ECM). Once activated, TGFβ released in the matrix binds to TGFβ receptor type II (TGFBR2), which then activates TGFβ receptor type I (TGFBR1) inducing a cascade of nuclear translocation and phosphorylation of receptor-actived Smad proteins 2 and 3 that associate with a co-Smad (Smad 4) and subsequent expression of target molecules, including matrix metalloproteinases (MMPs) leading to proteolysis of the ECM (El-Hamamsy and Yacoub, 2009a).

Enhanced TGFβ signalling, as assessed by nuclear phosphorylated Smad2 (pSmad2) accummulation, has been reported in syndromic and non-syndromic ascending aortic aneurysms, including patients with BAV (Gomez et al., 2009). A hypothesis of lineage-specific capacity in TGFβ responsiveness has been recently proposed (Lindsay and Dietz, 2011). The proximal ascending aorta is a mosaic of VSMCs derived from the cardiogenic mesoderm (second heart field) and the ectodermal cardiac neural crest (CNC), whereas the VSMCs in the aortic root are purely of mesoderm origin (Figure 4.2a) (Lindsay and Dietz, 2011). Based on experiments on the aorta of chick embryos, ectodermal VSMCs respond to TGFβ stimulation with increased DNA synthesis whereas mesodermal VSMCs show little activation with growth-inhibition (Topouzis and Majesky, 1996). Thus, in patients with BAV it can be hypothesized that the aortic root, which lies on the boundary of the CNC developmental field, would respond differentially to primary insults, such as genetic or haemodynamic aberrations, compared to the neighbouring ascending aorta. The aim of this study was to assess the degree of histological abnormalities and TGFβ signalling in aortic segments of distinct embryologic origin, which may explain the occurrence of diverse clinical phenotypes in BAV disease.

Figure 4.2 Developmental field boundaries in the thoracic ascending aorta (A). Binary nuclear pSmad2 activation (B). Two cell populations of either strong (brown nuclei) or absent (blue nuclei) pSmad2 signalling can be observed in the ascending aortic media of a patient with bicuspid aortic valve (x200 magnification).

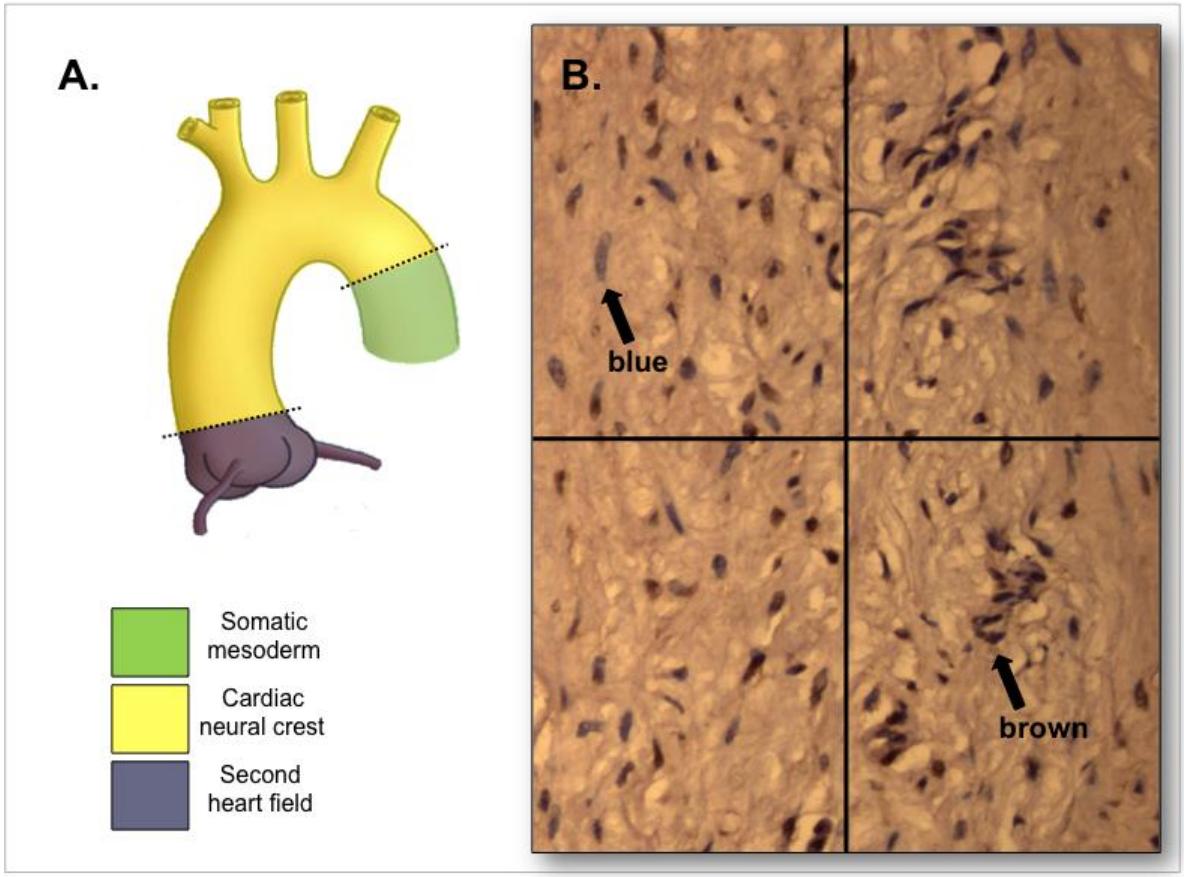

4.3 Methods

4.3.1 Aortic specimens

Informed consent was obtained from BAV patients planned to undergo surgery at the Royal Brompton Hospital, London. During the operation, tissue specimens (4mm x 2mm) were collected from the aortic root (within the sinuses) and the distal ascending aorta (>1cm above the sinutubular junction). Preoperative CMR imaging (Siemens 1.5T) was used for examination of BAV morphological subtypes, presence of valvular disease, and aortic diameter measurements. An electronic calculator was employed for calculation of z-scores at

the presented CMR-standardized aortic sites (aortic sinus and ascending aorta at the level of the right pulmonary artery) (Kaiser et al., 2008).

For the control group, age-matched structurally normal hearts were retrieved from patients who had not died from cardiovascular disease, held at the Cardiac Morphology Unit and the Department of Histopathology of the Royal Brompton Hospital. Coronary sinus and ascending aortic sections were obtained from the controls and compared to the surgical tissue samples from BAV patients.

Chapter 2 includes a detailed description of histological and immunohistochemical analyses. Figure 4.2b provides an example of image analysis application (**Chapter 2**) to assess pSmad2 immunolabeled frame areas of the media.

4.4 Results

4.4.1 Patient characteristics

Aortic tissue specimens from 18 BAV patients (22.5 years, [2-39]) were compared to 12 controls (27.5 years [6-41]). Three paediatric cases (age < 16 years) were included in each group. Thirteen out of the 18 BAV patients underwent targeted sequencing for a number of genes related to inherited aortopathy and BAV disease (results included in Table 4.6 under discussion, detailed description in **Chapter 7**). The majority of BAV patients (67%) were male and underwent aortic root replacement (50%). All BAV patients had valvular disease with predominant AR in 67% (Table 4.1). Standardized z-scores were used for assessment of aortic diameters in BAV subjects due to their wide age range. In the aortic root, median z-score was 4.91, [-1.14–9.94], with normal diameter ($-2 \leq z < 2$) in 6 (33%), mild dilation ($2 \leq z < 4$) in 1 (6%), and marked dilatation ($z \geq 4$) in 11 (61%) patients. Median z-score in the ascending aorta was 7.14, [1.19–16.72], with normal diameter in 2 (12%), mild dilation in 3 (17%), and marked dilatation in 13 (72%) patients.

As this was a relatively young population of BAV patients, none of the recruited subjects had any acquired cardiovascular disease risk factors or was on any anti-hypertensive pharmacological treatment, including ACE-inhibitors and angiotensin receptor blockers (ARBs) that might have affected the degree of pSmad2 signalling.

Table 4.1. Patient characteristics. CoA, coarctation of the aorta; CVD, cardiovascular disease; L-N, fusion of left and non-coronary leaflets; PDA, patent arterial duct; R-L, fusion of right and left-coronary leaflets; R-N, fusion of right and non-coronary leaflets; VSD, ventricular septal defect.

Patient characteristics (n=18)	
Age (y)	22.5 (2–39)
Male gender (n, %)	12 (66.7)
BAV type (n, %)	
True	6 (33.3)
R-N	5 (27.8)
R-L	4 (22.2)
L-N	1 (5.6)
Not available	2 (11.1)
Predominant BAV disease (n, %)	
Aortic regurgitation	12 (66.7)
Aortic stenosis	6 (33.3)
Type of operation (n, %)	
Ross	7 (38.8)
Root replacement	9 (50)
Bentall	2 (11.2)
Z score (median, range)	
Aortic root	4.91 (-1.14–9.94)
Ascending aorta	7.14 (1.19–16.72)
CVD risk factors (n, %)	
Hypertension	0 (0)
Diabetes	0 (0)
Smoking	0 (0)
Other CHD lesions (n, %)	
VSD	2 (11.1)
CoA	0 (0)
PDA	1 (5.5)

4.4.2 Histological findings

Severe medial wall abnormalities (≥ grade 2) were present in the aorta of BAV patients (Table 4.2). Paired analyses revealed significantly greater elastic fragmentation (12, 66.7% versus 6, 33.3%; p=0.034) and fibrosis (11, 61.1% versus 4, 22.2%, p=0.02) in the ascending

aorta compared to the aortic root of BAV subjects. Cyst-like formations occurred with similar frequency in the ascending aorta and root (8, 44.4% versus 10, 55.6%; p=0.48) whereas medionecrosis was absent in both segments. The overall histology grading score was greater in BAV patients compared to controls, both in the root (p<0.001) and in the ascending aorta (p<0.001; Table 4.2). Paired analysis in BAV patients reported a higher cumulative histology grading score in the ascending aorta compared to the root (5.5, [2-9] versus 4, [2-7]; p=0.004).

Table 4.2 Histological abnormalities in examined aortic specimens.

Variable	Control (n=12)		BAV (n=18)		P value*
	Root	Ascending aorta	Root	Ascending Aorta	
Histological Abnormalities (≥ grade 2), n (%)					
Elastic Fragmentation	0 (0)	0 (0)	**6 (33.3)**	**12 (66.7)**	**0.034**
Fibrosis	2 (16.7)	0 (0)	**4 (22.2)**	**11 (61.1)**	**0.02**
Medionecrosis	0 (0)	0 (0)	0 (0)	0 (0)	1
Cyst-like formations	0(0)	0 (0)	10 (55.6)	8 (44.4)	0.48
Histology grading score, median (range)	1 (0-3)	1 (0-1)	**4 (2-7)**	**5.5 (2-9)**	**0.004**
* Aortic root versus ascending aorta in BAV patients (paired analysis)					

No differences in histology grading score were noticed when BAV patients were subdivided by morphological subtypes. Paired analysis revealed a significantly higher histology score in the ascending aorta compared to the root (6, [2-9] versus 4, [2-6]; p=0.026) of BAV patients with regurgitant valve disease. No other histological differences were noticed between regurgitant and stenotic BAVs (Table 4.4). Overall, BAV patients with either ascending aortic or root dilatation (z-score ≥ 2) had greater medial wall degeneration in their ascending aorta compared to the root (paired analysis, Table 4.5). Similarly, comparison between BAV patients without and with aortic root dilatation, revealed significantly greater histology scores in the ascending aorta of the latter (4, [2-6] versus 6, [3-9]; p=0.029).

4.4.3 Immunohistochemical findings

Immohistochemical staining for pSmad2 was significantly greater in all three aortic wall layers of BAV patients compared to controls (Table 4.3, Figure 4.5). The cumulative pSmad2 staining was higher in the aortic root (38.1, [17-58] versus 12.1, [2-29]; p<0.001) and the ascending aorta (40.3, [8-49] versus 8.2, [4-37]; p<0.001) of BAV patients compared to controls (Table 4.3). Within BAV patients, there were no significant differences in pSmad2 signalling between the ascending aorta and the aortic root, both as a cumulative total percentage and in any of the separate aortic wall layers (Table 4.3).

Table 4.3 Percentage of pSmad2 signalling in patients and controls.

pSmad2%	BAV (n=18)	Control (n=12)	p value
Aortic root			
Intima	38.2 (6-79)	11.5 (2-19)	0.001
Media	38.7 (14-61)	10.7 (2-36)	<0.001
Adventitia	39.9 (25-59)	7.6 (2-15)	<0.001
Total	38.1 (17-58)	12.1 (2-29)	<0.001
Ascending Aorta			
Intima	30.5 (8-54)	7.6 (6-17)	<0.001
Media	40.3 (4-54)	7.9 (3-46)	0.001
Adventitia	43.9 (10-74)	10.2 (4-19)	<0.001
Total	40.3 (8-49)	8.2 (4-37)	<0.001

Morphological subtypes of BAV did not differ in levels of pSmad2 activation. Patients with regurgitant BAV disease had higher pSmad2 signalling in the media of the ascending aorta compared to those with stenotic valvular disease (44.6, [24-54] versus 18.1, [4-38]; p=0.001, Table 4.4). In contrast, paired analyses revealed that patients with stenotic BAVs had greater pSmad2 activation in the aortic root compared to the ascending aortic media (35.4, [30-61] versus 18.1, [4-38]; p=0.046, Table 4.4). No differences in pSmad2 activation in the media were noticed between patients with or without aortic dilation (z-score < 2) in either the root or the ascending aorta (Table 4.5). Patients without aortic root dilatation had greater pSmad2

signalling in the adventitia of their ascending aorta compared to those with root dilatation (55.8, [22-74] versus 29.1, [10-60]; p=0.039, Table 4.5). Paired analysis in BAV patients with aortic roots of normal diameters reported higher pSmad2 activation in the intima of the aortic root compared to the ascending aorta (41.4, [22-73] versus 22.8, [8-41]; p=0.046, Table 4.5).

In the overall population, a positive correlation was noticed between the percentage of pSmad2 signalling in the media and the degree of medial wall abnormalities, both in the aortic root (ρ=0.57; p=0.001) and the ascending aorta (ρ=0.6; p<0.001, Figure 4.3). When the grading score was broken down to its histological features, positive correlations were observed between pSmad2 activation in the ascending aortic media and the respective degree of elastic fragmentation (ρ=0.49; p=0.006), fibrosis (ρ=0.39; p=0.033), and cyst-like formations (ρ=0.59; p=0.001). In the aortic root, positive associations were noticed between pSmad2 signalling in the media and the levels of elastic fragmentation (ρ=0.38; p=0.036) and cyst-like formations (ρ=0.64; p<0.001) in the same area.

Table 4.4 Histological and immunohistochemical findings divided by aortic valvular disease.

Variable	Controls (n=12)	Regurgitant BAV (n=12)	Stenotic BAV (n=6)	P value*
Intima pSmad2%				
Aortic root	11.5 (2-19)	31.1 (6-73)	43.5 (8-79)	0.38
Ascending aorta	7.6 (6-17)	34.9 (8-54)	23 (10-45)	0.43
Media pSmad2%				
Aortic root	10.7 (2-36)	39.2 (14-58)	**35.4 (30-61)** †	0.96
Ascending aorta	11.8 (3-46)	**44.6 (24-54)**	**18.1 (4-38)**	**0.001**
Adventitia pSmad2%				
Aortic root	7.6 (2-15)	39.8 (25-59)	36.9 (25-53)	0.75
Ascending aorta	10.2 (4-19)	48.8 (10-74)	22.5 (15-61)	0.49
Total pSmad2%				
Aortic root	10.8 (2-29)	38.1 (17-58)	**37.2 (30-52)** †	0.89
Ascending aorta	8.2 (4-37)	**43 (21-49)**	**21 (8-41)**	**0.003**
Histology grading score				
Aortic root	1 (0-3)	**4 (2-6)** †	3 (2-7)	0.39
Ascending aorta	1 (0-1)	**6 (2-9)**	4 (4-6)	0.55

* Regurgitant versus stenotic BAV; †P <0.05, aortic root versus ascending aorta (Wilcoxon signed-rank test).

Table 4.5 Histological and immunohistochemical findings divided by absence (z-score < 2) or presence (z-score ≥ 2) of aortic dilatation.

Variable	Aortic root Z < 2 (n=6)	Aortic root Z ≥ 2 (n=12)	P value*¹	Ascending aorta Z < 2 (n=2)	Ascending aorta Z ≥ 2 (n=16)	P value*²
Intima pSmad2%						
Aortic root	**41.4 (22-73) †**	25.2 (6-79)	0.26	40.5 (8-73)	38 (6-79)	0.89
Ascending aorta	**22.8 (8-41)**	33.6 (10-54)	0.30	32 (23-41)	30.6 (8-54)	0.78
Media pSmad2%						
Aortic root	36.5 (30-52)	40.2 (14-61)	0.57	34.9 (31-38)	39.3 (14-61)	0.48
Ascending aorta	41.4 (18-47)	39 (4-54)	0.77	24.3 (4-44)	40.3 (14-54)	0.39
Adventitia pSmad2%						
Aortic root	37.6 (34-55)	39.3 (25-59)	0.92	36.4 (36-37)	39.9 (25-29)	0.39
Ascending aorta	**55.8 (22-74)**	**29.1 (10-60)**	**0.039**	34.9 (21-48)	44.4 (10-74)	0.57
Total pSmad2%						
Aortic root	38.6 (32-46)	36.8 (17-58)	0.92	34.8 (30-39)	38.1 (17-58)	0.67
Ascending aorta	41.7 (19-45)	34.9 (8-49)	0.77	26.2 (8-45)	40.3 (19-49)	0.57
Histology grading score						
Aortic root	2.5 (2-5)	**4 (2-7) †**	0.12	4.5 (4-5)	**3.5 (2-7)†**	0.39
Ascending aorta	**4 (2-6)**	**6 (3-9)**	**0.029**	5 (4-6)	**5.5 (2-9)**	0.94

***¹** Z score < 2 versus Z > 2 in the aortic root; ***²** Z score < 2 versus Z > 2 in the ascending aorta; †P <0.05, aortic root versus ascending aorta (paired analysis)

Figure 4.3 Correlation between medial pSmad2 signalling and histology grading score. The cumulative histology grading score for medial wall abnormalities in the aortic root **(A)** and the ascending aorta **(B)** correlated positively with the respective degree of pSmad2 signalling in the overall population.

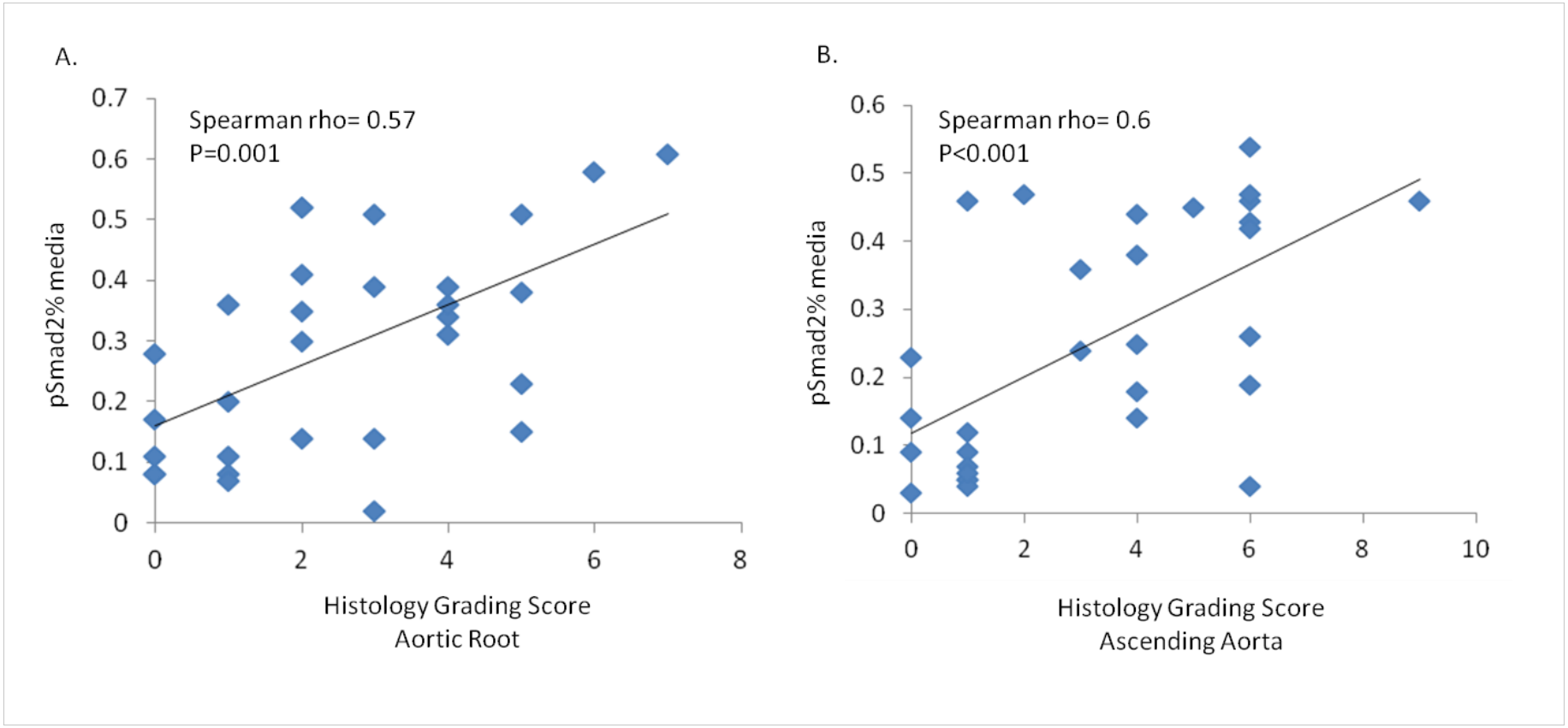

Figure 4.5 Representative overview of medial wall abnormalities and pSmad2 signalling in adjacent serial sections of the aortic root and the ascending aorta. The initrarily aligned and sparser elastic lamellae (*purple,* marked with arrows) of the healthy aortic root media can be seen in the elastic van Gieson (EVG) stained-sections. Immunolabelling for pSmad2 was uniformly distributed in the media of BAV patients and located in the proximity of mucoid degeneration areas (*pale blue*; corresponding alcian blue-stained sections, marked with asterisks). x200 magnification in all sections.

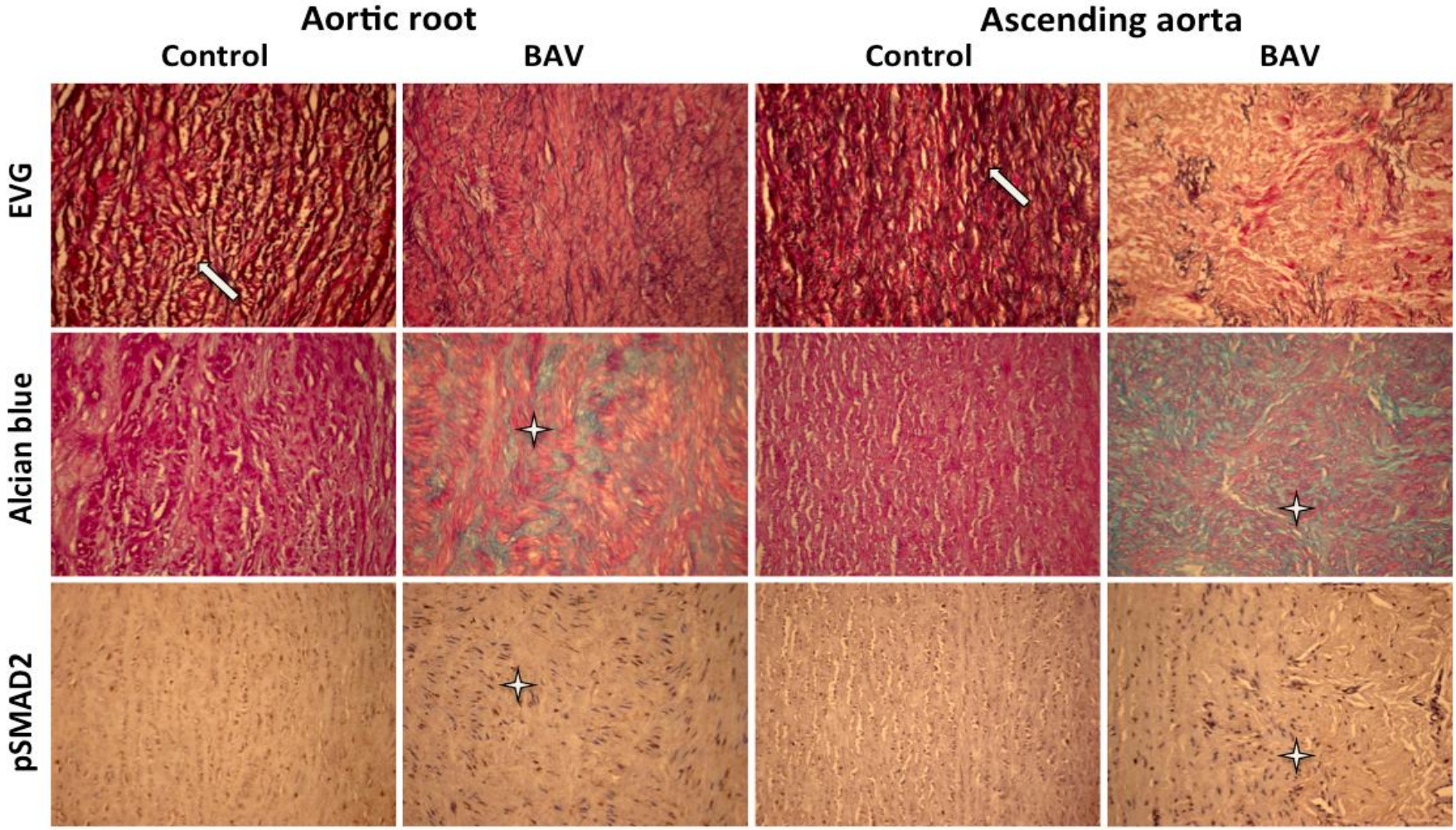

4.5 Discussion

This study demonstrates that severe structural abnormalities are present in the media of the aortic root and the ascending aorta of BAV patients, with an overall greater histology grading score in the ascending aortic segment, even in the presence of aortic root dilatation. Enhanced nuclear pSmad2 signaling was observed in the VSMCs of all aortic wall layers of BAV patients, with the presence of two distinct populations with either strong or absent immunostaining in both studied aortic segments. In the overall population, a positive correlation was noticed between the degree of medial pSmad2 activation and corresponding histology grading score in the aortic root and the ascending aorta, respectively.

4.5.1 The dilated root phenotype

Despite the existence of extensive literature on histological abnormalities of the dilated ascending aorta of BAV patients, the often affected aortic root in the same cohort has rarely been investigated (Girdauskas et al., 2011a). Aneurysms of the sinuses of Valsalva are infrequent and can be acquired or congenital, with concomitant valve abnormalities found in approximately 10% of patients (Ott, 2006). The relative paucity of the aneurysmal aortic root may also account for the lack of information on the morphology of the healthy sinuses (Iliopoulos et al., 2013). As illustrated by our histological findings and in agreement with a recent communication, the "bulge-shaped" non-pathologic sinuses have a more complex medial microstructure with arbitrarily aligned and sparser elastic lamellae compared to the bordering ascending aorta with coherent circumferential alignment of its elastic components (Figure 4.5) (Iliopoulos et al., 2013). This observation is of particular importance to future histological studies addressing the aneurysmal aortic root which mandates consideration of the less symmetric morphology of the healthy sinuses.

The "aortic root phenotype" has been increasingly recognized in BAV disease with up to 15% of affected patients presenting at a young age with predominant dilatation at the level of

the sinuses and various degrees of accompanying aortic valve annular dilatation with aortic insufficiency (Della Corte et al., 2007). Flow-induced changes secondary to BAV morphological variations may account for the observed different risks of aortic dilatation; fusion of the coronary leaflets has been linked to aortic root enlargement at a younger age whereas fusion of the right and non-coronary leaflets correlated with increased aortic arch dimensions (Schaefer et al., 2008, Schaefer et al., 2007, Russo et al., 2008). In this study, no histological differences were noticed between diverse BAV morphological subtypes. However, a greater histology grading score was observed in the ascending aorta compared to the root of patients with regurgitant BAV disease (Table 4.4). Similarly, BAV patients with root dilatation had greater degrees of medial wall degeneration in their ascending aorta compared to those without (Table 4.5). The above findings are in agreement with Roberts et al. who reported a much greater likelihood of significant elastic fragmentation in the ascending aorta of BAV patients with pure AR (Roberts et al., 2011). These observations would support the application of a lower threshold for surgical replacement of the BAV dilated ascending aorta in the instance of concomitant aortic root dilatation and/or predominant regurgitant valve disease (Roberts et al., 2011).

The genetic origin of BAV aortopathy has been supported by evidence of progressive ascending aortic dilatation following isolated aortic valve replacement (AVR), and thus removal of any additive haemodynamic factors secondary to the malformed valve (Girdauskas et al., 2011a). In contrast, incremental enlargement of the sinuses of Valsalva has rarely been reported following AVR (Park et al., 2011). In this study, when only BAV patients with present aortic root or ascending aortic dilatation (z-score ≥ 2) were considered, paired analyses reported a consistently higher histology grading score in the ascending aorta compared to the root of both groups (Table 4.5). Thus, this finding could explain the lower observed rates of aortic root dilatation in BAV disease and may advocate a more judicious

approach to prophylactic aortic root replacement in the presence of moderately dilated sinuses of Valsalva (Park et al., 2011).

4.5.2 TGFβ signalling

The culprit lesion in BAV aortic wall disease remains unknown although recent evidence point to a shared activation of the TGFβ/Smad pathway in TAAs of diverse aetiology, with the common end-result of medial wall degeneration (Milewicz et al., 2008, Gomez et al., 2009). High levels of pSmad2 activation have been observed in the aneurysmal ascending aorta of patients with syndromic TAA, such as MFS and LDS syndrome, and other non-syndromic forms including BAV and degenerative disease (Gomez et al., 2009, Maleszewski et al., 2009). Gomez et al. reported an average 46% nuclear pSmad2 staining in the media of the dilated ascending aorta of 15 BAV patients compared to our 40% in 16 BAV subjects with a respective z-score ≥ 2 (Table 4.5) (Gomez et al., 2009). Notably, the not-previously investigated aortic root and non-dilated ascending aorta were also examined in our study with significantly higher pSmad2 activation in BAV patients compared to controls (Tables 4.3, 4.5). Similarly to previous findings, pSmad2 immunolabelling was uniformly distributed in the media and located in the proximity of mucoid degeneration areas (Figure 4.5) (Gomez et al., 2009, Maleszewski et al., 2009). Overall, a positive correlation was noticed between the percentage of pSmad2 signalling in the media and the degree of medial wall abnormalities, both in the aortic root and the ascending aorta, which was in agreement with Gomez et al. who reported a similar association between the cumulative medial pSmad2 activation and elastic fragmentation in the aneurysmal ascending aortic wall of different aetiologies (Figure 4.4) (Gomez et al., 2009).

Despite the above associations, the exact sequence of mechanisms leading to medial wall degeneration downstream TGFβ signalling remains elusive (Figure 4.1). The general mechanistic hypothesis in MFS is that fibrillin-1 (FBN1) deficiency, secondary to *FBN1* gene

mutations, makes sequestered TGFβ more accessible to activation with subsequent matrix proteolysis via release of MMP-2 and -9 (El-Hamamsy and Yacoub, 2009a, Carta et al., 2009). The paradox of amplified TGFβ signalling in LDS patients with *TGFBR1* or *TGFBR2* mutations is less well understood with potential mechanisms including activation of SMAD2/3 in response to TGFβ1 by other signalling mediators without direct interaction with TGFβ receptors (Jones et al., 2009, Gomez et al., 2009). Preliminary genetic sequencing in 13 out of 18 BAV subjects participating in this study revealed novel variants in the *NOTCH1* gene, which has been linked to calcified BAV disease and associated aneurysm formation (Table 4.6) (Garg et al., 2005). Despite the reported absence of *FBN1* gene mutations in isolated BAV disease in the literature, a reduction in fibrillin-1 expression in the extracellular matrix of dilated BAV aortas has been described and in fact, two of our studied subjects tested positive for *FBN1* mutations which merit further investigation (Laforest and Nemer, 2012, Nataatmadja et al., 2003). None of our sequenced patients tested positive for mutations in *TGFBR1* or *TGFBR2* genes, although a single patient had a mutation in the gene encoding for *TGFβ1*. Finally, all genetically tested patients carried a *SMAD3* known common variant, albeit mutations in this gene have been linked to aortic aneurysms with early-onset osteoarthritis (van de Laar et al., 2011). Next-generation sequencing results are discussed in more detail in **Chapter 7**.

Table 4.6 Next-generation sequencing results (selected genes) in BAV patients. AA; amino-acid, * mutations in the same individual.

BAV subjects (n)	Gene	AA change	Clinical significance
13/13	*SMAD3*	Tyr85Cys	Common variant
3/13	*NOTCH1*	Ser2170Asn* Asn197Lys Arg1761Gln	Novel (putative benign) Novel (probably damaging) Novel (possibly damaging)
2/13	*FBN1*	Val670Met Pro809Leu*	Probable-pathogenic Novel (probably damaging)
1/13	*TGFB1*	Leu8Met	Novel (probably damaging)

Another potential mechanism underlying increased TGFβ signalling in aortopathy relates to the embryologic origin of VSMCs in neighbouring thoracic aortic segments and their differential TGFβ responsiveness (Figure 4.2a) (Topouzis and Majesky, 1996, Lindsay and Dietz, 2011). It is hypothesized that VSMCs in the aortic root and neighbouring ascending aorta respond differentially to primary insults, such as FBN1 deficiency or loss of function mutations of TGFBR1 and TGFBR2, with the more "vulnerable" mesodermal cells in the root loosing TGFβ feedback inhibition and the more "tolerant" ectodermal cells in the ascending aorta responding to compensatory mechanisms of increased TGFβ ligand expression (Lindsay and Dietz, 2011). The binary status of nuclear pSmad2 signalling, with either strong or absent activity in VSMCs of the media, as shown in the aortic root of a LDS patient by Lindsay et al. and in BAV disease by our study, would favour this theory (Figure 4.2b) (Lindsay and Dietz, 2011). However, we were unable to detect any significant differences across all aortic wall layers in the degree of pSmad2 immuno-labelling between the BAV aortic root and ascending aorta (Table 4.1).

Overall, the initial trigger for increased TGFβ signalling in the BAV aorta remains to be identified, although the presence of equally increased pSmad2 activation in dilated and non-dilated aortic segments points to a genetic substrate (Table 4.5). VSMCs have also been shown to be responsive to haemodynamic perturbations with downstream alteration of their proliferative, contractile, or synthetic properties, including TGFβ1 expression induced by increased shear stress (El-Hamamsy and Yacoub, 2009a, Topper et al., 1996, Ohno et al., 1995). However, unexpected findings were revealed upon examination of the haemodynamic influence on pSmad2 activation; patients with regurgitant BAV disease had increased signalling in their ascending aorta whereas paired analyses revealed higher signals in the aortic root of patients with stenotic BAV disease (Table 4.4). If haemodynamic alterations were indeed in operation, the opposite effect would be expected, as regurgitant BAVs are

thought to increase wall tension, due to higher stroke volumes, and correlate with aortic root dilatation whereas stenotic BAVs generate a high-velocity jet imposing increased longitudinal stress on the ascending aorta (Tadros et al., 2009).

4.5.3 Limitations

This study is limited by the small number of tissue samples and longer formalin-fixation of control samples (stored at the biobank of the Cardiac Morphology Unit, Royal Brompton Hospital) which may have affected our immunohistochemical analyses. However, it is the first study of its kind including histology of both the aortic root and ascending aortic segments with uniform application of optimized pSmad2 antibody concentration in all studied tissue samples. Genetic testing was available in a subset of BAV patients and merits further validation. Immunostaining for TGFβ1 and potential co-localization with pSmad2 activation was not performed, albeit outside the scope of this study which was to provide preliminary data on the aortic root phenotype in BAV disease. Sub-group analyses in BAV patients with and without aortic dilatation may have been underpowered due to the limited number of patients in the non-dilated groups. Interquartile range of z-scores could have been used to sub-divide our population as an alternative method. However, it was decided to use the cut-off z score of greater or less than 2, for clinically relevant interpretation of data.

4.6 Conclusions

Patients with BAV have marked histological abnormalities in both their aortic root and ascending aorta. The dilated aortic root phenotype may represent the primarily genetic form of BAV disease as patients with either root dilatation and/or predominant regurgitant valve disease had greater levels of medial wall degeneration in their ascending aorta. In contrast, structural abnormalities in the aortic root per se were lower compared to these seen in the ascending aorta, even in the presence of root dilatation, and may advocate a more judicious approach to prophylactic aortic root replacement in this cohort. Increased nuclear pSmad2

signalling was observed in the BAV aorta and did not differ significantly between the mesoderm-derived root and the ectoderm-derived ascending aorta. The presence of enhanced pSmad2 activation in non-dilated BAV aortic segments points to a genetic trigger whereas any haemodynamic influence secondary to valvular disease appears less operative. It was thus, decided to further investigate the genetic basis of BAV disease and associated aortopathy with application of state-of-the-art genetic sequencing tools (**Chapters 6 and 7**).

Chapter 5. PAH model of aortopathy

Abbreviations

Ao Aortic
ASD Atrial septal defect
ASO arterial switch operation
BAV Bicuspid aortic valve
CHD Congenital heart disease
ES Eisenmenger syndrome
HGS Histology grading score
LPA Left pulmonary artery
LV Left ventricular
MFS Marfan syndrome
PAH Pulmonary arterial hypertension
PDA Patent arterial duct
PT Pulmonary trunk
PT/Ao MT Pulmonary trunk-to-aortic media thickness
RPA Right pulmonary artery
STJ Sinutubular junction
TAA Thoracic aortic aneurysm
TGA Transposition of the great arteries
TOF Tetralogy of Fallot
VSD Ventricular septal defect

5.2 Abstract

Background: Pulmonary arterial hypertension (PAH) is considered primarily a disease of the distal pulmonary arteries but also affects the larger proximal pulmonary arteries causing them to become aneurysmal. With this study, we aimed to examine arterial wall remodelling in PAH associated with CHD, which can serve as an aortopathy model for medial wall changes in relation to elevated haemodynamic stress.

Methods: Tissue samples from the great arteries (pulmonary trunk and aorta) of 10 formalin-fixed human hearts from patients with PAH/CHD were examined via light microscopy and compared to age-matched healthy controls. A detailed histology grading score was used to assess the severity of medial wall abnormalities.

Results: Significant medial wall abnormalities (grade ≥ 2) were present in the pulmonary trunk (PT), including fibrosis (80%), and atypical elastic pattern (80%). Cyst-like formations were present in less than one third of patients and were severe in a single case leading to wall rupture. The cumulative PT histology grading score was significantly higher in PAH/CHD cases compared to controls ($p<0.0001$) and correlated positively with larger vessel diameter ($\rho=0.812$, $p<0.0001$) and greater degrees of medial wall hypertrophy ($\rho=0.749$, $p<0.0001$). Significant medial wall abnormalities were also found in the aorta of PAH/CHD patients, including fibrosis (60%), elastic fragmentation (10%), and medionecrosis (10%).

Conclusion: Chronic PAH in association with CHD results in marked medial wall abnormalities in the large pulmonary arteries. Structural defects also existed in the aorta of PAH/CHD patients, suggestive of inherent abnormalities of the great arterial walls which are further enhanced in the PT due to elevated intravascular pressures.

5.3 Introduction

As seen in **Chapters 3 & 4**, medial wall abnormalities are found at different segments of the BAV aorta and their asymmetrical patterns of dilatation may be owing to haemodynamic vascular remodelling on the background of an inherent structural weakness. Histological abnormalities underlying TAA formation and dissection have been described as early as the 1930s with the term "cystic medial necrosis" established by Erdheim, although later disputed (Niwa et al., 2001, Erdheim, 1930). MFS has served as the typical aortopathy model in inherited TAA disease since the discovery of causative fibrillin-1 mutations by Dietz and colleagues in 1991 (Dietz et al., 1991). As thoracic aortic complications in patients with congenital heart disease (CHD) became increasingly recognised, research focus broadened from connective tissue disorders to a wide array of inborn heart defects. In fact, medial wall abnormalities, similar to those seen in MFS and BAV, have been described in a wider range of disparate congenital heart defects, including coarctation of the aorta, Tetralogy of Fallot (TOF), complete transposition of the great arteries (TGA), atrial septal defect (ASD) and ventricular septal defect (VSD) (Niwa et al., 2001).

The above abnormalities can affect both the proximal aorta and pulmonary trunks of CHD patients and are thought to be associated with or account for progressive vessel wall dilatation with aneurysm formation and rupture. Approximately 10% of adults with CHD develop PAH of variable severity, with Eisenmenger syndrome representing its extreme manifestation (Diller and Gatzoulis, 2007). Apart from the distal small muscular pulmonary arteries, the pulmonary trunk and its large elastic branches are also affected in this setting, with previous reports of aneurysmal dilatation, atherosclerosis and thrombosis (Heath et al., 1960, Daliento et al., 2002, Broberg et al., 2007). It remains unknown whether structural defects of the pulmonary trunk wall is purely the result of distal pulmonary vascular disease and PAH or

whether there is an additional contribution from the above described intrinsic abnormalities associated with the underlying cardiac defect (Botney, 1999, Prapa et al., 2013).

Normally, morphological changes in the elastic pulmonary artery take place after birth and relate to the imposed intravascular pressures. Due to the presence of pulmonary hypertension in the healthy foetus, the media of the pulmonary trunk resembles that of the aorta during the first six months of life, with long, parallel and uniform elastic lamellae (Heath and Edwards, 1960). By the second year, pressures in the pulmonary artery fall and the media acquires its normal "adult" configuration with short fragmented fibrils and sparser elastic tissue. In patients with CHD associated with pulmonary hypertension, the pulmonary trunk may retain its "aortic" configuration or undergo transition to its "adult" elastic pattern, depending on whether the hypertension dates from birth or develops later in life (Heath and Edwards, 1960).

Aneurysms of the hypertensive pulmonary trunk have been described in a number of CHD lesions, including PDA, ASD, VSD, and TGA with nonrestrictive VSD (Niwa et al., 2001, Veldtman et al., 2003). The aim of this study was to assess the histological features of the large elastic pulmonary arteries and aorta in adult patients with PAH/CHD, with an aim to apply this knowledge to an 'aortopathy' model for haemodynamically-induced vascular remodelling in the setting of BAV, as investigated in **Chapter 3**.

5.4 Methods

5.4.1 Tissue specimens

Heart specimens from adult PAH/CHD patients, who died between 1975 and 1999, were retrieved from our cardiac morphology archive (Royal Brompton Hospital, London, UK) of formalin-fixed hearts. For the control group, age-matched structurally normal hearts were

retrieved from subjects who were not known to have suffered from any congenital heart abnormality and had not died from a cardiovascular cause.

5.4.2 Macroscopic analysis

Circumference measurements of the luminal surface of the pulmonary trunk (PT) and aorta were made 5mm above the sinutubular junction (STJ) with additional measurements of the internal circumference of the right and left main pulmonary artery (RPA and LPA), just above the PT bifurcation. All diameter measurements were indexed to the length of the left ventricle (LV), defined as the left atrioventricular junction to left ventricular apex distance, to account for differences in age/patient size and presence of a rudimentary morphological right ventricle in 3 patients with congenital heart defects.

5.4.3 Microscopic analysis

Full thickness sections of the PT and aorta were dissected 5mm distally to the STJ. RPA and LPA sections were obtained directly above the bifurcation level. **Chapter 2** provides a detailed description of histological analyses undertaken for examination of the aorta. The same methods were used for examination of the elastic pulmonary arteries (PT, RPA and LPA) which were also assessed for medionecrosis, fibrosis, and cystic-like formations, applying histological criteria adopted for the pulmonary artery (grades 0-3) (Bedard et al., 2009, de Sa et al., 1999).

As described above, by the second year of life the healthy PT looses its resemblance to the aorta and acquires its adult pattern with short fragmented fibrils and sparser elastic tissue. The media also becomes thinner with a pulmonary trunk-to-aortic media thickness (PT/Ao MT) ratio of 0.4 to 0.7 (Heath et al., 1959). In this study, the PT elastic tissue configuration was examined using the Heath classification and the PT/Ao MT ratio was calculated (Heath and Edwards, 1960). Due to these physiological morphologic adaptations of the PT, an ‘inversed’ score was used to evaluate the severity of elastic fragmentation in the pulmonary

arteries compared to that of the aorta. Thus, specimens with the normal pulmonary pattern of short, overlapping and fragmented lamellae were graded as 0 whereas those with complete absence of elastic fragmentation resembling the 'aortic' phenotype (Heath and Edwards, 1960), were classified as grade 3 atypical elastic pattern (Figure 5.1c).

The elastic components of the PT and aortic media were also examined using elastic van Gieson stain and colour image analysis (Quantimet 500C QWIN V02.00B, *Leica, Cambridge, UK*) (Salih et al., 2004). Following identification of populations of elastic fibres crossing the midline of a frame area (20x magnification), the percentage of elastin and collagen exhibiting staining for each population was measured. For each examined tissue specimen, the mean elastin/collagen ratio was calculated by obtaining a percentage of elastin and collagen in 5 frame areas.

5.4.4 Histology grading scores

As detailed in **Chapter 2**, a histology grading score (HGS) was calculated to assess the severity of medial wall abnormalities in the great arteries (Tan et al., 2005). In the case of the pulmonary arteries, the HGS included the 'atypical elastic pattern' (grades 0 to 3) described above to report the severity of elastic fragmentation.

5.5 Results

Tissue specimens were collected from 10 formalin-fixed hearts from adult PAH/CHD patients (29.5 years, [22 years-83 years]) and compared to 10 healthy controls (44.5 years, [19years-70 years]). Patient clinical characteristics are summarised in Table 5.1. None of the CHD patients had undergone surgery apart from the 24-year-old female with situs inversus and ASD who underwent atrial partition with mitral valve repair at the age of 19 years. Branch pulmonary arteries were not available in the control hearts and the LPA was not available in a single PAH/CHD patient.

Table 5.1 Patient characteristics. Abbreviations: ASD, atrial septal defect; CFH, congestive heart failure; DILV, double inlet left ventricle; LPA, left pulmonary artery; MV, mitral valve; PDA, patent ductus arteriosus; PAH, pulmonary arterial hypertension; TGA, transposition of the great arteries; TV, tricuspid valve; VSD, ventricular septal defect; SCD, sudden cardiac death

Age deceased	Gender	Mode of death	CHD	Lung histology
22y	male	CHF	TV atresia, ASD, VSD	Medial/intimal hyperplasia
24y	female	SCD	Situs inversus, ASD, cleft MV	Medial/intimal hyperplasia
29y	male	SCD	DILV, VSD, PDA	Dilated plexiform lesions
29y	female	CHF	VSD, PDA	Dilated plexiform lesions
29y	female	Non-cardiac	ASD, VSD, PDA	Dilated plexiform lesions
30y	male	CHF	DILV, TGA, VSD	Mild hypertensive changes
35y	male	SCD	PDA	Medial/intimal hyperplasia
55y	female	CHF	PDA	Dilated plexiform lesions
59y	female	CHF	ASD	Mild hypertensive changes
83y	female	CHF	ASD	Consistent with PAH but no dilatation/plexiform lesions

5.5.1 Pulmonary trunk

The PT/LV index of PAH/CHD patients (median 1.33, [0.94-2.07]) was significantly higher compared to controls (0.75, [0.57- 0.92]; p <0.0001). The majority of PAH/CHD patients had severe medial wall abnormalities (≥ grade 2) in their PT, including fibrosis (80%) and atypical elastic pattern (80%) (Figure 5.2). Only a single case (10%) had medionecrosis and cyst-like formations, which were both of mild degree (grade 1). The PT elastic tissue configuration was abnormal in all PAH/CHD patients: 8 (80%) had transitional and 2 (20%) had aortic configuration (Figure 5.1c). The PT/Ao MT ratio was significantly higher in PAH/CHD (1.0, [0.5-1.8]) compared to controls (0.5, [0.4 to 0.7]; p<0.0001). The cumulative HGS for PT medial wall abnormalities was significantly higher in PAH/CHD (6, [4 to 7])

compared to controls (3, [2 to 3]; p<0.0001) (Figure 5.3). Overall, the cumulative PT HGS correlated positively with the degree of medial hypertrophy (PT/Ao MT ratio) (ρ=0.749, p <0.0001) as well as PT diameter (PT/LV index) (ρ=0.812, p <0.0001) (Figure 5.4).

5.5.2 Main pulmonary artery branches

The median diameter of the LPA and RPA at bifurcation level was 2.5cm [1.4-3.1] and 2.1cm [1.6-3.5], respectively. Significant medial wall abnormalities (grade ≥ 2) were present in the pulmonary artery branches of the majority of patients, including fibrosis (60%, right; 44%, left), atypical elastic pattern (90%, right; 100%, left), medionecrosis (20%, right; 22%, left) and cyst-like formations (11%, left branch only) (Figure 5.2). All patients had abnormal elastic tissue configuration, which was transitional in 90% and aortic in 10% of the RPA branches, and transitional in 88% and aortic in 11% of the LPA branches. The cumulative HGS was similar in the branches and PT of PAH/CHD patients (PT 6, [4 to 7]) versus LPA (5, [4-8]; p=0.72 and RPA (6, [4-7]; p=0.56).

Figure 5.1 A. The vicious circle of vascular remodelling in pulmonary arterial hypertension (PAH). PAs, pulmonary arteries; PAP, pulmonary arterial pressure; RV, right ventricle; VVC, ventricular-vascular coupling. Diagram based on figure by Wang and Chesler (Wang and Chesler, 2012). **B. Correlation between elastin/collagen ratio and age.** Patients and controls are highlighted in red triangles and blue dots, respectively. **C. Elastic tissue configuration and histological abnormalities in the pulmonary trunk (PT) of congenital heart disease (CHD) PAH patients.** Normally, the PT elastic tissue configuration loses its resemblance to the aorta (*aortic; transitional*) by the second year of life and acquires its adult pattern (*adult pulmonary*) with short fragmented fibrils and sparser elastic tissue. Principal histological features in the PT of PAH/CHD patients included fibrosis and atypical elastic pattern resembling that of the aorta (*PAH/CHD*). Elastic van Gieson stain, magnification x200.

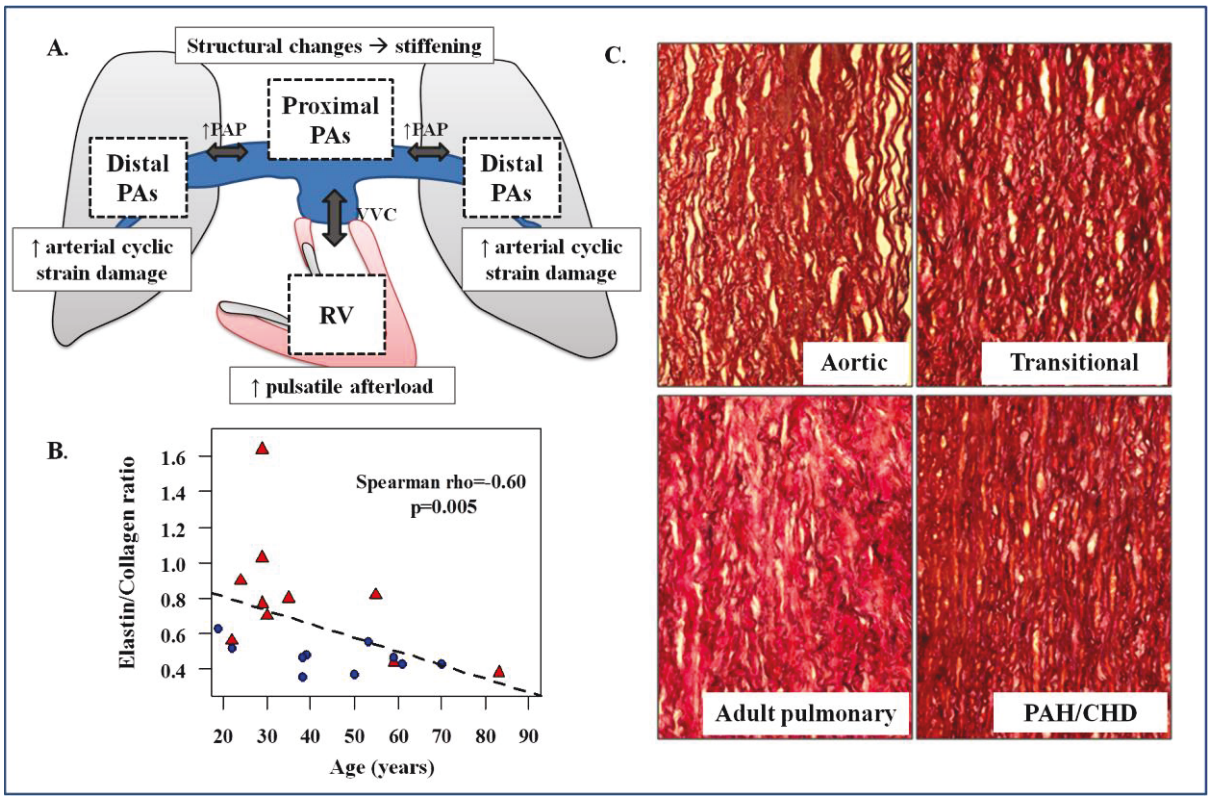

5.5.3 Aorta

The aortic diameter (Ao/LV index) of PAH/CHD cases and controls did not differ significantly (0.27, [0.18-0.47] versus 0.29, [0.22-0.36]; p=0.94). Significant medial wall abnormalities (grade ≥ 2) were present in the aorta of PAH/CHD patients, including fibrosis (60%), elastic fragmentation (10%), and medionecrosis (10%). Cyst-like formations were absent in all cases (Figure 5.2). Medial wall hypertrophy was significantly lower in PAH/CHD compared to controls (p<0.0001). The cumulative HGS for aortic medial abnormalities was significantly higher in PAH/CHD patients compared to controls (2.5, [0-4] versus 1, [0-2]; p=0.008) (Figure 5.3).

5.5.4 Elastic components of the media

The median elastin/collagen ratio was significantly higher in PAH/CHD patients compared to controls (0.78 [0.38-1.64] versus 0.46 [0.38-1.64]; p=0.009). Advanced age correlated with lower elastin/collagen ratio in the overall study population (ρ=-0.587, p=0.006) (Figure 5.1b).

Figure 5.2 Histological changes in the great arteries. Histological changes in the media (≥ grade 2) and intima of the pulmonary trunk, right and left pulmonary arteries (RPA, LPA) **(A)** and aorta **(B)**. Significant fibrosis with diffuse intimal thickening were common findings in the pulmonary arteries **(C*1)** whereas cyst-like formations were rarely seen **(C*2)**. Elastic van Gieson (C*1) and alcian blue (C*2) stain, magnification x200.

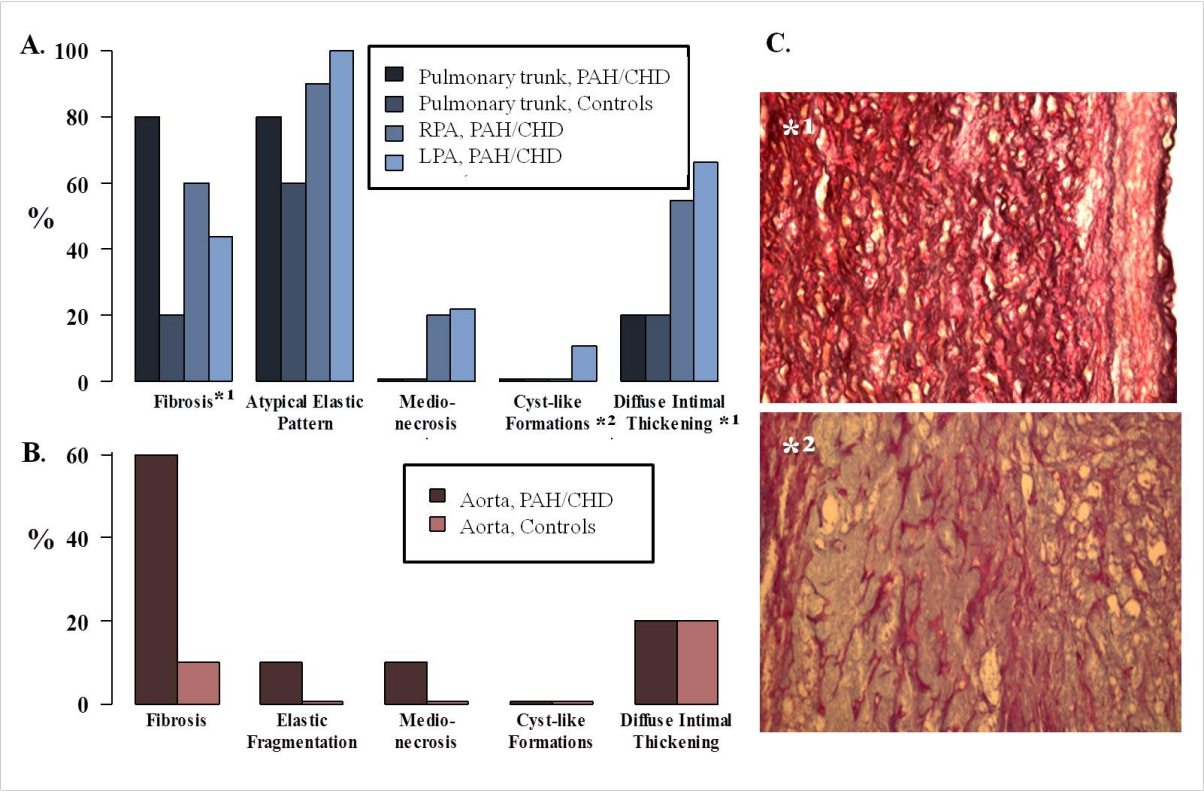

Figure 5.3 Histology grading scores (HGS) for the great arteries. The cumulative HGS for medial wall abnormalities in the pulmonary trunk **(A)** and aorta **(B)** was significantly higher in PAH/CHD cases versus controls.

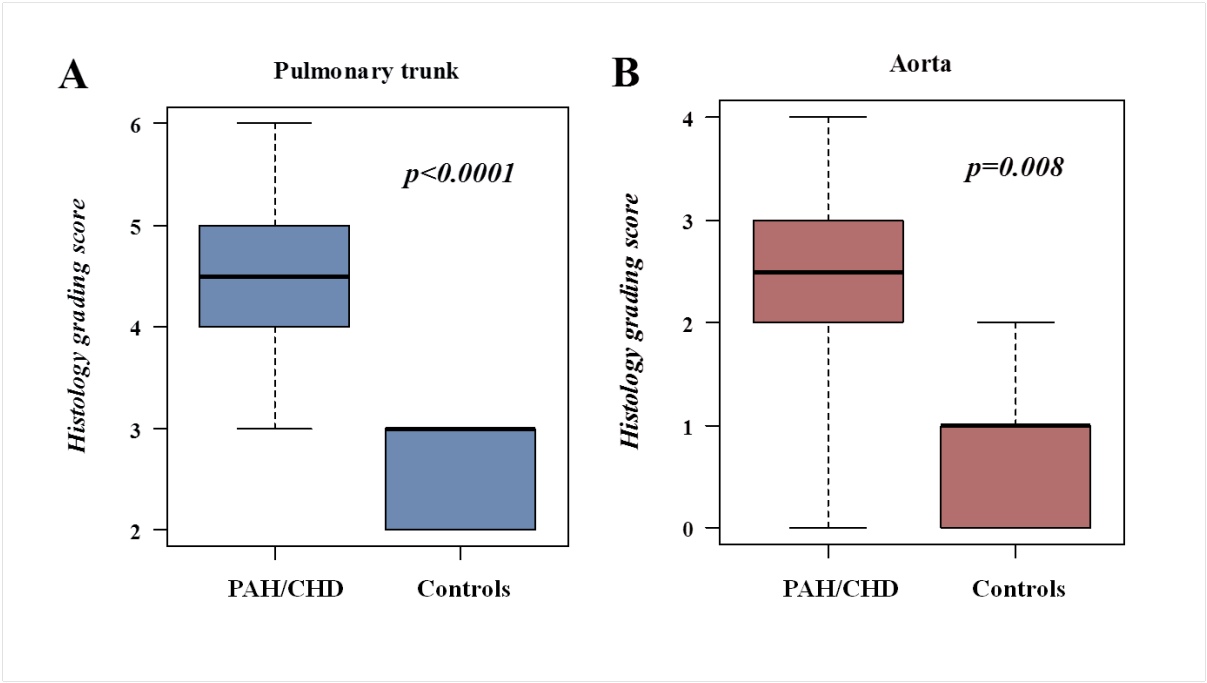

5.6 Discussion

In patients with PAH/CHD, histological abnormalities are not restricted in the small muscular pulmonary arteries but are also present in the pulmonary trunk and its large elastic branches. Commonly encountered histological findings included fibrosis and atypical elastic pattern whereas cyst-like formations and medionecrosis were rarely seen, which together with the aortic phenotype of the media, may explain the low incidence of dissection of aneurysmal PTs in PAH/CHD (Tredal et al., 1974). Structural abnormalities were also found in the aorta of PAH/CHD patients, suggestive of inherent abnormalities of the great arterial walls.

Figure 5.4 Correlation between PT HGS, vessel diameter and medial hypertrophy. The cumulative histology grading score (HGS) for medial wall abnormalities of the pulmonary trunk (PT) correlated positively with the degree of medial wall thickness **(A)** and larger vessel diameter **(B)**. LV, left ventricle. Patients are depicted in red triangles and controls in blue dots.

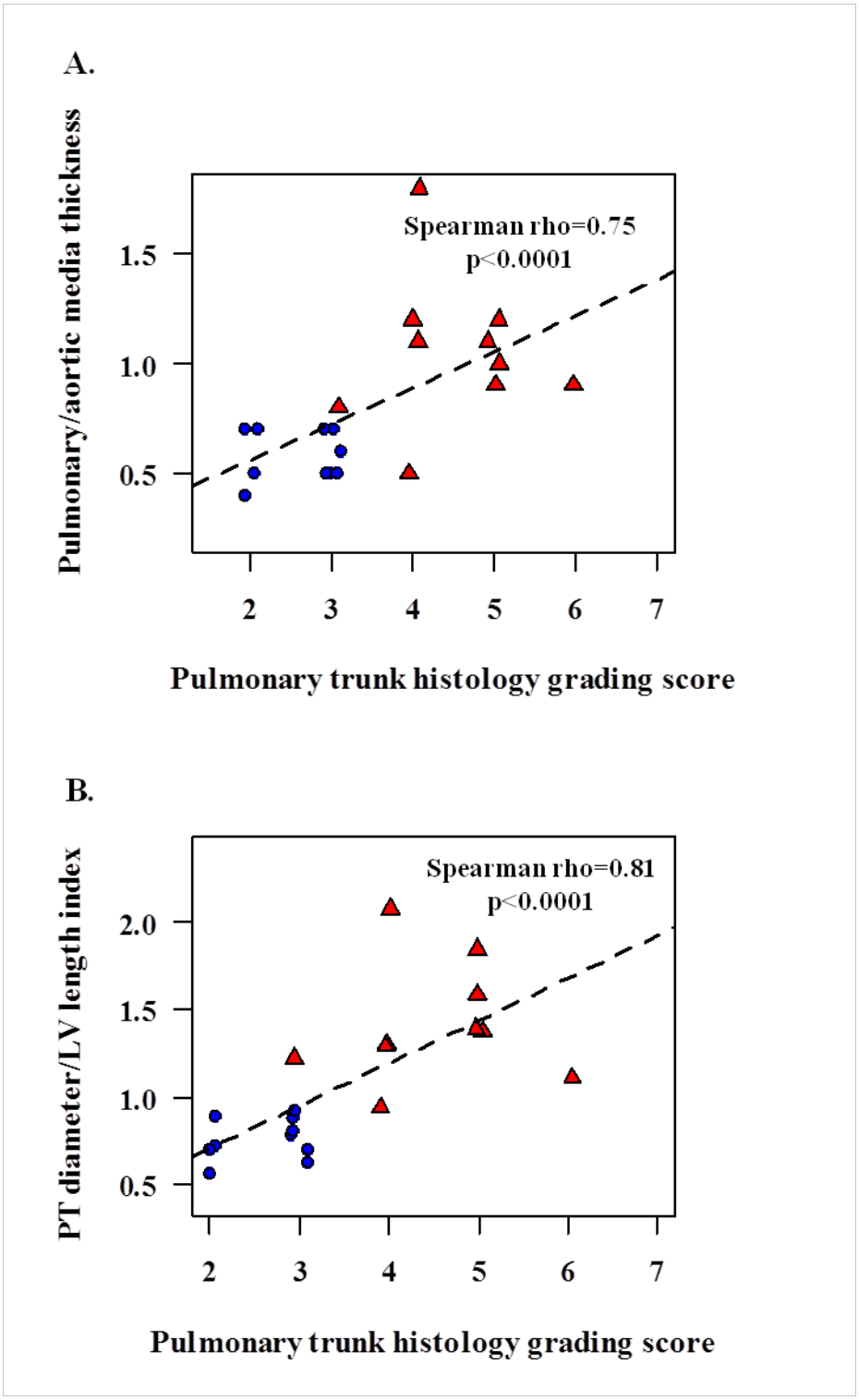

5.5.1 Medial wall abnormalities in the elastic pulmonary arteries

Significant abnormalities (grade ≥ 2) were present in the majority of the elastic PAs of PAH/CHD patients (Tredal et al., 1974, Niwa et al., 2001). Fibrosis was the predominant described histological feature in the media, with atypical architecture of the elastic lamellae similar to that of the aorta. Similarly, fibrotic changes were present in the BAV aorta (**Chapter 3**) which correlated strongly with the degree of mechanical stress exerted to the aortic wall. Haemodynamic data were incomplete in this data set and thus, correlations between stress and histological changes in the hypertensive PT could not be made in analogy to the BAV aorta. However, the significant volume and pressure overload of the pulmonary circulation in the setting of PAH may equally account for these changes.

Arterial wall remodelling in response to increased radial stress has been studied in patients with systemic hypertension with findings of altered contribution of the elastic components of the media (elastic lamellae fracture and increased collagen turnover) and dilatation of the vessel wall dilatation with hypertrophy and increased stiffness (Humphrey, 2008). In this study, a greater elastin/collagen ratio was noticed in the PAH-CHD cases compared to controls, with an abundance of collagen as age increased in the overall population (Figure 5.1b). The close correlation between the above medial changes, vessel size and medial hypertrophy (Figure 5.4), supports the pathophysiological link between the severity of PAH and the structural abnormalities (Prapa et al., 2013).

Conversely, cyst-like formations were present in less than one third of PAH patients and only in a single case (24y female with situs inversus and atrial septal defect, Table 5.1) were they significant (grade 2) and resulted in recurrent wall rupture of the left pulmonary artery, which was proven fatal. Medial cyst-like formations have been described as the only potential histological feature differentiating the dissecting aorta from normotensive and hypertensive controls (Manley, 1964). It has been previously suggested that the relatively low rate of

dissection and pulmonary artery rupture in PAH/CHD may be due to the rarity of cyst-like formations as an underlying histological feature (Tredal et al., 1974). In patients with BAV, cyst-like formations are more frequently found (**Chapters 3 and 4**) and may reflect a proteolytic process which renders the arterial wall susceptible to dissection and rupture.

5.5.2 Determinants of aortopathy in CHD lesions

Interestingly, a higher cumulative histology grading score was noted not only in the PT but also in the aorta of PAH/CHD cases compared to controls. Inherent abnormalities of the great arteries have been previously reported in normotensive subjects with a variety of CHD lesions and may reflect the paradigm of BAV disease affecting both of the great vessels, possibly due to perturbations in their common embryologic origin, the conotruncus (**Chapter 1**) (Niwa et al., 2001). Similar to the haemodynamic theory of aortopathy in BAV disease, the above findings raise the possibility of elevated intravascular pressures further enhancing intrinsic structural defects of the pulmonary trunk in the setting of PAH.

Medial wall abnormalities also exist in the normotensive dilated pulmonary trunk of patients with pulmonary valve stenosis, either isolated or as part of TOF (Niwa et al., 2001, Veldtman et al., 2003, Bedard et al., 2009). It is postulated that in utero haemodynamic perturbations secondary to the malformed pulmonary valve contribute to degeneration of the pulmonary artery media, similar to the so-called "post-stenotic" dilatation in BAV disease. Importantly, changes in the media of the TOF pulmonary trunk persist even after reparative surgery, suggestive of irreversible remodelling of the vessel wall (Bedard et al., 2009) resembling the progressive aortic dilation seen in BAV patients following aortic valve replacement (Andrus et al., 2003).

5.5.2 Clinical implications of PT wall abnormalities

Regardless of the origin of structural abnormalities in the pulmonary artery, their existence may have important implications in surgical planning and late post-operative complications.

An exemplary case is that of arterial switch operation (ASO) for anatomical repair of complete transposition of the great arteries. Medial wall abnormalities are present in the pulmonary trunk (neoaorta) leading to development of neoaortic root dilation and aortic regurgitation in 16% of patients approximately 5 years following ASO (Losay et al., 2001). Similarly, pulmonary valve auto-transplantation (Ross procedure) remains controversial in young patients with BAV in need of aortic valve replacement with histological abnormalities of the pulmonary root potentially accounting for postoperative pulmonary autograft dilation (**Chapter 1**) (de Sa et al., 1999).

The histological changes detected in this study are also likely to affect the compliance of the proximal pulmonary arteries and have a negative impact on pulmonary perfusion and right ventricular function. The healthy PT wall is intrinsically more compliant compared to that of the aorta, due to the greater wall thickness of the latter and differences in the medial structure (Harris et al., 1965). In PAH, several studies have illustrated reduced extensibility of the PT which has been attributed to altered distribution of medial elastic components (Zuckerman et al., 1991, Reuben, 1971, Jarmakani et al., 1971). Pulmonary arterial stiffness has a key role in the vicious circle of vascular remodelling in PAH, with elastance of the pulmonary circulation comprising an essential component of afterload maintenance via adequacy of the right ventricular - pulmonary arterial coupling (Wang and Chesler, 2012).

Narrowing of the distal pulmonary arteries in PAH increases mean pulmonary arterial pressure leading to exertion of enhanced circumferential stress to the proximal large pulmonary vessels with distension and hypertrophy of the arterial wall (Figure 5.1a). The above changes contribute to proximal vascular stiffening which, in turn, results in increased downstream flow pulsatility and damage of the microvascular pulmonary endothelium (Bedard et al., 2009). Current therapies for PAH are primarily focused on remodelling of the small muscular pulmonary arteries (Diller and Gatzoulis, 2007). In view of the significant

potential impact of PT stiffness on both the right ventricle and distal vasculature, the large elastic pulmonary arteries consist emerging novel therapeutic targets in PAH/CHD.

5.6 Study limitations

This study is restricted by the small number of tissue specimens and lack of PT branches in control subjects. Indexed PT and aortic diameters could not be compared directly to normograms due to the shrinkage of arterial tissue secondary to formalin fixation. However, all studied specimens were prepared and stored in similar methods and any changes in diameter should be uniform. Despite sufficient clinical information on all CHD subjects, haemodynamic data were incomplete and hence not included in the analyses.

5.7 Conclusion

Patients with PAH/CHD have marked histological lesions in their proximal elastic pulmonary arteries, which correlated positively with increased vessel wall diameter and thickness. Fibrosis with atypical architecture of the elastic components of the media were predominant features and may constitute novel therapeutic targets in PAH. Structural wall abnormalities also existed in the aorta of PAH/CHD patients, suggestive of inherent abnormalities of the great arterial walls which are further enhanced in the PT due to elevated intravascular pressures. The following chapters (**chapter 6 & 7**) investigate further the genetic component of the aforementioned histological abnormalities contributing to aortopathy in CHD lesions and particularly, BAV disease.

Chapter 6. Copy number variation

Abbreviations

ACE Angiotensin converting enzyme
ALP Alkaline phosphatase
AS Aortic stenosis
AT1 Angiotensin II receptor type
AVR Aortic valve replacement
BAV Bicuspid aortic valve
CHD Congenital heart disease
CNV Copy number variation
CNVE Copy number variation event
CGH Comparative genomic hybridization
CNS Central nervous system
DDR Deletion-to-duplication ratio
FBN1 Fibrillin-1
GABA gamma-aminobutyric acid
HLHS Hypoplastic left heart syndrome
LOD score Logarithm (base 10) of odds
LVOTO Left ventricular outflow tract obstruction
MAD Median absolute deviation
MFS Marfan syndrome
QC Quality control
RAS Renin-angiotensin system
R-L Fusion of right- and left-coronary leaflets
SAC Sum of auto-correlation
TAA Thoracic aortic aneurysm
TGFβ Transforming growth factor beta

6.1 Abstract

Background: BAV disease encompasses a spectrum of left-sided cardiac lesions with a strong, yet not fully elucidated, genetic component. Recent evidence points to the presence of chromosomal copy number variants (CNVs) as a cause for inherited and sporadic structural heart disease. In this study, we hypothesized that BAV patients exhibit rare, clinically significant CNVs that are not present in healthy controls.

Methods: Genomic DNA from 94 BAV patients (mean age 35 ± 13years) was hybridized to the Affymetrix 6.0 array for CGH and the frequency of identified CNVs was compared to a data-set from the Wellcome Trust Control Consortium 2 containing 5,919 genotyped donors of European ancestry.

Results: Post CNV-calling quality control and filtering gave rise to 4,842 CNVs (81.2% deletions) with a median size of 23.2kb in 93 BAV patients (single case excluded) and 341,194 CNVs (78.7% deletions) with a median size of 23.6kb in 5,919 controls. When CNVs where clustered into events (CNVEs), a significantly greater incidence of rare (frequency < 1%) and large (100-200kb) deletions was detected in sporadic BAV cases compared to controls. However, none of the recurrent rare events survived multiple test correction for identification of likely pathogenic CNVs. Individual review of CNV calls encompassing genes with BAV functional relatedness revealed a 20kb heterozygous deletion on chromosome 17 in a single patient, overlapping with more than 2/3 of the *ACE* gene. Additional CNVs encompassing genes expressed in the heart included a recurrent duplication on chromosome 2 overlapping *ALPPL2* and a single deletion on chromosome X located 1kb upstream of *GABRE*.

Conclusion: Patients with BAV disease harbour a significantly greater number of rare, large deletions compared to controls, although these are unlikely to be clinically significant.

Identified CNVs encompassed several genes including *ACE*, a key element of the angiotensin-aldosterone system contributing to vascular function and disease. Future studies in larger BAV cohorts and families are needed to assess the role of structural genomic variants in this complex disease.

6.2 Introduction

As discussed in **Chapter 1**, BAV appears to be a complex heterogeneous trait with a strong genetic component; not only is it considered to be a disease of the entire aortic root and ascending aorta but also, a part of a broader spectrum of left-sided cardiac malformations (Tadros et al., 2009, Hinton et al., 2009). This phenotypic diversity along with the additive influence of haemodynamic factors may account for the lack of firm conclusions on the genetic basis of BAV disease (Girdauskas et al., 2011a). To date, the majority of investigators have adopted a candidate gene approach, focusing mainly on genes encoding proteins of vital importance for the conservation of the structural integrity of the aortic wall (*FBN1*, *ACTA2*, *TGFβ*) and genes encoding products involved in cardiac development (*NKX2.5*, *UFD1L*) (Laforest and Nemer, 2012, Guo et al., 2007, Girdauskas et al., 2011b, Majumdar et al., 2006, Mohamed et al., 2005, Arrington et al., 2008). Other authors have performed linkage studies in affected kindreds, leading to identification of genetically relevant loci (5q, 13q, 18q) and mapped genes (*NOTCH1* on 9q) (Martin et al., 2007, Garg et al., 2005).

Array-CGH is a technique which allows the identification of submicroscopic chromosomal CNVs at the genome wide level, the resolution of which is platform-specific (**Chapter 2**). The utilisation of this technique has revealed the overlap of CNVs with genes and the association of CNVs with levels of gene expression and specific clinical phenotypes (Aitman et al., 2006, Fanciulli et al., 2007). Structural genomic variants have also been reported in patients with CHD and additional birth malformations, although BAV disease has not been

examined in isolation (Thienpont et al., 2007, Richards et al., 2008, Greenway et al., 2009). These findings imply that CNVs may account for a significant component of human phenotypic variation, including structural heart disease, and can lead to identification of novel disease related genes and loci. The aim of this study was to examine the presence of CNVs in BAV disease in comparison to a well-characterised large control cohort from the Wellcome Trust Control Consortium, Sanger Institute, Cambridge, UK.

6.3 Methods

6.3.1 Patient recruitment

Patient recruitment and phenotypic assessment is described in **Chapter 2**. Blood samples were collected from the majority of patients with alternative collection of saliva from participants who refused blood sampling. For the control group, data from the Wellcome Trust Control Consortium 2 containing 5,919 genotyped donors of European ancestry were used (Bochukova et al., 2010).

Methods of DNA extraction and purification are included in **Chapter 2**.

6.3.2 CNV discovery

Following DNA extraction, samples were stored at -20˚C and sent to the Wellcome Trust Sanger Institute, Cambridge, UK for further quality testing and genotyping. DNA samples were run on Affymetrix Genome-Wide Human SNP Array 6.0 (Aros, Inc.), and compared to genotyping data from Wellcome Trust Control Consortium 2 donors assayed on the same platform. CNVs were discovered separately for cases and controls.

6.4 Results

6.4.1 Patient characteristics

A summary of patient characteristics is included in Table 5.1. The majority of patients were male (68%) and had functional BAVs with predominant R-L type (34%). Mean age was 35

years; all patients were adults with the exception of a single paediatric case. All genotyped BAV patients were isolated cases apart from the 2 year-old child whose father also had a BAV and was included in the analyses.

6.4.2 CNV calling

Pre-calling sample quality control (QC)

Raw intensities were regenerated and normalized across samples typed on the same plate from .CEL files using Affymetrix Power Tools. Intensities were transformed to log2 ratio using the plate median as the reference. A number of statistics, including median and median absolute deviation (MAD), were calculated from the log2 ratio for each sample and samples with MAD greater than 0.3 were removed (details in following sections).

CNV calling and QC

CNVs were called plate by plate using Birdseye from Birdsuite version 1.5.3, which generates a LOD score for each call that measures its likelihood of being in the called copy number state. A number of summary statistics was produced and parameters checked included the LOD score, the size of the call, the number of probes supporting the calling, and local probe density for the quality of the calls (Figure 5.1). The following criteria were set to filter CNV calls:

i) LOD score ≥ 10

ii) Size ≥ 1kb

iii) Number of probes ≥ 5

iv) Probe density ≥ 1 per 10kb

Table 6.1 Patient characteristics.

BAV population (n)	**94**
Sex (male n, %)	64 (68)
Age (years, mean)	35 (13)
BAV subtype (n, %)	
True	22 (23)
Right-left	32 (34)
Right-non	17 (18)
Left-non	2 (2)
Not known	21 (23)
Moderate- severe AVD (n, %)	
Aortic regurgitation	46 (49)
Aortic stenosis	50 (53)
Concomitant lesions (n, %)	
Thoracic aortic dilatation/aneurysm	52 (55)
Coarctation of the aorta	28 (30)
Ventricular septal defect	14 (15)
Patent arterial duct	5 (5)
Other (n, %)	
Family history of CHD	30 (32)
Previous endocarditis	3 (3)
Previous cardiac surgery (n, %)	72 (76)
Aortic valve replacement	26 (27)
Ross	18 (19)
Root replacement	13 (13)
Bentall	15 (16)
CVD risk factors (n, %)	
Hypertension	2 (2)
Diabetes	2 (2)
Smoking	1 (1)

Abbreviations: AVD, aortic valve disease; CHD, congenital heart disease; CVD, cardiovascular disease

Figure 6.1 Quality calling (QC) statistics of copy number variation (CNV) calling in BAV patients. The following plots can be viewed: i) distribution of size of CNV calls; ii) distribution of number of probes per CNV call; iii) distribution of density of probes per CNV call (ratio of size to number of probes); iv) size against number of probes for each CNV call; v) & vi) distribution of log2 ratio for each copy number and size of call; vii) Q-Q plot contrasting the number of CNV calls per sample against a fitted normal distribution; viii) Q-Q plot contrasting the total number of bases covered by CNV calls per sample against a fitted normal distribution; ix) number of deletion versus duplication calls in each sample. Dashed lines in (i-iii) mark the median.

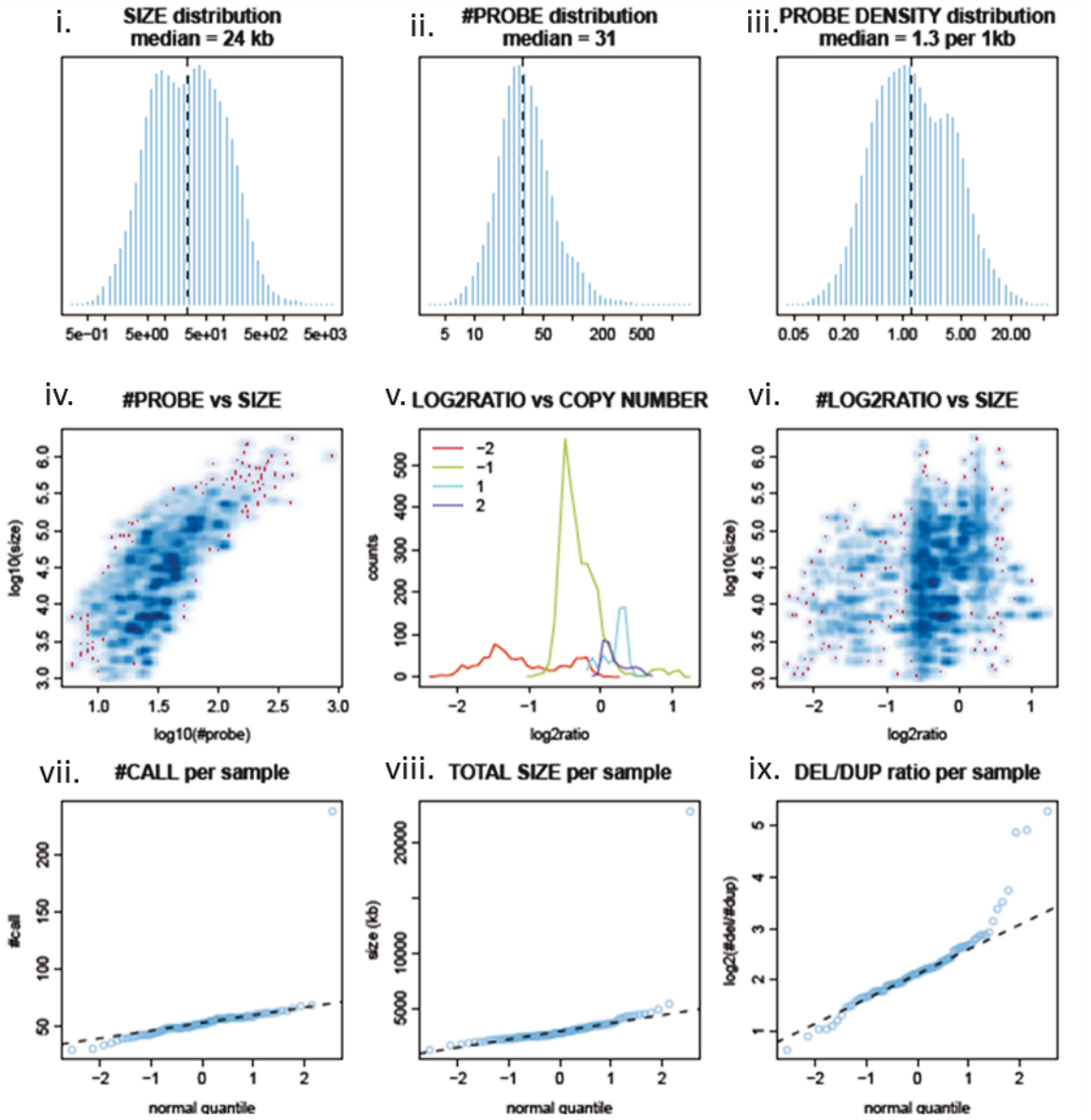

Following CNV calling and quality control, samples producing excessive CNV calls, that are most likely secondary to technical artefacts, were removed to keep the distribution of the number of CNV calls of all samples roughly normal. A linear function was used to model the negative correlation between the number of calls per sample and the sample's MAD of log

ratios (a measure of the level of noise in the data), whereby the parameters of the linear model were estimated using samples with a MAD<0.3 and a sum of auto-correlation (SAC) in the lower 90% to exclude the influence of samples with extreme level of noise or spatial auto-correlation. During this process, three BAV samples which after correction were more than four MADs from the fitted linear model were removed (Figure 6.2).

Figure 6.2 Number of CNV calls per sample as a function of sample's level of noise. Each dot represents a BAV sample with colour representing the level of sum of auto-correlation (SAC). The solid blue line denotes the fitted linear model and the dashed blue lines represent four times the median absolute deviation (MAD) of the residuals away from the fitted line. Dots encircled by red (not visible in this graph) were samples falling outside the blue dashed lines' region which were removed.

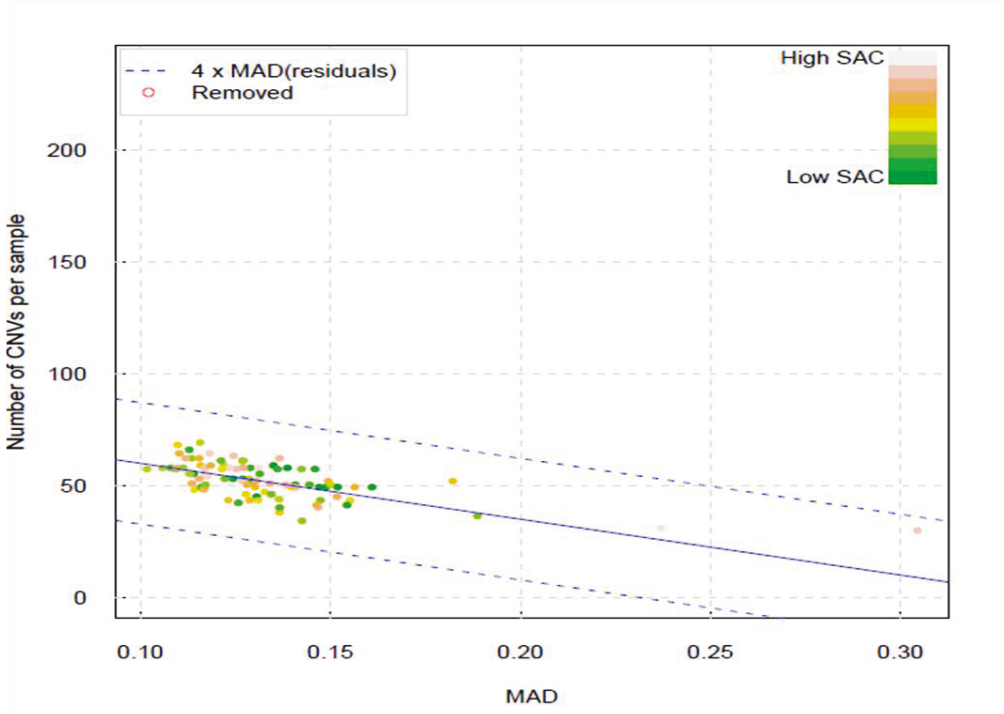

In addition to number of CNV calls in each sample, the deletion-to-duplication ratio (DDR) is also expected to be roughly stable across all samples, considering the identical CNV discovery algorithm and the reasonably large number of CNVs called per sample. Three BAV samples had a DDR above the upper bound (Figure 6.3) which also coincided with those having a high SAC and excessive CNV calls (same BAV cases as above).

Figure 6.3 Distribution of deletion-to-duplication ratio. Each dot represents a BAV sample with colour representing the level of sum of auto-correlation (SAC). The solid blue line represents the median of log2 deletion-to-duplication ratio and the dashed blue lines represent four times the median absolute deviation (MAD) of the residuals away from the fitted line. Dots encircled by red (two samples can be visualized in this graph) were cases falling outside the blue dashed lines' region to be removed.

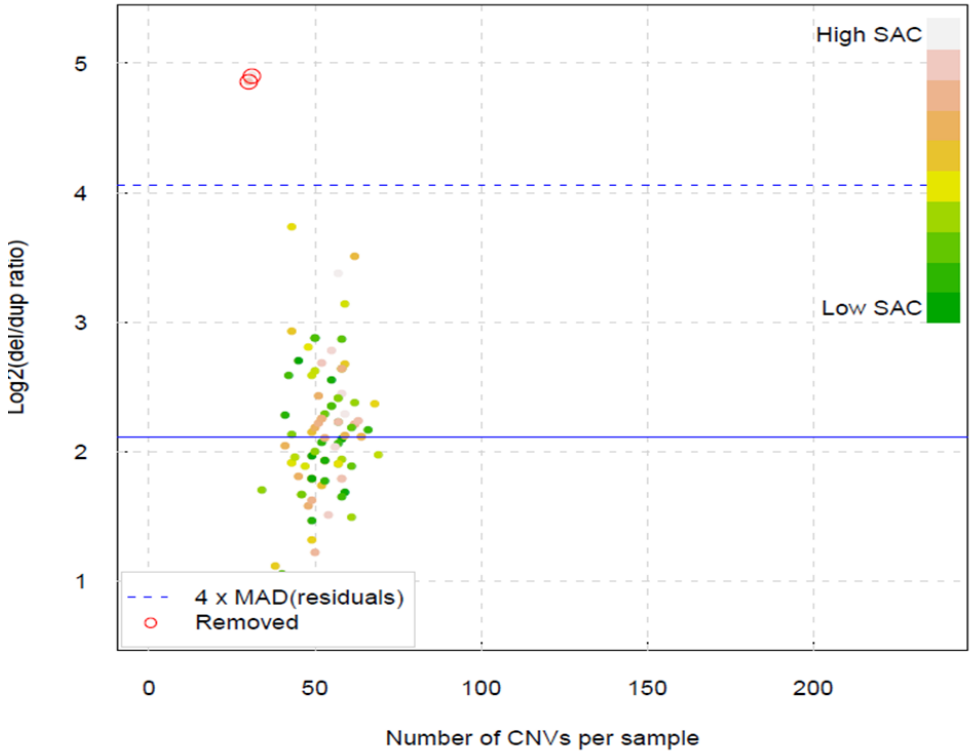

Following individual review of CNV calls generated by the above three BAV samples, two of these were manually re-included in the final analyses (Figure 6.4) and a single case was excluded for technical reasons, as outlined above.

Figure 6.4 Example of array data from BAV samples with excessive CNV calls. Log2 ratios of two samples (red line) in identical genomic regions of chromosome 1; other samples in the same genotyping plate are depicted in grey. Following individual visualisation of the total CNVs from these samples, it was decided to re-include them in the final analyses due to their overlap with CNVs from the remaining BAV samples.

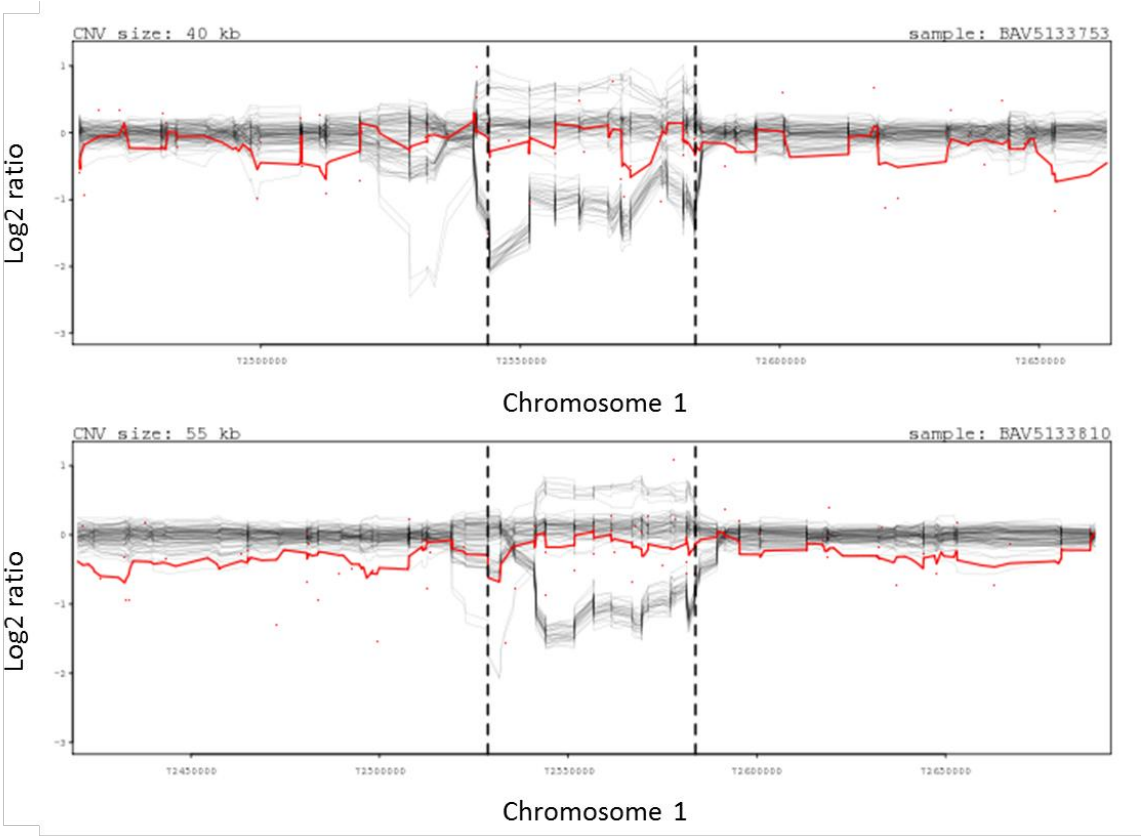

In the end, this process gave rise to 4,842 CNVs (81.2% deletions) with a median size of 23.2kb in 93 BAV cases and 341,194 CNVs (78.7% deletions) with a median size of 23.6kb in 5,919 controls.

Merging CNV calls

A clustering-like algorithm was used to merge CNV calls with extensive overlap into CNV events (CNVEs). These variables are likely to be identical with any slight differences in location owing to technical fluctuations in the precision of CNV discovery. The CNV calls among BAV cases were clustered into 869 CNVEs with a median size of 32.4kb; 704 of them overlapped reciprocally >50% with control CNVEs.

6.4.3 CNV Burden Analysis

We tested the hypothesis that BAV patients exhibit a greater burden of rare (<1% frequency) and large (>500kb) CNVs compared to controls. Statistical significance was established by 10,000 rounds of permutation. Since we observed differences in the distribution of noise between samples and controls, we performed a conditioned permutation to control for this effect (Tables 6.2 and 6.3, calculated p values according to two conditions: level of noise and total number of calls per sample).

Table 6.2 Global CNV burden analysis: CNV event (CNVE) type and frequency (annotated CNVs size 100-200kb). Presented p values conditioned for level of noise expressed by median absolute deviation (MAD, p1) and for total number of calls per sample (NCPS, p2).

CNVEs Type	CNVEs Frequency	Case rate	Control rate	Case/control ratio	p1 (MAD)	p2 (NCPS)
Losses and gains	Single occurrence	0.2795	0.1645	1.6989	0.0108	0.0046
Losses	Single occurrence	0.1612	0.0658	2.4478	0.0025	0.0021
Gains	Single occurrence	0.118	0.0986	1.1987	0.235	0.146
Losses and gains	2 - 6 occurrences	0.2150	0.1861	1.1550	0.252	0.157
Losses	2 - 6 occurrences	0.1075	0.0851	1.2628	0.159	0.107
Gains	2 - 6 occurrences	0.1075	0.1010	1.0643	0.399	0.311
Losses and gains	7 - 60 occurrences	0.3763	0.4941	0.7615	0.920	0.785
Losses	7 - 60 occurrences	0.2043	0.2042	1.0002	0.387	0.213
Gains	7 - 60 occurrences	0.1720	0.2899	0.5934	0.976	0.953
Losses and gains	All <1%	0.8709	0.8449	1.0308	0.326	0.117
Losses	All <1%	0.4731	0.3552	1.3316	0.021	0.0054
Gains	All <1%	0.3978	0.4896	0.8125	0.866	0.729

Table 6.3 Global CNV burden analysis: CNV event (CNVE) type and size (annotated CNVs frequency <1%). Presented p values conditioned for level of noise expressed by median absolute deviation (MAD, p1) and for total number of calls per sample (NCPS, p2).

CNVEs Type	CNVEs Size (kb)	Case rate	Control rate	Case/control ratio	p1 (MAD)	p2 (NCPS)
Losses and gains	100-200	0.8709	0.8449	1.0308	0.326	0.117
Losses	100-200	0.4731	0.3552	1.3316	0.021	0.0054
Gains	100-200	0.3978	0.4896	0.8125	0.866	0.729
Losses and gains	200-500	0.4408	0.5507	0.8004	0.923	0.797
Losses	200-500	0.1720	0.1833	0.9385	0.493	0.417
Gains	200-500	0.2688	0.3674	0.7315	0.946	0.857
Losses and gains	>500	0.1290	0.1905	0.6770	0.907	0.859
Losses	>500	0.0322	0.0471	0.6843	0.639	0.628
Gains	>500	0.0967	0.1434	0.6746	0.863	0.807

6.4.4 Identification of likely pathogenic CNVs

We performed the Fisher's exact test to examine CNVs that are rare (<1%) in the pooled population of cases and controls, but are specific or enriched in cases. The frequency of a CNV for this test was defined as the number of individuals that carry CNV calls overlapping more than 50% of the CNV in question since we were more interested in the affected genomic region rather than whether the CNVs correspond to a single mutation event. Overall, we observed 162 deletion CNVEs and 81 duplication CNVEs with a p-value < 0.05. However, (1) only two "dropped" duplications on chromosome 17 (Figure 5.5) survived multiple test corrections, (2) the vast majority of CNVEs were just singleton case CNVs not found in controls, and (3) some identified CNVEs could be under-called common CNVs or "false association" at the border of common CNVs, such as in the case of the "dropped" duplications. Other information, such as functional relatedness due to overlap of CNVEs with genes of interest, would be needed in order to support the argument that the failure of an association signal to survive multiple test correction was not just a random fluctuation of test statistics among a large number of tests. Individual review of the top eight recurrent CNV calls in BAV cases (Tables 6.4 and 6.5) revealed a single duplication on chromosome 2 overlapping alkaline phosphatase placental-like 2 (*ALPPL2*, ENSG00000163286) gene which has been shown to be expressed in human heart tissue, as discussed later (Figure 6.6).

Figure 6.5 "**Dropped" duplication on chromosome 17.** Due to the close clustering of CNVs calls in controls, many "normal" calls in the BAV cases may have been accounted as duplications whereas we would expect to see a clear separation of calls in order to interpret the significance of the duplication. Depicted log2 ratios correspond to number of copies; ratio > 1 indicates duplication and ratio < 1 indicates deletion.

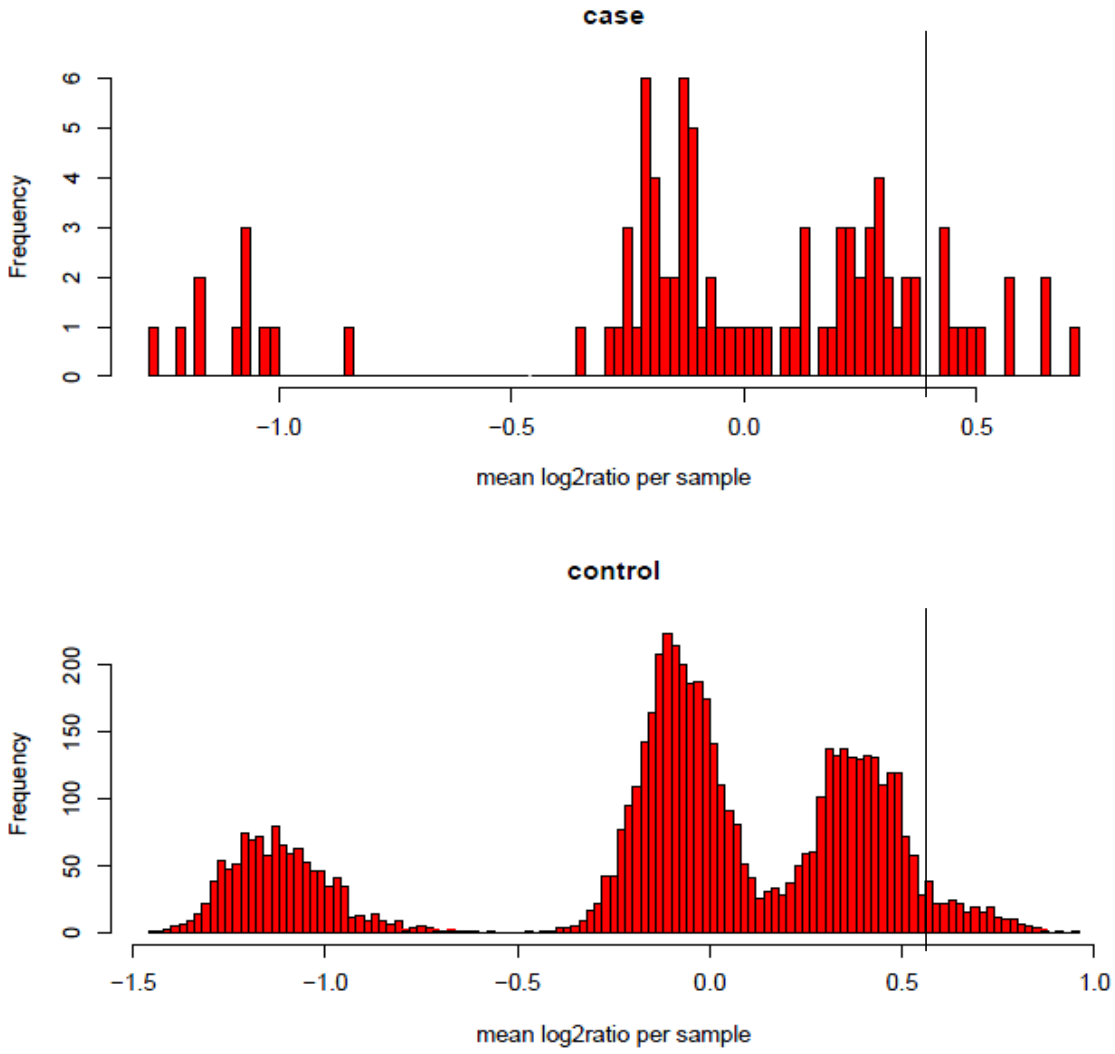

Table 6.4 Rare recurrent deletions in BAV cases.

Chromosome	Start	End	Size (bp)	Case (n)	Control (n)	Odd ratio	P
18	56267422	56272211	4790	3	23	8.535547	0.007201
3	7880524	7888516	7993	2	7	18.52006	0.007941
6	57018293	57060589	42297	2	7	18.52006	0.007941
1	1.51E+08	1.51E+08	14833	3	24	8.178987	0.008012
5	98795643	98842659	47017	3	24	8.178987	0.008012
1	1.51E+08	1.51E+08	6439	3	25	7.85109	0.008874
3	1.94E+08	1.94E+08	2431	4	50	5.272772	0.009409
3	1.27E+08	1.27E+08	22940	2	10	12.96779	0.014126

Table 6.5 Rare recurrent duplications in BAV cases.

Chromosome	Start	End	Size (bp)	Case (n)	Control (n)	Odd ratio	P
17	18296117	18353283	57167	23	18	106.9256	2.01E-32
17	18254555	18450883	196329	17	4	328.1796	2.04E-28
22	19872615	20247323	374709	4	19	13.93484	0.000379
1	2.07E+08	2.07E+08	6052	2	4	32.38166	0.00341
7	57599484	57741524	142041	2	5	25.92692	0.004727
7	57621147	57671281	50135	2	7	18.52006	0.007941
22	20038030	20264568	226539	4	51	5.167407	0.010029
2	2.33E+08	2.33E+08	79810	2	9	14.41078	0.01189

Figure 6.6 Rare recurrent duplication on chromosome 2. Duplications are depicted in green and deletions in red; each line represents a sample. The genomic region of interest (1Mb window, 500kb bilateral flanking) overlaps with alkaline phosphatase placental-like 2 (*ALPPL2*) gene, known to be expressed in human heart tissue.

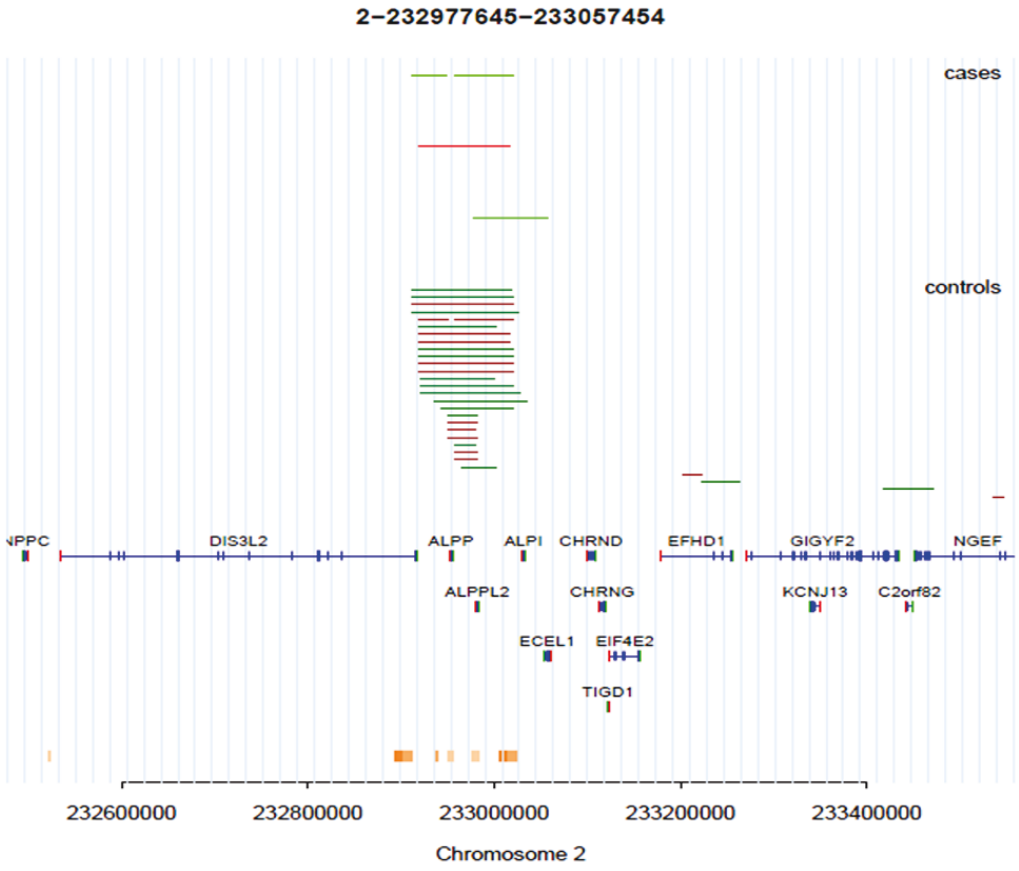

6.4.5 Candidate genes

We performed additional investigations for CNVs overlapping (1Mb window, 500kb flanking from each side) with selected genes of interest related to BAV and aneurysm formation (Table 6.6, gene selection discussed in more detail in **Chapter 7**). A 20kb heterozygous deletion in *ACE* gene (ENSG00000159640) was identified in a single 39 year-old male patient with a heavily calcified and severely stenotic functional BAV who

underwent aortic valve and hemi-root replacement (pre-operative aortic diameters of 50mm at the level of the root, 38mm at the sinutubular junction, and 47mm at the proximal ascending aorta, Figure 6.7). There was no known family history of CHD.

Table 6.6. Investigated genes of interest associated with BAV disease and TAA formation.

Ensebl Gene ID	Gene	Gene name	Chromosome
ENSG00000163221	S100A12	S100 calcium binding protein A12	1
ENSG00000177000	MTHFR	methylenetetrahydrofolate reductase	1
ENSG00000136634	IL10	Interleukin 10	1
ENSG00000060718	COL11A21	Collagen type XI	1
ENSG00000083444	PLOD1	lysyl hydroxylase 1	1
ENSG00000168542	COL3A1	Collagen alpha-1 (III)	2
ENSG00000115414	FN1	Fibronectin-1	2
ENSG00000084674	APOB	Apolipoprotein B	2
ENSG00000163513	TGFBR2	TGF- b receptor type 2	3
ENSG00000163884	KLF15	Kruppel-like factor 15	3
ENSG00000160791	CCR5	chemokine receptor 5	3
ENSG00000183072	NKX2.5	NK2 transcription factor related	5
ENSG00000113083	LOX	lysyl oxidase	5
ENSG00000152661	GJA1	gap junction protein, alpha 1	6
ENSG00000091831	ESR1	Estrogen receptor alpha	6
ENSG00000118523	CTGF	connective tissue growth factor	6
ENSG00000049540	ELN	Elastin	7
ENSG00000164867	NOS3/eNOS	Nitric oxide synthase 3	7
ENSG00000106366	PAI1/SERPINE1	serpin peptidase inhibitor	7
ENSG00000146648	EGFR	epidermal growth factor receptor	7
ENSG00000164692	COL1A2	Collagen type II	7
ENSG00000106397	PLOD3	lysyl hydroxylase 3	7
ENSG00000148400	NOTCH1	NOTCH1	9
ENSG00000106799	TGFBR1	TGF- b receptor type 1	9
ENSG00000106991	ENG	endoglin	9
ENSG00000107796	ACTA2	alpha smooth muscle actin	10
ENSG00000035403	VCL	vinculin	10
ENSG00000172638	EFEMP2	EGF containing fibulin-like extracellular matrix protein 2	11
ENSG00000166341	DSCHS1	Dachsous 1	11
ENSG00000139567	ACVRL1	activin receptor-like kinase-1	12

ENSG00000179295	PTPN11	Protein-tyrosine phosphatase	12
ENSG00000111424	VDR	Vitamin D receptor	12
ENSG00000187498	COL4A1	Collagen alpha-1(IV)	13
ENSG00000100644	HIF1A	hypoxia inducible factor 1, alpha subunit	14
ENSG00000119630	PGF	placental growth factor	14
ENSG00000072110	ACTN1	Alpha-actinin-1	14
ENSG00000134001	EIF2S1	eukaryotic translation initiation factor 2	14
ENSG00000166147	FBN1	Fibrillin-1	15
ENSG00000166949	SMAD3	SMAD family member 3	15
ENSG00000133392	MYH11	smooth muscle myosin, heavy chain 11	16
ENSG00000103197	TSC2	tuberin	16
ENSG00000103126	AXIN1	Axin-1	16
ENSG00000185615	PDIA2	protein disulfide isomerase family A, member 2	16
ENSG00000125398	SOX9	SRY-box 9	17
ENSG00000123700	KCNJ2	potassium inwardly-rectifying channel, subfamily J, member 2	17
ENSG00000196712	NF1	Neurofibromin-1	17
ENSG00000171298	GAA	lysosomal alpha-glucosidase	17
ENSG00000159640	ACE	angiotensin I converting enzyme	17
ENSG00000108821	COL1A1	Collagen Type I	17
ENSG00000131196	NFATc1	Nuclear factor of activated T-cells, calcineurin-dependant-1	18
ENSG00000127528	KLF2	Kruppel-like factor 2	19
ENSG00000130203	APOE	Apolipoprotein E	19
ENSG00000105329	TGFB1	TGF-beta 1	19
ENSG00000130700	GATA5	GATA binding protein 5	20
ENSG00000101384	JAG1	JAGGED1	20
ENSG00000197496	SLC2A10	glucose transporter type 10	20
ENSG00000100985	MMP9	matrix metallopeptidase 9	20
ENSG00000070010	UFD1L	ubiquitin fusion degradation 1 like	22
ENSG00000188153	COL4A5	Collagen alpha -5 (IV)	X
ENSG00000196924	FLNA	Filamen-A	X
ENSG00000184634	MED12	mediator complex subunit 12	X

Figure 6.7 Deletion on angiotensin-converting enzyme (*ACE*) gene. (A) Array data for sequenced BAV patients can be seen in grey with the log2 ratio of the single case with the 20kb heterozygous deletion encompassing ACE gene highlighted in red. Histology findings from the ascending aorta of the latter subject can be viewed, with predominant findings of elastic fragmentation in the convexity (B) and fibrotic changes in the concavity (C) of the media (x200 magnification, elastic van gieson stain).

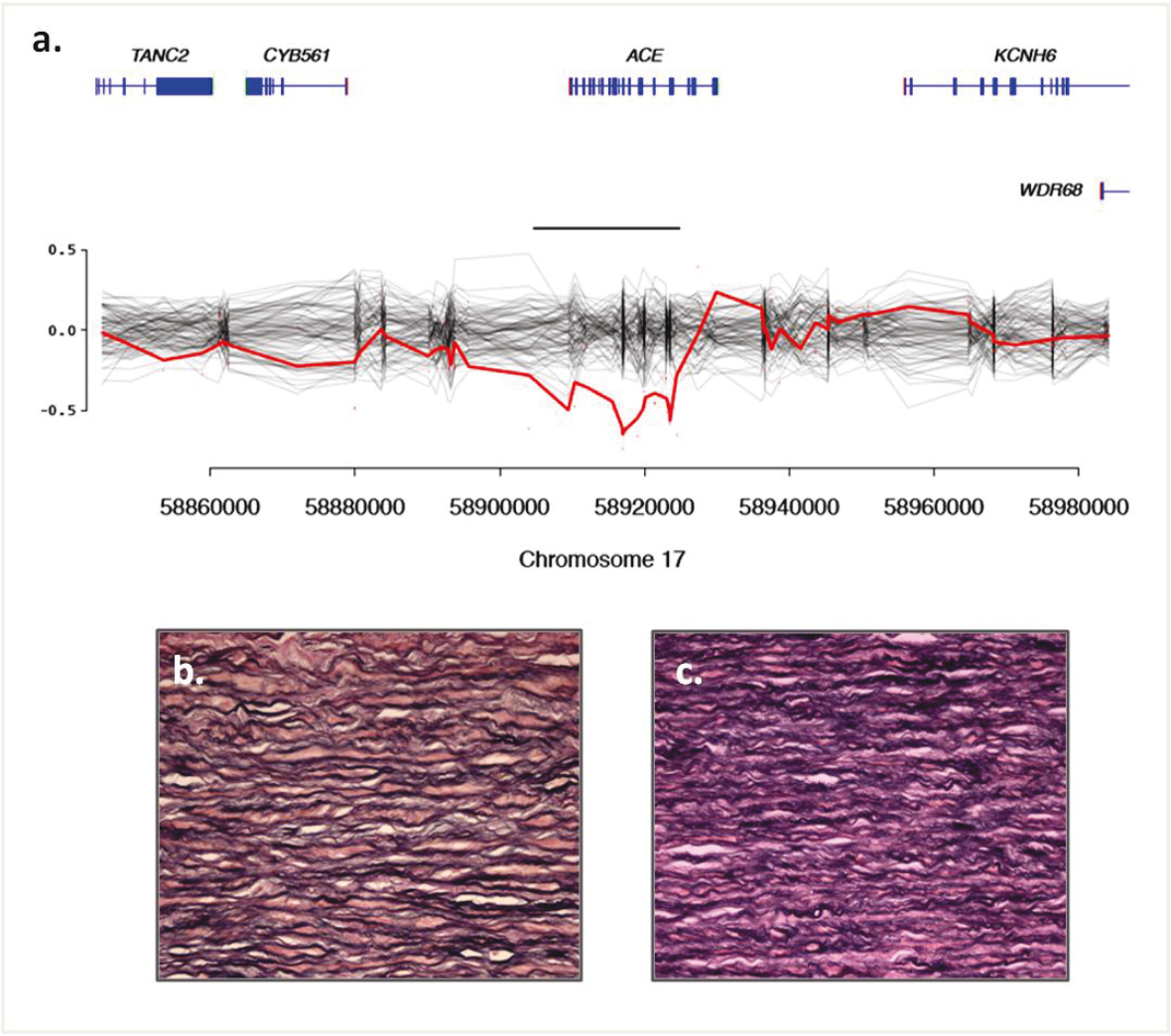

6.4.6 CNV calling for X chromosome

None of the identified rare CNVs on the X chromosome encompassed novel or selected genes of interest (Table 6.6). Tests were performed both separately and in combination, for males and females (Table 6.7). The only interesting finding was that of a 6kb heterozygous deletion (chr X: 150895188-150901132) in a single patient that was not present in controls; the patient was a 32 year-old female with a functional BAV and a history of AVR for severe AS. At the time of recruitment, she had normal aortic diameters with no other lesions and a negative family history for CHD. The deletion was just 1kb upstream of *GABRE* (ENSG00000102287), a gene coding a subunit of a chloride channel mediating synaptic transmission that is also expressed in the heart (to a lesser extent).

6.4.7 Supplementary data

CNV analyses were additionally performed in a single family and three trios following recruitment of consenting first-degree family members of BAV cases included in this study (pedigrees depicted in Figure 6.8). All family members were echocardiographically screened for heart disease with no detected abnormalities expect from a dilated thoracic ascending aorta in family #1 (Figure 6.8). Similar analyses applying the aforementioned methods did not detect any likely pathogenic CNVs harbouring genes of interest in the index cases or their family members.

Figure 6.8 Family pedigrees. Family trees are depicted for four bicuspid aortic valve (BAV) patients (index cases marked with arrows) and their first-degree family members. Circle depicts female and square, male patients with blue colour denoting cases with BAV and white colour, cases with tricuspid aortic valve (TAV). The horizontal line connecting the diagonal lines in family #4 denotes monozygotic twins. Abbreviations: R-L, right- and left-coronary; R-N, right- and non-coronary; TAA, thoracic aortic aneurysm.

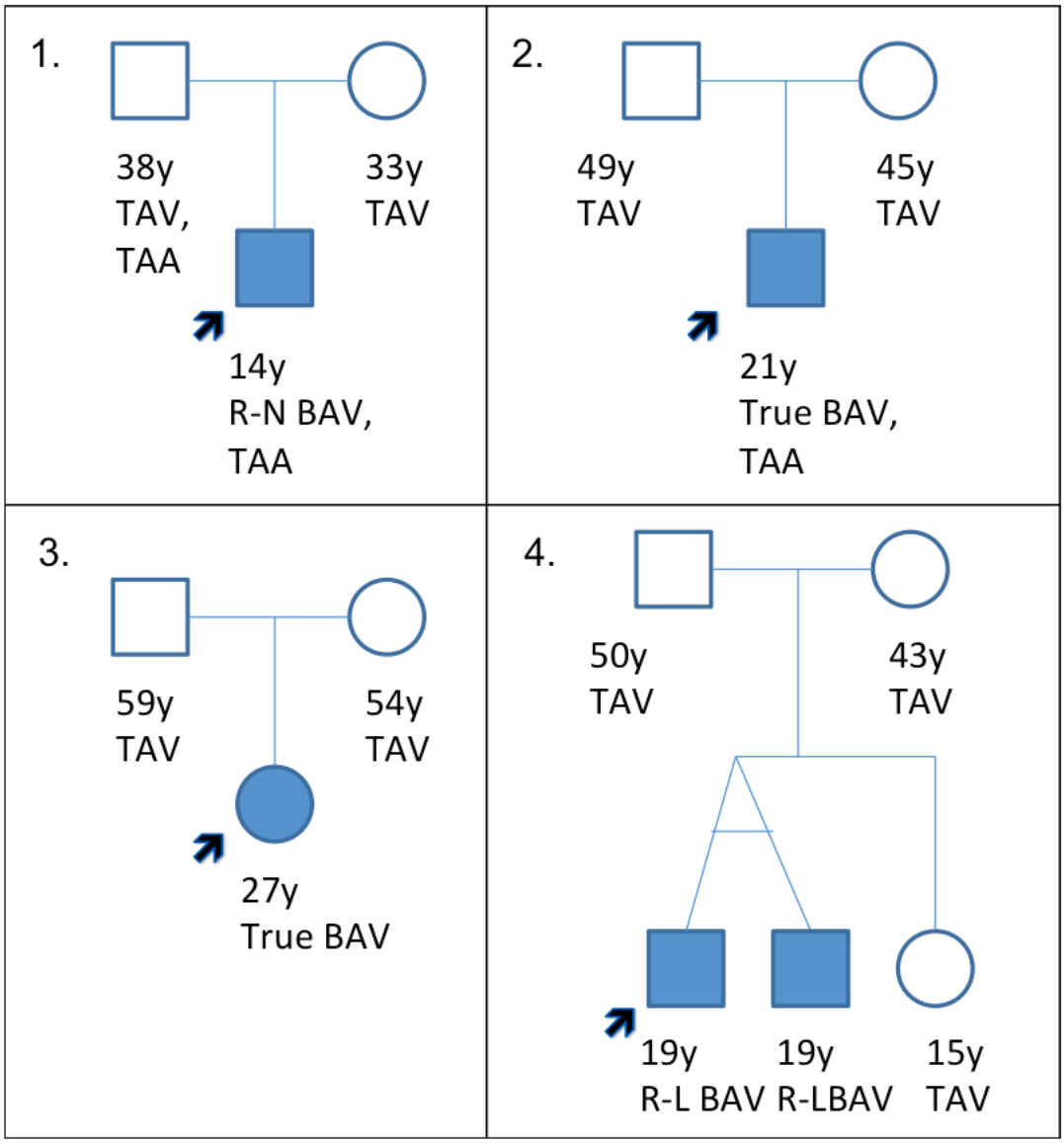

Table 6.7 Rare deletions and duplications on the X chromosome (combined results for male and female BAV patients). Abbreviations: Chr, chromosome; Del, deletion; Dup, duplication; Inf, infinite.

Chr	Start	End	Size (bp)	Del. Cases (n)	Del. Controls (n)	Dup. Cases (n)	Dup. Controls (n)	Del. Odds ratio	Del. p value	Dup. Odds ratio	Dup. p value
X	1.44E+08	1.44E+08	99291	1	0	0	2	Inf	1.77E-02	0	1.00E+00
X	1.49E+08	1.49E+08	23465	1	0	0	0	Inf	1.77E-02	0	1.00E+00
X	1.51E+08	1.51E+08	5945	1	0	0	0	Inf	1.77E-02	0	1.00E+00
X	88352266	88386448	34183	0	0	4	22	0	1.00E+00	10.47	1.03E-03
X	91195197	91241279	46083	0	0	3	17	0	1.00E+00	10.06	4.94E-03
X	91215681	91241279	25599	0	0	3	24	0	1.00E+00	7.11	1.16E-02
X	2778567	2825538	46972	0	4	1	0	0	1.00E+00	Inf	1.77E-02
X	57165332	57178738	13407	0	0	1	0	0	1.00E+00	Inf	1.77E-02
X	70451051	70504174	53124	0	0	1	0	0	1.00E+00	Inf	1.77E-02
X	89415789	89459641	43853	0	0	1	0	0	1.00E+00	Inf	1.77E-02
X	89578305	89876837	298533	0	0	1	0	0	1.00E+00	Inf	1.77E-02
X	1.14E+08	1.14E+08	22556	0	0	1	0	0	1.00E+00	Inf	1.77E-02
X	1.46E+08	1.46E+08	35491	0	1	1	0	0	1.00E+00	Inf	1.77E-02
X	1.49E+08	1.49E+08	367046	0	0	1	0	0	1.00E+00	Inf	1.77E-02
X	91455945	91472313	16369	0	0	1	1	0	1.00E+00	55.74	3.52E-02
X	1.52E+08	1.52E+08	376649	0	2	1	1	0	1.00E+00	55.74	3.52E-02

6.5 Discussion

This study demonstrates a significantly greater incidence of rare (< 1% frequency) and large (100-200kb) deletions in BAV patients compared to controls (Tables 6.2 & 6.3, Figure 6.9). However, none of the recurrent rare events survived multiple test correction for identification of likely pathogenic CNVs. Individual review of CNV calls encompassing genes with functional relatedness to BAV disease revealed a 20kb heterozygous deletion on chromosome 17 in a single patient, overlapping with more than 2/3 of the *ACE* gene (Figure 6.7a). Additional CNVs encompassing genes which are expressed in the heart to a lesser extent included a recurrent duplication on chromosome 2 overlapping *ALPPL2* and a single deletion on chromosome X located 1kb upstream of *GABRE*.

6.5.1 CNVs in CHD

Recent studies in patients with CHD have illustrated the presence of clinically significant CNVs as a cause for both inherited and sporadic structural heart disease (Greenway et al., 2009, Thienpont et al., 2007). Greenway et al. reported *de novo* CNVs at 10 loci accounting for at least 10% of non-syndromic sporadic cases of Tetralogy of Fallot whereas Thienpont and colleagues described chromosomal imbalances in patients with a variety of CHD lesions with additional phenotypic features suggestive of chromosomal aberrations (Greenway et al., 2009, Thienpont et al., 2007). Both authors identified CNVs encompassing genes known to cause CHD, such as *NKX2.5* and *NOTCH1*. In a different study including children with CHD and concomitant birth defects, a duplication of chromosome 2q33 was reported in a single BAV case with coarctation, developmental delay, and dysmorphic facies (Richards et al., 2008). Interestingly, chromosome 2q duplications have been previously linked to birth malformations (Bird and Mascarello, 2001) and despite the lack of syndromic features in all of our cases, two BAV patients had duplications overlapping *ALPPL2* gene located on chromosome 2q37 (Figure 6.6).

Figure 6.9 Overall distribution of rare autosomal deletions and duplications in BAV cases and controls.

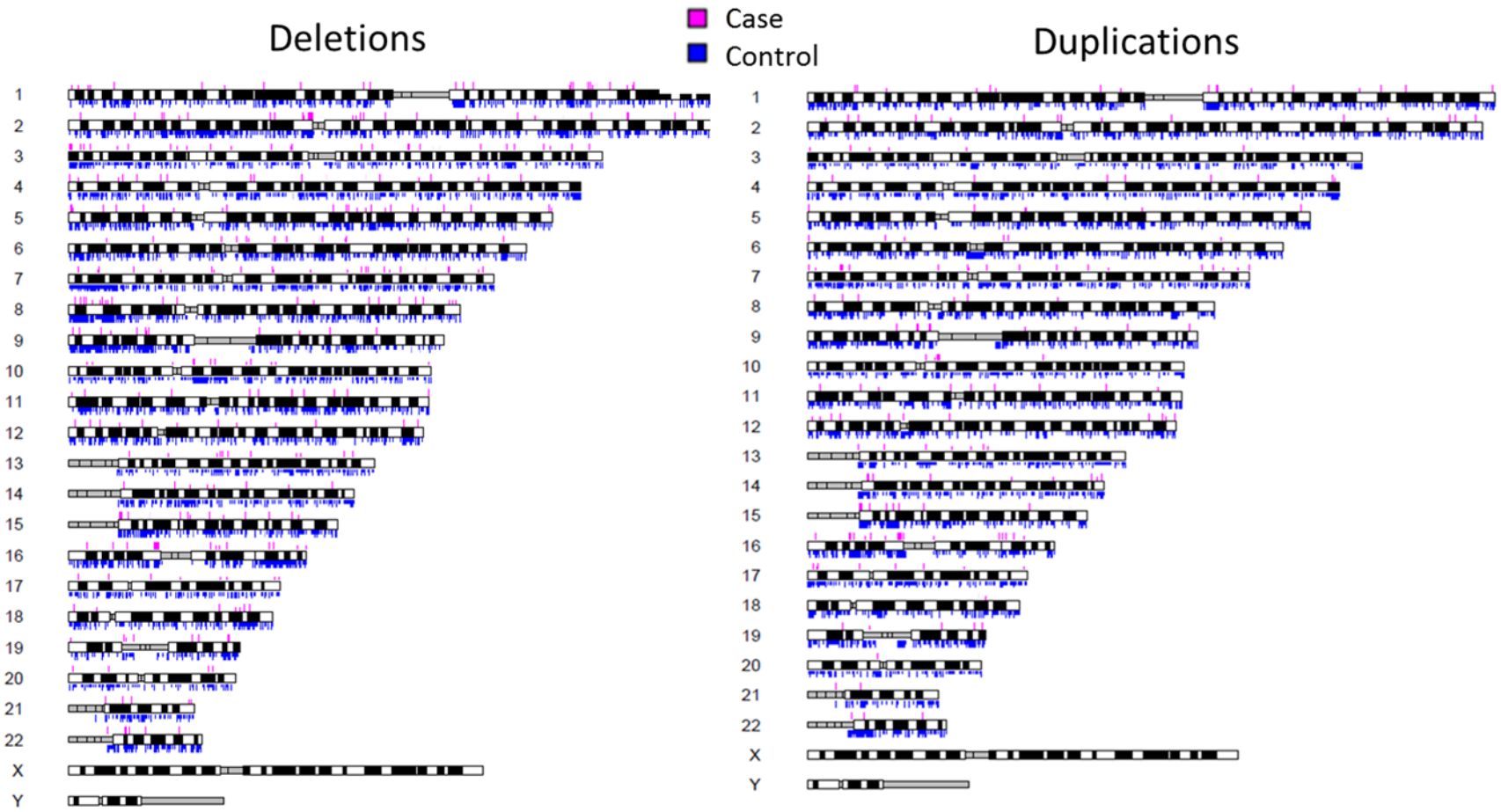

ALPPL2 belongs to the closely related family of alkaline phosphatase (ALP) genes, encodes for the placental ALP-like enzyme of the testis and thymus, and has been shown to be expressed in the heart (to a lesser extent) with no reported involvement in cardiac development(Knoll et al., 1988, Martin et al., 1987).

There is mounting evidence suggesting that BAV is part of a larger spectrum of cardiac malformations, including aortic valve stenosis, aortic coarctation, and hypoplastic left heart syndrome (HLHS), collectively known as left ventricular outflow tract obstruction (LVOTO) (Loffredo et al., 2004, Lewin et al., 2004, Hinton et al., 2009). Hitz et al. examined a large number of families segregating left-sided CHD lesions, including BAV, and reported a number of *de novo* and inherited CNVs contributing to 10% of their cases (Hitz et al., 2012). Identified chromosomal regions encompassed genes known to act in valvulogenesis pathways, such as *CTHRC1* and *MFAP4* (Hitz et al., 2012). The additional contribution of *CTHRC1* over-expression to calcific AS was suggestive of developmental gene defects leading to both early and adult onset valvular disease (Hitz et al., 2012, Bosse et al., 2009). In our study, *ACE* was the only gene with similar functional relatedness to BAV disease (O'Brien et al., 2002, Nishimoto et al., 2002), overlapping with a large heterozygous deletion in a single BAV case (Figure 6.7a).

6.5.2 *ACE* gene

Angiotensin I-converting enzyme, encoded by the *ACE* gene, is a key component of the renin-angiotensin system (RAS) hydrolysing angiotensin I into angiotensin II, a potent vasopressor that stimulates aldosterone (Heeneman et al., 2007). Recently, the RAS system has been suggested to play a key role in TAA formation with evidence of increased expression of *ACE* in the aneurysmal aortic wall (Heeneman et al., 2007, Nishimoto et al., 2002) and direct action of aldosterone and angiotensin II on VSMCs with transcription of genes involved in vascular fibrosis, inflammation, and calcification (Jaffe and Mendelsohn,

2005). Administration of AT1 blocker, losartan, has been shown to attenuate the aortic phenotype in both animal models and children with MFS (Habashi et al., 2006, Brooke et al., 2008). Thus, in our BAV patient carrying the heterozygous *ACE* deletion, a "protective" rather than "damaging" effect on the aorta would be expected provided that gene haploinsufficiency results in reduced angiotensin II levels. In contrast, histological examination of collected tissue specimens revealed severe fibrosis and elastic fragmentation in the concave and convex aspects of the aneurysmal ascending aorta (Figure 6.7b).

The functional effect of a single *ACE* allele has only been investigated in animal models so far, with step-wise reduction of *ACE* plasma activity by 25% in heterozygous mice (*ACE* +/-) and 70% in homozygous mice (*ACE* -/-) (Alexiou et al., 2005). ACE haploinsufficiency did not have a significant effect on angiotensin II, with similar plasma and heart tissue levels in heterozygous and wild type mice (Alexiou et al., 2005). Interestingly, human studies have linked a polymorphism involving the insertion (I) or deletion (D) of a 287bp DNA sequence in intron 16 of the *ACE* gene to aneurysm formation, with DD carriers having higher plasma and heart tissue *ACE* levels and increased predisposition to TAA formation, including patients with a BAV (Danser et al., 1995, Foffa et al., 2012). Therefore, it is possible that the quantitative level of *ACE* gene function does not influence angiotensin II activity, which can also be activated in an *ACE*-independent manner, or changes in *ACE* activity are attenuated by compensatory mechanisms (Uehara et al., 2013, Alexiou et al., 2005).

The presence of a single copy number of *ACE* may also impact earlier developmental processes. Similar to the observations by Hitz et al. who reported CNVs overlapping genes expressed during cardiac development (Hitz et al., 2012), *ACE* gene expression is present in the aortic valve and ascending aorta of wild-type mice during embryogenesis (Figure 6.9). Angiotensin II receptors are also widely expressed in the fetal tissue and have been shown to contribute to early embryologic development of the heart (Burrell et al., 2001). Interestingly,

expression of *ACE* and angiotensin II has also been exhibited in later onset severe calcific aortic stenosis, similar to the one seen in our BAV proband carrying the *ACE* deletion (O'Brien et al., 2002). The impact of reduced *ACE* expression on cardiac development can be examined by the fetopathy of *ACE*-inhibitors administered during human pregnancy. *In utero* exposure to these agents over the second and third trimesters of pregnancy has been associated with a number of conditions including oligohydramnios, hypocalvaria, abnormalities of the urinary tract and renal vascular system, renal failure, and death (Briggs, 2002, Tabacova et al., 2003, Pryde et al., 1993). Earlier exposure to *ACE*-inhibitors during the first trimester has been linked to a number of cardiovascular malformations, including atrial septal defect, patent ductus arteriosus, ventricular septal defect, and pulmonary stenosis (Cooper et al., 2006). The presence of a BAV was not mentioned in the aforementioned large epidemiological study, although it is a phenotype that can potentially be overlooked in the presence of other major cardiovascular defects.

Figure 6.9 The expression of ACE gene in the embryonic mouse heart. In situ hybridization for ACE gene expression performed on sagittal sections of a wild-type E14.5 mouse heart (a, b). Strong expression can be seen in the endothelium of the ascending aorta (asterisks) in both sections, with additional expression in the pulmonary valve (arrow), and aortic valve (arrowhead) seen in b. Source of pictures: www.eurexpress.org.

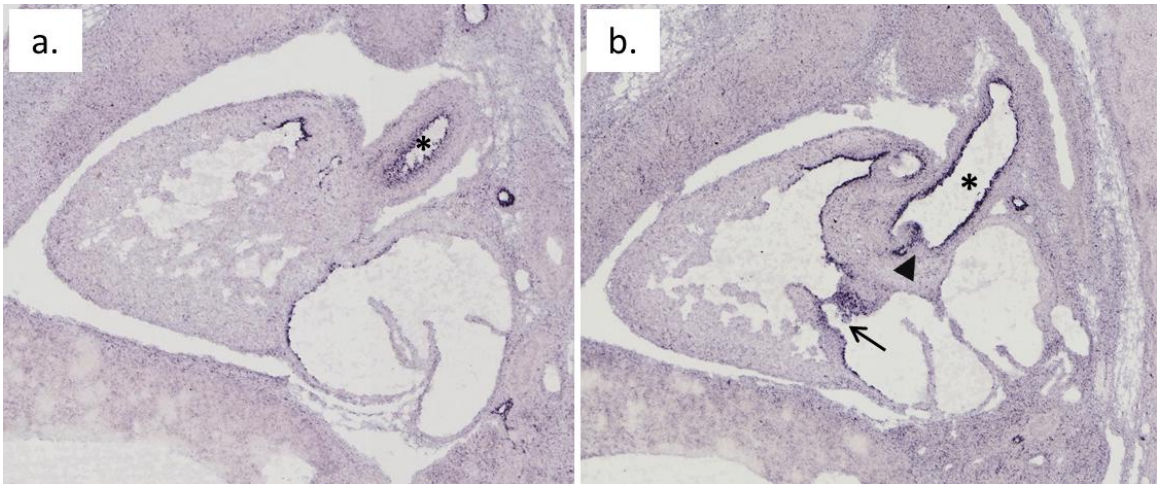

6.5.3 X- chromosome linkage theory

This study also investigated the suggested BAV linkage to X-chromosome, due to the disease's male predominance and its association with Turner syndrome (Tadros et al., 2009). Turner syndrome is characterized by complete or partial absence of one X chromosome in female patients, leading to early ovarian failure and a higher incidence of congenital cardiac malformations, including BAV, aortic valve disease, and coarctation of the aorta (Prandstraller et al., 1999). The 45X karyotype is associated with complex and more severe CHD, whereas the BAV phenotype is more frequent in X-structural abnormalities (X-rings and Xp monosomy) (Prandstraller et al., 1999, Sachdev et al., 2008). In our non-syndromic BAV probands, there was an absence of likely pathogenic CNVs located on the X chromosome. This was in agreement with a previous family-based heritability study that failed to identify BAV X-linkage (Martin et al., 2007).

When rare CNVs on the X-chromosome were examined for overlapping genes (Table 6.6), a 6kb heterozygous deletion 1kb upstream *GABRE* gene was reported in a female BAV patient that was absent in controls. *GABRE* gene, mapped to chromosome Xq28, encodes a subunit of the gamma-aminobutyric acid (GABA) receptor which mediates synaptic transmission in the central nervous system (CNS) (Wilke et al., 1997). An alternative GABA subunit, with up to 45% amino-acid sequence overlap with CNS subunits, has been shown to be expressed in the electrical conduction system of the human heart (Garret et al., 1997). Notably, despite the unknown role of *GABRE* gene in valve formation, another gene involved in electrical conduction has been linked to BAV disease. Mutations in *KCNJ2*, encoding the inward-rectifying potassium current Kir2.1, have been reported in BAV patients with Andersen syndrome, characterized by periodic paralysis, ventricular arrhythmias, and dysmorphic features (Plaster et al., 2001). Animal studies have shown that the function of inward-rectifying potassium current Kir2.1 is not restricted to excitable tissue, thus leading to

speculation of an important role of ion channels in organ development through signalling pathways (Plaster et al., 2001, Karschin and Karschin, 1997).

6.5.4 Limitations

This study is limited by the restricted number of BAV patients who had heterogeneous phenotypes and variable family history of CHD. The absence of adequate parental samples is an additional limiting factor; the small number of recruited family members did not allow the undertaking of an alternative method of "trio" analysis involving screening of probands and their unaffected parents for detection of CNVs (Greenway et al., 2009). Our preliminary results merit further validation through expression studies for proof of causation. Future analyses with larger cohorts will be needed to investigate the potential clinical significance of identified rare and large CNVs which did not survive multiple statistical test correction.

6.6 Conclusion

This study demonstrates that patients with BAV disease harbour a significantly greater number of rare, large deletions compared to controls, although unlikely to be clinically significant. Individual review of CNV calls overlapping genes with BAV functional relatedness revealed a 20kb heterozygous deletion in a single patient overlapping *ACE* gene, a key element of the angiotensin-aldosterone system contributing to vascular function and disease. Mutations in the *ACE* gene were further investigated via next-generation sequencing in the same BAV patient cohort (**Chapter 7**). Additional CNVs of interest included a recurrent duplication encompassing *ALPPL2* and a single deletion 1kb of *GABRE*, with no known involvement of the latter genes in cardiac development although found to be expressed in the heart. The functional effects of the above CNVs merit further validation in conjunction with genetic analyses in larger BAV cohorts.

Chapter 7. Next-generation sequencing

Abbreviations

AAA Abdominal aortic aneurysm
AS Aortic stenosis
AVR Aortic valve replacement
BAV Bicuspid aortic valve
BRU Biomedical research unit
CHD Congenital heart disease
CoA Coarctation of the aorta
ECM Extracellular matrix
HLHS Hypoplastic left heart syndrome
MAF Minor allele frequency
NGS Next generation sequencing
PDA Patent arterial duct
R-L Fusion of right- and left-coronary leaflets
SNP Single nucleotide polymorphism
TAA Thoracic aortic aneurysm
TGFβ Transforming growth factor beta
UTR Prime untranslated region
VSD Ventricular septal defect
VSMC Vascular smooth muscle cell

Abbreviated gene names are included in Table 7.1

7.1 Abstract

Background: BAV is a complex multifactorial disease encompassing a wide spectrum of phenotypic manifestations and associated genetic aberrations. Recent advances in genomics with the advent of cutting-edge NGS techniques, allow comprehensive genetic characterization of BAV patients in a timely and cost-efficient manner.

Methods: Genomic DNA from 94 BAV patients was used to construct DNA libraries (SureSelectXT Target Enrichment System for SOLiD 4) followed by NGS (SOLiD 5500 platform) of 63 genes of interest, known to be associated with BAV phenotypic traits.

Results: A total of 157 likely pathogenic variants were identified in 62 (66%) BAV cases, out of which 41 (44%) carried mutations in more than one genes. Previously reported variants were identified in *NOTCH1*, *COL3A1*, and *APOE* genes with additional discovery of a large number of novel variants, which are predicted to be harmful, in genes related to BAV formation, aortopathy, calcific aortic stenosis, and hypoplastic left heart syndrome. Sanger sequencing will be performed to confirm novel mutations in prioritized genes of interest.

Conclusion: Application of NGS techniques in BAV allows comprehensive assessment of a wide array of targeted genes and provides preliminary evidence on the polygenic nature of this complex heterogeneous trait.

7.2 Introduction

The effect of haemodynamic stress on the BAV aorta (**Chapter 3**) along with presence of CNVs in BAV patients encompassing a number of genes (**Chapter 6**) reinforced current views in the literature on the multifactorial nature of BAV disease (Laforest and Nemer, 2012, Hinton, 2012). In this chapter, recently available cutting-edge genomic techniques at the Royal Brompton Hospital campus (Cardiovascular BRU) were utilized to further

investigate the genetic basis of BAV disease via targeted NGS of a wide array of associated genes of interest.

Introduction of NGS technologies is currently changing the landscape of clinical genomics, with a dramatic increase in throughput at a constantly reducing cost (Ware et al., 2012). Targeted NGS is an especially attractive technique allowing selective sequencing of the coding regions of the human genome as opposed to costly, and occasionally unnecessary whole-genome sequencing (Biesecker, 2010, Choi et al., 2009). This approach has been applied successfully for research and diagnostics in several cardiovascular conditions, including inherited cardiomyopathies and arrhythmia syndromes (Meder et al., 2011, Herman et al., 2012, Ware et al., 2013). Application of this technique in BAV disease is particularly beneficial, in view of the wide spectrum of observed phenotypic manifestations with a large number of associated genetic aberrations (Hinton, 2012). The aim of this study was to create a library of genomic regions associated with various BAV phenotypic traits which, following further validation, may serve as a future clinical diagnostic tool for risk stratification in this population.

7.3 Methods

7.3.1 Sample collection

A total of 94 BAV patient samples were sequenced (cohort described in CNV study, **Chapter 6**). DNA extraction and purification methods are described in detail in **Chapter 2**.

7.3.2 Next-generation sequencing

Assay Design

General principles of targeted NGS are described in **Chapter 2**. For the design of the sequence capture array, current literature was reviewed and 63 genes of interest were selected (Table 7.1). In addition to genes known to be associated with syndromic and sporadic BAV

disease, a number of genes related to inherited forms of aortopathy, aneurysm formation, AS, and valve formation were also included in the library (subpanels in Table 7.1). Gene sequences were retrieved from a reference database (http://www.ensembl.org) and RNA baits were designed for all exons of Ensembl transcripts of the selected genes, using Agilent's eArray platform (https://earray.chem.agilent.com/earray). The final microarray design included UTRs and flanking exon/intron boundaries (+/-100 bp) with a total number of 16,216 unique 120 mer RNA baits covering a target region of 479,673bp. Applied standard eArray parameters to generate RNA baits included tiling frequency = 5x, bait length = 120, standard repeats = off, avoid overlap = 20, and layout strategy = centred.

Table 7.1 Summary of sequenced genes. Genes harboring likely pathogenic variants (post NGS): * isolated cases; ‡ recurrent or multiple.

Ensebl Gene ID	Gene	Chromosome	Function/signalling pathways	Human phenotype	Reference
Extracellular matrix proteins					
ENSG00000166147	*FBN1* (Fibrillin-1) ‡	15	Tissue elasticity, TGFβ	MFS, BAV Ao- increased expression	(Dietz et al., 1991, Gomez et al., 2009)
ENSG00000115414	*FN1* (Fibronectin-1) ‡	2	Marker of VSMC synthetic phenotype	Increased expression in convexity of Asc ao in stenotic BAV	(Della Corte et al., 2008)
ENSG00000049540	*ELN* (Elastin) ‡	7	Tissue elasticity	Williams-Beuren syndrome; BAV with supravalvular AS	(Szabo et al., 2006, Li et al., 1998)
ENSG00000168542	*COL3A1* (Collagen alpha-1 III) ‡	2	Collagen metabolism	EDS, type 4; frequent arterial dissection with infrequent aneurysm	(Liu et al., 1997, Superti-Furga et al., 1988)
ENSG00000188153	*COL4A5* (Collagen alpha-5 IV)	X	Collagen metabolism	X-linked Alport syndrome; Asc ao & abdominal aneurysm	(Kashtan et al., 2010)
ENSG00000187498	*COL4A1* (Collagen alpha-1IV) ‡	13	Collagen metabolism	Hereditary angiopathy,nephropathy, aneurysms and muscle cramps	(Plaisier et al., 2007, Poschl et al., 2004)
ENSG00000083444	*PLOD1* (lysyl hydroxylase 1) ‡	1	Collagen metabolism	EDS type 6, rare aneurysm	(Wenstrup et al., 1989, Takaluoma et al., 2007)
ENSG00000106397	*PLOD3* (lysyl hydroxylase 3) ‡	7	Collagen metabolism	Bone fragility, arterial rupture and deafness	(Salo et al., 2008, Ruotsalainen et al., 2006)
ENSG00000113083	*LOX* (lysyl oxidase) ‡	5	Collagen metabolism, TGFβ	Unknown, Ao aneurysm in KO mice	(Maki et al., 2002)
ENSG00000172638	*EFEMP2* (fibulin-4) *	11	Elastic fiber formation, connective tissue development	Cutis laxa with Asc ao aneurysm and arterial tortuosity	(Dasouki et al., 2007, Huang et al., 2010)
Transcription factors					
ENSG00000130700	*GATA5* (GATA binding protein 5) ‡	20	Cardiac development (aortic valve)	Unknown, BAV in 25% of KO mice	(Laforest et al., 2011)
ENSG00000125398	*SOX9* (SRY-box 9) *	17	Chondrogenesis	Unknown, calcific valvular disease in KO mice	(Peacock et al., 2010)
ENSG00000131196	*NFATc1* (Nuclear factor of activated T-cells calcineurin-dependant1) ‡	18	Cardiac development (endocardial cushion growth & remodelling)	Unknown	(de la Pompa et al., 1998)
ENSG00000183072	*NKX2.5* (NK2 transcription factor related) ‡	5	Cardiac development (cardiac homeobox gene)	BAV-TAA, ASD, VSD, TOF, Ebstein's, DORV	(Biben et al., 2000, Schott et al., 1998, Majumdar et al., 2006, Wang et al., 2011)
ENSG00000070010	*UFD1L* (ubiquitin fusion degradation 1 like)	22	Cardiac development (cardiac outflow tract)	BAV-TAA, DGS/VCFS (conotruncal cardiac defects)	(Mohamed et al., 2005)

Transmembrane proteins					
ENSG00000148400	*NOTCH1*‡	9	Cardiac development (cardiac outflow tract)	BAV, calcific aortic stenosis, VSD, TOF, mitral stenosis	(Garg et al., 2005, Niessen and Karsan, 2008)
ENSG00000106799	*TGFBR1* (TGFβ receptor type 1)	9	Connective tissue degradation, TGFβ	MFS-type 2, LDS, BAV Ao- increased expression	(Loeys et al., 2006, Gomez et al., 2009)
ENSG00000163513	*TGFBR2* (TGFβ receptor type 1)	3	Connective tissue degradation, TGFβ	MFS-type 2, LDS, BAV Ao- increased expression	(Loeys et al., 2006, Gomez et al., 2009)
ENSG00000106991	*ENG* (endoglin) ‡	9	Cardiac development (aortic valve formation), TGFβ superfamily	BAV	(Wooten et al., 2010)
ENSG00000101384	*JAG1* (JAGGED1) *	20	Cardiac development (aortic valve formation)	Allagile syndrome; BAV with characteristic facies, jaundice & skeletal abnormalities	(McElhinney et al., 2002)
ENSG00000123700	*KCNJ2*	17	Excitable myocardial tissue (inward-rectifying potassium current Kir2.1)	Andersen syndrome; BAV with periodic paralysis, ventricular arrhythmias & dysmorphic features	(Andelfinger et al., 2002)
ENSG00000152661	*GJA1* (connexin-43)	6	Connexin gap junction- development of normal cardiac architecture and ventricular conduction	Hypoplastic left heart syndrome	(Yu et al., 2004)
ENSG00000139567	*ACVRL1* (activin receptor-like kinase-1)	12	TGFβ superfamily	Hereditary haemorrahagic telangiectasia, arterial aneurysms	(Andersen et al., 2010, Oh et al., 2000)
ENSG00000197496	*SLC2A10* (glucose transporter type 10)	20	Glucose homeostasis	Arterial tortuosity syndrome	(Coucke et al., 2006)
Cytoplasmic proteins					
ENSG00000166949	*SMAD3* (SMAD family member 3)	15	Connective tissue degradation, TGFβ	LDS, aortic aneurysm with osteoarthritis	(van de Laar et al., 2011)
ENSG00000107796	*ACTA2* (alpha smooth muscle actin)	10	Vascular contractility, TGFβ	Familial aortic aneurysm; BAV with livedo reticularis	(Guo et al., 2007)
ENSG00000133392	*MYH11* (smooth muscle myosin, heavy chain 11) ‡	16	Vascular contractility, angiotensin II	Familial aortic aneurysm with patent ductus arteriosus	(Zhu et al., 2006, Pannu et al., 2007)
ENSG00000196924	*FLNA* (Filamin-A) ‡	X	Actin cytoskeleton, TGFβ	Periventricular nodular heterotopia with EDS, Asc ao aneurysm and valvular dystrophy	(Sheen et al., 2005, Feng et al., 2006)
ENSG00000196712	*NF1* (Neurofibromin-1) ‡	17	Ras-MEK-ERK	Neurofibromatosis, arterial aneurysm and stenosis	(Friedman et al., 2002)
ENSG00000179295	*PTPN11* (Protein-tyrosine phosphatase 2C)	12	Ras-MEK-ERK	Noonan syndrome, coronary artery aneurysm and rare Asc ao aneurysm	(Purnell et al., 2005, Araki et al., 2004, Iwasaki et al., 2009)
ENSG00000103197	*TSC2* (tuberin) ‡	16	Tumour suppression, mammalian target of	Tuberous sclerosis, diffuse	(Cao et al., 2010)

			rapamycin (mTOR)	thoracoabdominal aneurysm	
ENSG00000163221	*S100A12* (S100 calcium binding protein A12)	1	Interleukin-6, TGFβ	Increased expression in MYH11-mutation aneurysm	(Hofmann Bowman et al., 2010)
ENSG00000164867	*NOS3/eNOS* (endothelial nitric oxide synthase) *	7	Cardiac development, stress-induced vascular remodelling	Abdominal aortic aneurysm, BAV in KO mice	(Atli et al., 2010, Fernandez et al., 2009)
ENSG00000103126	*AXIN1* (Axin-1) ‡	16	Cardiac development (cardiac valve, outflow tract), Wnt	BAV	(Wooten et al., 2010)
ENSG00000185615	*PDIA2* ‡	16	Protein disulfide isomerase family A, member 2	BAV	(Wooten et al., 2010)
ENSG00000171298	*GAA* ‡	17	Lysosomal alpha-glucosidase	Acid maltase deficiency, intracranial aneurysm, lysosomal accumulation in heart and aorta of KO mice	(Raben et al., 1998)
Nuclear protein					
ENSG00000127528	*KLF2* (Kruppel-like factor 2)	19	Unknown	Unknown, Ao aneurysm and dissection in KO mice	(Kuo et al., 1997)
ENSG00000163884	*KLF15* (Kruppel-like factor 15) *	3	Inhibition of VSMC proliferation and migration, thrombospondin-2, p53, TGFβ	Unknown, Ao aneurysm and cardiomyopathy in KO mice	(Haldar et al., 2010, Lu et al., 2010)
ENSG00000184634	*MED12* (mediator complex subunit 12) ‡	X	WNT-β-catenin, WNT-PCP	Lujan–Fryns syndrome with ao root dilation	(Schwartz et al., 2007, Rocha et al., 2010)
Vascular endothelial growth factor (VEGF) pathway members					
ENSG00000100644	*HIF1A* (hypoxia inducible factor 1, alpha subunit) ‡	14	Proangiogenic transcriptional factor, VEGF	Hypoplastic lef heart syndrome with BAV	(Hinton et al., 2009)
ENSG00000119630	*PGF* (placental growth factor)	14	Embryogenesis (angiogenesis), VEGF	Hypoplastic lef heart syndrome with BAV, atherosclerosis	(Hinton et al., 2009)
ENSG00000072110	*ACTN1* (Alpha-actinin-1) ‡	14	Cardiac development (cardiac valve), VEGF	Hypoplastic lef heart syndrome with BAV	(Hinton et al., 2009)
ENSG00000134001	*EIF2S1*	14	Eukaryotic translation initiation factor 2, subunit 1 alpha, VEGF	Hypoplastic lef heart syndrome with BAV	(Hinton et al., 2009)
ENSG00000035403	*VCL* (vinculin) *	10	Cytoskeletal protein, VEGF	Hypoplastic lef heart syndrome, dilated cardiomyopathy	(Hinton et al., 2009)
Enzymes regulating nitric oxide generation					
ENSG00000153904	*DDAH1**	1	dimethylarginine dimethylaminohydrolase 1	Type II diabetes	(Abhary et al., 2010)
ENSG00000213722	*DDAH2*	6	dimethylarginine dimethylaminohydrolase 2	Type II diabetes	(Abhary et al., 2010)

Associated with abdominal aortic aneurysm (AAA)					
ENSG00000100985	*MMP9* (matrix metallopeptidase 9) ‡	20	Connective tissue degradation, TGFβ	BAV-TAA with autoimmune disease (case report), AAA	(Foffa et al., 2009)
ENSG00000159640	*ACE* (angiotensin I converting enzyme) ‡	17	Connective tissue degradation, angiotensin II	BAV-TAA, AAA, left ventricular hypertrophy	(Foffa et al., 2009, Foffa et al., 2012)
ENSG00000177000	*MTHFR* (methylene-tetrahydrofolate reductase *	1	Connective tissue degradation	BAV-TAA with autoimmune disease (case report), AAA, coronary artery disease	(Foffa et al., 2009)
ENSG00000106366	*PAI1/SERPINE1* (serpin peptidase inhibitor) *	7	Connective tissue degradation	BAV-TAA with autoimmune disease (case report), AAA, coronary artery disease	(Foffa et al., 2009)
Associated with aortic stenosis					
ENSG00000130203	*APOE* (apolipoprotein E) ‡	19	Catabolism of triglyceride-rich lipoprotein constituents	Aortic stenosis-BAV (case report), atherosclerosis, Alzheimer's	(Saravanan and Kadir, 2009)
ENSG00000084674	*APOB* (apolipoprotein B) ‡	2	Primary apolipoproteins of chylomicrons & low-density lipoproteins	Calcific aortic stenosis, atherosclerosis	(Anger et al., 2006)
ENSG00000111424	*VDR* (Vitamin D receptor) *	12	Transcription factor, mineral metabolism	Calcific aortic stenosis, type II vitamin D-resistant rickets	(Ortlepp et al., 2001)
ENSG00000091831	*ESR1* (Estrogen receptor alpha)	6	Transcription factor	Calcific aortic stenosis, cancer, osteoporosis	(Anger et al., 2006)
ENSG00000136634	*IL10* (Interleukin 10)	1	Anti-inflammatory cytokine	Calcific aortic stenosis, HIV-1 infection, rheumatoid arthritis	(Ortlepp et al., 2004)
ENSG00000160791	*CCR5* (chemokine receptor 5) ‡	3	Transmembrane protein, anti-inflammatory properties	Calcific aortic stenosis, HIV-1 infection	(Ortlepp et al., 2004)
ENSG00000118523	*CTGF* (connective tissue growth factor) ‡	6	Chondrocyte proliferation	Calcific aortic stenosis, systemic sclerosis	(Ortlepp et al., 2004)
ENSG00000146648	*EGFR* (epidermal growth factor receptor)	7	Transmembrane protein, cell proliferation	Calcific aortic stenosis, lung cancer	(Anger et al., 2006)
Associated with mitral valve prolapse (MVP)					
ENSG00000105329	*TGFB1* (TGF-beta1) ‡	19	Connective tissue degradation, TGFβ	MVP, increased expression in LDS aorta	(Lindsay et al., 2012, Hagler et al., 2013)
ENSG00000108821	*COL1A1* (Collagen Type I) ‡	17	Collagen metabolism	MVP, EDS, osteogenesis imperfecta	(Sykes et al., 1990, De Paepe, 1998, Malfait et al., 2007)
ENSG00000164692	*COL1A2* (Collagen type II) ‡	7	Collagen metabolism	MVP, osteogenesis imperfecta	(Sykes et al., 1990, De Paepe, 1998)

ENSG00000060718	*COL11A1* (Collagen type XI) ‡	1	Collagen metabolism	MVP, EDS, Stickler syndrome, Marshall syndrome	(Griffith et al., 1998, Khalifa et al., 2012)
ENSG00000166341	*DCHS1* (Dachsous 1) ‡	11	Cadherin family member, expressed in fibroblasts	MVP, zebrafish model - no valve (personal communication to S.Cook)	(Freed et al., 2003)

Abbreviations: AAA, abdominal aortic aneurysm; Ao, aorta; AS, aortic stenosis; Asc Ao, ascending aortic; ASD, atrial septal defect; BAV, bicuspid aortic valve; DGS/VCFS, DiGeorge syndrome/Velo-cardio-facial syndrome; DORV, double outlet right ventricle; EDS, Ehlers Danlos syndrome; KO, knock-out; LDS, Loyes Dietz syndrome; MFS, Marfan syndrome; MVP, mitral valve prolapse; TAA, thoracic aortic aneurysm; TOF, Tetralogy of Fallot; VSD, ventricular septal defect.

Library preparation and sequencing

Targeted exons and adjacent introns were enriched and barcoded, followed by next-generation sequencing to screen for sequence variants. First, 3µg of genomic DNA was sheared using the Covaris S2 system and libraries constructed using the SureSelectXT Target Enrichment System for SOLiD 4. Libraries were multiplexed and 32 samples pooled per lane for sequencing on the SOLiD 5500 platform, to generate paired end reads (75bp + 35bp).

7.3.3 Data analysis

SOLiD 5500xl reads were demultiplexed and aligned in colour space using LifesScope v2.5.1 "Targeted re-sequencing" pipeline (http://www.lifetechnologies.com/us/en/home/technical-resources/software-downloads/lifescope-genomic-analysis-software.html).

SOLiD Accuracy Enhancement Tool (SAET) was used to improve color call accuracy prior to mapping. SAET implements a spectral alignment error correction algorithm that uses quality values and properties of color space. All the parameters were used as default to streamline the data analysis. Duplicate reads were marked by LifeScope and created a subset file (ontarget) based on reads mapping quality > 8. In LifeScope "diBayes" algorithm was used to find single nucleotide polymorphisms (SNPs) and "smallindel" algorithm to call small insertion/deletions (indels).

Local realignment around indels, and base quality score recalibration process were done in The Genome Analysis Toolkit (GATK) v1.5-20-gd3f2bc4 (McKenna et al., 2010). Alignment summary metrics, callability and coverage report were calculated using Picard v1.65 (http://picard.sourceforge.net), BedTools v2.11.2 (Quinlan and Hall, 2010) and in house perl scripts. The same "ontarget" file was used in LifeScope, GATK and Samtools

v0.1.18 (Li et al., 2009) programs to make consistent variant calls. Only SNPs that had at least one copy of the non-reference allele, a sequencing depth of >4x, mapping and base quality score >30 were considered for analysis for each test sample. Variants were functionally annotated using the Ensembl API v70_37 (McLaren et al., 2010) and HGMD Professional version 2012.2(Stenson et al., 2003).

7.4 Results

7.4.1 Analysis of variants

A total of 2,746 variants were mapped in the sequenced 63 selected genes. To determine the functional relatedness of called indels and SNPs, variants were filtered in a stepwise approach (Figure 7.1). Selection of radical (frameshift, stop lost/gained, essential splice site) and potentially pathogenic (non-synonymous SNPs, other splice site, inframe indels) variants, led to a total of 370 calls. For non-synonymous variants affecting coding regions, the additional likely effect on protein function was predicted using SIFT (Sorts Intolerant from Tolerant) and Polyphen (Polymorphism Phenotyping) online tools (http://sift.jcvi.org, http://genetics.bwh.harvard.edu/pph2). Selection of variants with damaging and/or conflicting predictions on SIFT and Polyphen limited the total number of likely pathogenic variants to 254. Finally, due to the 0.5-2% incidence of BAV disease in the general population (Braverman et al., 2005), all variants with a minor allele frequency (MAF) of more than 2% (http://www.1000genomes.org) were excluded, leading to a total of 157 calls.

Table 7.2 includes BAV cases that show likely pathogenic alterations in the selected sequenced genes, excluding missense mutations with conflicting predictions on SIFT and Polyphen. Previously annotated variants on dbSNP (http://www.ncbi.nlm.nih.gov/SNP)

are included with an “rs” prefix, with known disease causing mutations high-lighted in bold. Out of the 94 sequenced BAV patients, 62 (66%) harboured likely pathogenic mutations in their genome, with 41 (44%) carrying mutations in more than one gene.

Figure 7.1 Analysis of variants. The process of variant filtering can be viewed. MAF, minor allele frequency.

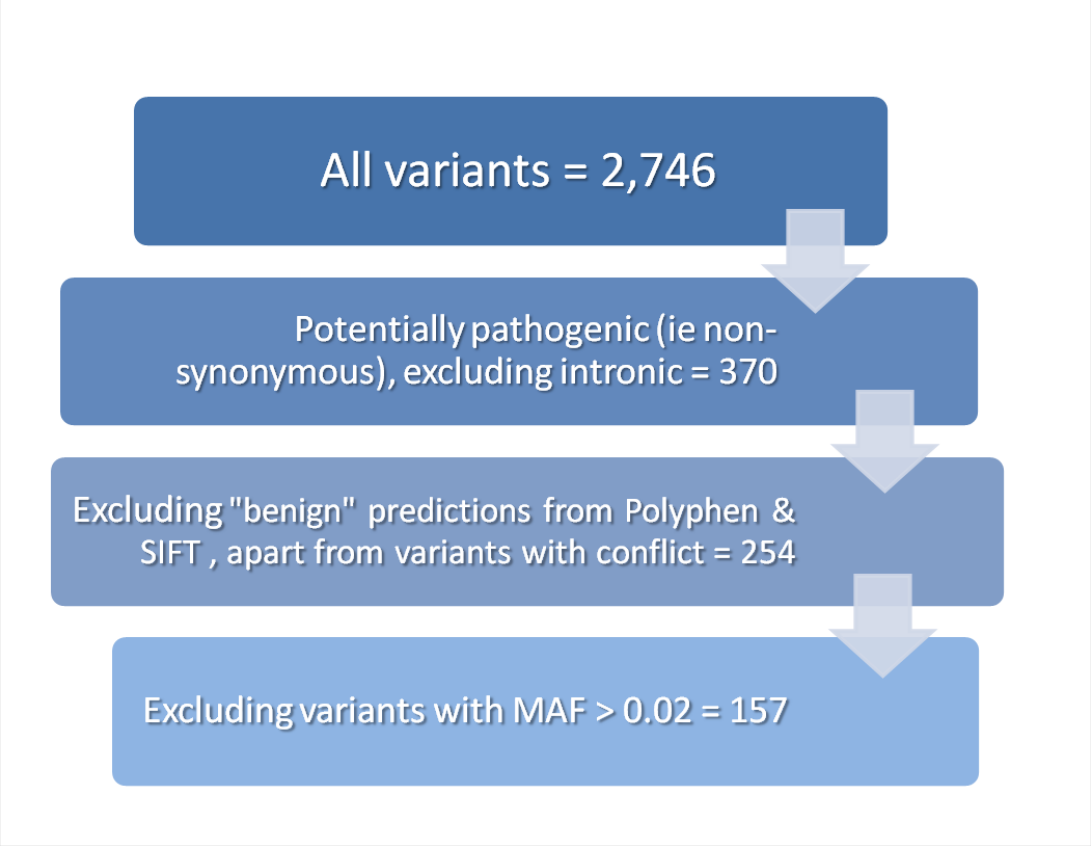

Table 7.2 Next-generation sequencing preliminary results. Sift and polyphen predictions are included for missense mutations (D: deleterious, PD: probably damaging, pD: possibly damaging, U: unknown) unless known to cause disease (high-lighted in bold).

Case ID (#)	Gene	Mutation	Consequence type	
			Missense Sift/Polyphen	Other
Extracellular matrix proteins				
1984	***FBN1***	c.2425C>T, p.Pro809Leu	D/PD	
1985, 2040	***FN1***	c.4213C>T, Arg1405Trp	D/PD	
2014		c.371C>A, p.Thr124Asn	D/pD	
2052		c.1313-7T>C (rs202045892)		Splice
2053, 2021		c.1070G>A, p.Gly357Glu	D/pD	
2008	***ELN***	c.614-8C>T (rs201859539)		Splice
2056		c.391+8C>T (rs55868272)		Splice
2059, 2010		c.2132G>A		Splice
1991, 1993		c.572G>A, p.Gly191Asp	D/PD	
1984	***COL3A1***	**c.2002C>A, p.Pro668Thr (rs1801183)**	**Familial aortic aneurysm (Tromp et al., 1993)**	
2013	***COL4A1***	c.3026G>A, p.Gly1009Glu	D/pD	
2037		c.4077_4078insAGAG		Frameshift_elongation
2040		c.365T>G, p.Ile122Ser	D/U	
2004, 2031	***PLOD1***	c.1675C>T, p.Arg559Cys	D/PD	
2016	***PLOD3***	c.*191C>T		3 prime UTR
2058, 1978, 1979, 1996		c.516G>C, p.Asp173His	D/PD	
2055	***LOX***	c.740+6G>A (rs41478244)		Splice
Transcription factors				
2000	***SOX9***	c.685+8G>A (rs117696751)		Splice
2015	***NFATc1***	c.*1427C>T (rs150249025)		3 prime UTR
1984	***NKX2.5***	c.428G>A, p.Arg143Gln	U	
2008		c.61G>C, p.Glu21Gln (rs104893904)	D/PD	
2031		c.763G>A, p.Ala255Thr	D/pD	

Transmembrane proteins				
1993	***NOTCH1***	c.1649dupA, p.Tyr550X		Frameshift elongation
2018, 2046		**c.2080G>A, p.Glu694Lys (rs79782048)**	**AS (McBride et al., 2008)**	
2025		c.591C>A, p.Asn197Lys	D/PD	
2026		c.5282G>A, p.Arg1761Gln	D/pD	
2031		c.6356T>A, p.Val2119Glu	D/Pd	
2032		**c.4168C>A, p.Pro1390Thr (rs191645600)**	**BAV-TAA(McKellar et al., 2007)**	
2038		c.3644-4G>C		Splice
2055		c.7652C>T, p.Pro2551Leu	D/pD	
2059		c.1127delG, p.Cys376SerfsX255		Frameshift truncation
1991, 1993	***ENG***	c.572G>A, p.Gly191Asp	D/PD	
2046	***JAG1***	c.1244T>A, p.Val415Glu	D/PD	
Cytoplasmic proteins				
1988	***MYH11***	c.5787-11_5787-8delCTCT		Splice
2049		c.2665A>C, p.Lys889Gln	D/PD	
1989	***FLNA***	c.901C>T, p.Arg301Trp	D/pD	
1992		c.-116-7T>C		Splice
1996		c.5972C>T, p.Ser1991Leu	D/pD	
2043		c.1068T>C		Splice
2059		c.1286C>T, p.Thr429Met (rs36051194)	D/PD	
2047	***NF1***	n.376+1G>A (rs184954044)		Splice
1978, 2009, 2054	***TSC2***	c.52C>T, p.Thr18Met	U	
1979		c.4368+6C>T		Splice
2026		c.1915C>T, p.Arg639Trp	D/PD	
2032, 1988		c.1747G>A, p.Ala583Thr	D/PD	
2045, 2053		c.3883+5C>T		Splice
2003	***NOS3/eNOS***	c.271-84_276del		Splice
2053, 1999	***AXIN1***	c.2186+7C>T (rs189357878)		Splice

1977, 2040, 1999		c.334C>T, p.Thr112Met	D/pD	Splice
1998	***PDIA2***	c.531-3C>T, p.Gln195X (rs45619835)		
2054		c.1388_1389delCT, p.Leu464GlnfsX13		Frameshift truncation
2014	***GAA***	c.1192C>T		Splice
2029		c.858+6_858+12delGCGGCGG		Splice
Nuclear protein				
2037	***MED12***	c.6339delAinsACAGCAACAGCAG, p.Gln2109_Gln2112dup		Inframe insertion
Vascular endothelial growth factor (VEGF) pathway members				
2033	***HIF1A***	c.1267G>T, p.Asp423Tyr	D/pD	
1978	***ACTN1***	c.1397A>G, p.Tyr466Cys	D/PD	
2016		n.95+4A>C		Splice
Enzymes regulating nitric oxide generation				
2033, 2009	***DDAH1***	c.260C>T, p.Thr87Met	D/PD	
Associated with abdominal aortic aneurysm				
1979		c.886G>A, p.Gly296Ser	D/PD	
2012		c.773C>T, p.Thr258Ile	D/PD	
2023	***MMP9***	c.734delC, p.Thr246ProfsX92		Frameshift truncation
2065		c.1751-6C>T		Splice
2068		c.1232A>G, p.His411Arg	D/pD	
2031, 2029, 2066		c.731A>G, p.Tyr244Cys	D/PD	
2045		c.1306+5C>T		Splice
2046, 2059, 1977	***ACE***	c.1025C>T, p.Thr342Met	D/PD	
2052		c.1513C>G, p.Pro505Ala	D/PD	
2052		c.1586+8C>T		Splice
Associated with aortic stenosis				
2006, 2016	***APOE***	**c.805C>G, p.Arg269Gly**	**Hyperlipidaemia(Marduel et al., 2013)**	

1980		c.3025G>A, p.Gly1009Arg	D/PD	
1988		c.11477C>T, p.Thr3826Met	D/PD	
1992		c.10672C>T, p.Arg3558Cys (rs12713559)	D/PD	
1994		c.5066G>A, p.Arg1689His (rs151009667)	D/pD	
2000	***APOB***	c.4850G>A, p.Gly1617Glu (rs146341569)	D/PD	
2010		c.3843C>T		Splice
2025		c.10294C>G, p.Gln3432Glu	D/PD	
2034		c.6639_6641delTGA, p.Asp2213del		Inframe deletion
2044		c.2981C>T, p.Pro994Leu	D/PD	
2063	***VDR***	c.909C>T		Splice
2000	***CCR5***	c.-10G>C		Splice
2036, 2057	***CTGF***	c.290-6C>T		Splice
Associated with mitral valve prolapse				
1983		c.71delGinsCGGGC, p.Gly24AlafsX78		Frameshift
2009, 2043, 2018	***TGFB1***	c.713-8delC (rs28365167; rs55659002)		Splice
2036		c.463C>G, p.Leu155Val	D/PD	
2061		c.887G>A, p.Arg296Gln	D/PD	
2013	***COL1A1***	c.2708A>G, p.Lys903Arg	D/U	
2050		c.935G>A, p.Arg312His	D/U	
1994	***COL1A2***	c.594+5A>T		Splice
2046		c.3853A>C, p.Asn1285His	D/U	
2044	***COL11A1***	c.4258C>G, p.Pro1420Ala	D/U	
2004		c.6508C>T, p.Arg2170Cys	D/PD	
2003, 1993	***DCHS1***	c.5160A>T (rs117031105)		Splice
2034		c.1160G>A, p.Arg387His	D/PD	
2068		c.5036-5C>G		Splice

Abbreviations: AS, aortic stenosis; BAV, bicuspid aortic valve; TAA, thoracic aortic aneurysm.

7.5 Discussion

NGS is an advantageous technology allowing parallel sequencing of selected genomic regions at a continuously reducing cost (Ware et al., 2012). Application of high-throughput techniques is particularly promising for genetically heterogeneous traits such as BAV disease. While the preliminary results described here will require further validation by conventional Sanger sequencing, this study exhibits that NGS is capable of detecting both known and potentially novel pathogenic variants related to the diverse BAV phenotype (Figure 7.2). Selected subsets of investigated genes are discussed in the following sections.

7.5.1 Genetic risk factors for aortic stenosis

Patients with BAV have an increased lifetime risk of cardiac complications, the commonest of which is AS requiring AVR (Ward, 2000, Davies et al., 1996). AS predominantly occurs during the middle age of BAV patients and is characterised by calcific aortic valve degeneration (Ward, 2000). Sclerotic changes in the valve leaflets start earlier, in the second decade of life, with a more rapid progression of AS if the BAV leaflets are asymmetrical or in the anteroposterior position (Mautner et al., 1993, Beppu et al., 1993).

Known genetic risk factors for aortic valve disease in the general population have rarely been investigated in BAV patients. Chan et al. assessed the role of conventional atherosclerotic risk factors in BAV disease and found that hypercholesterolemia and systemic hypertension are associated with development of AS (Chan et al., 2001). Following on from this, a single case report in the literature has shown the presence of e3/e4 apolipoprotein E genotypes, associated with hypercholesterolaemia, in a pair of

monozygotic twins with severely stenotic and calcified R-L BAVs (Saravanan and Kadir, 2009).

Figure 7.2 Previously investigated genes for association with BAV disease and/or hypoplastic left heart syndrome. Following next-generation sequencing, genes harboring likely pathogenic variants are denoted as * (in a single patient) or ‡ (recurrent or multiple variants).

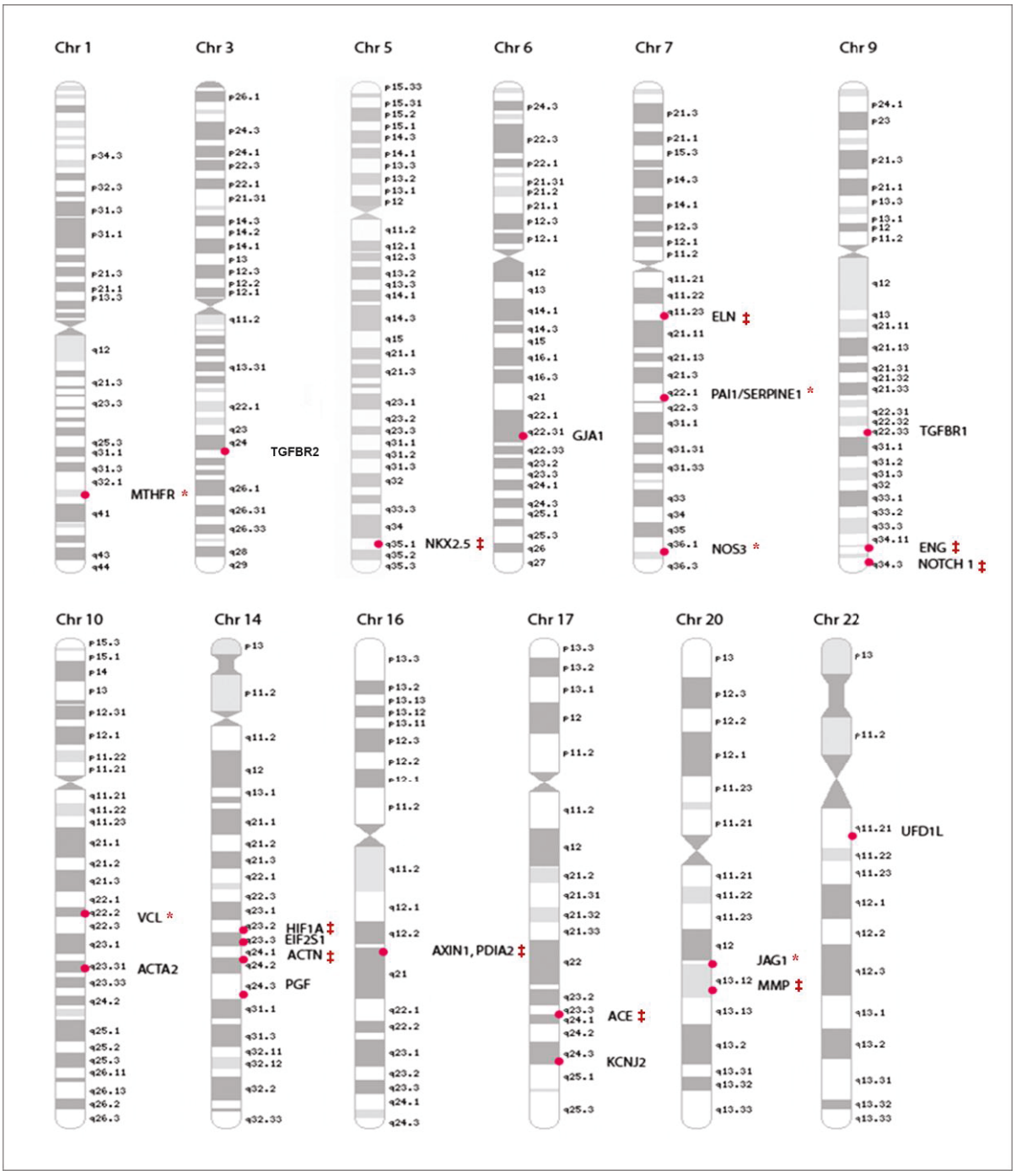

In this study, the presence of known genetic aberrations that could be assessed for risk of AS in BAV was further investigated, including known polymorphisms in *IL-10*, *CTGF*, *CCR5*, and *VDR* (Table 7.1) (Ortlepp et al., 2004, Ortlepp et al., 2001). A previously reported polymorphism in *APOE* gene (c.805C>G, p.Arg269Gly) was found in 2 BAV subjects, out of which one (#2016, Table 7.2) had stenotic valve disease (Marduel et al., 2013). Other potentially pathogenic variants were reported in *APOB*, *VDR, CCR5*, and *CTGF* genes with 4 BAV patients having AS (#1980, #2044, #2063, #2036, Table 6.2). A genotype–phenotype relationship could be suggested by these preliminary findings in selected BAV patients, whereby increased predisposition to AS would be owing to genetic variants that are not unique to the BAV population (Figure 7.3a).

7.5.2 Genes related to BAV formation

A number of genes encoding for transcription factors with a key role in aortic valve development were included in our NGS library (Table 7.1 and **Chapter 1, Figure 1.4**). Mutations in *NOTCH1*, previously associated with BAV and aortic valve calcification (Garg et al., 2005), were present in 10 BAV subjects (Table 7.2). Out of these, 4 patients had sclerotic changes in their aortic valves (#1993, # 2026, #2038, #2056) and 3 harboured previously described mutations (#2018, #2046, #2032, Table 6.2) (McBride et al., 2008, McKellar et al., 2007). A few of these patients had variants in more than one genes, including a young male BAV patient with stenotic calcified BAV and TAA (Figure 7.3c), who also carried a likely pathogenic mutation in *ENG* gene (#1993, Table 7.2). Similar to *NOTCH1*, *ENG* participates in valve formation during embryogenesis and has been associated with BAV (Niessen and Karsan, 2008, Qu et al., 1998, Wooten et al., 2010). Mutations in these two genes may also contribute to aortopathy seen in this

subject, as *NOTCH1* missense variants have been reported in patients with BAV-TAA phenotype (McKellar et al., 2007), and *ENG* is part of the TGFβ receptor complex (**Chapter 1, Figure 1.6)** with a key role in angiogenesis (Li et al., 1999).

Potentially pathogenic variants were found in additional genes involved in cardiac valve development, including *NFATc1* and *JAG1* (Table 7.2) (de la Pompa et al., 1998, McElhinney et al., 2002). Surprisingly, despite the strong association between eNOs deficiency and development of BAV in mice (Lee et al., 2000), only a single patient was found to have a variant in *eNOS* and two patients shared a variant in *DDAH1*, encoding an enzyme regulating nitric oxide generation (Table 7.2) (Abhary et al., 2010).

6.5.3 Genes related to aneurysm formation

The BAV aorta is known to be intrinsically abnormal, yet the culprit underlying genetic defect remains elusive. Affected family members may have isolated thoracic aortic dilatation or increased aortic stiffness in the absence of BAV (Hiratzka et al., 2010, Loscalzo et al., 2007), suggesting a common genetic background for BAV and TAA as variable manifestations of the same condition. Several signalling pathways share critical roles in the development of the aortic valve and the great vessels, such as *NOTCH1*, TGFβ, and Wnt signalling (**Chapter 1, Figure 1.6**) (Hinton, 2012). Although *NOTCH1* mutations have been linked to the TAA phenotype in sporadic BAV disease, familial studies show that they are exceedingly rare and do not contribute significantly to the non-calcific BAV-TAA phenotype (Kent et al., 2013, McKellar et al., 2007). In our study, 11% of the sequenced BAV patients harboured likely pathogenic or known *NOTCH1* variants, out of which 40% had TAA. Sequencing of two critical members of the Wnt pathway, *AXIN1* and *MED12*, led to identification of possibly damaging variants in 3

patients, with one having a BAV-TAA phenotype (#2037, Table 7.2) (Wooten et al., 2010, Rocha et al., 2010).

Histopathological changes seen in the BAV aorta are also present in a number of inherited forms of aortopathy, as discussed in **Chapter 1**. Patients with BAV have been previously reported to be negative for *FNB1* mutations (Robinson and Godfrey, 2000) despite the common findings with the MFS aortic media of decreased fibrillin-1 expression (Fedak et al., 2003) and increased TGFβ signalling (**Chapter 4**) (Gomez et al., 2009). Interestingly, a 25 year-old BAV patient with TAA in our study was found to have a likely pathogenic *FBN1* variant, without a diagnosis of MFS (#1984, Table 7.2). The same patient also carried a mutation in *COL3A1* gene (rs1801183) which has been associated with familial aortic aneurysm (Tromp et al., 1993). Family members were not examined at the time of the study although the patient reported a negative family history of aneurysm formation and/or other CHD lesions.

Screening for mutations in *TGFBR1* and *TGFBR2* genes associated with MFS type-2 and LDS was negative in BAV patients, in agreement with previous findings (Arrington et al., 2008). Mutations in *MYH11* gene, encoding the major contractile protein βMHC in VSMCs, have been linked to familial TAA associated with PDA and less frequently, BAV (Zhu et al., 2006, Pannu et al., 2007). In this study, 2 patients with BAV-TAA had likely pathogenic variants in *MYH11*, with no presence of PDA and a positive uninvestigated family history of sudden cardiac death in one of the probands (#2049, Table 7.2). Surprisingly, all patients tested negative for *ACTA2* mutations, despite its previous associations with familial aortic aneurysm and BAV disease (Guo et al., 2007).

Additional candidate genes for BAV aortopathy include genes encoding key components of the aortic ECM and genes associated with AAA formation (Table 7.1). An interesting novel candidate arising from our NGS is *FN1* encoding for fibronectin-1, a marker of VSMC synthetic phenotype (Zhang et al., 1995, Thyberg and Hultgardh-Nilsson, 1994), with likely pathogenic variants identified in 6 BAV patients (Table 7.2 and Figure 7.3b). Stress-dependent upregulation of *FN1* has been previously shown in the BAV ascending aorta (Della Corte et al., 2008) and thus, mutations in this gene may represent an initial genetic insult which is further enhanced by *in vivo* haemodynamic perturbations. Multiple variants were also identified in genes associated with AAA, including *MMP9* and *ACE*, suggestive of genetic aberrations in BAV patients that may individually contribute to the TAA (rather than BAV) phenotype (Foffa et al., 2009, Foffa et al., 2012). Although speculative, the latter theory would be further supported by the fact that more than 60% of BAV patients carrying *ACE* mutations also had likely pathogenic variants in other sequenced genes, including *NOTCH1* mutations (#2046, #2059, Table 7.2).

7.5.4 Syndromic forms of BAV disease

BAV can be a component part of a number of syndromes, outside the scope of familial TAA (McElhinney et al., 2002, Andelfinger et al., 2002, Szabo et al., 2006, Hinton et al., 2009). Targeted sequencing for mutations in *JAG1* (Allagile syndrome) and *KCNJ2* (Andersen syndrome) did not reveal any likely pathogenic variants whereas 6 BAV patients had mutations in *ELN* gene, associated with Williams-Beuren syndrome and supravalvular AS, which absence of the latter feature in our subjects with *ELN* mutations (Table 7.2) (McElhinney et al., 2002, Andelfinger et al., 2002, Szabo et al., 2006, Li et al., 1998). BAV can also be part of hypoplastic left heart syndrome (HLHS),

encompassing abnormalities of the left ventricular myocardium, aortic and mitral valves, and ascending aorta (Hinton et al., 2009). Sequencing of genes associated with HLHS revealed variants in *HIF1A* in a single patient with TAA, coarctation of the aorta (CoA), and absent valvular disease (#2033), and in *ACTN1* in 2 patients with stenotic BAV with no other associated lesions (#1978, #2016, Table 7.2) (Hinton et al., 2009).

Other phenotypic associations of BAV disease include a wide variety of cardiovascular malformations, such as CoA, ventricular septal defect (VSD), and mitral valve dysfunction (Braverman et al., 2005). Sequencing of genes related to mitral valve prolapse (Table 7.2) identified likely pathogenic variants in a number of candidate genes (*TGFB1, COL1A1, COL1A2, COL11A1, DCHS1*) (Hagler et al., 2013, Sykes et al., 1990, Freed et al., 2003, Griffith et al., 1998). None of these patients had reported mitral valve abnormalities although, interestingly, a number of them had associated CHD lesions including VSD (#2013, #2044), and CoA (#1994, #2044, #2033, Table 6.2). Finally, sequencing of the cardiac homeobox gene *NKX2.5* previously associated with a wide variety of CHD lesions (Schott et al., 1998, Wang et al., 2011), led to identification of variants in 3 BAV patients, out of which one (#2008, Figure 7.3d) had concomitant VSD, PDA, and CoA and another (#2031, Table 7.2) had VSD and CoA.

7.5.5 Towards a uniform theory

Preliminary results arising from this study in conjunction with the known complex BAV inheritance pattern (Loscalzo et al., 2007, Huntington et al., 1997) suggest a multifactorial model for phenotypic expression of BAV disease characterized by a number of susceptibility genes with different liability thresholds (Figure 7.4) (Hinton, 2012). Molecular networks sense and react to genetic and environmental perturbations

that in turn, affect disease risk (Schadt, 2009). Therefore, gene networks related to variable BAV manifestations, such as AS and TAA, may be affected by primary genetic insults but also, by epigenetic modifications and altered haemodynamics secondary to the malformed aortic valve (Nagy and Back, 2012, Shah et al., 2012, Hope et al., 2010).

The effect of epigenetic modifications on BAV phenotypes has been increasingly reported in the literature, with evidence of Smad2 overexpression in TAA, similar to the one seen in our BAV samples (**Chapter 4**), influenced by increased acetylation and methylation of the histone protein H3 in the medial layer of BAV-TAAs (Gomez et al., 2011). Furthermore, VSMC reprogramming has been shown to take place in response to TAA formation with epigenetically induced overexpression of protease nexin-1 (*PN-1*) promoting anti-proteolytic activity which may limit the risk of acute dissection and thus, imposing TAA patients with absence of these responsive processes to enhanced risk of wall rupture (Gomez et al., 2013).

In a different study comparing gene methylation in aneurysmal ascending aortic tissue samples from BAV and TAV patients, differential signature patterns of DNA methylation and expression were highlighted with the most profound differences found in the protein tyrosine phosphatase, non-receptor type 22 (*PTPN22*), a gene involved in T-cell receptor signalling (Shah et al., 2012). Development of calcific BAV stenosis may also be epigenetically influenced with calcified aortic valve tissue exhibiting decreased DNA-methylation in the promoter region of the pro-inflammatory enzyme 5-lipoxygenase (*5-LO*) gene, leading to its overexpression (Nagy and Back, 2012).

In conclusion, the above proposed multifactorial model (Figure 7.4) could explain the presence of intrinsic abnormalities in the BAV aorta but also the different risks of aortic

dilatation carried by BAV morphological subtypes, thus merging the "genetic" and "haemodynamic" hypothesis of BAV aortopathy into a uniform theory (Prapa and Ho, 2012, Tadros et al., 2009).

Figure 7.3. Proposed genotype-phenotype correlartions. Different genotypes in BAV disease may account for the wide variety of observed phenotypes. These associations are hypothetical and merit further investigation. A. Mutation in ApoB gene associated with calcific BAV disease (seen in red, histology of the aortic valve leaflet). B. Mutation in FN1 gene associated with aortic root dilatation and corresponding severe elastic fragmentation of the media on histology. C. Mutations in NOTCH1 and ENG genes associated with aortic stenosis and aortopathy. D. Mutations in NKX2.5 gene associated with a variety of cardiovascular malformations. A; haematoxylin and eosin stain, B-D; elastic van gieson stain, A-D x 20 magnification. Histology specimens and aortic images (three-dimensional models from Chapter 3) are patient-specific (subject IDs: a;#3/1980, b;#4/2021, c;#1/1993, d;#7/2008). AS; aortic stenosis, AVD; aortic valve disease, CoA; coarctation of the aorta, PDA; patent arterial duct; TAA; thoracic aortic aneurysm, VSD; ventricular septal defect.

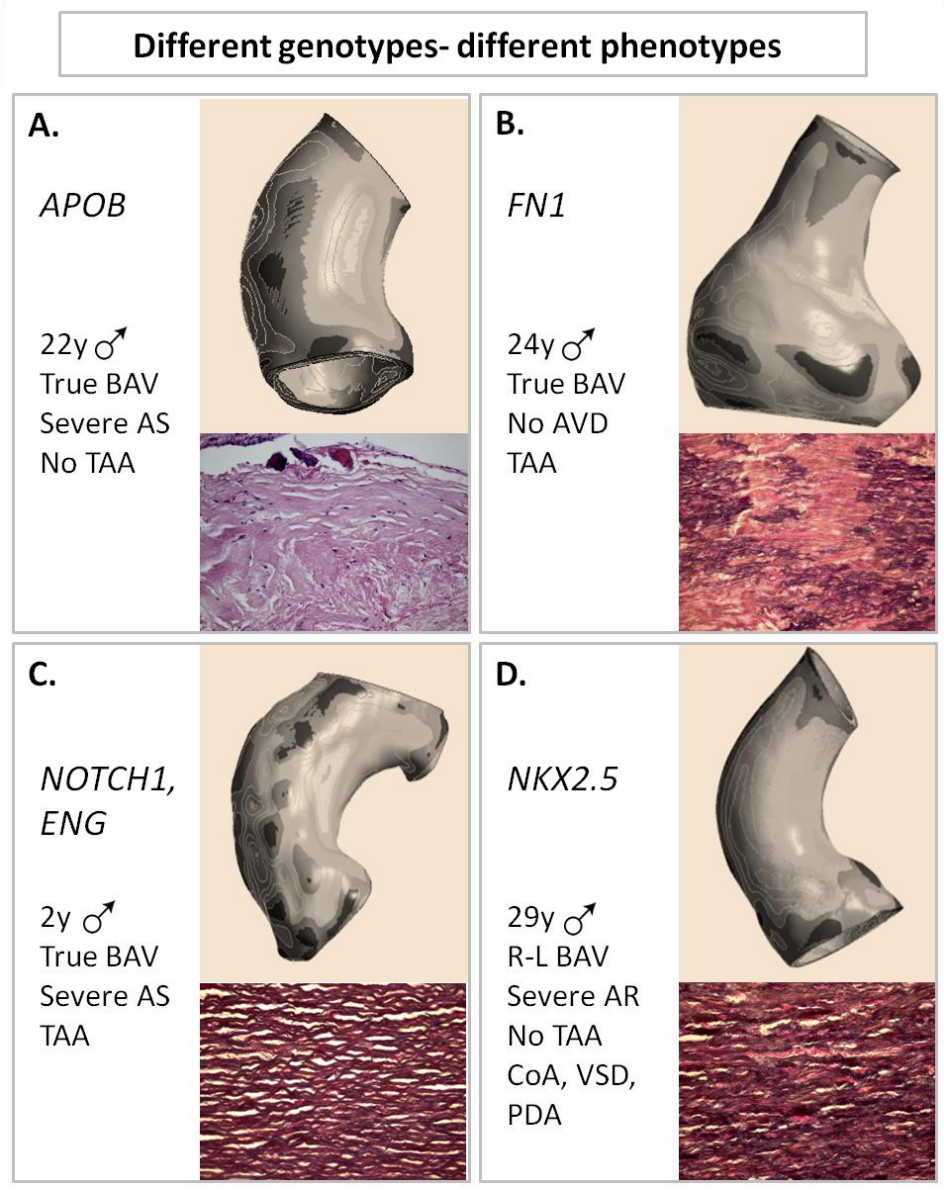

Figure 7.4. Hypothetical multifactorial model for BAV phenotypic expression. A. Multifactorial model characterized by a number of susceptibility genes with different liability thresholds affecting phenotypic expression of BAV disease. The interplay between primary genetic insults (blue) and epigenetic modifications (pink) can be seen. **B.** Hypothetical threshold model for phenotypic manifestations of BAV disease. Numerous susceptibility genes contribute to BAV phenotypes, with partial overlap (eg. Ca2+; a-c, BAV; b-e, TAA; e-h, HLHS; i-j). Assuming that each phenotype is dependent on different liability thresholds of predisposing variants (marked in blue), for example greater ≥2 variants for Ca2+, BAV, and HLHS, and ≥3 variants for TAA, then variable phenotypes manifest. Ca2+; calcification, HLHS, hypoplastic left heart syndrome; TAA; thoracic aortic aneurysm. Figure b. adjusted by Hinton (Hinton, 2012).

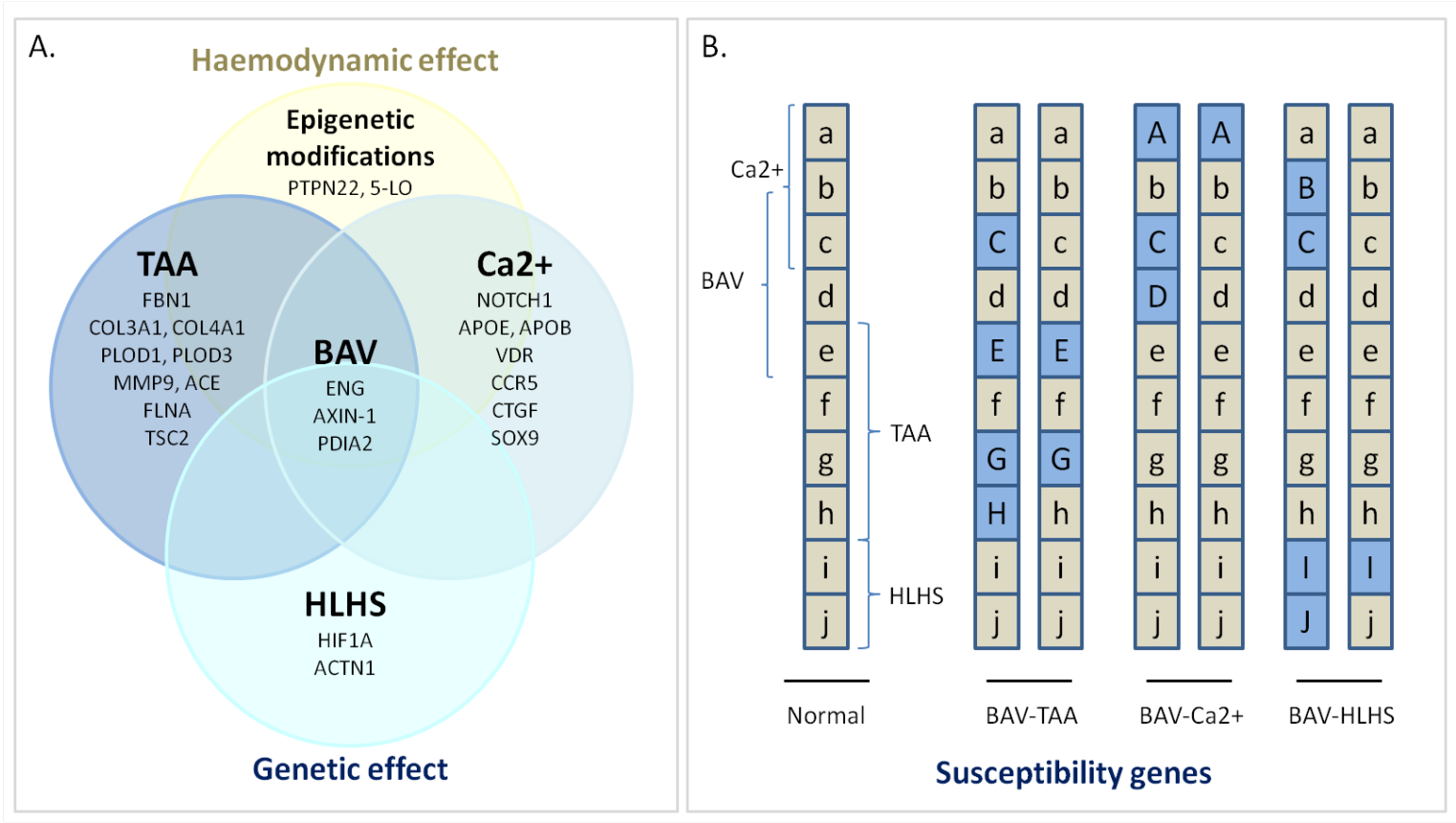

7.5.6 Limitations

Variants presented in this chapter are the result of preliminary analyses and require further validation via Sanger sequencing. Presented data are currently being processed in conjunction with NGS results from a different BAV cohort obtained via collaboration with St George's Hospital, London, UK. Following completion of preliminary analyses, likely pathogenic variants in well-conserved genes with potential phenotypic correlations will be prioritized and further evaluated via causation studies.

7.6 Conclusion

Application of NGS techniques in BAV disease allowed comprehensive assessment of a wide array of targeted genes in a timely and cost-effective manner. Previously reported variants were identified in *NOTCH1*, *COL3A1*, and *APOE* genes with additional discovery of a large number of likely pathogenic variants in genes related to BAV formation, aortopathy, calcific AS, and HLHS. While the reported preliminary results merit further validation by conventional Sanger sequencing, the concomitant presence of variants in different genes in 44% of sequenced patients suggests that BAV is a polygenic trait.

Chapter 8. General discussion

Abbreviations

AAA Abdominal aortic aneurysm
ACE Angiotensin converting enzyme
BAV Bicuspid aortic valve
CHD Congenital heart disease
CNV Copy number variation
MRI Magnetic resonance imaging
PAH Pulmonary arterial hypertension
TAA Thoracic aortic aneurysm
TGFβ Transforming growth factor beta
VSD Ventricular septal defect
VSMC Vascular smooth muscle cell
WSS Wall shear stress

In summary, multiple facets of BAV aortopathy were examined with application of distinct research methodologies. Novel data arising from these studies support a multifactorial rather than single (haemodynamic or genetic) origin of aortic abnormalities in BAV disease and may contribute to future individualised risk stratification of BAV patients for aortic complications.

8.1 Haemodynamic influence

Computational modelling techniques were applied to examine the effect of geometrical features of BAV aortic phenotypes on generated circumferential stress (exerted perpendicular to the aorta) and corresponding histological abnormalities of the media (**Chapter 3**). Aortic pathology is thought to occur when radial stress exceeds the tensile strength of the aortic wall (Nathan et al., 2011a). In agreement with a previous study, maximal circumferential stress in the majority of our studied BAV subjects occurred above the left-coronary sinus instead of the right-coronary sinus, where type A dissections typically occur (Nathan et al., 2011b). However, a pattern of shifting stress location was noticed from the convex to the concave aspect of the ascending aorta as the typical anterolateral bulge (seen in "post-stenotic" dilatation) became more asymmetrical (Figure 8.1).

Novel correlations between the degree of circumferential stress and the severity of corresponding histological abnormalities revealed strong associations between normalised mechanical stress, fibrosis, and cyst-like formations in the aortic root and a weaker association between stress and fibrosis in the ascending aorta. These findings suggest that mechanical stress may have a greater pathophysiologic effect on the dilated root as opposed to the ascending aorta of BAV patients, which is also subjected to elevated WSS due to abnormal recirculation flow vortices (Hope et al., 2010).

The effect of elevated pressures on arterial wall remodelling was also investigated in the setting of PAH and CHD with evidence of predominant fibrotic changes and a close

correlation between increasing vessel diameters and severity of medial wall changes in the hypertensive pulmonary artery (**Chapter 5**). Interestingly, despite its dilatation, the PAH/CHD pulmonary artery rarely dissects and this may be owning to the low frequency of cyst-like formations in the medial layer (Tredal et al., 1974). The latter formations have been described as the only potential histological feature differentiating the dissecting aorta from normotensive and hypertensive age- and sex-matched controls (Manley, 1964). In our studied PAH/CHD specimens, cyst-like formations of a significant degree were only found in a single specimen with recurrent pulmonary arterial wall rupture. In contrast, extensive cyst-like lesions were seen in up to 55% of BAV aortic specimens and may render the arterial wall more susceptible to dissection and rupture compared to the PAH/CHD great vessels (**Chapters 3 and 4**).

The above histopathological findings underlie a proteolytic process which constitutes the first necessary step for arterial wall "tear" formation. The secondary environmental triggers leading to aortic dissection and/or rupture remain elusive. So far, the main culprits include emotional stress and physical exertion resulting in acute hypertension and increased radial stress exceeding the tensile strength of the aortic wall (Nathan et al., 2011a). Thus, pharmacological treatment to reduce blood pressure to the lowest tolerated level is recommended in patients with TAA (Hiratzka et al., 2010). Moreover, heavy weight lifting accompanied by extreme isometric exercise is advised against as unusual sudden stress on the aorta may precipitate aortic dissection/rupture.

Studies investigating critical levels of mechanical stress at which aortic dissection is more likely to occur are currently lacking. Despite investigations by our group (**Chapter 3**) and others (Nathan et al., 2011b) exhibiting elevated mechanical stresses in the BAV aorta, the next necessary step would be that of sequential computational studies in enlarging or dissected BAV aortas to validate the prognostic value of maximal mechanical stress, similar

to AAA disease (Fillinger et al., 2003). However, application of structural analysis in clinical practice would still be challenging as it requires input of a large number of data, such as patient-specific arterial wall material properties, which is both time consuming and currently unavailable to clinicians.

The above obstacles may be overtaken in the future by fluid-structure interaction analyses which, in conjuction with functional imaging by positron emission tomography, have highlighted a spatiotemporal link between elevated tensile wall stresses and accelerated metabolic activity in the aortic wall of 5 patients with thoracic or abdominal aortic aneurysm (Xu et al., 2010). Despite these exciting preliminary findings, fluid-structure interaction analyses require a significant amount of workload, restricting their current use as a research rather than clinical tool (Scotti et al., 2005). Alternatively, phase contrast MRI allows real-time wall shear (rather than mechanical) stress measurements and may serve as an additional risk stratification tool in BAV disease, provided that such data fit the clinical context of progressive arterial disease (Barker et al., 2010).

Overall, advances in computational imaging, such as the ones explored in this thesis, can potentially hold a promising future in tailored risk stratification of BAV patients with aortic aneurysms. However, there is currently an increased need for a focused stepwise approach towards clinical translation of this biomechanical data. Moreover, the reproducibility and cost-effectiveness of the above time-consuming techniques needs to be assessed before their application in a clinical setting.

8.2 Developmental aspects

Our immunohistochemical findings confirmed the presence of increased TGFβ signalling in the aneurysmal BAV aorta, similar to other connective tissue disorders such as LDS and MFS (**Chapter 4**) (Gomez et al., 2009). The binary status of nuclear pSmad2 signalling seen in the BAV mesoderm derived root and the ectoderm derived ascending aorta favoured the theory

of differential TGFβ responsiveness in VSMCs of distinct embryologic origin, proposed by Lindsay and Dietz (Lindsay and Dietz, 2011). Moreover, increased TGFβ signalling was noticed for the first time in non-dilated BAV aortic segments, pointing to a genetic trigger. However, the primary genetic insult in BAV aortopathy remains to be found as BAV sequenced subjects tested negative for *TGFBR1* or *TGFBR2* gene mutations.

Another important aspect of this study was the histological examination of the BAV aortic root which has been largely overlooked in this context (**Chapter 4**). BAV patients with aortic root dilatation and/or predominant regurgitant valve disease had significantly greater medial wall degeneration in their ascending aorta, in agreement with previous findings (Roberts et al., 2011). Thus, the dilated root phenotype may represent the primarily genetic form of BAV aortopathy and constitute a risk factor for the presence of severe intrinsic abnormalities in the ascending aorta (Figure 8.1). This finding would be of significance to current surgical guidelines and would support the application of a lower threshold for surgical replacement of the BAV dilated ascending aorta in the instance of concomitant root dilatation and/or predominant regurgitant valve disease (Roberts et al., 2011). Equally, a higher threshold could be suggested for root replacement in BAV, as the aortic root *per se*, exhibited significantly less abnormalities compared to the ascending aorta, even in the presence of root dilatation. These observations highlight the need for further surgical studies with targeted tissue sampling at the level of the BAV aortic root as well as, imaging studies focusing on the dilated root rather than ascending aortic BAV phenotype.

Importantly, a study published at the time of completion of this thesis confirmed the above observations; by definition of aortic phenotypes of "ascending" (dilated ascending aorta with normal or less dilated root) versus "root" (dilated root with normal or less dilated ascending aorta) phenotype, Della Corte and colleagues found that the root phenotype was an important predictor of fast progression of ascending aortic dilation in 133 BAV adult patients

undergoing echocardiographic follow-up (Della Corte et al., 2013). The presence of aortic regurgitation also predicted an increase in ascending aortic diameter over time. These findings are in direct agreement with our histological findings of greater medial wall degeneration in the ascending aorta of BAV patients with aortic root dilatation and/or predominant regurgitant valve disease and reinforce the view of closer surveillance and potential earlier intervention in BAV patients presenting with predominant dilatation at the root level.

8.3 Genetic aberrations

Different sequencing techniques were employed to investigate the presence of genetic variants in BAV patients, at both the nucleotide and submicroscopic chromosomal level (**Chapters 6 and 7**). CNV analyses revealed a large heterozygous deletion in the *ACE* gene of a patient with heavily calcified BAV and extensive aortopathy. *ACE* mutations have been previously linked to BAV-TAA (Foffa et al., 2012) and were further investigated via targeted next-generation sequencing, revealing a number of likely pathogenic variants in 8% of our sequenced BAV patients. Development of a wide panel of genes associated with various phenotypic manifestations of BAV led to identification of previously reported variants in *NOTCH1*, *COL3A1*, and *APOE* genes with additional discovery of a large number of likely pathogenic variants in genes associated with BAV formation, aortopathy, calcific aortic stenosis, and hypoplastic left heart syndrome.

While these preliminary results require further validation via Sanger sequencing, the presence of multiple gene variants in 44% of sequenced patients support a multifactorial model for phenotypic expression of BAV disease characterized by a number of susceptibility genes with different liability thresholds (Figure 8.1). Gene networks related to variable BAV manifestations, such as aortic stenosis and TAA, might be affected by primary genetic insults as well as haemodynamic and epigenetic modifications (Nagy and Back, 2012, Shah et al.,

2012, Hope et al., 2010), thus merging the "genetic" and "haemodynamic" theory of BAV aortopathy into a uniform model.

Genetic screening is currently recommended for diagnosis of a number of syndromic and non-syndromic forms of TAA (**Chapter 1**) (Hiratzka et al., 2010). Despite the rapidly accumulating evidence that genetic abberations predispose BAV patients to certain phenotypes, including aneurysm formation, we are still on the verge of effective genetic screening to risk stratify this highly heterogeneous patient population. Application of cost- and time-efficient next-generation sequencing methods led to identification of a number of mutations in key BAV-associated genes (**Chapter 7**). However, more evidence is needed to support the causality of fundamental genetic mutations before we embark on genetic screening of BAV patients in a clinical, rather than experimental, context. Alternative approaches, such as whole genome gene expression profiles, have led to identification of signature sets of biomarker genes in asymptomatic TAA disease and may also hold a promising future (Wang et al., 2007).

Figure 8.1 Proposed novel risk stratification tools in BAV aortopathy. Equation for hypothetical interaction between genes and external haemodynamic impulses by Sievers et al. (Sievers and Sievers, 2011).

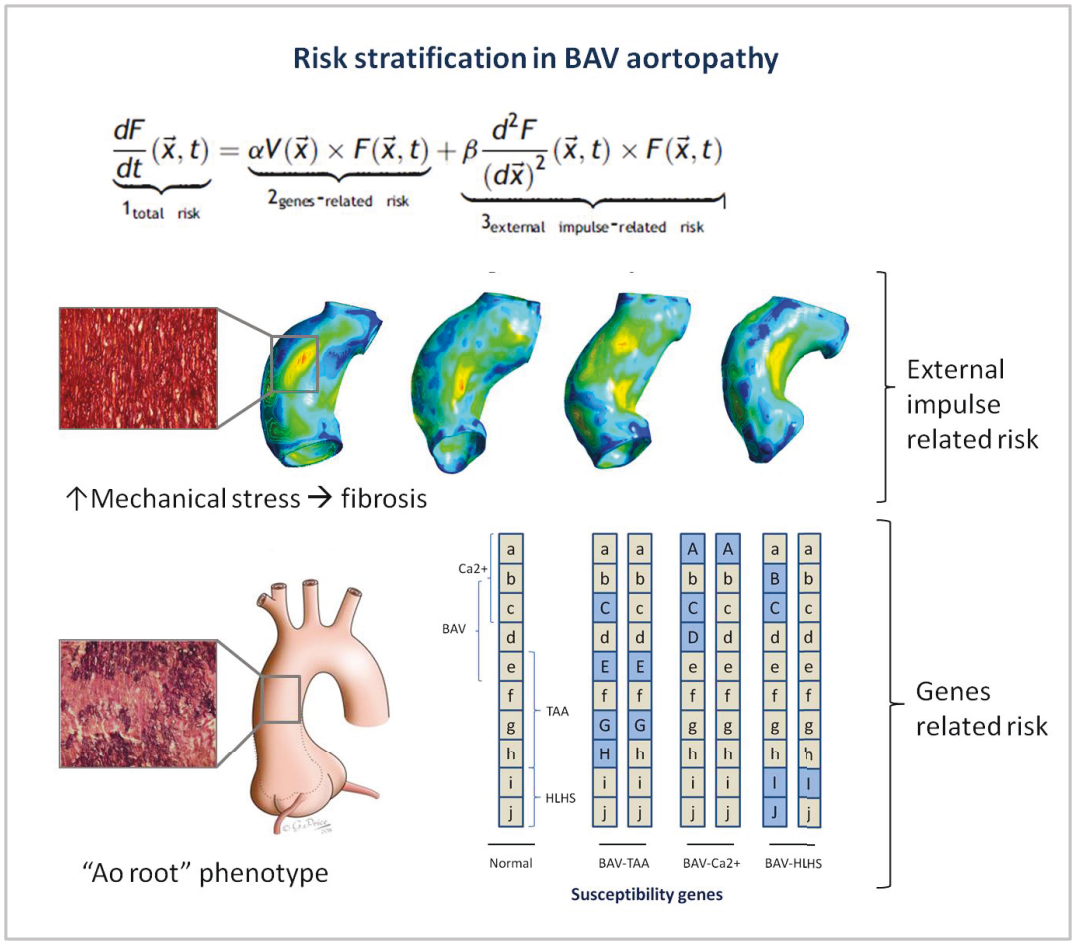

8.4 Conclusion

The described findings identified important new research areas in BAV aortopathy. Focus on the dilated root phenotype is incremental as it may constitute the primarily genetic form of BAV disease with predisposition to greater degrees of medial wall degeneration in the ascending aorta. As NGS techniques become less costly and more efficient, the role of genetic testing in clinical management of BAV disease is expected to increase. Genetic sequencing, in conjunction with assessment of local haemodynamics via MRI or computational methods, may lead the way to individualised risk stratification for TAA formation in BAV (Figure 8.1).

Chapter 9: Appendices

9.1 Personal contribution to the research

Several collaborations were necessary for completion of this multidisciplinary work. With regards to personal contribution, I set up the research protocol and ethics for the whole of this study, recruited patients and collected samples, performed the computational modelling, histological, and immunohistochemical analyses, and completed the statistical analyses. Pre-operative imaging data (CT and echocardiography) was obtained by radiographers of the Royal Brompton Hospital, whereas I completed the post-processing of CT angiograms to generate 3D models of the aorta and further structural analyses. NGS was performed by collaborating team members of the Cardiovascular BRU, Royal Brompton Hospital, and CNV analyses by members of Dr. Matthew Hurles' team, Wellcome Trust Sanger Institute, Cambridge. With regards to genetic analyses, I performed the DNA extraction and purification, conducted an extensive literature review for gene selection for targeted NGS and worked with bioinformaticians at the Royal Brompton Campus (John Shibu) for the design of the capture library and at the Sanger Institute (Ni Huang) for post-CNV calling processing of data. Preliminary NGS results were processed by Katie Fletcher, PhD student within the Cardiovascular BRU, who will undertake the further validation of novel likely pathogenic variants, as a direct extension of this work. In collaboration with Katie, I performed the interpretation of the processed preliminary NGS results and prioritized genes of interest.

All figures in this dissertation were produced by me, unless stated otherwise. Figures 1.3, 1.5, and 6.2 were produced with the assistance of Lucy Coleman, postdoctoral fellow of the Cardiovascular BRU, and figure 6.1 with the assistance of Katie Fletcher.

9.2 Prizes and grants

2012 Best Poster Award, Frontiers in Cardiovascular Biology, European Society of Cardiology, London

2012 Best Poster Presentation in Sub-topic "Integrative mechanisms, novel diagnostic and therapeutic approaches", Frontiers in Cardiovascular Biology, European Society of Cardiology, London

2010 NIHR Cardiovascular Biomedical Research Unit Pump Prime Grant

2010 Travel grant (Imperial College London) for Employability and Entrepreneurship Summer School, Tsinghua University, Beijing, China

9.3 Publications

Pending validation of described genetic variants, a number of publications on integrated results is currently in preparation.

Prapa M, et al. Histopathology of the great vessels in patients with pulmonary arterial hypertension in association with congenital heart disease: large pulmonary arteries matter too. Int J Cardiol 2013 [Epub ahead of print]

Fernandez-Jimenez R, Kempny A, **Prapa M**, et al. Giant Saphenous Vein Graft Aneurysm Compressing Right Ventricular Outflow Tract and Main Pulmonary Artery. Circulation (in press)

Prapa M, K Dimopoulos. Editorial comment: Arterial switch repair to transposition of great arteries: so far so good. Int J Cardiol 2012; 160(1):1-3

Prapa M, Ho SY. Editorial comment: Risk stratification in bicuspid aortic valve disease: still more work to do. Eur J Cardiothorac Surg 2012; 41(2):327-8

Prapa M, et al. E-letter: Erythrocytosis versus polycythaemia in Eisenmenger syndrome: not a conundrum. BMJ Case Reports 2011 [Epub ahead of print]

Diller GP, Inuzuka R, Kempny A, Alonso-Gonzalez R, Liodakis E, Borgia F, Lockhart CJ, **Prapa M**, et al. Detrimental impact of socioeconomic status on exercise capacity in adults with congenital heart disease. Int J Cardiol 2011 [Epub ahead of print]

Radojevic J, Inuzuka R, Alonso-Gonzalez R, Borgia F, Giannakoulas G, **Prapa M**, et al. Peak oxygen uptake correlates with disease severity and predicts outcome in adult patients with Ebstein's anomaly of the tricuspid valve. Int J Cardiol 2011 [Epub ahead of print]

Tay EL, Frogoudaki A, Inuzuka R, Giannakoulas G, **Prapa M**, et al. Exercise intolerance in patients with congenitally corrected transposition of the great arteries relates to right ventricular filling pressures. Int J Cardiol 2011; 147(2):219-23

9.3.1 Published abstracts

Prapa M, McCarthy KP, Krexi D, Gatzoulis MA, Ho SY. Bicuspid aortic valve disease: evidence for increased TGF-ß signalling in aortic regions of distinct embryologic origin. ESC Working Group "Development, Anatomy and Pathology" Meeting, Amsterdam, 2012

Prapa M, McCarthy KP, Dimopoulos K, Sheppard MN, Gatzoulis MA, Ho SY. Gross histological abnormalities in the pulmonary trunk of patients with Eisenmenger syndrome: evidence of a causative mechanism for reduced compliance and progressive dilatation. ESC Working Group "Development, Anatomy and Pathology" Meeting, Liblice, 2011

Prapa M, McCarthy KP, Kilner PJ , Xu XY, Johnson MR, Ho SY, Gatzoulis MA. Elevated mechanical stress underlying thoracic aortic aneurysm formation in patients with bicuspid aortic valve: an integrated analysis. Annual Postgraduate Research Student Presentation Day, National Heart and Lung Institute, Imperial College London, 2011

Liodakis E, Dimopoulos K, Diller GP, Shiina Y, **Prapa M**, Wustmann K, Uebing A, Swan L, Gatzoulis MA. Low body mass index predicts outcome in adult congenital heart disease: the role of cachexia. ESC Congress, Paris, 2011

Prapa M. Neighbourhood socioeconomic context and survival in adult congenital heart disease population. "A Symposium in Honour of the Late Philip Poole-Wilson", National Heart and Lung Institute, Imperial College London, 2010

9.3.2 Chapters in BooksDF Shore**, M Prapa**. Late Repair and Reoperations in Adults with Congenital Heart Disease. In: MA Gatzoulis, GH Webb, PEF Daubeney, eds. Diagnosis and Management of Adult Congenital Heart Disease. UK: Elsevier 2009

M Prapa, K Dimopoulos, DF Shore, M Petrou, MA Gatzoulis. Adult Congenital Heart Disease. In: C Mavroudis, CL Backer, eds. Pediatric Cardiac Surgery 4th Edition US: Mosby 2010; in press

M Prapa, JP Pepper, MA Gatzoulis. Abnormalities of the Aortic Root. In: HD Allen, DJ Driscoll, RE Shaddy, TF Feltes, eds. Moss and Adams' Heart Disease in Infants, Children, and Adolescents US: Lippincott Williams and Wilkins 2012

9.4 Presentations

International/national

Nov 2012 (poster): Bicuspid aortic valve disease: evidence for increased TGF-ß signalling in aortic regions of distinct embryologic origin, European Society of Cardiology Working Group "Development, Anatomy and Pathology" Meeting, Amsterdam

Mar 2012 (poster): Biomechanical perspectives of thoracic aortic aneurysm formation in patients with a bicuspid aortic valve: an integrated analysis, European Society of Cardiology, Frontiers in Cardiovascular Biology, London

Nov 2011 (oral): Histopathology of the great arteries in Eisenmenger syndrome: large

pulmonary arteries matter too, Pulmonary Hypertension Physicians' Research Forum, London

Oct 2011 (oral): Histology and Histopathology of the Great Arteries, Hands-on Cardiac Morphology Workshop for Cardiologists, Royal Brompton Hospital

Sep 2011 (poster): Gross histological abnormalities in the pulmonary trunk of patients with Eisenmenger syndrome, European Society of Cardiology Working Group " Development, Anatomy and Pathology" Meeting, Liblice

Local

June 2012 (oral): Bicuspid Aortic Valve disease, Annual Postgraduate Research Day, South Kensington Campus

May 2012 (poster): Biomechanical aspects of aneurysm formation in patients with a bicuspid aortic valve, Annual Academic Trainees Event, Hammersmith Campus

Oct 2011 (oral): Bicuspid Aortic Valve and associated aortopathy, Joint Academic and Clinical Seminars (NHLI-JACS), International Centre for Circulatory Health, St Mary's campus

May 2011 (poster): Elevated mechanical stress underlying thoracic aortic aneurysm formation in bicuspid aortic valve disease, NHLI Postgraduate Meeting, South Kensington Campus

April 2011 (poster): Biomechanical aspects of bicuspid aortic valve and associated ascending aortic dilatation: in vivo tensile stress analysis employing computed tomography versus magnetic resonance imaging data, BHF Centre Student Symposium, South Kensington Campus

Bibliography

ABHARY, S., BURDON, K. P., KUOT, A., JAVADIYAN, S., WHITING, M. J., KASMERIDIS, N., PETROVSKY, N. & CRAIG, J. E. 2010. Sequence variation in DDAH1 and DDAH2 genes is strongly and additively associated with serum ADMA concentrations in individuals with type 2 diabetes. *PLoS One,* 5**,** e9462.

ACHARYA, A., HANS, C. P., KOENIG, S. N., NICHOLS, H. A., GALINDO, C. L., GARNER, H. R., MERRILL, W. H., HINTON, R. B. & GARG, V. 2011. Inhibitory role of Notch1 in calcific aortic valve disease. *PLoS One,* 6**,** e27743.

AICHER, D., URBICH, C., ZEIHER, A., DIMMELER, S. & SCHAFERS, H. J. 2007. Endothelial nitric oxide synthase in bicuspid aortic valve disease. *Ann Thorac Surg,* 83**,** 1290-4.

AIKAWA, E., NAHRENDORF, M., SOSNOVIK, D., LOK, V. M., JAFFER, F. A., AIKAWA, M. & WEISSLEDER, R. 2007. Multimodality molecular imaging identifies proteolytic and osteogenic activities in early aortic valve disease. *Circulation,* 115**,** 377-86.

AITMAN, T. J., DONG, R., VYSE, T. J., NORSWORTHY, P. J., JOHNSON, M. D., SMITH, J., MANGION, J., ROBERTON-LOWE, C., MARSHALL, A. J., PETRETTO, E., HODGES, M. D., BHANGAL, G., PATEL, S. G., SHEEHAN-ROONEY, K., DUDA, M., COOK, P. R., EVANS, D. J., DOMIN, J., FLINT, J., BOYLE, J. J., PUSEY, C. D. & COOK, H. T. 2006. Copy number polymorphism in Fcgr3 predisposes to glomerulonephritis in rats and humans. *Nature,* 439**,** 851-5.

ALEXIOU, T., BOON, W. M., DENTON, D. A., NICOLANTONIO, R. D., WALKER, L. L., MCKINLEY, M. J. & CAMPBELL, D. J. 2005. Angiotensinogen and angiotensin-converting enzyme gene copy number and angiotensin and bradykinin peptide levels in mice. *J Hypertens,* 23**,** 945-54.

ANDELFINGER, G., TAPPER, A. R., WELCH, R. C., VANOYE, C. G., GEORGE, A. L., JR. & BENSON, D. W. 2002. KCNJ2 mutation results in Andersen syndrome with sex-specific cardiac and skeletal muscle phenotypes. *Am J Hum Genet,* 71**,** 663-8.

ANDERSEN, N. D., DUBOSE, J., SHAH, A., LEE, T., WECHSLER, S. B. & HUGHES, G. C. 2010. Thoracic endografting in a patient with hereditary hemorrhagic telangiectasia presenting with a descending thoracic aneurysm. *J Vasc Surg,* 51**,** 468-70.

ANDERSON, R. H. 2007. The surgical anatomy of the aortic root. *Multimed Man Cardiothorac Surg,* 2007**,** mmcts 2006 002527.

ANDRUS, B. W., O'ROURKE, D. J., DACEY, L. J. & PALAC, R. T. 2003. Stability of ascending aortic dilatation following aortic valve replacement. *Circulation,* 108 Suppl 1**,** II295-9.

ANGER, T., EKICI, A. B., DANIEL, W. G. & GARLICHS, C. D. 2006. [Gene polymorphisms leading to calcified and stenotic aortic valves]. *Herz,* 31**,** 635-43.

ARAKI, T., MOHI, M. G., ISMAT, F. A., BRONSON, R. T., WILLIAMS, I. R., KUTOK, J. L., YANG, W., PAO, L. I., GILLILAND, D. G., EPSTEIN, J. A. & NEEL, B. G. 2004. Mouse model of Noonan syndrome reveals cell type- and gene dosage-dependent effects of Ptpn11 mutation. *Nat Med,* 10**,** 849-57.

ARMSTRONG, E. J. & BISCHOFF, J. 2004. Heart valve development: endothelial cell signaling and differentiation. *Circ Res,* 95**,** 459-70.

ARRINGTON, C. B., SOWER, C. T., CHUCKWUK, N., STEVENS, J., LEPPERT, M. F., YETMAN, A. T. & BOWLES, N. E. 2008. Absence of TGFBR1 and TGFBR2 mutations in patients with bicuspid aortic valve and aortic dilation. *Am J Cardiol,* 102**,** 629-31.

ATLI, F. H., MANDUZ, S., KATRANCIOGLU, N., OZUM, U., DISLI, O. M., ATAHAN, E., OZDEMIR, O., DOGAN, K. & BERKAN, O. 2010. eNOS G894T polymorphism and abdominal aortic aneurysms. *Angiology,* 61**,** 125-30.

BARKER, A. J., LANNING, C. & SHANDAS, R. 2010. Quantification of hemodynamic wall shear stress in patients with bicuspid aortic valve using phase-contrast MRI. *Ann Biomed Eng,* 38**,** 788-800.

BASSO, C., BOSCHELLO, M., PERRONE, C., MECENERO, A., CERA, A., BICEGO, D., THIENE, G. & DE DOMINICIS, E. 2004. An echocardiographic survey of primary school children for bicuspid aortic valve. *Am J Cardiol,* 93**,** 661-3.

BAUER, M., GLIECH, V., SINIAWSKI, H. & HETZER, R. 2006. Configuration of the ascending aorta in patients with bicuspid and tricuspid aortic valve disease undergoing aortic valve replacement with or without reduction aortoplasty. *J Heart Valve Dis,* 15**,** 594-600.

BAUMGARTNER, D., BAUMGARTNER, C., MATYAS, G., STEINMANN, B., LOFFLER-RAGG, J., SCHERMER, E., SCHWEIGMANN, U., BALDISSERA, I., FRISCHHUT, B., HESS, J. & HAMMERER, I. 2005. Diagnostic power of aortic elastic properties in young patients with Marfan syndrome. *J Thorac Cardiovasc Surg,* 129**,** 730-9.

BEDARD, E., MCCARTHY, K. P., DIMOPOULOS, K., GIANNAKOULAS, G., GATZOULIS, M. A. & HO, S. Y. 2009. Structural abnormalities of the pulmonary trunk in tetralogy of Fallot and potential clinical implications: a morphological study. *J Am Coll Cardiol,* 54**,** 1883-90.

BEPPU, S., SUZUKI, S., MATSUDA, H., OHMORI, F., NAGATA, S. & MIYATAKE, K. 1993. Rapidity of progression of aortic stenosis in patients with congenital bicuspid aortic valves. *Am J Cardiol,* 71**,** 322-7.

BERGLUND, E. C., KIIALAINEN, A. & SYVANEN, A. C. 2011. Next-generation sequencing technologies and applications for human genetic history and forensics. *Investig Genet,* 2**,** 23.

BERIDZE, N. & FRISHMAN, W. H. 2012. Vascular Ehlers-Danlos syndrome: pathophysiology, diagnosis, and prevention and treatment of its complications. *Cardiol Rev,* 20**,** 4-7.

BEROUKHIM, R. S., ROOSEVELT, G. & YETMAN, A. T. 2006. Comparison of the pattern of aortic dilation in children with the Marfan's syndrome versus children with a bicuspid aortic valve. *Am J Cardiol,* 98**,** 1094-5.

BIBEN, C., WEBER, R., KESTEVEN, S., STANLEY, E., MCDONALD, L., ELLIOTT, D. A., BARNETT, L., KOENTGEN, F., ROBB, L., FENELEY, M. & HARVEY, R. P. 2000. Cardiac septal and valvular dysmorphogenesis in mice heterozygous for mutations in the homeobox gene Nkx2-5. *Circ Res,* 87**,** 888-95.

BIESECKER, L. G. 2010. Exome sequencing makes medical genomics a reality. *Nat Genet,* 42**,** 13-4.

BIRD, L. M. & MASCARELLO, J. T. 2001. Chromosome 2q duplications: case report of a de novo interstitial duplication and review of the literature. *Am J Med Genet,* 100**,** 13-24.

BOCHUKOVA, E. G., HUANG, N., KEOGH, J., HENNING, E., PURMANN, C., BLASZCZYK, K., SAEED, S., HAMILTON-SHIELD, J., CLAYTON-SMITH, J., O'RAHILLY, S., HURLES, M. E. & FAROOQI, I. S. 2010. Large, rare

chromosomal deletions associated with severe early-onset obesity. *Nature,* 463**,** 666-70.

BONOW, R. O., CARABELLO, B. A., CHATTERJEE, K., DE LEON, A. C., JR., FAXON, D. P., FREED, M. D., GAASCH, W. H., LYTLE, B. W., NISHIMURA, R. A., O'GARA, P. T., O'ROURKE, R. A., OTTO, C. M., SHAH, P. M., SHANEWISE, J. S., SMITH, S. C., JR., JACOBS, A. K., ADAMS, C. D., ANDERSON, J. L., ANTMAN, E. M., FUSTER, V., HALPERIN, J. L., HIRATZKA, L. F., HUNT, S. A., NISHIMURA, R., PAGE, R. L. & RIEGEL, B. 2006. ACC/AHA 2006 guidelines for the management of patients with valvular heart disease: a report of the American College of Cardiology/American Heart Association Task Force on Practice Guidelines (writing Committee to Revise the 1998 guidelines for the management of patients with valvular heart disease) developed in collaboration with the Society of Cardiovascular Anesthesiologists endorsed by the Society for Cardiovascular Angiography and Interventions and the Society of Thoracic Surgeons. *J Am Coll Cardiol,* 48**,** e1-148.

BORGHI, A., WOOD, N. B., MOHIADDIN, R. H. & XU, X. Y. 2006. 3D geometric reconstruction of thoracic aortic aneurysms. *Biomed Eng Online,* 5**,** 59.

BOSSE, Y., MIQDAD, A., FOURNIER, D., PEPIN, A., PIBAROT, P. & MATHIEU, P. 2009. Refining molecular pathways leading to calcific aortic valve stenosis by studying gene expression profile of normal and calcified stenotic human aortic valves. *Circ Cardiovasc Genet,* 2**,** 489-98.

BOTNEY, M. D. 1999. Role of hemodynamics in pulmonary vascular remodeling: implications for primary pulmonary hypertension. *Am J Respir Crit Care Med,* 159**,** 361-4.

BRAVERMAN, A. C., GUVEN, H., BEARDSLEE, M. A., MAKAN, M., KATES, A. M. & MOON, M. R. 2005. The bicuspid aortic valve. *Curr Probl Cardiol,* 30**,** 470-522.

BRIGGS, G. G. 2002. Drug effects on the fetus and breast-fed infant. *Clin Obstet Gynecol,* 45**,** 6-21.

BROBERG, C. S., UJITA, M., PRASAD, S., LI, W., RUBENS, M., BAX, B. E., DAVIDSON, S. J., BOUZAS, B., GIBBS, J. S., BURMAN, J. & GATZOULIS, M. A. 2007. Pulmonary arterial thrombosis in eisenmenger syndrome is associated with biventricular dysfunction and decreased pulmonary flow velocity. *J Am Coll Cardiol,* 50**,** 634-42.

BROOKE, B. S., HABASHI, J. P., JUDGE, D. P., PATEL, N., LOEYS, B. & DIETZ, H. C., 3RD 2008. Angiotensin II blockade and aortic-root dilation in Marfan's syndrome. *N Engl J Med,* 358**,** 2787-95.

BURRELL, J. H., HEGARTY, B. D., MCMULLEN, J. R. & LUMBERS, E. R. 2001. Effects of gestation on ovine fetal and maternal angiotensin receptor subtypes in the heart and major blood vessels. *Exp Physiol,* 86**,** 71-82.

BUXTON, D. B. 2012. Molecular imaging of aortic aneurysms. *Circ Cardiovasc Imaging,* 5**,** 392-9.

CANADAS, V., VILACOSTA, I., BRUNA, I. & FUSTER, V. 2010. Marfan syndrome. Part 1: pathophysiology and diagnosis. *Nat Rev Cardiol,* 7**,** 256-65.

CAO, J., GONG, L., GUO, D. C., MIETZSCH, U., KUANG, S. Q., KWARTLER, C. S., SAFI, H., ESTRERA, A., GAMBELLO, M. J. & MILEWICZ, D. M. 2010. Thoracic aortic disease in tuberous sclerosis complex: molecular pathogenesis and potential therapies in Tsc2+/- mice. *Hum Mol Genet,* 19**,** 1908-20.

CARTA, L., SMALDONE, S., ZILBERBERG, L., LOCH, D., DIETZ, H. C., RIFKIN, D. B. & RAMIREZ, F. 2009. p38 MAPK is an early determinant of promiscuous

Smad2/3 signaling in the aortas of fibrillin-1 (Fbn1)-null mice. *J Biol Chem,* 284**,** 5630-6.
CHAKRABORTY, S., COMBS, M. D. & YUTZEY, K. E. 2010. Transcriptional regulation of heart valve progenitor cells. *Pediatr Cardiol,* 31**,** 414-21.
CHAN, K. L., GHANI, M., WOODEND, K. & BURWASH, I. G. 2001. Case-controlled study to assess risk factors for aortic stenosis in congenitally bicuspid aortic valve. *Am J Cardiol,* 88**,** 690-3.
CHAN, K. L., STINSON, W. A. & VEINOT, J. P. 1999. Reliability of transthoracic echocardiography in the assessment of aortic valve morphology: pathological correlation in 178 patients. *Can J Cardiol,* 15**,** 48-52.
CHENG, Z., TAN, F. P., RIGA, C. V., BICKNELL, C. D., HAMADY, M. S., GIBBS, R. G., WOOD, N. B. & XU, X. Y. 2010. Analysis of flow patterns in a patient-specific aortic dissection model. *J Biomech Eng,* 132**,** 051007.
CHOI, M., SCHOLL, U. I., JI, W., LIU, T., TIKHONOVA, I. R., ZUMBO, P., NAYIR, A., BAKKALOGLU, A., OZEN, S., SANJAD, S., NELSON-WILLIAMS, C., FARHI, A., MANE, S. & LIFTON, R. P. 2009. Genetic diagnosis by whole exome capture and massively parallel DNA sequencing. *Proc Natl Acad Sci U S A,* 106**,** 19096-101.
CHOUDHURY, N., BOUCHOT, O., ROULEAU, L., TREMBLAY, D., CARTIER, R., BUTANY, J., MONGRAIN, R. & LEASK, R. L. 2009. Local mechanical and structural properties of healthy and diseased human ascending aorta tissue. *Cardiovasc Pathol,* 18**,** 83-91.
CHUNG, A. W., YANG, H. H., RADOMSKI, M. W. & VAN BREEMEN, C. 2008. Long-term doxycycline is more effective than atenolol to prevent thoracic aortic aneurysm in marfan syndrome through the inhibition of matrix metalloproteinase-2 and -9. *Circ Res,* 102**,** e73-85.
CLEVERS, H. & NUSSE, R. 2012. Wnt/beta-catenin signaling and disease. *Cell,* 149**,** 1192-205.
COHN, R. D., VAN ERP, C., HABASHI, J. P., SOLEIMANI, A. A., KLEIN, E. C., LISI, M. T., GAMRADT, M., AP RHYS, C. M., HOLM, T. M., LOEYS, B. L., RAMIREZ, F., JUDGE, D. P., WARD, C. W. & DIETZ, H. C. 2007. Angiotensin II type 1 receptor blockade attenuates TGF-beta-induced failure of muscle regeneration in multiple myopathic states. *Nat Med,* 13**,** 204-10.
COOPER, W. O., HERNANDEZ-DIAZ, S., ARBOGAST, P. G., DUDLEY, J. A., DYER, S., GIDEON, P. S., HALL, K. & RAY, W. A. 2006. Major congenital malformations after first-trimester exposure to ACE inhibitors. *N Engl J Med,* 354**,** 2443-51.
CORDENONSI, M., DUPONT, S., MARETTO, S., INSINGA, A., IMBRIANO, C. & PICCOLO, S. 2003. Links between tumor suppressors: p53 is required for TGF-beta gene responses by cooperating with Smads. *Cell,* 113**,** 301-14.
COTRUFO, M. & DELLA CORTE, A. 2009. The association of bicuspid aortic valve disease with asymmetric dilatation of the tubular ascending aorta: identification of a definite syndrome. *J Cardiovasc Med (Hagerstown),* 10**,** 291-7.
COTRUFO, M., DELLA CORTE, A., DE SANTO, L. S., QUARTO, C., DE FEO, M., ROMANO, G., AMARELLI, C., SCARDONE, M., DI MEGLIO, F., GUERRA, G., SCARANO, M., VITALE, S., CASTALDO, C. & MONTAGNANI, S. 2005. Different patterns of extracellular matrix protein expression in the convexity and the concavity of the dilated aorta with bicuspid aortic valve: preliminary results. *J Thorac Cardiovasc Surg,* 130**,** 504-11.

COUCKE, P. J., WILLAERT, A., WESSELS, M. W., CALLEWAERT, B., ZOPPI, N., DE BACKER, J., FOX, J. E., MANCINI, G. M., KAMBOURIS, M., GARDELLA, R., FACCHETTI, F., WILLEMS, P. J., FORSYTH, R., DIETZ, H. C., BARLATI, S., COLOMBI, M., LOEYS, B. & DE PAEPE, A. 2006. Mutations in the facilitative glucose transporter GLUT10 alter angiogenesis and cause arterial tortuosity syndrome. *Nat Genet,* 38**,** 452-7.

DALIENTO, L., REBELLATO, L., ANGELINI, A., FRESCURA, C., MAZZOTTI, E., ROTUNDO, M. & THIENE, G. 2002. Fatal outcome in Eisenmenger syndrome. *Cardiovasc Pathol,* 11**,** 221-8.

DANSER, A. H., SCHALEKAMP, M. A., BAX, W. A., VAN DEN BRINK, A. M., SAXENA, P. R., RIEGGER, G. A. & SCHUNKERT, H. 1995. Angiotensin-converting enzyme in the human heart. Effect of the deletion/insertion polymorphism. *Circulation,* 92**,** 1387-8.

DASOUKI, M., MARKOVA, D., GAROLA, R., SASAKI, T., CHARBONNEAU, N. L., SAKAI, L. Y. & CHU, M. L. 2007. Compound heterozygous mutations in fibulin-4 causing neonatal lethal pulmonary artery occlusion, aortic aneurysm, arachnodactyly, and mild cutis laxa. *Am J Med Genet A,* 143A**,** 2635-41.

DAVIES, M. J., TREASURE, T. & PARKER, D. J. 1996. Demographic characteristics of patients undergoing aortic valve replacement for stenosis: relation to valve morphology. *Heart,* 75**,** 174-8.

DAVIES, R. R., KAPLE, R. K., MANDAPATI, D., GALLO, A., BOTTA, D. M., JR., ELEFTERIADES, J. A. & COADY, M. A. 2007. Natural history of ascending aortic aneurysms in the setting of an unreplaced bicuspid aortic valve. *Ann Thorac Surg,* 83**,** 1338-44.

DE LA POMPA, J. L., TIMMERMAN, L. A., TAKIMOTO, H., YOSHIDA, H., ELIA, A. J., SAMPER, E., POTTER, J., WAKEHAM, A., MARENGERE, L., LANGILLE, B. L., CRABTREE, G. R. & MAK, T. W. 1998. Role of the NF-ATc transcription factor in morphogenesis of cardiac valves and septum. *Nature,* 392**,** 182-6.

DE PAEPE, A. 1998. Heritable collagen disorders: from phenotype to genotype. *Verh K Acad Geneeskd Belg,* 60**,** 463-82; discussion 482-4.

DE SA, M., MOSHKOVITZ, Y., BUTANY, J. & DAVID, T. E. 1999. Histologic abnormalities of the ascending aorta and pulmonary trunk in patients with bicuspid aortic valve disease: clinical relevance to the ross procedure. *J Thorac Cardiovasc Surg,* 118**,** 588-94.

DELLA CORTE, A., BANCONE, C., BUONOCORE, M., DIALETTO, G., COVINO, F. E., MANDUCA, S., SCOGNAMIGLIO, G., D'ORIA, V. & DE FEO, M. 2013. Pattern of ascending aortic dimensions predicts the growth rate of the aorta in patients with bicuspid aortic valve. *JACC Cardiovasc Imaging,* 6**,** 1301-10.

DELLA CORTE, A., BANCONE, C., QUARTO, C., DIALETTO, G., COVINO, F. E., SCARDONE, M., CAIANIELLO, G. & COTRUFO, M. 2007. Predictors of ascending aortic dilatation with bicuspid aortic valve: a wide spectrum of disease expression. *Eur J Cardiothorac Surg,* 31**,** 397-404; discussion 404-5.

DELLA CORTE, A., QUARTO, C., BANCONE, C., CASTALDO, C., DI MEGLIO, F., NURZYNSKA, D., DE SANTO, L. S., DE FEO, M., SCARDONE, M., MONTAGNANI, S. & COTRUFO, M. 2008. Spatiotemporal patterns of smooth muscle cell changes in ascending aortic dilatation with bicuspid and tricuspid aortic valve stenosis: focus on cell-matrix signaling. *J Thorac Cardiovasc Surg,* 135**,** 8-18, 18 e1-2.

DERYNCK, R. & ZHANG, Y. E. 2003. Smad-dependent and Smad-independent pathways in TGF-beta family signalling. *Nature,* 425**,** 577-84.

DIETZ, H. C., CUTTING, G. R., PYERITZ, R. E., MASLEN, C. L., SAKAI, L. Y., CORSON, G. M., PUFFENBERGER, E. G., HAMOSH, A., NANTHAKUMAR, E. J., CURRISTIN, S. M. & ET AL. 1991. Marfan syndrome caused by a recurrent de novo missense mutation in the fibrillin gene. *Nature,* 352**,** 337-9.

DILLER, G. P. & GATZOULIS, M. A. 2007. Pulmonary vascular disease in adults with congenital heart disease. *Circulation,* 115**,** 1039-50.

EL-HAMAMSY, I. & YACOUB, M. H. 2009a. Cellular and molecular mechanisms of thoracic aortic aneurysms. *Nat Rev Cardiol,* 6**,** 771-86.

EL-HAMAMSY, I. & YACOUB, M. H. 2009b. A measured approach to managing the aortic root in patients with bicuspid aortic valve disease. *Curr Cardiol Rep,* 11**,** 94-100.

ELEFTERIADES, J. A. & FARKAS, E. A. 2010. Thoracic aortic aneurysm clinically pertinent controversies and uncertainties. *J Am Coll Cardiol,* 55**,** 841-57.

ENCISO, J. M., GRATZINGER, D., CAMENISCH, T. D., CANOSA, S., PINTER, E. & MADRI, J. A. 2003. Elevated glucose inhibits VEGF-A-mediated endocardial cushion formation: modulation by PECAM-1 and MMP-2. *J Cell Biol,* 160**,** 605-15.

ERDHEIM, J. 1930. Medionecrosis aortae idiopathica cystica. *Virchows Arch Pathol Anat,* 276**,** 187–229.

FANCIULLI, M., NORSWORTHY, P. J., PETRETTO, E., DONG, R., HARPER, L., KAMESH, L., HEWARD, J. M., GOUGH, S. C., DE SMITH, A., BLAKEMORE, A. I., FROGUEL, P., OWEN, C. J., PEARCE, S. H., TEIXEIRA, L., GUILLEVIN, L., GRAHAM, D. S., PUSEY, C. D., COOK, H. T., VYSE, T. J. & AITMAN, T. J. 2007. FCGR3B copy number variation is associated with susceptibility to systemic, but not organ-specific, autoimmunity. *Nat Genet,* 39**,** 721-3.

FARBER, H. W. & LOSCALZO, J. 2004. Pulmonary arterial hypertension. *N Engl J Med,* 351**,** 1655-65.

FATIGATI, V. & MURPHY, R. A. 1984. Actin and tropomyosin variants in smooth muscles. Dependence on tissue type. *J Biol Chem,* 259**,** 14383-8.

FAZEL, S. S., MALLIDI, H. R., LEE, R. S., SHEEHAN, M. P., LIANG, D., FLEISCHMAN, D., HERFKENS, R., MITCHELL, R. S. & MILLER, D. C. 2008. The aortopathy of bicuspid aortic valve disease has distinctive patterns and usually involves the transverse aortic arch. *J Thorac Cardiovasc Surg,* 135**,** 901-7, 907 e1-2.

FEDAK, P. W., DE SA, M. P., VERMA, S., NILI, N., KAZEMIAN, P., BUTANY, J., STRAUSS, B. H., WEISEL, R. D. & DAVID, T. E. 2003. Vascular matrix remodeling in patients with bicuspid aortic valve malformations: implications for aortic dilatation. *J Thorac Cardiovasc Surg,* 126**,** 797-806.

FEDAK, P. W., VERMA, S., DAVID, T. E., LEASK, R. L., WEISEL, R. D. & BUTANY, J. 2002. Clinical and pathophysiological implications of a bicuspid aortic valve. *Circulation,* 106**,** 900-4.

FENG, Y., CHEN, M. H., MOSKOWITZ, I. P., MENDONZA, A. M., VIDALI, L., NAKAMURA, F., KWIATKOWSKI, D. J. & WALSH, C. A. 2006. Filamin A (FLNA) is required for cell-cell contact in vascular development and cardiac morphogenesis. *Proc Natl Acad Sci U S A,* 103**,** 19836-41.

FERNANDES, S. M., KHAIRY, P., SANDERS, S. P. & COLAN, S. D. 2007. Bicuspid aortic valve morphology and interventions in the young. *J Am Coll Cardiol,* 49**,** 2211-4.

FERNANDEZ, B., DURAN, A. C., FERNANDEZ-GALLEGO, T., FERNANDEZ, M. C., SUCH, M., ARQUE, J. M. & SANS-COMA, V. 2009. Bicuspid aortic valves with different spatial orientations of the leaflets are distinct etiological entities. *J Am Coll Cardiol,* 54**,** 2312-8.

FEUK, L., CARSON, A. R. & SCHERER, S. W. 2006. Structural variation in the human genome. *Nat Rev Genet,* 7**,** 85-97.

FILLINGER, M. F., MARRA, S. P., RAGHAVAN, M. L. & KENNEDY, F. E. 2003. Prediction of rupture risk in abdominal aortic aneurysm during observation: wall stress versus diameter. *J Vasc Surg,* 37**,** 724-32.

FOFFA, I., FESTA, P. L., AIT-ALI, L., MAZZONE, A., BEVILACQUA, S. & ANDREASSI, M. G. 2009. Ascending aortic aneurysm in a patient with bicuspid aortic valve, positive history of systemic autoimmune diseases and common genetic factors: a case report. *Cardiovasc Ultrasound,* 7**,** 34.

FOFFA, I., MURZI, M., MARIANI, M., MAZZONE, A. M., GLAUBER, M., AIT ALI, L. & ANDREASSI, M. G. 2012. Angiotensin-converting enzyme insertion/deletion polymorphism is a risk factor for thoracic aortic aneurysm in patients with bicuspid or tricuspid aortic valves. *J Thorac Cardiovasc Surg,* 144**,** 390-5.

FREED, L. A., ACIERNO, J. S., JR., DAI, D., LEYNE, M., MARSHALL, J. E., NESTA, F., LEVINE, R. A. & SLAUGENHAUPT, S. A. 2003. A locus for autosomal dominant mitral valve prolapse on chromosome 11p15.4. *Am J Hum Genet,* 72**,** 1551-9.

FRIEDMAN, J. M., ARBISER, J., EPSTEIN, J. A., GUTMANN, D. H., HUOT, S. J., LIN, A. E., MCMANUS, B. & KORF, B. R. 2002. Cardiovascular disease in neurofibromatosis 1: report of the NF1 Cardiovascular Task Force. *Genet Med,* 4**,** 105-11.

GARG, V., MUTH, A. N., RANSOM, J. F., SCHLUTERMAN, M. K., BARNES, R., KING, I. N., GROSSFELD, P. D. & SRIVASTAVA, D. 2005. Mutations in NOTCH1 cause aortic valve disease. *Nature,* 437**,** 270-4.

GARRET, M., BASCLES, L., BOUE-GRABOT, E., SARTOR, P., CHARRON, G., BLOCH, B. & MARGOLSKEE, R. F. 1997. An mRNA encoding a putative GABA-gated chloride channel is expressed in the human cardiac conduction system. *J Neurochem,* 68**,** 1382-9.

GATEHOUSE, P. D., KEEGAN, J., CROWE, L. A., MASOOD, S., MOHIADDIN, R. H., KREITNER, K. F. & FIRMIN, D. N. 2005. Applications of phase-contrast flow and velocity imaging in cardiovascular MRI. *Eur Radiol,* 15**,** 2172-84.

GAUSSIN, V., VAN DE PUTTE, T., MISHINA, Y., HANKS, M. C., ZWIJSEN, A., HUYLEBROECK, D., BEHRINGER, R. R. & SCHNEIDER, M. D. 2002. Endocardial cushion and myocardial defects after cardiac myocyte-specific conditional deletion of the bone morphogenetic protein receptor ALK3. *Proc Natl Acad Sci U S A,* 99**,** 2878-83.

GIANNAKOULAS, G., DIMOPOULOS, K. & XU, X. Y. 2009. Modelling in congenital heart disease. Art or science? *Int J Cardiol,* 133**,** 141-4.

GIANNAKOULAS, G., GIANNOGLOU, G., SOULIS, J., FARMAKIS, T., PAPADOPOULOU, S., PARCHARIDIS, G. & LOURIDAS, G. 2005. A computational model to predict aortic wall stresses in patients with systolic arterial hypertension. *Med Hypotheses,* 65**,** 1191-5.

GIANNOGLOU, G., GIANNAKOULAS, G., SOULIS, J., CHATZIZISIS, Y., PERDIKIDES, T., MELAS, N., PARCHARIDIS, G. & LOURIDAS, G. 2006. Predicting the risk of rupture of abdominal aortic aneurysms by utilizing various geometrical parameters: revisiting the diameter criterion. *Angiology,* 57**,** 487-94.

GIRDAUSKAS, E., BORGER, M. A., SECKNUS, M. A., GIRDAUSKAS, G. & KUNTZE, T. 2011a. Is aortopathy in bicuspid aortic valve disease a congenital defect or a result of abnormal hemodynamics? A critical reappraisal of a one-sided argument. *Eur J Cardiothorac Surg,* 39**,** 809-14.

GIRDAUSKAS, E., SCHULZ, S., BORGER, M. A., MIERZWA, M. & KUNTZE, T. 2011b. Transforming growth factor-beta receptor type II mutation in a patient with bicuspid aortic valve disease and intraoperative aortic dissection. *Ann Thorac Surg,* 91**,** e70-1.

GITLER, A. D., LU, M. M., JIANG, Y. Q., EPSTEIN, J. A. & GRUBER, P. J. 2003. Molecular markers of cardiac endocardial cushion development. *Dev Dyn,* 228**,** 643-50.

GOMEZ, D., AL HAJ ZEN, A., BORGES, L. F., PHILIPPE, M., GUTIERREZ, P. S., JONDEAU, G., MICHEL, J. B. & VRANCKX, R. 2009. Syndromic and non-syndromic aneurysms of the human ascending aorta share activation of the Smad2 pathway. *J Pathol,* 218**,** 131-42.

GOMEZ, D., COYET, A., OLLIVIER, V., JEUNEMAITRE, X., JONDEAU, G., MICHEL, J. B. & VRANCKX, R. 2011. Epigenetic control of vascular smooth muscle cells in Marfan and non-Marfan thoracic aortic aneurysms. *Cardiovasc Res,* 89**,** 446-56.

GOMEZ, D., KESSLER, K., BORGES, L. F., RICHARD, B., TOUAT, Z., OLLIVIER, V., MANSILLA, S., BOUTON, M. C., ALKODER, S., NATAF, P., JANDROT-PERRUS, M., JONDEAU, G., VRANCKX, R. & MICHEL, J. B. 2013. Smad2-dependent protease nexin-1 overexpression differentiates chronic aneurysms from acute dissections of human ascending aorta. *Arterioscler Thromb Vasc Biol,* 33**,** 2222-32.

GOUMANS, M. J., LIU, Z. & TEN DIJKE, P. 2009. TGF-beta signaling in vascular biology and dysfunction. *Cell Res,* 19**,** 116-27.

GREENWAY, S. C., PEREIRA, A. C., LIN, J. C., DEPALMA, S. R., ISRAEL, S. J., MESQUITA, S. M., ERGUL, E., CONTA, J. H., KORN, J. M., MCCARROLL, S. A., GORHAM, J. M., GABRIEL, S., ALTSHULER, D. M., QUINTANILLA-DIECK MDE, L., ARTUNDUAGA, M. A., EAVEY, R. D., PLENGE, R. M., SHADICK, N. A., WEINBLATT, M. E., DE JAGER, P. L., HAFLER, D. A., BREITBART, R. E., SEIDMAN, J. G. & SEIDMAN, C. E. 2009. De novo copy number variants identify new genes and loci in isolated sporadic tetralogy of Fallot. *Nat Genet,* 41**,** 931-5.

GRIFFITH, A. J., SPRUNGER, L. K., SIRKO-OSADSA, D. A., TILLER, G. E., MEISLER, M. H. & WARMAN, M. L. 1998. Marshall syndrome associated with a splicing defect at the COL11A1 locus. *Am J Hum Genet,* 62**,** 816-23.

GROENENDIJK, B. C., HIERCK, B. P., GITTENBERGER-DE GROOT, A. C. & POELMANN, R. E. 2004. Development-related changes in the expression of shear stress responsive genes KLF-2, ET-1, and NOS-3 in the developing cardiovascular system of chicken embryos. *Dev Dyn,* 230**,** 57-68.

GUO, D. C., PANNU, H., TRAN-FADULU, V., PAPKE, C. L., YU, R. K., AVIDAN, N., BOURGEOIS, S., ESTRERA, A. L., SAFI, H. J., SPARKS, E., AMOR, D., ADES, L., MCCONNELL, V., WILLOUGHBY, C. E., ABUELO, D., WILLING, M., LEWIS, R. A., KIM, D. H., SCHERER, S., TUNG, P. P., AHN, C., BUJA, L. M., RAMAN, C. S., SHETE, S. S. & MILEWICZ, D. M. 2007. Mutations in smooth muscle alpha-actin (ACTA2) lead to thoracic aortic aneurysms and dissections. *Nat Genet,* 39**,** 1488-93.

HABASHI, J. P., JUDGE, D. P., HOLM, T. M., COHN, R. D., LOEYS, B. L., COOPER, T. K., MYERS, L., KLEIN, E. C., LIU, G., CALVI, C., PODOWSKI, M., NEPTUNE, E. R., HALUSHKA, M. K., BEDJA, D., GABRIELSON, K., RIFKIN,

D. B., CARTA, L., RAMIREZ, F., HUSO, D. L. & DIETZ, H. C. 2006. Losartan, an AT1 antagonist, prevents aortic aneurysm in a mouse model of Marfan syndrome. *Science,* 312**,** 117-21.

HAGLER, M. A., HADLEY, T. M., ZHANG, H., MEHRA, K., ROOS, C. M., SCHAFF, H. V., SURI, R. M. & MILLER, J. D. 2013. TGF-beta signalling and reactive oxygen species drive fibrosis and matrix remodelling in myxomatous mitral valves. *Cardiovasc Res*.

HALDAR, S. M., LU, Y., JEYARAJ, D., KAWANAMI, D., CUI, Y., EAPEN, S. J., HAO, C., LI, Y., DOUGHMAN, Y. Q., WATANABE, M., SHIMIZU, K., KUIVANIEMI, H., SADOSHIMA, J., MARGULIES, K. B., CAPPOLA, T. P. & JAIN, M. K. 2010. Klf15 deficiency is a molecular link between heart failure and aortic aneurysm formation. *Sci Transl Med,* 2**,** 26ra26.

HARRIS, P., HEATH, D. & APOSTOLOPOULOS, A. 1965. Extensibility of the pulmonary trunk in heart disease. *Br Heart J,* 27**,** 660-6.

HEATH, D. & EDWARDS, J. E. 1960. Configuration of elastic tissue of pulmonary trunk in idiopathic pulmonary hypertension. *Circulation,* 21**,** 59-62.

HEATH, D., WOOD, E. H., DUSHANE, J. W. & EDWARDS, J. E. 1959. The structure of the pulmonary trunk at different ages and in cases of pulmonary hypertension and pulmonary stenosis. *J Pathol Bacteriol,* 77**,** 443-56.

HEATH, D., WOOD, E. H., DUSHANE, J. W. & EDWARDS, J. E. 1960. The relation of age and blood pressure to atheroma in the pulmonary arteries and thoracic aorta in congenital heart disease. *Lab Invest,* 9**,** 259-72.

HEENEMAN, S., SLUIMER, J. C. & DAEMEN, M. J. 2007. Angiotensin-converting enzyme and vascular remodeling. *Circ Res,* 101**,** 441-54.

HERMAN, D. S., LAM, L., TAYLOR, M. R., WANG, L., TEEKAKIRIKUL, P., CHRISTODOULOU, D., CONNER, L., DEPALMA, S. R., MCDONOUGH, B., SPARKS, E., TEODORESCU, D. L., CIRINO, A. L., BANNER, N. R., PENNELL, D. J., GRAW, S., MERLO, M., DI LENARDA, A., SINAGRA, G., BOS, J. M., ACKERMAN, M. J., MITCHELL, R. N., MURRY, C. E., LAKDAWALA, N. K., HO, C. Y., BARTON, P. J., COOK, S. A., MESTRONI, L., SEIDMAN, J. G. & SEIDMAN, C. E. 2012. Truncations of titin causing dilated cardiomyopathy. *N Engl J Med,* 366**,** 619-28.

HINTON, R. B. 2012. Bicuspid aortic valve and thoracic aortic aneurysm: three patient populations, two disease phenotypes, and one shared genotype. *Cardiol Res Pract,* 2012**,** 926975.

HINTON, R. B., MARTIN, L. J., RAME-GOWDA, S., TABANGIN, M. E., CRIPE, L. H. & BENSON, D. W. 2009. Hypoplastic left heart syndrome links to chromosomes 10q and 6q and is genetically related to bicuspid aortic valve. *J Am Coll Cardiol,* 53**,** 1065-71.

HIRATZKA, L. F., BAKRIS, G. L., BECKMAN, J. A., BERSIN, R. M., CARR, V. F., CASEY, D. E., JR., EAGLE, K. A., HERMANN, L. K., ISSELBACHER, E. M., KAZEROONI, E. A., KOUCHOUKOS, N. T., LYTLE, B. W., MILEWICZ, D. M., REICH, D. L., SEN, S., SHINN, J. A., SVENSSON, L. G. & WILLIAMS, D. M. 2010. 2010 ACCF/AHA/AATS/ACR/ASA/SCA/SCAI/SIR/STS/SVM guidelines for the diagnosis and management of patients with Thoracic Aortic Disease: a report of the American College of Cardiology Foundation/American Heart Association Task Force on Practice Guidelines, American Association for Thoracic Surgery, American College of Radiology, American Stroke Association, Society of Cardiovascular Anesthesiologists, Society for Cardiovascular Angiography and Interventions, Society of

Interventional Radiology, Society of Thoracic Surgeons, and Society for Vascular Medicine. *Circulation,* 121**,** e266-369.

HITZ, M. P., LEMIEUX-PERREAULT, L. P., MARSHALL, C., FEROZ-ZADA, Y., DAVIES, R., YANG, S. W., LIONEL, A. C., D'AMOURS, G., LEMYRE, E., CULLUM, R., BIGRAS, J. L., THIBEAULT, M., CHETAILLE, P., MONTPETIT, A., KHAIRY, P., OVERDUIN, B., KLAASSEN, S., HOODLESS, P., AWADALLA, P., HUSSIN, J., IDAGHDOUR, Y., NEMER, M., STEWART, A. F., BOERKOEL, C., SCHERER, S. W., RICHTER, A., DUBE, M. P. & ANDELFINGER, G. 2012. Rare copy number variants contribute to congenital left-sided heart disease. *PLoS Genet,* 8**,** e1002903.

HOFMANN BOWMAN, M., WILK, J., HEYDEMANN, A., KIM, G., REHMAN, J., LODATO, J. A., RAMAN, J. & MCNALLY, E. M. 2010. S100A12 mediates aortic wall remodeling and aortic aneurysm. *Circ Res,* 106**,** 145-54.

HOPE, M. D., HOPE, T. A., CROOK, S. E., ORDOVAS, K. G., URBANIA, T. H., ALLEY, M. T. & HIGGINS, C. B. 2011. 4D flow CMR in assessment of valve-related ascending aortic disease. *JACC Cardiovasc Imaging,* 4**,** 781-7.

HOPE, M. D., HOPE, T. A., MEADOWS, A. K., ORDOVAS, K. G., URBANIA, T. H., ALLEY, M. T. & HIGGINS, C. B. 2010. Bicuspid aortic valve: four-dimensional MR evaluation of ascending aortic systolic flow patterns. *Radiology,* 255**,** 53-61.

HUANG, J., DAVIS, E. C., CHAPMAN, S. L., BUDATHA, M., MARMORSTEIN, L. Y., WORD, R. A. & YANAGISAWA, H. 2010. Fibulin-4 deficiency results in ascending aortic aneurysms: a potential link between abnormal smooth muscle cell phenotype and aneurysm progression. *Circ Res,* 106**,** 583-92.

HUMPHREY, J. D. 2008. Mechanisms of arterial remodeling in hypertension: coupled roles of wall shear and intramural stress. *Hypertension,* 52**,** 195-200.

HUNTINGTON, K., HUNTER, A. G. & CHAN, K. L. 1997. A prospective study to assess the frequency of familial clustering of congenital bicuspid aortic valve. *J Am Coll Cardiol,* 30**,** 1809-12.

HURLSTONE, A. F., HARAMIS, A. P., WIENHOLDS, E., BEGTHEL, H., KORVING, J., VAN EEDEN, F., CUPPEN, E., ZIVKOVIC, D., PLASTERK, R. H. & CLEVERS, H. 2003. The Wnt/beta-catenin pathway regulates cardiac valve formation. *Nature,* 425**,** 633-7.

IKONOMIDIS, J. S., JONES, J. A., BARBOUR, J. R., STROUD, R. E., CLARK, L. L., KAPLAN, B. S., ZEESHAN, A., BAVARIA, J. E., GORMAN, J. H., 3RD, SPINALE, F. G. & GORMAN, R. C. 2007. Expression of matrix metalloproteinases and endogenous inhibitors within ascending aortic aneurysms of patients with bicuspid or tricuspid aortic valves. *J Thorac Cardiovasc Surg,* 133**,** 1028-36.

ILIOPOULOS, D. C., KRITHARIS, E. P., BOUSSIAS, S., DEMIS, A., ILIOPOULOS, C. D. & SOKOLIS, D. P. 2013. Biomechanical properties and histological structure of sinus of Valsalva aneurysms in relation to age and region. *J Biomech,* 46**,** 931-40.

IWASAKI, Y., HORIGOME, H., TAKAHASHI-IGARI, M., KATO, Y., RAZZAQUE, M. A. & MATSUOKA, R. 2009. Coronary artery dilatation in LEOPARD syndrome. A child case and literature review. *Congenit Heart Dis,* 4**,** 38-41.

JAFFE, I. Z. & MENDELSOHN, M. E. 2005. Angiotensin II and aldosterone regulate gene transcription via functional mineralocortocoid receptors in human coronary artery smooth muscle cells. *Circ Res,* 96**,** 643-50.

JARMAKANI, J. M., GRAHAM, T. P., JR., BENSON, D. W., JR., CANENT, R. V., JR. & GREENFIELD, J. C., JR. 1971. In vivo pressure-radius relationships of the pulmonary artery in children with congenital heart disease. *Circulation,* 43**,** 585-92.

JOHNSON, E. N., LEE, Y. M., SANDER, T. L., RABKIN, E., SCHOEN, F. J., KAUSHAL, S. & BISCHOFF, J. 2003. NFATc1 mediates vascular endothelial growth factor-induced proliferation of human pulmonary valve endothelial cells. *J Biol Chem,* 278**,** 1686-92.

JONES, J. A., SPINALE, F. G. & IKONOMIDIS, J. S. 2009. Transforming growth factor-beta signaling in thoracic aortic aneurysm development: a paradox in pathogenesis. *J Vasc Res,* 46**,** 119-37.

KAISER, T., KELLENBERGER, C. J., ALBISETTI, M., BERGSTRASSER, E. & VALSANGIACOMO BUECHEL, E. R. 2008. Normal values for aortic diameters in children and adolescents--assessment in vivo by contrast-enhanced CMR-angiography. *J Cardiovasc Magn Reson,* 10**,** 56.

KARSCHIN, C. & KARSCHIN, A. 1997. Ontogeny of gene expression of Kir channel subunits in the rat. *Mol Cell Neurosci,* 10**,** 131-48.

KASHTAN, C. E., SEGAL, Y., FLINTER, F., MAKANJUOLA, D., GAN, J. S. & WATNICK, T. 2010. Aortic abnormalities in males with Alport syndrome. *Nephrol Dial Transplant,* 25**,** 3554-60.

KEANE, J. F., DRISCOLL, D. J., GERSONY, W. M., HAYES, C. J., KIDD, L., O'FALLON, W. M., PIERONI, D. R., WOLFE, R. R. & WEIDMAN, W. H. 1993. Second natural history study of congenital heart defects. Results of treatment of patients with aortic valvar stenosis. *Circulation,* 87**,** I16-27.

KENT, K. C., CRENSHAW, M. L., GOH, D. L. & DIETZ, H. C. 2013. Genotype-phenotype correlation in patients with bicuspid aortic valve and aneurysm. *J Thorac Cardiovasc Surg,* 146**,** 158-165 e1.

KHALIFA, O., IMTIAZ, F., ALLAM, R., AL-HASSNAN, Z., AL-HEMIDAN, A., AL-MANE, K., ABUHARB, G., BALOBAID, A., SAKATI, N., HYLAND, J. & AL-OWAIN, M. 2012. A recessive form of Marshall syndrome is caused by a mutation in the COL11A1 gene. *J Med Genet,* 49**,** 246-8.

KIM, H. K., GOTTLIEBSON, W., HOR, K., BACKELJAUW, P., GUTMARK-LITTLE, I., SALISBURY, S. R., RACADIO, J. M., HELTON-SKALLY, K. & FLECK, R. 2011. Cardiovascular anomalies in Turner syndrome: spectrum, prevalence, and cardiac MRI findings in a pediatric and young adult population. *AJR Am J Roentgenol,* 196**,** 454-60.

KIM, R. Y., ROBERTSON, E. J. & SOLLOWAY, M. J. 2001. Bmp6 and Bmp7 are required for cushion formation and septation in the developing mouse heart. *Dev Biol,* 235**,** 449-66.

KIRBY, M. L., GALE, T. F. & STEWART, D. E. 1983. Neural crest cells contribute to normal aorticopulmonary septation. *Science,* 220**,** 1059-61.

KNOLL, B. J., ROTHBLUM, K. N. & LONGLEY, M. 1988. Nucleotide sequence of the human placental alkaline phosphatase gene. Evolution of the 5' flanking region by deletion/substitution. *J Biol Chem,* 263**,** 12020-7.

KUO, C. T., VESELITS, M. L., BARTON, K. P., LU, M. M., CLENDENIN, C. & LEIDEN, J. M. 1997. The LKLF transcription factor is required for normal tunica media formation and blood vessel stabilization during murine embryogenesis. *Genes Dev,* 11**,** 2996-3006.

LACRO, R. V., DIETZ, H. C., WRUCK, L. M., BRADLEY, T. J., COLAN, S. D., DEVEREUX, R. B., KLEIN, G. L., LI, J. S., MINICH, L. L., PARIDON, S. M., PEARSON, G. D., PRINTZ, B. F., PYERITZ, R. E., RADOJEWSKI, E., ROMAN, M. J., SAUL, J. P., STYLIANOU, M. P. & MAHONY, L. 2007.

Rationale and design of a randomized clinical trial of beta-blocker therapy (atenolol) versus angiotensin II receptor blocker therapy (losartan) in individuals with Marfan syndrome. *Am Heart J,* 154**,** 624-31.
LAFOREST, B., ANDELFINGER, G. & NEMER, M. 2011. Loss of Gata5 in mice leads to bicuspid aortic valve. *J Clin Invest,* 121**,** 2876-87.
LAFOREST, B. & NEMER, M. 2012. Genetic insights into bicuspid aortic valve formation. *Cardiol Res Pract,* 2012**,** 180297.
LARSON, E. W. & EDWARDS, W. D. 1984. Risk factors for aortic dissection: a necropsy study of 161 cases. *Am J Cardiol,* 53**,** 849-55.
LEE, T. C., ZHAO, Y. D., COURTMAN, D. W. & STEWART, D. J. 2000. Abnormal aortic valve development in mice lacking endothelial nitric oxide synthase. *Circulation,* 101**,** 2345-8.
LEE, Y. C., HUANG, H. Y., CHANG, C. J., CHENG, C. H. & CHEN, Y. T. 2010. Mitochondrial GLUT10 facilitates dehydroascorbic acid import and protects cells against oxidative stress: mechanistic insight into arterial tortuosity syndrome. *Hum Mol Genet,* 19**,** 3721-33.
LEHOUX, S., TRONC, F. & TEDGUI, A. 2002. Mechanisms of blood flow-induced vascular enlargement. *Biorheology,* 39**,** 319-24.
LEMAIRE, S. A., WANG, X., WILKS, J. A., CARTER, S. A., WEN, S., WON, T., LEONARDELLI, D., ANAND, G., CONKLIN, L. D., WANG, X. L., THOMPSON, R. W. & COSELLI, J. S. 2005. Matrix metalloproteinases in ascending aortic aneurysms: bicuspid versus trileaflet aortic valves. *J Surg Res,* 123**,** 40-8.
LEWIN, M. B., MCBRIDE, K. L., PIGNATELLI, R., FERNBACH, S., COMBES, A., MENESSES, A., LAM, W., BEZOLD, L. I., KAPLAN, N., TOWBIN, J. A. & BELMONT, J. W. 2004. Echocardiographic evaluation of asymptomatic parental and sibling cardiovascular anomalies associated with congenital left ventricular outflow tract lesions. *Pediatrics,* 114**,** 691-6.
LEWIN, M. B. & OTTO, C. M. 2005. The bicuspid aortic valve: adverse outcomes from infancy to old age. *Circulation,* 111**,** 832-4.
LI, D. Y., BROOKE, B., DAVIS, E. C., MECHAM, R. P., SORENSEN, L. K., BOAK, B. B., EICHWALD, E. & KEATING, M. T. 1998. Elastin is an essential determinant of arterial morphogenesis. *Nature,* 393**,** 276-80.
LI, D. Y., SORENSEN, L. K., BROOKE, B. S., URNESS, L. D., DAVIS, E. C., TAYLOR, D. G., BOAK, B. B. & WENDEL, D. P. 1999. Defective angiogenesis in mice lacking endoglin. *Science,* 284**,** 1534-7.
LI, H., HANDSAKER, B., WYSOKER, A., FENNELL, T., RUAN, J., HOMER, N., MARTH, G., ABECASIS, G. & DURBIN, R. 2009. The Sequence Alignment/Map format and SAMtools. *Bioinformatics,* 25**,** 2078-9.
LIN, A. E., LIPPE, B. & ROSENFELD, R. G. 1998. Further delineation of aortic dilation, dissection, and rupture in patients with Turner syndrome. *Pediatrics,* 102**,** e12.
LIN, C. Y., LIN, C. J., CHEN, C. H., CHEN, R. M., ZHOU, B. & CHANG, C. P. 2012. The secondary heart field is a new site of calcineurin/Nfatc1 signaling for semilunar valve development. *J Mol Cell Cardiol,* 52**,** 1096-102.
LINDSAY, M. E. & DIETZ, H. C. 2011. Lessons on the pathogenesis of aneurysm from heritable conditions. *Nature,* 473**,** 308-16.
LINDSAY, M. E., SCHEPERS, D., BOLAR, N. A., DOYLE, J. J., GALLO, E., FERT-BOBER, J., KEMPERS, M. J., FISHMAN, E. K., CHEN, Y., MYERS, L., BJEDA, D., OSWALD, G., ELIAS, A. F., LEVY, H. P., ANDERLID, B. M., YANG, M. H., BONGERS, E. M., TIMMERMANS, J., BRAVERMAN, A. C., CANHAM, N., MORTIER, G. R., BRUNNER, H. G., BYERS, P. H., VAN EYK, J., VAN LAER,

L., DIETZ, H. C. & LOEYS, B. L. 2012. Loss-of-function mutations in TGFB2 cause a syndromic presentation of thoracic aortic aneurysm. *Nat Genet,* 44**,** 922-7.
LIU, X., WU, H., BYRNE, M., KRANE, S. & JAENISCH, R. 1997. Type III collagen is crucial for collagen I fibrillogenesis and for normal cardiovascular development. *Proc Natl Acad Sci U S A,* 94**,** 1852-6.
LIU, Y., LU, X., XIANG, F. L., LU, M. & FENG, Q. 2013. Nitric oxide synthase-3 promotes embryonic development of atrioventricular valves. *PLoS One,* 8**,** e77611.
LOEYS, B. L., SCHWARZE, U., HOLM, T., CALLEWAERT, B. L., THOMAS, G. H., PANNU, H., DE BACKER, J. F., OSWALD, G. L., SYMOENS, S., MANOUVRIER, S., ROBERTS, A. E., FARAVELLI, F., GRECO, M. A., PYERITZ, R. E., MILEWICZ, D. M., COUCKE, P. J., CAMERON, D. E., BRAVERMAN, A. C., BYERS, P. H., DE PAEPE, A. M. & DIETZ, H. C. 2006. Aneurysm syndromes caused by mutations in the TGF-beta receptor. *N Engl J Med,* 355**,** 788-98.
LOFFREDO, C. A., CHOKKALINGAM, A., SILL, A. M., BOUGHMAN, J. A., CLARK, E. B., SCHEEL, J. & BRENNER, J. I. 2004. Prevalence of congenital cardiovascular malformations among relatives of infants with hypoplastic left heart, coarctation of the aorta, and d-transposition of the great arteries. *Am J Med Genet A,* 124A**,** 225-30.
LOSAY, J., TOUCHOT, A., SERRAF, A., LITVINOVA, A., LAMBERT, V., PIOT, J. D., LACOUR-GAYET, F., CAPDEROU, A. & PLANCHE, C. 2001. Late outcome after arterial switch operation for transposition of the great arteries. *Circulation,* 104**,** I121-6.
LOSCALZO, M. L., GOH, D. L., LOEYS, B., KENT, K. C., SPEVAK, P. J. & DIETZ, H. C. 2007. Familial thoracic aortic dilation and bicommissural aortic valve: a prospective analysis of natural history and inheritance. *Am J Med Genet A,* 143A**,** 1960-7.
LU, Y., HALDAR, S., CROCE, K., WANG, Y., SAKUMA, M., MOROOKA, T., WANG, B., JEYARAJ, D., GRAY, S. J., SIMON, D. I. & JAIN, M. K. 2010. Kruppel-like factor 15 regulates smooth muscle response to vascular injury--brief report. *Arterioscler Thromb Vasc Biol,* 30**,** 1550-2.
MA, C., TARNUZZER, R. W. & CHEGINI, N. 1999. Expression of matrix metalloproteinases and tissue inhibitor of matrix metalloproteinases in mesothelial cells and their regulation by transforming growth factor-beta1. *Wound Repair Regen,* 7**,** 477-85.
MAJUMDAR, R., YAGUBYAN, M., SARKAR, G., BOLANDER, M. E. & SUNDT, T. M., 3RD 2006. Bicuspid aortic valve and ascending aortic aneurysm are not associated with germline or somatic homeobox NKX2-5 gene polymorphism in 19 patients. *J Thorac Cardiovasc Surg,* 131**,** 1301-5.
MAKI, J. M., RASANEN, J., TIKKANEN, H., SORMUNEN, R., MAKIKALLIO, K., KIVIRIKKO, K. I. & SOININEN, R. 2002. Inactivation of the lysyl oxidase gene Lox leads to aortic aneurysms, cardiovascular dysfunction, and perinatal death in mice. *Circulation,* 106**,** 2503-9.
MALESZEWSKI, J. J., MILLER, D. V., LU, J., DIETZ, H. C. & HALUSHKA, M. K. 2009. Histopathologic findings in ascending aortas from individuals with Loeys-Dietz syndrome (LDS). *Am J Surg Pathol,* 33**,** 194-201.
MALFAIT, F., SYMOENS, S., DE BACKER, J., HERMANNS-LE, T., SAKALIHASAN, N., LAPIERE, C. M., COUCKE, P. & DE PAEPE, A. 2007. Three arginine to cysteine substitutions in the pro-alpha (I)-collagen chain cause Ehlers-

Danlos syndrome with a propensity to arterial rupture in early adulthood. *Hum Mutat,* 28**,** 387-95.
MANLEY, G. 1964. Histology of the Aortic Media in Dissecting Aneurysms. *J Clin Pathol,* 17**,** 220-4.
MARDUEL, M., OUGUERRAM, K., SERRE, V., BONNEFONT-ROUSSELOT, D., MARQUES-PINHEIRO, A., ERIK BERGE, K., DEVILLERS, M., LUC, G., LECERF, J. M., TOSOLINI, L., ERLICH, D., PELOSO, G. M., STITZIEL, N., NITCHKE, P., JAIS, J. P., ABIFADEL, M., KATHIRESAN, S., LEREN, T. P., RABES, J. P., BOILEAU, C. & VARRET, M. 2013. Description of a large family with autosomal dominant hypercholesterolemia associated with the APOE p.Leu167del mutation. *Hum Mutat,* 34**,** 83-7.
MARTIN, D., TUCKER, D. F., GORMAN, P., SHEER, D., SPURR, N. K. & TROWSDALE, J. 1987. The human placental alkaline phosphatase gene and related sequences map to chromosome 2 band q37. *Ann Hum Genet,* 51**,** 145-52.
MARTIN, L. J., RAMACHANDRAN, V., CRIPE, L. H., HINTON, R. B., ANDELFINGER, G., TABANGIN, M., SHOONER, K., KEDDACHE, M. & BENSON, D. W. 2007. Evidence in favor of linkage to human chromosomal regions 18q, 5q and 13q for bicuspid aortic valve and associated cardiovascular malformations. *Hum Genet,* 121**,** 275-84.
MAUTNER, G. C., MAUTNER, S. L., CANNON, R. O., 3RD, HUNSBERGER, S. A. & ROBERTS, W. C. 1993. Clinical factors useful in predicting aortic valve structure in patients > 40 years of age with isolated valvular aortic stenosis. *Am J Cardiol,* 72**,** 194-8.
MCBRIDE, K. L., PIGNATELLI, R., LEWIN, M., HO, T., FERNBACH, S., MENESSES, A., LAM, W., LEAL, S. M., KAPLAN, N., SCHLIEKELMAN, P., TOWBIN, J. A. & BELMONT, J. W. 2005. Inheritance analysis of congenital left ventricular outflow tract obstruction malformations: Segregation, multiplex relative risk, and heritability. *Am J Med Genet A,* 134A**,** 180-6.
MCBRIDE, K. L., RILEY, M. F., ZENDER, G. A., FITZGERALD-BUTT, S. M., TOWBIN, J. A., BELMONT, J. W. & COLE, S. E. 2008. NOTCH1 mutations in individuals with left ventricular outflow tract malformations reduce ligand-induced signaling. *Hum Mol Genet,* 17**,** 2886-93.
MCELHINNEY, D. B., KRANTZ, I. D., BASON, L., PICCOLI, D. A., EMERICK, K. M., SPINNER, N. B. & GOLDMUNTZ, E. 2002. Analysis of cardiovascular phenotype and genotype-phenotype correlation in individuals with a JAG1 mutation and/or Alagille syndrome. *Circulation,* 106**,** 2567-74.
MCKELLAR, S. H., TESTER, D. J., YAGUBYAN, M., MAJUMDAR, R., ACKERMAN, M. J. & SUNDT, T. M., 3RD 2007. Novel NOTCH1 mutations in patients with bicuspid aortic valve disease and thoracic aortic aneurysms. *J Thorac Cardiovasc Surg,* 134**,** 290-6.
MCKENNA, A., HANNA, M., BANKS, E., SIVACHENKO, A., CIBULSKIS, K., KERNYTSKY, A., GARIMELLA, K., ALTSHULER, D., GABRIEL, S., DALY, M. & DEPRISTO, M. A. 2010. The Genome Analysis Toolkit: a MapReduce framework for analyzing next-generation DNA sequencing data. *Genome Res,* 20**,** 1297-303.
MCKUSICK, V. A. 1972. Association of congenital bicuspid aortic valve and erdheim's cystic medial necrosis. *Lancet,* 1**,** 1026-7.
MCLAREN, W., PRITCHARD, B., RIOS, D., CHEN, Y., FLICEK, P. & CUNNINGHAM, F. 2010. Deriving the consequences of genomic variants with the Ensembl API and SNP Effect Predictor. *Bioinformatics,* 26**,** 2069-70.

MEDER, B., HAAS, J., KELLER, A., HEID, C., JUST, S., BORRIES, A., BOISGUERIN, V., SCHARFENBERGER-SCHMEER, M., STAHLER, P., BEIER, M., WEICHENHAN, D., STROM, T. M., PFEUFER, A., KORN, B., KATUS, H. A. & ROTTBAUER, W. 2011. Targeted next-generation sequencing for the molecular genetic diagnostics of cardiomyopathies. *Circ Cardiovasc Genet,* 4**,** 110-22.

METZKER, M. L. 2010. Sequencing technologies - the next generation. *Nat Rev Genet,* 11**,** 31-46.

MILEWICZ, D. M., CHEN, H., PARK, E. S., PETTY, E. M., ZAGHI, H., SHASHIDHAR, G., WILLING, M. & PATEL, V. 1998. Reduced penetrance and variable expressivity of familial thoracic aortic aneurysms/dissections. *Am J Cardiol,* 82**,** 474-9.

MILEWICZ, D. M., DIETZ, H. C. & MILLER, D. C. 2005. Treatment of aortic disease in patients with Marfan syndrome. *Circulation,* 111**,** e150-7.

MILEWICZ, D. M., GUO, D. C., TRAN-FADULU, V., LAFONT, A. L., PAPKE, C. L., INAMOTO, S., KWARTLER, C. S. & PANNU, H. 2008. Genetic basis of thoracic aortic aneurysms and dissections: focus on smooth muscle cell contractile dysfunction. *Annu Rev Genomics Hum Genet,* 9**,** 283-302.

MIQUEROL, L., GERTSENSTEIN, M., HARPAL, K., ROSSANT, J. & NAGY, A. 1999. Multiple developmental roles of VEGF suggested by a LacZ-tagged allele. *Dev Biol,* 212**,** 307-22.

MOHAMED, S. A., HANKE, T., SCHLUETER, C., BULLERDIEK, J. & SIEVERS, H. H. 2005. Ubiquitin fusion degradation 1-like gene dysregulation in bicuspid aortic valve. *J Thorac Cardiovasc Surg,* 130**,** 1531-6.

NAGY, E. & BACK, M. 2012. Epigenetic regulation of 5-lipoxygenase in the phenotypic plasticity of valvular interstitial cells associated with aortic valve stenosis. *FEBS Lett,* 586**,** 1325-9.

NATAATMADJA, M., WEST, M., WEST, J., SUMMERS, K., WALKER, P., NAGATA, M. & WATANABE, T. 2003. Abnormal extracellular matrix protein transport associated with increased apoptosis of vascular smooth muscle cells in marfan syndrome and bicuspid aortic valve thoracic aortic aneurysm. *Circulation,* 108 Suppl 1**,** II329-34.

NATHAN, D. P., XU, C., GORMAN, J. H., 3RD, FAIRMAN, R. M., BAVARIA, J. E., GORMAN, R. C., CHANDRAN, K. B. & JACKSON, B. M. 2011a. Pathogenesis of acute aortic dissection: a finite element stress analysis. *Ann Thorac Surg,* 91**,** 458-63.

NATHAN, D. P., XU, C., PLAPPERT, T., DESJARDINS, B., GORMAN, J. H., 3RD, BAVARIA, J. E., GORMAN, R. C., CHANDRAN, K. B. & JACKSON, B. M. 2011b. Increased ascending aortic wall stress in patients with bicuspid aortic valves. *Ann Thorac Surg,* 92**,** 1384-9.

NIESSEN, K. & KARSAN, A. 2008. Notch signaling in cardiac development. *Circ Res,* 102**,** 1169-81.

NISHIMOTO, M., TAKAI, S., FUKUMOTO, H., TSUNEMI, K., YUDA, A., SAWADA, Y., YAMADA, M., JIN, D., SAKAGUCHI, M., NISHIMOTO, Y., SASAKI, S. & MIYAZAKI, M. 2002. Increased local angiotensin II formation in aneurysmal aorta. *Life Sci,* 71**,** 2195-205.

NISTRI, S., GRANDE-ALLEN, J., NOALE, M., BASSO, C., SIVIERO, P., MAGGI, S., CREPALDI, G. & THIENE, G. 2008. Aortic elasticity and size in bicuspid aortic valve syndrome. *Eur Heart J,* 29**,** 472-9.

NISTRI, S., SORBO, M. D., MARIN, M., PALISI, M., SCOGNAMIGLIO, R. & THIENE, G. 1999. Aortic root dilatation in young men with normally functioning bicuspid aortic valves. *Heart,* 82**,** 19-22.

NIWA, K., PERLOFF, J. K., BHUTA, S. M., LAKS, H., DRINKWATER, D. C., CHILD, J. S. & MINER, P. D. 2001. Structural abnormalities of great arterial walls in congenital heart disease: light and electron microscopic analyses. *Circulation,* 103**,** 393-400.

O'BRIEN, K. D., SHAVELLE, D. M., CAULFIELD, M. T., MCDONALD, T. O., OLIN-LEWIS, K., OTTO, C. M. & PROBSTFIELD, J. L. 2002. Association of angiotensin-converting enzyme with low-density lipoprotein in aortic valvular lesions and in human plasma. *Circulation,* 106**,** 2224-30.

OH, S. P., SEKI, T., GOSS, K. A., IMAMURA, T., YI, Y., DONAHOE, P. K., LI, L., MIYAZONO, K., TEN DIJKE, P., KIM, S. & LI, E. 2000. Activin receptor-like kinase 1 modulates transforming growth factor-beta 1 signaling in the regulation of angiogenesis. *Proc Natl Acad Sci U S A,* 97**,** 2626-31.

OHNO, M., COOKE, J. P., DZAU, V. J. & GIBBONS, G. H. 1995. Fluid shear stress induces endothelial transforming growth factor beta-1 transcription and production. Modulation by potassium channel blockade. *J Clin Invest,* 95**,** 1363-9.

OKAMOTO, R. J., XU, H., KOUCHOUKOS, N. T., MOON, M. R. & SUNDT, T. M., 3RD 2003. The influence of mechanical properties on wall stress and distensibility of the dilated ascending aorta. *J Thorac Cardiovasc Surg,* 126**,** 842-50.

ORTLEPP, J. R., HOFFMANN, R., OHME, F., LAUSCHER, J., BLECKMANN, F. & HANRATH, P. 2001. The vitamin D receptor genotype predisposes to the development of calcific aortic valve stenosis. *Heart,* 85**,** 635-8.

ORTLEPP, J. R., SCHMITZ, F., MEVISSEN, V., WEISS, S., HUSTER, J., DRONSKOWSKI, R., LANGEBARTELS, G., AUTSCHBACH, R., ZERRES, K., WEBER, C., HANRATH, P. & HOFFMANN, R. 2004. The amount of calcium-deficient hexagonal hydroxyapatite in aortic valves is influenced by gender and associated with genetic polymorphisms in patients with severe calcific aortic stenosis. *Eur Heart J,* 25**,** 514-22.

OTT, D. A. 2006. Aneurysm of the sinus of valsalva. *Semin Thorac Cardiovasc Surg Pediatr Card Surg Annu***,** 165-76.

OWENS, G. K. & WISE, G. 1997. Regulation of differentiation/maturation in vascular smooth muscle cells by hormones and growth factors. *Agents Actions Suppl,* 48**,** 3-24.

PANNU, H., FADULU, V. T., CHANG, J., LAFONT, A., HASHAM, S. N., SPARKS, E., GIAMPIETRO, P. F., ZALESKI, C., ESTRERA, A. L., SAFI, H. J., SHETE, S., WILLING, M. C., RAMAN, C. S. & MILEWICZ, D. M. 2005. Mutations in transforming growth factor-beta receptor type II cause familial thoracic aortic aneurysms and dissections. *Circulation,* 112**,** 513-20.

PANNU, H., TRAN-FADULU, V., PAPKE, C. L., SCHERER, S., LIU, Y., PRESLEY, C., GUO, D., ESTRERA, A. L., SAFI, H. J., BRASIER, A. R., VICK, G. W., MARIAN, A. J., RAMAN, C. S., BUJA, L. M. & MILEWICZ, D. M. 2007. MYH11 mutations result in a distinct vascular pathology driven by insulin-like growth factor 1 and angiotensin II. *Hum Mol Genet,* 16**,** 2453-62.

PARAI, J. L., MASTERS, R. G., WALLEY, V. M., STINSON, W. A. & VEINOT, J. P. 1999. Aortic medial changes associated with bicuspid aortic valve: myth or reality? *Can J Cardiol,* 15**,** 1233-8.

PARK, C. B., GREASON, K. L., SURI, R. M., MICHELENA, H. I., SCHAFF, H. V. & SUNDT, T. M., 3RD 2011. Fate of nonreplaced sinuses of Valsalva in bicuspid aortic valve disease. *J Thorac Cardiovasc Surg,* 142**,** 278-84.

PEACOCK, J. D., LEVAY, A. K., GILLASPIE, D. B., TAO, G. & LINCOLN, J. 2010. Reduced sox9 function promotes heart valve calcification phenotypes in vivo. *Circ Res,* 106**,** 712-9.

PLAISIER, E., GRIBOUVAL, O., ALAMOWITCH, S., MOUGENOT, B., PROST, C., VERPONT, M. C., MARRO, B., DESMETTRE, T., COHEN, S. Y., ROULLET, E., DRACON, M., FARDEAU, M., VAN AGTMAEL, T., KERJASCHKI, D., ANTIGNAC, C. & RONCO, P. 2007. COL4A1 mutations and hereditary angiopathy, nephropathy, aneurysms, and muscle cramps. *N Engl J Med,* 357**,** 2687-95.

PLASTER, N. M., TAWIL, R., TRISTANI-FIROUZI, M., CANUN, S., BENDAHHOU, S., TSUNODA, A., DONALDSON, M. R., IANNACCONE, S. T., BRUNT, E., BAROHN, R., CLARK, J., DEYMEER, F., GEORGE, A. L., JR., FISH, F. A., HAHN, A., NITU, A., OZDEMIR, C., SERDAROGLU, P., SUBRAMONY, S. H., WOLFE, G., FU, Y. H. & PTACEK, L. J. 2001. Mutations in Kir2.1 cause the developmental and episodic electrical phenotypes of Andersen's syndrome. *Cell,* 105**,** 511-9.

POSCHL, E., SCHLOTZER-SCHREHARDT, U., BRACHVOGEL, B., SAITO, K., NINOMIYA, Y. & MAYER, U. 2004. Collagen IV is essential for basement membrane stability but dispensable for initiation of its assembly during early development. *Development,* 131**,** 1619-28.

PRANDSTRALLER, D., MAZZANTI, L., PICCHIO, F. M., MAGNANI, C., BERGAMASCHI, R., PERRI, A., TSINGOS, E. & CACCIARI, E. 1999. Turner's syndrome: cardiologic profile according to the different chromosomal patterns and long-term clinical follow-Up of 136 nonpreselected patients. *Pediatr Cardiol,* 20**,** 108-12.

PRAPA, M. & HO, S. Y. 2012. Risk stratification in bicuspid aortic valve disease: still more work to do. *Eur J Cardiothorac Surg,* 41**,** 327-8.

PRAPA, M., MCCARTHY, K. P., DIMOPOULOS, K., SHEPPARD, M. N., KREXI, D., SWAN, L., WORT, S. J., GATZOULIS, M. A. & HO, S. Y. 2013. Histopathology of the great vessels in patients with pulmonary arterial hypertension in association with congenital heart disease: Large pulmonary arteries matter too. *Int J Cardiol*.

PRYDE, P. G., SEDMAN, A. B., NUGENT, C. E. & BARR, M., JR. 1993. Angiotensin-converting enzyme inhibitor fetopathy. *J Am Soc Nephrol,* 3**,** 1575-82.

PURNELL, R., WILLIAMS, I., VON OPPELL, U. & WOOD, A. 2005. Giant aneurysms of the sinuses of Valsalva and aortic regurgitation in a patient with Noonan's syndrome. *Eur J Cardiothorac Surg,* 28**,** 346-8.

QU, R., SILVER, M. M. & LETARTE, M. 1998. Distribution of endoglin in early human development reveals high levels on endocardial cushion tissue mesenchyme during valve formation. *Cell Tissue Res,* 292**,** 333-43.

QUINLAN, A. R. & HALL, I. M. 2010. BEDTools: a flexible suite of utilities for comparing genomic features. *Bioinformatics,* 26**,** 841-2.

RABEN, N., NAGARAJU, K., LEE, E., KESSLER, P., BYRNE, B., LEE, L., LAMARCA, M., KING, C., WARD, J., SAUER, B. & PLOTZ, P. 1998. Targeted disruption of the acid alpha-glucosidase gene in mice causes an illness with critical features of both infantile and adult human glycogen storage disease type II. *J Biol Chem,* 273**,** 19086-92.

REDAELLI A, R. G., ARRIGONI S, DI MARTINO E, ORIGGI D, FAZIO F, MONTEVECCHI F. 2002. An assisted automated procedure for vessel geometry reconstruction and hemodynamic simulations from clinical imaging. *Comput Med Imaging Graph,* 26**,** 143-52.

RENGIER, F., GEISBUSCH, P., VOSSHENRICH, R., MULLER-ESCHNER, M., KARMONIK, C., SCHOENHAGEN, P., VON TENGG-KOBLIGK, H. & PARTOVI, S. 2013. State-of-the-art aortic imaging: part I - fundamentals and perspectives of CT and MRI. *Vasa,* 42**,** 395-412.

REUBEN, S. R. 1971. Compliance of the human pulmonary arterial system in disease. *Circ Res,* 29**,** 40-50.

RICHARDS, A. A., SANTOS, L. J., NICHOLS, H. A., CRIDER, B. P., ELDER, F. F., HAUSER, N. S., ZINN, A. R. & GARG, V. 2008. Cryptic chromosomal abnormalities identified in children with congenital heart disease. *Pediatr Res,* 64**,** 358-63.

ROBERTS, W. C., MORROW, A. G., MCINTOSH, C. L., JONES, M. & EPSTEIN, S. E. 1981. Congenitally bicuspid aortic valve causing severe, pure aortic regurgitation without superimposed infective endocarditis. Analysis of 13 patients requiring aortic valve replacement. *Am J Cardiol,* 47**,** 206-9.

ROBERTS, W. C., VOWELS, T. J., KO, J. M., FILARDO, G., HEBELER, R. F., JR., HENRY, A. C., MATTER, G. J. & HAMMAN, B. L. 2011. Comparison of the structure of the aortic valve and ascending aorta in adults having aortic valve replacement for aortic stenosis versus for pure aortic regurgitation and resection of the ascending aorta for aneurysm. *Circulation,* 123**,** 896-903.

ROBICSEK, F., THUBRIKAR, M. J., COOK, J. W. & FOWLER, B. 2004. The congenitally bicuspid aortic valve: how does it function? Why does it fail? *Ann Thorac Surg,* 77**,** 177-85.

ROBINSON, P. N. & GODFREY, M. 2000. The molecular genetics of Marfan syndrome and related microfibrillopathies. *J Med Genet,* 37**,** 9-25.

ROCHA, P. P., SCHOLZE, M., BLEISS, W. & SCHREWE, H. 2010. Med12 is essential for early mouse development and for canonical Wnt and Wnt/PCP signaling. *Development,* 137**,** 2723-31.

RODRIGUEZ-VITA, J., SANCHEZ-LOPEZ, E., ESTEBAN, V., RUPEREZ, M., EGIDO, J. & RUIZ-ORTEGA, M. 2005. Angiotensin II activates the Smad pathway in vascular smooth muscle cells by a transforming growth factor-beta-independent mechanism. *Circulation,* 111**,** 2509-17.

ROSSI-FOULKES, R., ROMAN, M. J., ROSEN, S. E., KRAMER-FOX, R., EHLERS, K. H., O'LOUGHLIN, J. E., DAVIS, J. G. & DEVEREUX, R. B. 1999. Phenotypic features and impact of beta blocker or calcium antagonist therapy on aortic lumen size in the Marfan syndrome. *Am J Cardiol,* 83**,** 1364-8.

RUOTSALAINEN, H., SIPILA, L., VAPOLA, M., SORMUNEN, R., SALO, A. M., UITTO, L., MERCER, D. K., ROBINS, S. P., RISTELI, M., ASZODI, A., FASSLER, R. & MYLLYLA, R. 2006. Glycosylation catalyzed by lysyl hydroxylase 3 is essential for basement membranes. *J Cell Sci,* 119**,** 625-35.

RUSSO, C. F., CANNATA, A., LANFRANCONI, M., VITALI, E., GARATTI, A. & BONACINA, E. 2008. Is aortic wall degeneration related to bicuspid aortic valve anatomy in patients with valvular disease? *J Thorac Cardiovasc Surg,* 136**,** 937-42.

SACHDEV, V., MATURA, L. A., SIDENKO, S., HO, V. B., ARAI, A. E., ROSING, D. R. & BONDY, C. A. 2008. Aortic valve disease in Turner syndrome. *J Am Coll Cardiol,* 51**,** 1904-9.

SALERNO, J. C., HARRIS, D. E., IRIZARRY, K., PATEL, B., MORALES, A. J., SMITH, S. M., MARTASEK, P., ROMAN, L. J., MASTERS, B. S., JONES, C. L., WEISSMAN, B. A., LANE, P., LIU, Q. & GROSS, S. S. 1997. An

autoinhibitory control element defines calcium-regulated isoforms of nitric oxide synthase. *J Biol Chem,* 272**,** 29769-77.
SALIH, C., MCCARTHY, K. P. & HO, S. Y. 2004. The fibrous matrix of ventricular myocardium in hypoplastic left heart syndrome: a quantitative and qualitative analysis. *Ann Thorac Surg,* 77**,** 36-40.
SALO, A. M., COX, H., FARNDON, P., MOSS, C., GRINDULIS, H., RISTELI, M., ROBINS, S. P. & MYLLYLA, R. 2008. A connective tissue disorder caused by mutations of the lysyl hydroxylase 3 gene. *Am J Hum Genet,* 83**,** 495-503.
SANS-COMA, V., FERNANDEZ, B., DURAN, A. C., THIENE, G., ARQUE, J. M., MUNOZ-CHAPULI, R. & CARDO, M. 1996. Fusion of valve cushions as a key factor in the formation of congenital bicuspid aortic valves in Syrian hamsters. *Anat Rec,* 244**,** 490-8.
SARAVANAN, P. & KADIR, I. 2009. Apolipoprotein E alleles and bicuspid aortic valve stenosis in monozygotic twins. *Interact Cardiovasc Thorac Surg,* 8**,** 687-8.
SCHADT, E. E. 2009. Molecular networks as sensors and drivers of common human diseases. *Nature,* 461**,** 218-23.
SCHAEFER, B. M., LEWIN, M. B., STOUT, K. K., BYERS, P. H. & OTTO, C. M. 2007. Usefulness of bicuspid aortic valve phenotype to predict elastic properties of the ascending aorta. *Am J Cardiol,* 99**,** 686-90.
SCHAEFER, B. M., LEWIN, M. B., STOUT, K. K., GILL, E., PRUEITT, A., BYERS, P. H. & OTTO, C. M. 2008. The bicuspid aortic valve: an integrated phenotypic classification of leaflet morphology and aortic root shape. *Heart,* 94**,** 1634-8.
SCHLATMANN, T. J. & BECKER, A. E. 1977. Pathogenesis of dissecting aneurysm of aorta. Comparative histopathologic study of significance of medial changes. *Am J Cardiol,* 39**,** 21-6.
SCHOTT, J. J., BENSON, D. W., BASSON, C. T., PEASE, W., SILBERBACH, G. M., MOAK, J. P., MARON, B. J., SEIDMAN, C. E. & SEIDMAN, J. G. 1998. Congenital heart disease caused by mutations in the transcription factor NKX2-5. *Science,* 281**,** 108-11.
SCHWARTZ, C. E., TARPEY, P. S., LUBS, H. A., VERLOES, A., MAY, M. M., RISHEG, H., FRIEZ, M. J., FUTREAL, P. A., EDKINS, S., TEAGUE, J., BRIAULT, S., SKINNER, C., BAUER-CARLIN, A., SIMENSEN, R. J., JOSEPH, S. M., JONES, J. R., GECZ, J., STRATTON, M. R., RAYMOND, F. L. & STEVENSON, R. E. 2007. The original Lujan syndrome family has a novel missense mutation (p.N1007S) in the MED12 gene. *J Med Genet,* 44**,** 472-7.
SCOTTI, C. M., SHKOLNIK, A. D., MULUK, S. C. & FINOL, E. A. 2005. Fluid-structure interaction in abdominal aortic aneurysms: effects of asymmetry and wall thickness. *Biomed Eng Online,* 4**,** 64.
SHAH, A., FENG, S., KRUPP, D., HAYNES, C., GRASS, E., LIN, S., HAUSER, E., KRAUS, W., GREGORY, S., SHAH, S. & HUGHES, G. C. 2012. Abstract 9035: Epigenetic Modifications are Associated with Ascending Thoracic Aneurysm Formation in Patients with Bicuspid Aortic Valve. *Circulation,* 126.
SHEEN, V. L., JANSEN, A., CHEN, M. H., PARRINI, E., MORGAN, T., RAVENSCROFT, R., GANESH, V., UNDERWOOD, T., WILEY, J., LEVENTER, R., VAID, R. R., RUIZ, D. E., HUTCHINS, G. M., MENASHA, J., WILLNER, J., GENG, Y., GRIPP, K. W., NICHOLSON, L., BERRY-KRAVIS, E., BODELL, A., APSE, K., HILL, R. S., DUBEAU, F., ANDERMANN, F., BARKOVICH, J.,

ANDERMANN, E., SHUGART, Y. Y., THOMAS, P., VIRI, M., VEGGIOTTI, P., ROBERTSON, S., GUERRINI, R. & WALSH, C. A. 2005. Filamin A mutations cause periventricular heterotopia with Ehlers-Danlos syndrome. *Neurology,* 64**,** 254-62.

SHI, Y. & MASSAGUE, J. 2003. Mechanisms of TGF-beta signaling from cell membrane to the nucleus. *Cell,* 113**,** 685-700.

SHORES, J., BERGER, K. R., MURPHY, E. A. & PYERITZ, R. E. 1994. Progression of aortic dilatation and the benefit of long-term beta-adrenergic blockade in Marfan's syndrome. *N Engl J Med,* 330**,** 1335-41.

SIEVERS, H. H. & SCHMIDTKE, C. 2007. A classification system for the bicuspid aortic valve from 304 surgical specimens. *J Thorac Cardiovasc Surg,* 133**,** 1226-33.

SIEVERS, H. H. & SIEVERS, H. L. 2011. Aortopathy in bicuspid aortic valve disease - genes or hemodynamics? or Scylla and Charybdis? *Eur J Cardiothorac Surg,* 39**,** 803-4.

SONODA, M., TAKENAKA, K., UNO, K., EBIHARA, A. & NAGAI, R. 2008. A larger aortic annulus causes aortic regurgitation and a smaller aortic annulus causes aortic stenosis in bicuspid aortic valve. *Echocardiography,* 25**,** 242-8.

STENSON, P. D., BALL, E. V., MORT, M., PHILLIPS, A. D., SHIEL, J. A., THOMAS, N. S., ABEYSINGHE, S., KRAWCZAK, M. & COOPER, D. N. 2003. Human Gene Mutation Database (HGMD): 2003 update. *Hum Mutat,* 21**,** 577-81.

STRINGFELLOW, M. M., LAWRENCE, P. F. & STRINGFELLOW, R. G. 1987. The influence of aorta-aneurysm geometry upon stress in the aneurysm wall. *J Surg Res,* 42**,** 425-33.

SUPERTI-FURGA, A., GUGLER, E., GITZELMANN, R. & STEINMANN, B. 1988. Ehlers-Danlos syndrome type IV: a multi-exon deletion in one of the two COL3A1 alleles affecting structure, stability, and processing of type III procollagen. *J Biol Chem,* 263**,** 6226-32.

SYKES, B., OGILVIE, D., WORDSWORTH, P., WALLIS, G., MATHEW, C., BEIGHTON, P., NICHOLLS, A., POPE, F. M., THOMPSON, E., TSIPOURAS, P. & ET AL. 1990. Consistent linkage of dominantly inherited osteogenesis imperfecta to the type I collagen loci: COL1A1 and COL1A2. *Am J Hum Genet,* 46**,** 293-307.

SZABO, Z., CREPEAU, M. W., MITCHELL, A. L., STEPHAN, M. J., PUNTEL, R. A., YIN LOKE, K., KIRK, R. C. & URBAN, Z. 2006. Aortic aneurysmal disease and cutis laxa caused by defects in the elastin gene. *J Med Genet,* 43**,** 255-8.

TABACOVA, S., LITTLE, R., TSONG, Y., VEGA, A. & KIMMEL, C. A. 2003. Adverse pregnancy outcomes associated with maternal enalapril antihypertensive treatment. *Pharmacoepidemiol Drug Saf,* 12**,** 633-46.

TADROS, T. M., KLEIN, M. D. & SHAPIRA, O. M. 2009. Ascending aortic dilatation associated with bicuspid aortic valve: pathophysiology, molecular biology, and clinical implications. *Circulation,* 119**,** 880-90.

TAKALUOMA, K., HYRY, M., LANTTO, J., SORMUNEN, R., BANK, R. A., KIVIRIKKO, K. I., MYLLYHARJU, J. & SOININEN, R. 2007. Tissue-specific changes in the hydroxylysine content and cross-links of collagens and alterations in fibril morphology in lysyl hydroxylase 1 knock-out mice. *J Biol Chem,* 282**,** 6588-96.

TAKKENBERG, J. J., KLIEVERIK, L. M., SCHOOF, P. H., VAN SUYLEN, R. J., VAN HERWERDEN, L. A., ZONDERVAN, P. E., ROOS-HESSELINK, J. W., EIJKEMANS, M. J., YACOUB, M. H. & BOGERS, A. J. 2009. The Ross

procedure: a systematic review and meta-analysis. *Circulation,* 119**,** 222-8.

TAN, J. L., DAVLOUROS, P. A., MCCARTHY, K. P., GATZOULIS, M. A. & HO, S. Y. 2005. Intrinsic histological abnormalities of aortic root and ascending aorta in tetralogy of Fallot: evidence of causative mechanism for aortic dilatation and aortopathy. *Circulation,* 112**,** 961-8.

THIENPONT, B., MERTENS, L., DE RAVEL, T., EYSKENS, B., BOSHOFF, D., MAAS, N., FRYNS, J. P., GEWILLIG, M., VERMEESCH, J. R. & DEVRIENDT, K. 2007. Submicroscopic chromosomal imbalances detected by array-CGH are a frequent cause of congenital heart defects in selected patients. *Eur Heart J,* 28**,** 2778-84.

THYBERG, J. & HULTGARDH-NILSSON, A. 1994. Fibronectin and the basement membrane components laminin and collagen type IV influence the phenotypic properties of subcultured rat aortic smooth muscle cells differently. *Cell Tissue Res,* 276**,** 263-71.

TOPOUZIS, S. & MAJESKY, M. W. 1996. Smooth muscle lineage diversity in the chick embryo. Two types of aortic smooth muscle cell differ in growth and receptor-mediated transcriptional responses to transforming growth factor-beta. *Dev Biol,* 178**,** 430-45.

TOPPER, J. N., CAI, J., FALB, D. & GIMBRONE, M. A., JR. 1996. Identification of vascular endothelial genes differentially responsive to fluid mechanical stimuli: cyclooxygenase-2, manganese superoxide dismutase, and endothelial cell nitric oxide synthase are selectively up-regulated by steady laminar shear stress. *Proc Natl Acad Sci U S A,* 93**,** 10417-22.

TREDAL, S. M., CARTER, J. B. & EDWARDS, J. E. 1974. Cystic medial necrosis of the pulmonary artery: association with pulmonary hypertension. *Arch Pathol,* 97**,** 183-6.

TROMP, G., WU, Y., PROCKOP, D. J., MADHATHERI, S. L., KLEINERT, C., EARLEY, J. J., ZHUANG, J., NORRGARD, O., DARLING, R. C., ABBOTT, W. M. & ET AL. 1993. Sequencing of cDNA from 50 unrelated patients reveals that mutations in the triple-helical domain of type III procollagen are an infrequent cause of aortic aneurysms. *J Clin Invest,* 91**,** 2539-45.

UEHARA, Y., MIURA, S., YAHIRO, E. & SAKU, K. 2013. Non-ACE Pathway-induced Angiotensin II Production. *Curr Pharm Des,* 19**,** 3054-9.

VAN DE LAAR, I. M., OLDENBURG, R. A., PALS, G., ROOS-HESSELINK, J. W., DE GRAAF, B. M., VERHAGEN, J. M., HOEDEMAEKERS, Y. M., WILLEMSEN, R., SEVERIJNEN, L. A., VENSELAAR, H., VRIEND, G., PATTYNAMA, P. M., COLLEE, M., MAJOOR-KRAKAUER, D., POLDERMANS, D., FROHN-MULDER, I. M., MICHA, D., TIMMERMANS, J., HILHORST-HOFSTEE, Y., BIERMA-ZEINSTRA, S. M., WILLEMS, P. J., KROS, J. M., OEI, E. H., OOSTRA, B. A., WESSELS, M. W. & BERTOLI-AVELLA, A. M. 2011. Mutations in SMAD3 cause a syndromic form of aortic aneurysms and dissections with early-onset osteoarthritis. *Nat Genet,* 43**,** 121-6.

VELDTMAN, G. R., DEARANI, J. A. & WARNES, C. A. 2003. Low pressure giant pulmonary artery aneurysms in the adult: natural history and management strategies. *Heart,* 89**,** 1067-70.

VENKATASUBRAMANIAM, A. K., FAGAN, M. J., MEHTA, T., MYLANKAL, K. J., RAY, B., KUHAN, G., CHETTER, I. C. & MCCOLLUM, P. T. 2004. A comparative study of aortic wall stress using finite element analysis for ruptured and non-ruptured abdominal aortic aneurysms. *Eur J Vasc Endovasc Surg,* 28**,** 168-76.

VORP, D. A., RAGHAVAN, M. L. & WEBSTER, M. W. 1998. Mechanical wall stress in abdominal aortic aneurysm: influence of diameter and asymmetry. *J Vasc Surg,* 27**,** 632-9.

WAIN, L. V., ARMOUR, J. A. & TOBIN, M. D. 2009. Genomic copy number variation, human health, and disease. *Lancet,* 374**,** 340-50.

WANG, J., XIN, Y. F., LIU, X. Y., LIU, Z. M., WANG, X. Z. & YANG, Y. Q. 2011. A novel NKX2-5 mutation in familial ventricular septal defect. *Int J Mol Med,* 27**,** 369-75.

WANG, Y., BARBACIORU, C. C., SHIFFMAN, D., BALASUBRAMANIAN, S., IAKOUBOVA, O., TRANQUILLI, M., ALBORNOZ, G., BLAKE, J., MEHMET, N. N., NGADIMO, D., POULTER, K., CHAN, F., SAMAHA, R. R. & ELEFTERIADES, J. A. 2007. Gene expression signature in peripheral blood detects thoracic aortic aneurysm. *PLoS One,* 2**,** e1050.

WANG, Z. & CHESLER, N. C. 2012. Role of collagen content and cross-linking in large pulmonary arterial stiffening after chronic hypoxia. *Biomech Model Mechanobiol,* 11**,** 279-89.

WARD, C. 2000. Clinical significance of the bicuspid aortic valve. *Heart,* 83**,** 81-5.

WARE, J. S., JOHN, S., ROBERTS, A. M., BUCHAN, R., GONG, S., PETERS, N. S., ROBINSON, D. O., LUCASSEN, A., BEHR, E. R. & COOK, S. A. 2013. Next generation diagnostics in inherited arrhythmia syndromes : a comparison of two approaches. *J Cardiovasc Transl Res,* 6**,** 94-103.

WARE, J. S., ROBERTS, A. M. & COOK, S. A. 2012. Next generation sequencing for clinical diagnostics and personalised medicine: implications for the next generation cardiologist. *Heart,* 98**,** 276-81.

WENSTRUP, R. J., MURAD, S. & PINNELL, S. R. 1989. Ehlers-Danlos syndrome type VI: clinical manifestations of collagen lysyl hydroxylase deficiency. *J Pediatr,* 115**,** 405-9.

WILFINGER, W. W., MACKEY, K. & CHOMCZYNSKI, P. 1997. Effect of pH and ionic strength on the spectrophotometric assessment of nucleic acid purity. *Biotechniques,* 22**,** 474-6, 478-81.

WILKE, K., GAUL, R., KLAUCK, S. M. & POUSTKA, A. 1997. A gene in human chromosome band Xq28 (GABRE) defines a putative new subunit class of the GABAA neurotransmitter receptor. *Genomics,* 45**,** 1-10.

WOOTEN, E. C., IYER, L. K., MONTEFUSCO, M. C., HEDGEPETH, A. K., PAYNE, D. D., KAPUR, N. K., HOUSMAN, D. E., MENDELSOHN, M. E. & HUGGINS, G. S. 2010. Application of gene network analysis techniques identifies AXIN1/PDIA2 and endoglin haplotypes associated with bicuspid aortic valve. *PLoS One,* 5**,** e8830.

XU, X. Y., BORGHI, A., NCHIMI, A., LEUNG, J., GOMEZ, P., CHENG, Z., DEFRAIGNE, J. O. & SAKALIHASAN, N. 2010. High levels of 18F-FDG uptake in aortic aneurysm wall are associated with high wall stress. *Eur J Vasc Endovasc Surg,* 39**,** 295-301.

YONEDA, A., USHAKOV, D., MULTHAUPT, H. A. & COUCHMAN, J. R. 2007. Fibronectin matrix assembly requires distinct contributions from Rho kinases I and -II. *Mol Biol Cell,* 18**,** 66-75.

YU, Q., SHEN, Y., CHATTERJEE, B., SIEGFRIED, B. H., LEATHERBURY, L., ROSENTHAL, J., LUCAS, J. F., WESSELS, A., SPURNEY, C. F., WU, Y. J., KIRBY, M. L., SVENSON, K. & LO, C. W. 2004. ENU induced mutations causing congenital cardiovascular anomalies. *Development,* 131**,** 6211-23.

ZHANG, Z., VUORI, K., REED, J. C. & RUOSLAHTI, E. 1995. The alpha 5 beta 1 integrin supports survival of cells on fibronectin and up-regulates Bcl-2 expression. *Proc Natl Acad Sci U S A,* 92**,** 6161-5.

ZHOU, Y., POCZATEK, M. H., BERECEK, K. H. & MURPHY-ULLRICH, J. E. 2006. Thrombospondin 1 mediates angiotensin II induction of TGF-beta activation by cardiac and renal cells under both high and low glucose conditions. *Biochem Biophys Res Commun,* 339**,** 633-41.

ZHU, L., VRANCKX, R., KHAU VAN KIEN, P., LALANDE, A., BOISSET, N., MATHIEU, F., WEGMAN, M., GLANCY, L., GASC, J. M., BRUNOTTE, F., BRUNEVAL, P., WOLF, J. E., MICHEL, J. B. & JEUNEMAITRE, X. 2006. Mutations in myosin heavy chain 11 cause a syndrome associating thoracic aortic aneurysm/aortic dissection and patent ductus arteriosus. *Nat Genet,* 38**,** 343-9.

ZUCKERMAN, B. D., ORTON, E. C., STENMARK, K. R., TRAPP, J. A., MURPHY, J. R., COFFEEN, P. R. & REEVES, J. T. 1991. Alteration of the pulsatile load in the high-altitude calf model of pulmonary hypertension. *J Appl Physiol,* 70**,** 859-68.